

LOS ANGELES PUBLIC LIBRARY

APR 25 1956

JET PROPULSION

Journal of the

— AMERICAN ROCKET SOCIETY —

Rocketry Jet Propulsion Sciences Astronautics

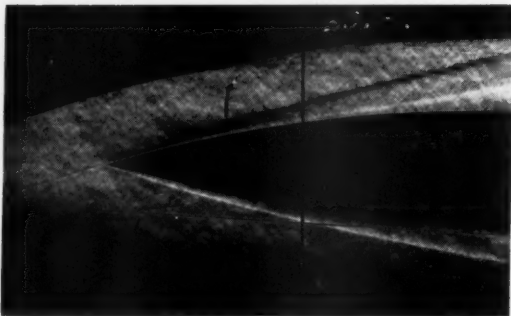
VOLUME 26

APRIL 1956

NUMBER 4

Hypersonic Aerodynamics Issue

- Hypersonic Studies of the Leading Edge Effect on the Flow Over a Flat Plate A. G. Hammitt and S. M. Bogdonoff 241
- Aerodynamics at Very High Altitudes. S. A. Schaaf 247
- Ballistic Missile Performance J. W. Reece, R. D. Joseph, and D. Shaffer 251
- Effect of Chemical Reactions in the Boundary Layer on Convective Heat Transfer D. Altman and H. Wise 256
- Laminar Heat Transfer Over Blunt-Nosed Bodies at Hypersonic Flight Speeds L. Lees 259
- On Laminar Boundary Layers With Heat Transfer W. D. Hayes 270
- Technical Notes**
- Sun-Follower for High Altitude Sounding Rocket. D. D. Terwilliger and G. J. Granros 275
- Heat-Up Time of Wire Glow Plugs S. K. Clark 278
- Comments on "Manifolds for Solid Propellant Rocket Motors" H. Verdier 279
- Measurement of Total Emissivity of Porous Materials in Use for Transpiration Cooling E. R. G. Eckert, J. P. Hartnett, and T. F. Irvine, Jr. 280
- The Near-Constancy of Full-Power Duration for Unboosted Rocket Vehicles W. P. Berggren 282



Gas Dynamics Laboratory, Princeton University

Hypersonic flow at Mach 12.7
Helium wind tunnel at 1000 psi stagnation pressure

- Jet Propulsion News 284
- ARS News 290
- New Equipment and Processes. 301
- New Patents 304
- Book Reviews 308
- Technical Literature Digest. 313

*When you
gotta go...*

you GO!

RMI POWER ENGINEERING is developing a new concept for safer, more reliable ejection systems—another example of increasing diversification in the application of rocket technology.

Engineers and Scientists: creative and rewarding opportunities exist for all types of technical specialists in the research and development of rocket power devices. Send complete resume and salary requirements to employment manager.

PRIMARY AND AUXILIARY ROCKET POWER FOR:

Missile Boosters and Sustainers, Aircraft, Target Drones, Ordnance Rockets, Ejection Systems, Launching Devices.

Power for Progress

RMI

REACTION MOTORS, INC.

DENVILLE, NEW JERSEY

A MEMBER OF THE OMAR TEAM

Scope of JET PROPULSION

JET PROPULSION, the Journal of the American Rocket Society, is devoted to the advancement of the field of jet propulsion through the publication of original papers disclosing new knowledge and new developments. The term "jet propulsion" as used herein is understood to embrace all engines that develop thrust by rearward discharge of a jet through a nozzle or duct; and thus it includes systems utilizing atmospheric air and underwater systems, as well as rocket engines. JET PROPULSION is open to contributions, either fundamental or applied, dealing with specialized aspects of jet and rocket propulsion, such as fuels and propellants, combustion, heat transfer, high temperature materials, mechanical design analyses, flight mechanics of jet-propelled vehicles, astronautics, and so forth. JET PROPULSION endeavors, also, to keep its subscribers informed of the affairs of the Society and of outstanding events in the rocket and jet propulsion field.

Limitation of Responsibility

Statements and opinions expressed in JET PROPULSION are to be understood as the individual expressions of the authors and do not necessarily reflect the views of the Editors or the Society.

Subscription Rates

One year (twelve monthly issues).....	\$12.50
Foreign countries, additional postage.....	add .50
Single copies.....	1.25
Special issues, single copies.....	2.50
Back numbers.....	2.00

Change of Address

Notices of change of address should be sent to the Secretary of the Society at least 30 days prior to the date of publication.

Information for Authors

Preparation of Manuscripts

Manuscripts must be double spaced on one side of paper only with wide margins to allow for instructions to printer. Submit two copies: original and first carbon. Include a 100-200 word abstract of paper. The title of the paper should be brief to simplify indexing. The author's name should be given without title, degree, or honor. A footnote on the first page should indicate the author's position and affiliation. Include only essential illustrations, tables, and mathematics. References should be grouped at the end of the manuscript; footnotes are reserved for comments on the text. Use American Standard symbols and abbreviations published by the American Standards Association. Greek letters should be identified clearly for the printer. References should be given as follows: For Journal Articles: Authors, Title, Journal, Volume, Year, Page Numbers. For Books: Author, Title, Publisher, City, Edition, Year, Page Numbers. Line drawings must be made with India ink on white paper or tracing cloth. Lettering on drawings should be large enough to permit reduction to standard one-column width, except for unusually complex drawings where such reduction would be prohibitive. Photographs should be clear, glossy prints. Legends must accompany each illustration submitted and should be listed in order on a separate sheet of paper.

Security Clearance

Manuscripts must be accompanied by written assurance as to security clearance in the event the subject matter of the manuscript is considered to lie in a classified area. Alternatively, written assurance that clearance is unnecessary should be submitted. Full responsibility for obtaining authoritative clearance rests with the author.

Submission of Manuscripts

Manuscripts should be submitted in duplicate to the Editor-in-Chief, Martin Summerfield, Professor of Aeronautical Engineering, Princeton University, Princeton, N. J.

Manuscripts Presented at ARS Meetings

A manuscript submitted to the ARS Program Chairman and accepted for presentation at a national meeting will automatically be referred to the Editors for consideration for publication in JET PROPULSION, unless a contrary request is made by the author.

To Order Reprints

Prices for reprints will be sent to the author with the galley proof, and orders should accompany the corrected galley when it is returned to the Assistant Editor.

JET PROPULSION, the Journal of the American Rocket Society, published monthly by the American Rocket Society at 20th and Northampton Streets, Easton, Pa., U.S.A. The Editorial Office is located at 500 5th Ave., New York 36, N. Y. Price \$1.25 per copy, \$12.50 per year: Entered as second-class matter at the Post Office at Easton, Pa., under the Act of March 3, 1879. © Copyright, 1956, by the American Rocket Society, Inc. Permission for reprinting may be obtained by written application to the Assistant Editor.

JET PROPULSION

Journal of the
AMERICAN ROCKET SOCIETY

EDITOR-IN-CHIEF

MARTIN SUMMERFIELD
Princeton University

ASSISTANT EDITOR

H. K. WILGUS

ART EDITOR

N. KOCHANSKY

ASSOCIATE EDITORS

ALI BULENT CAMEL

Northwestern University

IRVIN GLASSMAN

Princeton University

M. H. SMITH

Princeton University

A. J. ZAEHRINGER

American Rocket Company

CONTRIBUTORS

NORMAN L. BAKER

Indiana Technical College

MARSHALL FISHER

Princeton University

G. F. McLAUGHLIN

K. R. STEHLING

Naval Research Laboratory

EDITORIAL BOARD

D. ALTMAN

California Institute of Technology

L. CROCCO

Princeton University

P. DUWEZ

California Institute of Technology

R. D. GECKLER

Aerojet-General Corporation

C. A. CONGWER

Aerojet-General Corporation

C. A. MEYER

Westinghouse Electric Corporation

P. F. WINTERITZ

New York University

K. WOHL

University of Delaware

M. J. ZUCROW

Purdue University

ADVISORS ON PUBLICATION POLICY

L. G. DUNN

Ramo-Wooldridge Corporation
Los Angeles, California

R. G. FOLSOM

Director, Engineering Research Institute
University of Michigan

R. E. GIBSON

Director, Applied Physics Laboratory
Johns Hopkins University

H. F. GUGGENHEIM

President, The Daniel and Florence
Guggenheim Foundation

R. P. KROON

Director of Research, AGT Div.
Westinghouse Electric Corporation

ABE SILVERSTEIN

Associate Director, Lewis Laboratory
National Advisory Committee for
Aeronautics

T. VON KÁRMÁN

Chairman, Advisory Group for
Aeronautical Research and Development, NATO

W. E. ZISCH

Vice-President and General Manager
Aerojet-General Corporation

OFFICERS

President

Vice-President

Executive Secretary

Secretary

Treasurer

General Counsel

Noah S. Davis

Robert C. Truax

James J. Harford

A. C. Slade

Robert M. Lawrence

Andrew G. Haley

BOARD OF DIRECTORS

Terms expiring on dates indicated

J. B. Cowen, 1956

Andrew G. Haley, 1957

S. K. Hoffman, 1958

H. W. Ritchey, 1956

Milton W. Rosen, 1957

H. S. Seifert, 1958

K. R. Stehling, 1958

George P. Sutton, 1956

Wernher von Braun, 1957

Advertising Representatives

EMERY-HARFORD

155 East 42 St., New York, N. Y. 6535 Wilshire Blvd., Los Angeles, Calif.

Telephone: MU 4-7232

JIM SUMMERS

400 N. Michigan Ave.

Chicago, Ill.

Telephone: Su 7-1641

J. C. GALLOWAY & J. W. HARBISON

Telephone: Olive 3-3223

R. F. PICKRELL AND ASSOCIATES

318 Stephenson Bldg.

Detroit, Mich.

Telephone: Trinity 1-0790

HAROLD SHORT

Holt Rd., Andover, Mass.

Telephone: Andover 2212

engineers
ANNOUNCING
EXPANSION
OF THE
ROCKET
ENGINE
SECTION of
General Electric's
Aircraft
Gas
Turbine
Development
Department

The performance records of rockets as power plants for supersonic missiles and aircraft have led to accelerated design and development activities in this field. Our huge satellite program is now under way. Engineers who wish to contribute to advances in propulsion will be interested in the following openings created by expansion at GE.

ROCKETS

- Design and develop rocket engine valves, seals and piping. Establish and maintain standards and instructions for their manufacture, test, installation and operation.
- Design, develop, construct and test rocket engine seals and piping. Prepare standards and instructions for their manufacture, test and use.
- Assemble and test rocket engines from their functional components. Design and develop supporting members needed to mount engine components.
- Design, develop, construct and test propellant pumps.
- Design, develop, construct and test turbines. Conduct performance analysis.
- Create advanced inlet designs for high performance rockets; provide data on aerodynamic design and performance of such inlets, and conduct theoretical and experimental investigations of designs created.

You'll be working with top men in the field, in small groups which stimulate exchange of ideas. Here, your talents can be easily recognized and rewarded. Educational assistance programs and specialized technical courses are also available to you.

Openings in both
MALTA, NEW YORK
and
CINCINNATI, OHIO

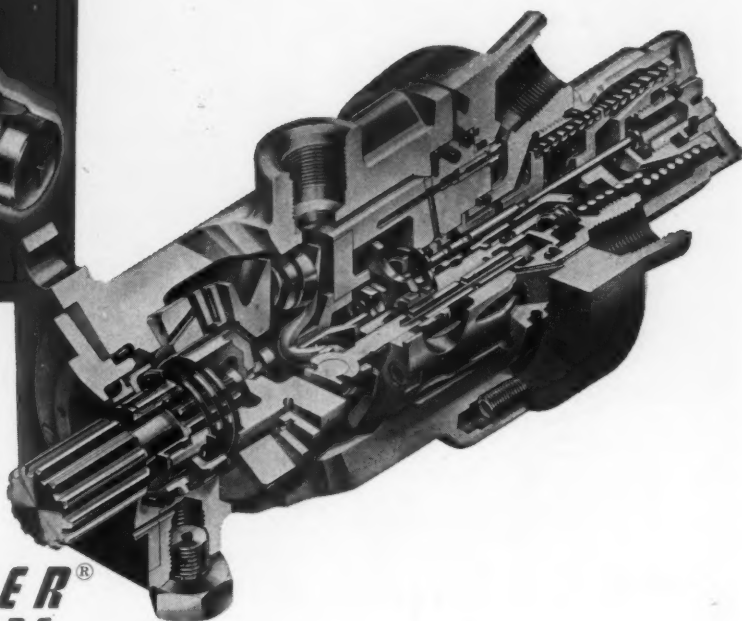
For further information, please write to:

Mr. Mark Peters
TECHNICAL RECRUITING, BLDG. 100
CINCINNATI 15, OHIO

Mr. William E. Potter
ROCKET SECTION, MALTA TEST STATION
BALLSTON SPA, N. Y.

GENERAL  ELECTRIC

Are You One of the 728 Engineers Who Needs This
New Variable Delivery **STRATOPOWER[®]**
HYDRAULIC PUMP



This New Series
65W
STRATOPOWER[®]
HYDRAULIC PUMPS

Answers Many of Your Demands for...

The quiet efficiency of this new 65W Series of STRATOPOWER Variable Delivery Pumps excites the interest of design and project engineers because this efficiency spells better performance.

Again, STRATOPOWER has come forward with a significant development in hydraulic equipment, geared to your advanced thinking. Compacted into a smaller envelope, and with a remarkably low weight/horsepower ratio, STRATOPOWER 65W Pumps operate at system pressures to 3000 psi and the smaller sizes at 10,000 rpm continuous speed!

Whether your project concerns jet propelled aircraft, rockets or guided missiles, consider STRATOPOWER Hydraulic Pumps as the heart of your Hydraulic system.

LIGHTER WEIGHT



SMALLER ENVELOPE



HIGHER SPEEDS



HIGHER ALTITUDES



HIGHER PRESSURES



HIGHER TEMPERATURES

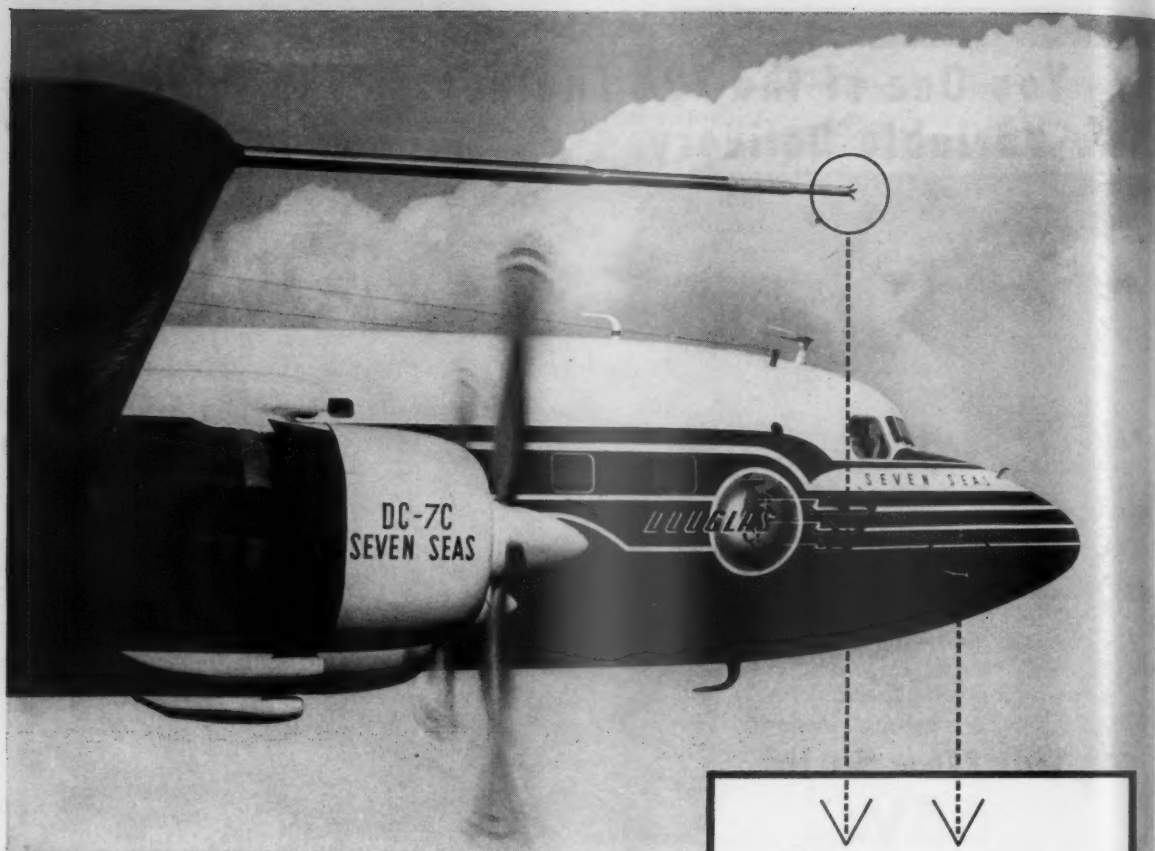


WATERTOWN DIVISION
THE NEW YORK AIR BRAKE COMPANY

STARBUCK AVENUE • WATERTOWN • N. Y.
INTERNATIONAL SALES OFFICE, 90 WEST ST., NEW YORK 6, N. Y.



APRIL 1956



ANNOUNCING
A CRUISE CONTROL SYSTEM
WITH NO MOVING PARTS...

*The Giannini-Douglas Differential
 Pressure Flight Angle Computer*

Differential pressure probes with no moving parts sense cruise control air data on Douglas Aircraft's newest overseas transport, the DC-7C. The probes are an integral part of a completely new angle-of-attack measuring system, the Giannini-Douglas Differential Pressure Flight Angle Computer, which was designed to have the greatest reliability and longest operating life possible in a cruise control sensing instrument.

In the Giannini-Douglas developed unit, small impact probes are accurately positioned on the head of a short stub boom mounted on the side of the fuselage; or for flight test,

on a free airstream boom. The probes are connected to sensitive Giannini pressure transducers which supply electrical signals proportional to air data to a passive network computer having no vacuum tubes. The output of this integrating unit can be fed directly into an automatic flight control system or can be used to activate a panel indicator.

System accuracy in the control range is $\pm 0.1^\circ$ to $\pm 0.2^\circ$ and angle of attack data can be sensed over a range of $\pm 20^\circ$ from Mach 0.3 to 2.0. Less than 0.25 ampere at standard aircraft voltage is required for continuous operation.

Thoroughly proven in wind tunnel and flight test, the Giannini-Douglas Differential Pressure Flight Angle Computer is one more outstanding example of recent advances in aeronautical progress made possible by the ingenuity and skill of today's research and design engineers in the field of avionics.

Giannini

AIRBORNE SYSTEMS DIVISION

REGIONAL SALES OFFICES

NEW YORK 1, N.Y., Empire State Bldg., CHickering 4-4700
 CHICAGO, Ill., 8 So. Michigan Ave., ANdover 3-5272
 PASADENA, Calif., 918 E. Green St., RYan 1-7152

G. M. GIANNINI & CO., INC. 918 EAST GREEN STREET • PASADENA, CALIFORNIA

THE SKY IS FULL OF VITAL CLARY CONTROLS

*...in missiles, rockets
and aircraft!*

LIKE SO MANY missile developers, the designers of the Firestone "Corporal," the North American "Navaho," and four other classified missiles, specified *Clary* for vital automatic controls. Every control that bears the Clary name combines delicate precision (up to seven-one-millionths of an inch tolerance) with bulldog construction and supreme reliability. Our long experience in manufacturing to the stringent requirements of missiles also gives us an outstanding background in producing vital rocket and aircraft components... for air-to-air rockets, jet engine after-burner actuators, fuel system emergency valves and others that cannot be named.

WE INVITE YOU to come to Clary, where our expanding engineering and manufacturing facilities provide you with—

- **DESIGNING AND TESTING** to established specifications and envelope drawings.
- **PRODUCTION-ENGINEERING** of parts or complete components covered by your prototype sketches or drawings.
- **MANUFACTURING** of precision components to established drawings and specifications.

TYPICAL CLARY AUTOMATIC CONTROLS



Servo actuator
for the "Corporal"



Gate-type propellant
valve for the "Navaho"



Gyroscope
for the "Corporal"



After-burner actuator
for jet engines

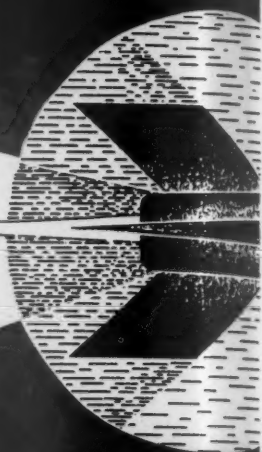


AUTOMATIC CONTROLS DIVISION

CLARY CORPORATION
Dept. J46, San Gabriel, Calif.

MANUFACTURER OF BUSINESS MACHINES, ELECTRONIC DATA HANDLING EQUIPMENT AND AIRCRAFT AND MISSILE COMPONENTS

TALOS



Department Heads needed in:

MISSILE FLIGHT TEST...

To organize and direct group of Flight Test Engineers engaged in all phases of instrumentation, ground based radar, telemetering and check-out equipment, data processing.

AEROELASTICITY AND FLUTTER...

Will direct all division activity concerning the problems of missile aeroelasticity, subsonic and supersonic flutter.

Openings also exist in the fields of:

Stability and Control Analysis — Dynamic Systems Calculations — Preliminary and Advanced Design — Aerodynamic and Hi-Speed Heat Problems — Structural Analysis — Airloads and Flight Criteria — Servo-Mechanisms — Computers

TALOS is but one of seven missile development projects in which our Missile Division is presently active.

Write in confidence to:

TECHNICAL PLACEMENT SUPERVISOR
P. O. Box 516 • St. Louis 3, Missouri

MCDONNELL *Aircraft Corporation*

DESIGNERS

for MISSILE SYSTEMS

■ *New activities at Lockheed Missile Systems Division have created positions for Designers capable of performing creative basic layout and design of structural, mechanical, electro-mechanical and electronic packaging of missile assemblies and components.*

■ *Those who will qualify will cope with new problems in a field of scientific endeavor that grows daily in complexity. A knowledge of new materials, finishes, specifications and experience on small precision devices will prove helpful in meeting the challenge of Missile Systems research and development.*

Those possessing a high order of ability applicable to these areas of endeavor are invited to write:

VARIED ASSIGNMENTS

Designers are not limited to specific functions under Missile Systems Division's philosophy of operation. Diversified assignments provide stimulating challenge, enable Designers to acquire the broadest possible background in the field of missile systems design. For example: it is not uncommon for a Missile Systems Designer to work on diverse problems in structures, controls, hydraulics, pneumatics, electro-mechanical packaging, fuel systems and other fields within the span of a few months.

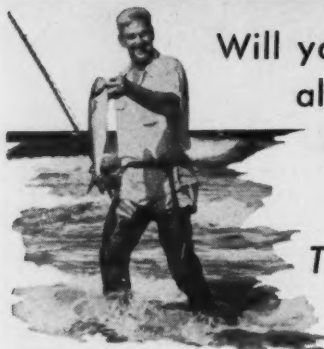
Lockheed **MISSILE SYSTEMS DIVISION**
research and engineering staff

LOCKHEED AIRCRAFT CORPORATION • VAN NUYS, CALIFORNIA

ENGINEERS... LOOK TEN YEARS AHEAD!



A Douglas engineer lives here



Will your income and location
allow you to live in a home
like this...spend your
leisure time like this?

*They can...if you start your
career now at Douglas!*

Take that ten year ahead look. There's a fine career opportunity in the engineering field you like best waiting for you at Douglas.

And what about the Douglas Aircraft Company? It's the biggest, most successful, most stable unit in one of the fastest growing industries in the world. It has giant military contracts involving some of the most exciting projects ever conceived...yet its commercial business is greater than that of any other aviation company.

The Douglas Company's size and variety mean that you'll be in the

work you like best—side by side with the men who have engineered the finest aircraft and missiles on the American scene today. And you'll have every prospect that ten years from now you'll be where you want to be career-wise, money-wise and location-wise.

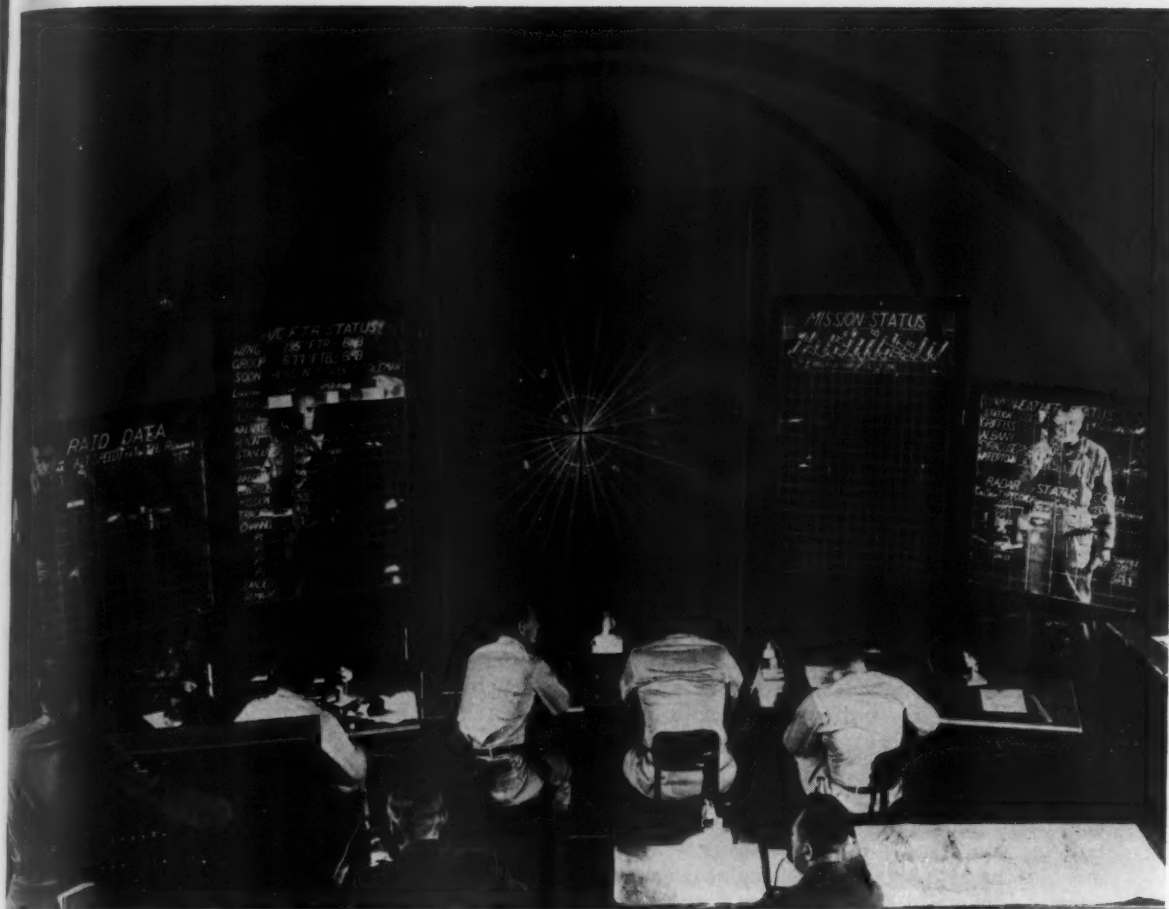
For further information about opportunities with Douglas at Santa Monica, El Segundo and Long Beach, California and Tulsa, Oklahoma, write today to:

DOUGLAS AIRCRAFT COMPANY, INC.
C. C. LaVene, 3000 Ocean Park Blvd.
Santa Monica, California

DOUGLAS



First in Aviation



Official U.S. Air Force Photograph

Friend or foe? Tactical defense officers in MINK control center watch movements of aircraft as reported from radar warning sites. This is equipment developed under the direction of Rome Air Development Center.

ROME AIR DEVELOPMENT CENTER PROVIDES AIR DEFENSE EQUIPMENT FOR OUR AIR FORCE

One development agency for the Air Force's ground-based electronic equipment is Rome Air Development Center, located at Griffiss AFB in Rome, N. Y. One of the ten centers of the Air Research and Development Command, RADC is concerned with the air defense of our nation, with providing equipment for tactical supremacy, and with developing ground complexes for various navigation systems to aid all aircraft. In addition, RADC is charged with data handling improvements for the Air Force intelligence mission.

RADC is the responsible center for development,

through its various contractors, of such end products as radar sites, including improved tubes, circuits, antennae, and shelters; ground communications equipment and associated support items; IFF (Identification Friend or Foe) environments, and electronic countermeasures.

Bringing complex systems from the written requirements to the actual hardware items to be used in the various Air Force commands is a long and tedious business which draws upon the skills of RADC's 500 civilian and military engineers and their many counterparts in private industry.



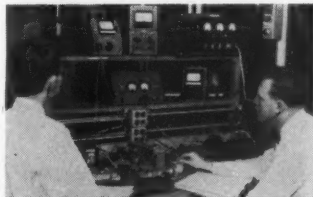
FORD INSTRUMENT COMPANY

DIVISION OF SPERRY RAND CORPORATION

31-10 Thomson Ave., Long Island City 1, N. Y.

This is one of a series of ads on the technical activities of the Department of Defense.

Engineers at Ford Instrument Company working on a special Air Force project in one of the company's laboratories.



WHY ENGINEERS FEEL AT HOME AT ROCKETDYNE

First and foremost, ROCKETDYNE talks your language—and understands it too. Your associates and supervisors here are professional people like you. They respect your status, your thinking, your ideas and your interest in technical advancement.

ROCKETDYNE will encourage you to choose the field that is most satisfying and rewarding... truly best for you. This is possible because its activity includes the full range of rocket engine development from preliminary design to field testing and production... because its programs include development of the largest liquid-propellant rocket engine in the Western World... because it has contracts with all branches of the Armed Services and the guided missile industry for broad variety of rocket engine types and sizes.

It may surprise you to know you can qualify for a career at ROCKETDYNE *with or without specific rocket engine experience!* Engineering experience in heating and ventilating, hydraulics, pumps, tur-

bines, combustion devices, controls, dynamics, structures and instrumentation are just a few of the related fields that could open your future at ROCKETDYNE.

ROCKETDYNE's design and manufacturing center and its nearby test laboratory house complete, advanced facilities... the vital tools you need to meet the challenges of rocket engine development.

ROCKETDYNE is North American's rocket engine division. It has just moved into new ultra-modern headquarters in Canoga Park, located in the beautiful West San Fernando Valley of Los Angeles. This area is famous for its fine residential sections, modern shopping-center convenience, varied recreational and entertainment facilities. Any point in the San Fernando Valley is just minutes drive from the beaches, and the weather is pleasant all year around. Many engineers are interested in advanced courses offered by fine schools like UCLA, USC and Cal Tech, all within a short drive from our headquarters.

THESE POSITIONS NOW OPEN AT ROCKETDYNE:

DESIGN & DEVELOPMENT ENGINEERS

Mechanical, Chemical, Electrical, Aeronautical, Standards, Structural and Stress. For rocket engine components and systems design or development. Turbine, pump, controls and combustion device experience preferred.

TEST ENGINEERS

Experienced on engine systems, combustion devices, turbines, pumps and engine instrumentation.

EQUIPMENT DESIGN ENGINEERS

Electrical, mechanical, structural, industrial. For design of facilities, specialized test, and handling equipment.

DYNAMICS ENGINEERS

To analyze rocket engine control systems utilizing electronic analog and digital computers, B.S., M.E., or B.S.E.E. necessary. Prefer advanced degree. Experience in servomechanisms, systems analysis desired.

THERMODYNAMICIST

To analyze, design and develop high speed subsonic and supersonic turbines. Jet engine or industrial steam turbine experience desired.

SYSTEMS ENGINEERS
ENVIRONMENTAL TEST ENGINEERS
STANDARDS ENGINEERS
TEST ENGINEERS—ELECTRICAL

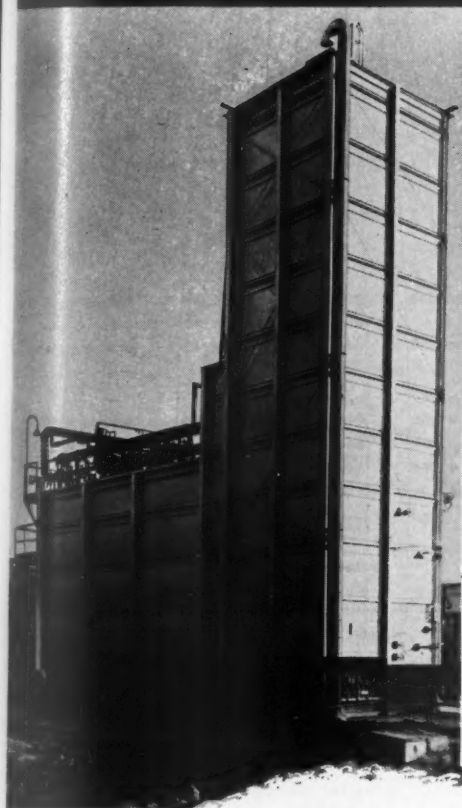
Write Mr. Grant Baldwin, Rocketdyne Engineering Personnel, Dept. 596-JP, 6633 Canoga Ave., Canoga Park, Calif.

ROCKETDYNE

A DIVISION OF NORTH AMERICAN AVIATION, INC.

B U I L D E R S O F P O W E R F O R O U T E R S P A C E

Air Products GENERATORS for abundant liquid oxygen at lowest cost



Large-scale "on-location" oxygen production is economically essential to major rocket research and operational facilities. Air Products Oxygen Generators provide the most dependable source of oxygen in unlimited quantities at lowest cost. This statement is amply supported by experience based on many successful installations.

We will provide and install an "on-location" oxygen and/or nitrogen generating station to suit your present and expanding oxygen requirements. This can be done on a lease basis, *without capital investment by you*. Operation and maintenance can be handled by you or by Air Products—at your option—with price guaranteed at all levels of consumption.

We design and manufacture generators for unlimited quantities of oxygen and nitrogen regardless of size, purity or cycle.

If you will advise us regarding your requirements, we will be glad to furnish you with actual costs and engineering information on oxygen generators designed for your particular needs.

More than 700 successful installations

Cost Analyses

• Process Design

• Apparatus Design

• Apparatus Manufacture

Air Products

INCORPORATED

Dept. O, Box 538 Allentown, Pa.



THE GPE CAPACITIES

Precision Mechanics, Optical Devices, Ceramics	●●●	●●	●●	□●●	●●	●●●		●●	●●●	□●●	●●	●●	●●	●●●
Electrical Equipment and Components	●●●	●	●			●●●		●●●	●●	□●●	●	●●	●	●●●
Electronics	●●●	●●	●●●	●●●		●●●		●	●●	□●●		●●●	●●	●●●
Hydraulics, Liquids Processing, Heat Exchange		●●			●●●		●●●					●●●		
Television: Studio, Theatre, Institutional, Business, Industrial	●	●●		●●●		●						●		
Instruments, Servos, Controls: Hydraulic, Pneumatic, Magnetic, Electronic	●●●	●	●●	□●●		●●●	●●●	●●	●●	□●●		●●●	●	●●●
Aircraft and Missile Guidance, Control, Simulation	●●●	●		●●●		●●●		●				●●	●	●●●
Automatic Computers and Components	●●●	●	●	□●●		●●●						●●●		●●●
Radar, Microwave, Ultrasonics	●●●	●●	●●	●●●		●●			●	□●●		●		
Motion Picture and Audio Equipment		●●●		□●●				●●	●●●		●●●		●●●	
Nuclear Power Components and Controls	●●●				●●					□●●		●●		●●●
Systems Engineering: Aeronautical, Naval, Industrial	●●●			●●●	●●●	●●●	●●●			□●●		●●●		●●●
	I	II	III	IV	V	VI	VII	VIII	IX	X	XI	XII	XIII	XIV

- I Kearfott Company, Inc.; Little Falls, New Jersey
 II International Projector Corporation; Bloomfield, New Jersey
 III Bludworth Marine; New York
 IV General Precision Laboratory Incorporated; Pleasantville, New York
 V The Grisco-Russell Company; Massillon, Ohio
 VI Link Aviation, Inc.; Binghamton, New York
 VII Shand and Jurs Co.; Berkeley, California
 VIII The Hertner Electric Company; Cleveland
 IX The Strong Electric Corporation; Toledo, Ohio
 X Precision Technology, Inc.; Livermore, California
 XI J. E. McAuley Mfg. Co.; Chicago
 XII Askania Regulator Company; Chicago
 XIII Ampco Corporation; Chicago
 XIV Librascope, Incorporated; Glendale, California

● Manufacturing ●● Manufacturing and product development ●●● Manufacturing, product development and research
 □●● Pilot manufacturing, product development and research



to "speak softly..."

More than a year ago, one of the operating companies of General Precision Equipment Corporation—after nearly 8 years of joint development work with the Air Force—placed in scheduled production the most advanced air navigation system known to exist. Called AN/APN-66, the system is based on "Doppler effect," a known natural phenomenon, but one which others said could never be applied to aviation engineering. Its successful development brought to culmination still another notable aviation engineering "first" by a GPE Company.

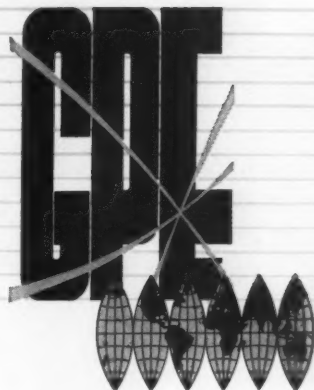
AN/APN-66 and related systems adapted for specific purposes compute air position with unprecedented accuracy and speed. They work independently of any ground-based reference, optical or electronic; are the only operational systems that are global. They provide a vitally needed element in the defensive-offensive power our country must have to speak softly, yet negotiate from strength.

For months now, these systems have been functioning as brain and nerve center in a substantial number of the Air Force's newest craft. In millions of miles of operational flight they have demonstrated their engineering genius. When put to civilian use, they will guide air liners to the remote corners of the globe with equal accuracy. Then, never again need a plane get lost anywhere...in any weather.

While the GPE Company primarily responsible for this AN/APN equipment is General Precision Laboratory, the systems are typical products of GPE Coordinated Precision Technology. Four other GPE Companies—Askania, International Projector, Kearfott and Librascope—participated with GPL in providing the components that made them possible. All now manufacture portions of the equipment.

As the chart on the opposite page shows, all of the producing companies in the GPE Group work in highly advanced fields. GPE Coordinated Precision Technology, a basic GPE operating policy, gives each GPE company access to the skills and facilities of the others and coordinates those which are relevant. This coordination has played an important part in amplifying the capabilities of all GPE companies, enabling them to solve highly advanced technological problems with vision. Frequently, as with these AN/APN systems, frontiers of science are pushed back on the way.

The GPE Producing Companies serve more than a dozen major industries. A brochure, "Serving Industry through Coordinated Precision Technology," describes their fields in some detail. It may well suggest products or facilities applicable to problems your company is facing. For a copy or other information, write:



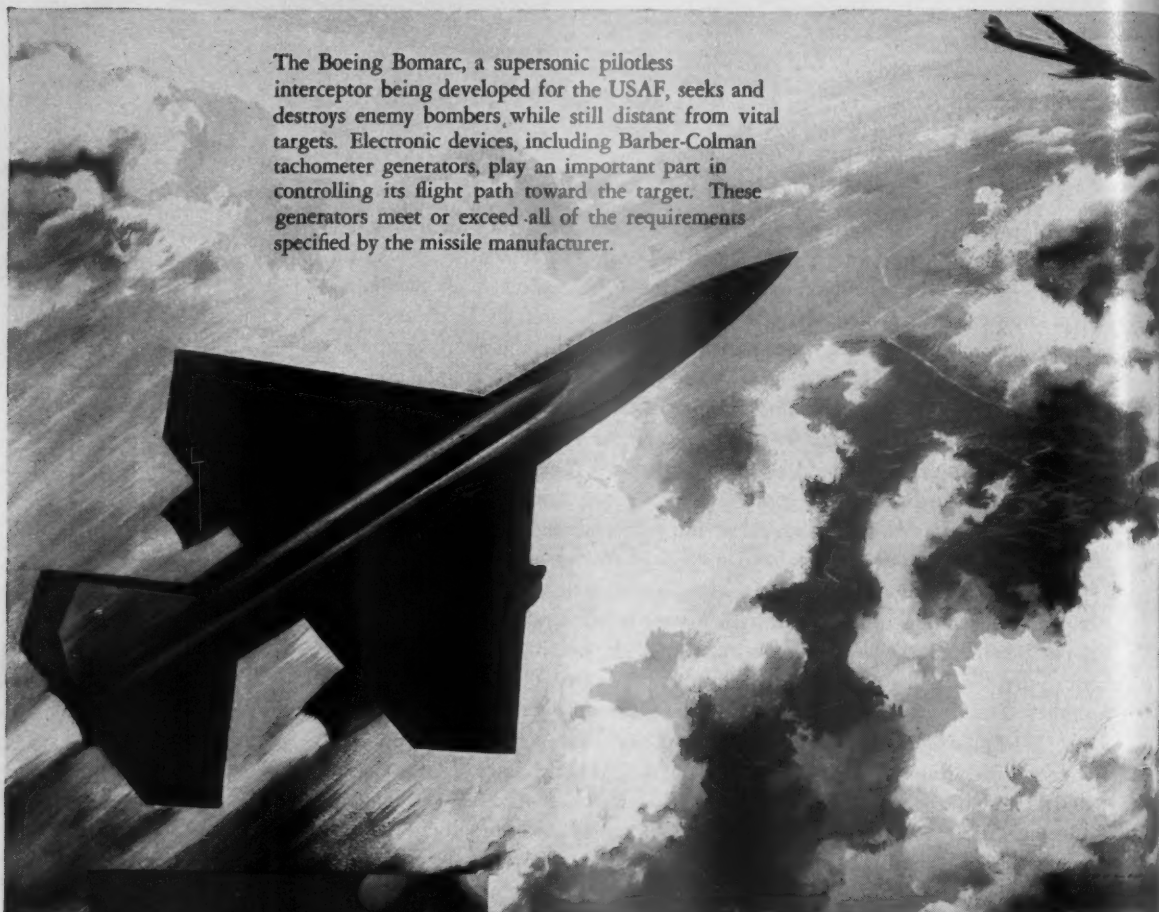
General Precision Equipment Corporation

92 Gold Street, New York 38, New York,



Aircraft Controls

help keep Boeing IM-99 missile accurately on course



The Boeing Bomarc, a supersonic pilotless interceptor being developed for the USAF, seeks and destroys enemy bombers while still distant from vital targets. Electronic devices, including Barber-Colman tachometer generators, play an important part in controlling its flight path toward the target. These generators meet or exceed all of the requirements specified by the missile manufacturer.

* Artist's conception of Boeing Bomarc



The Barber-Colman tach generator used on this missile application is a special adaptation of the widely known Barber-Colman line of high quality d-c motors for aircraft.

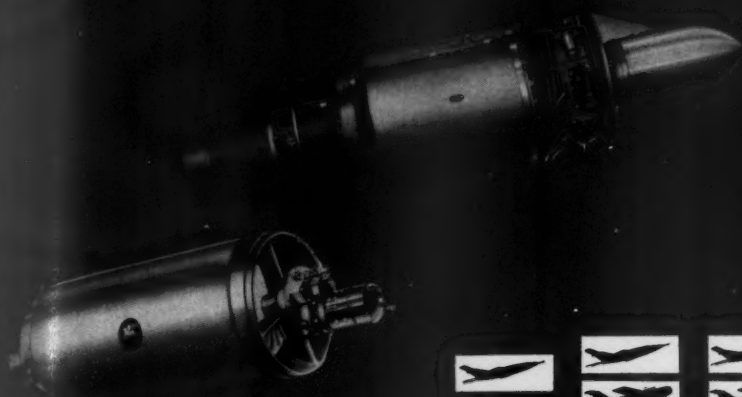
The complete line of Barber-Colman aircraft controls includes: Actuators; Positioning Controls; Temperature Controls; Small Motors; Valves; Ultra-Sensitive Relays; Thermo-Sensitive Elements. Write today for literature or consult the Barber-Colman engineering sales office nearest you . . . Los Angeles; Seattle; Baltimore; New York; Montreal, Melbourne.

Barber-Colman Company

DEPT. D, 1470 ROCK STREET, ROCKFORD, ILLINOIS

AIRCRAFT CONTROLS • AUTOMATIC CONTROLS • INDUSTRIAL INSTRUMENTS • SMALL MOTORS • AIR DISTRIBUTION PRODUCTS
OVERDOORS AND OPERATORS • MOLDED PRODUCTS • METAL CUTTING TOOLS • MACHINE TOOLS • TEXTILE MACHINERY

EVOLUTION



ANNUAL PRODUCTION

JUNE 1947 1948 1949 1950 1951 1952 1953 1954 1955

Here's how a new era in small jet development was pioneered. More than seven years ago, Fairchild Engine Division began work on the mighty J44, a power-packed, bantam-weight turbojet, to power guided missiles, target drones and pilotless planes.

Its 150-hour military qualification tests completed, the J44 can now be put to work as thrust assist on multi-engined military cargo and transport aircraft; or as part of auxiliary power and boundary layer control systems.




From the beginning, Fairchild engineers have continually designed increased performance, reliability and ruggedness into the J44. Faster speeds, higher altitudes were achieved, and with them, a wider and wider range of new applications.

FAIRCHILD

ENGINE DIVISION • DEER PARK, L. I., N. Y.
A Division of Fairchild Engine and Airplane Corporation

... WHERE THE FUTURE IS MEASURED IN LIGHT-YEARS!



 SPECIFICATION REQUIREMENTS
 PERFORMANCE DELIVERED
 PLANNED PERFORMANCE GROWTH





Vanguard chooses UDMH *For Satellite Second Stage*

The top performance characteristics of unsym-Dimethylhydrazine make this fuel the ideal choice for use under the difficult conditions involved in propelling this vehicle into outer space.

We welcome the opportunity to discuss UDMH and its properties with your staff.

Commercial quantities of UDMH are available from stock for immediate delivery.



DEVELOPMENT DEPARTMENT
Westvaco Chlor-Alkali Division
FOOD MACHINERY AND CHEMICAL CORPORATION
South Charleston 3, West Virginia

FMC CHEMICALS INCLUDE: *Various Fertilizer Chemicals • WESTVACO Alkalies, Chlorinated Chemicals and Carbon Disulfide • FMC And Associated Chemicals and Industrial Gases • ODDO-APEN Plasticizers and Chemicals • FAIRFIELD Pesticide Compounds and Organic Chemicals • WESTVACO Phosphates, Barium and Magnesium Chemicals*

Hypersonic Studies of the Leading Edge Effect on the Flow Over a Flat Plate

A. G. HAMMITT¹ and S. M. BOGDONOFF²

Forrestal Research Center, Princeton University, Princeton, N. J.

Using the Princeton helium hypersonic wind tunnel, the effect of leading edge thickness on the flow over a flat plate has been investigated. The study was carried out by optical measurements of the shock position over a wide range of leading edge thicknesses and surface pressure measurements for the thicker leading edges. The flow over the plate with a thick leading edge was found to be essentially inviscid, but viscosity was important for the case of thin leading edges. The strong inviscid effect caused by the finite thickness of the leading edge seemed to be sufficient to explain the discrepancies between viscous theory and experiment in the region near the leading edge.

Nomenclature

- C = linear viscosity coefficient in relation $\mu_w/\mu_1 = C(T_w/T_1)$
 δ_0 = boundary layer parameter depending on surface temperature
 M = Mach number
 p = pressure
 Δp = static pressure increment
 Re = Reynolds number
 t = leading edge thickness, inches
 T = temperature
 x = distance from leading edge
 y = distance of shock above plate surface
 w = velocity divided by maximum velocity on expanding to zero pressure
 γ = specific heat ratio
 δ^* = boundary layer displacement thickness
 μ = viscosity

Subscripts

- 1 = tunnel empty condition
 ∞ = stagnation
 l = based on leading edge thickness
 w = condition on wall
 z = based on distance from leading edge

Introduction

THE analysis of flows at many times the speed of sound are complicated by special problems which are unimportant at lower speeds. These problems can be broken down into two classes: (a) fluid dynamics problems, which depend on the conventional parameters of Mach number, Reynolds number, Nusselt number, and specific heat ratio; (b) molecular problems, which depend on temperature and involve the change of molecular structure at high temperatures.

Presented at the ARS 25th Anniversary Annual Meeting, Chicago, Ill., Nov. 14-18, 1955.

¹ Research Associate, Gas Dynamics Laboratory.

² Associate Professor.

³ Numbers in parentheses indicate References at end of paper.

The hypersonic fluid dynamic problems are governed by the same relations as other fluid dynamic problems. Considerable study has been given to the predominant fluid dynamics problems in the subsonic and supersonic range. At hypersonic speeds the relative magnitude of the various effects may be considerably different. This change in emphasis leads to several new problems which have received little attention. Effects of little importance at supersonic speeds may become dominant at hypersonic speeds, and vice versa.

The molecular problems are essentially new in aerodynamic applications. These problems only occur at high temperatures where the molecular structure may be considerably different than at conventional temperatures. Some of these problems have been encountered at the relatively low speeds and high temperatures which exist in rocket motors.

This paper describes a study of the flow about the leading edge of a flat plate and the experimental equipment used for this study. This flow involves several hypersonic fluid dynamics problems. At hypersonic speeds most shocks are strong and the entropy changes through the shocks cannot be neglected. The reflected waves, caused by the interaction of other waves with the strong shocks, are also important. Viscous forces are large and can cause important modifications in the inviscid external flow. All these factors combine in the flow about the leading edge of a flat plate. The study of this problem was carried out in a hypersonic wind tunnel using helium as the working fluid. The tunnel operates in a Reynolds number range where the fluid is essentially a continuum and slip phenomena are limited to very small distances. The work reported herein covers an analysis of shock shapes and pressure distributions of the hypersonic flow about a flat plate over a wide range of Reynolds numbers and leading edge thicknesses.

This work was carried out in the Gas Dynamics Laboratory of the Forrestal Research Center, Princeton University, and was sponsored by the United States Air Force, Aeronautical Research Laboratory, Wright Air Development Center, Wright Patterson Air Force Base, under contracts numbers AF 33(038)-250 and AF 33(616)-2547. More detailed descriptions of the helium tunnel and research are contained in (15)³ to (20).

Hypersonic Wind Tunnel

General Discussion

There are several techniques for making fluid dynamics experiments which have been proved useful. Wind tunnels, shock tubes, and free flight experiments all have important uses. The wind tunnel has proved to be very valuable for many investigations in the subsonic and supersonic range and

might be expected to be equally useful in the hypersonic range. The wind tunnel allows tests to be made over relatively long periods, under controlled conditions, with ease and nominal expense.

The main problem in operating a wind tunnel hypersonically is to heat the air enough so that it does not condense after expanding to high velocities. Stagnation temperatures of the order of 1300 to 1500 F are required to prevent condensation of the air in the test section at Mach number 10. To obtain stagnation temperatures high enough to study the molecular problems of hypersonic flow, of the order of 4000 to 6000 F, seems to be impractical in a wind tunnel. For this reason hypersonic wind tunnels are limited to a study of only the fluid dynamic problems. Another technique for avoiding condensation in the working section of a wind tunnel is to use a gas which does not condense. Since the wind tunnel cannot simulate the full flight problem, there is little loss for the purpose of fluid dynamics research in using a gas other than air. If a gas with low condensation temperature such as helium is used, Mach numbers in excess of 20 can be obtained at atmospheric stagnation temperatures. The elimination of the heater and the accompanying problems of a hot tunnel is such an important simplification that the helium tunnel seems to be the most satisfactory device for fluid dynamics research at Mach numbers greater than 10. The results obtained in the helium tunnel do not represent the complete answer to hypersonic flight but only lead to an understanding of the fluid dynamics problems. The data obtained from such a tunnel are directly comparable to the data obtained in hot air tunnels at the same Mach, Reynolds, and Nusselt numbers, corrected for the effect of the different specific heat ratio.

Princeton Helium Hypersonic Tunnel

The Princeton hypersonic wind tunnel is of the blow-down type using helium as the test fluid. Fluid dynamics problems may be studied in this tunnel up to Mach 20. A detailed description of the tunnel is given in (15). The helium is obtained at high pressures in tank semitrailers which are used as the storage system. From the trailer, the helium is piped through a regulating valve to the settling chamber. The tunnel may be run at stagnation pressures up to 2000 psia for periods of about 10 minutes. A stagnation pressure range of 800 to 1400 psia has been used in these tests. To obtain the high pressure ratios which are needed, an air operated ejector, using air at 1500 psi from a second high pressure storage system, is used downstream of the hypersonic diffuser. A general layout of the piping and tunnel is shown in Fig. 1.

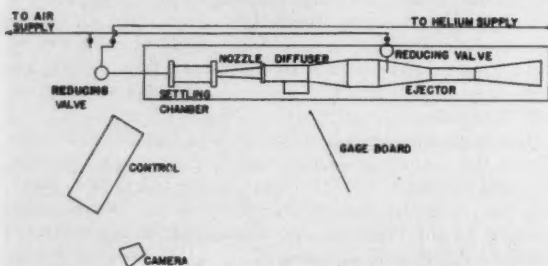


Fig. 1 Piping and control system for helium hypersonic tunnel

The first nozzle used, Fig. 2(a), was an axial symmetric conical nozzle with no windows and a maximum diameter of approximately 3 inches. The second nozzle, Fig. 2(b), is similar to the first one except that it has been cut open and windows installed. The disturbances from the windows do not effect the central core in the region of interest. The models and probe are supported in the test section by means of the sting and spider shown. The first nozzle was used on the initial surface pressure distribution tests and the second

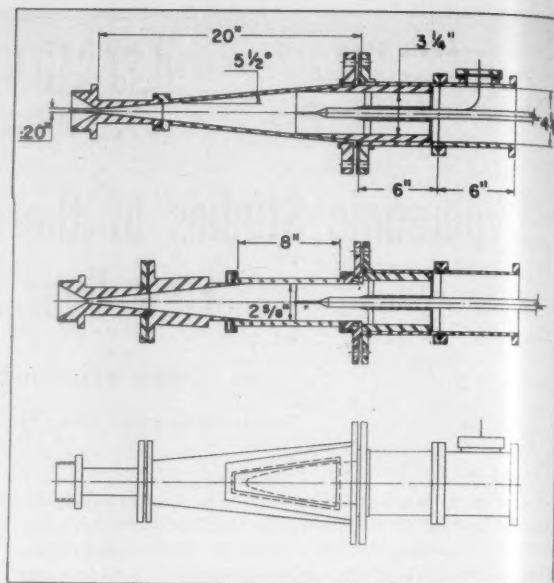


Fig. 2 Cross sections of hypersonic tunnel

Top: axial symmetric nozzle; center and bottom: axial symmetric nozzle with windows.

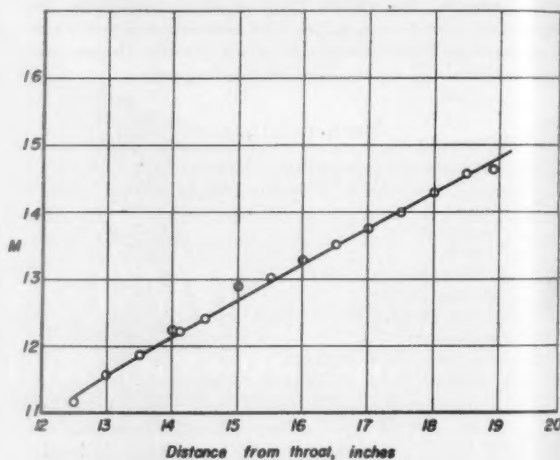


Fig. 3 Mach number distribution along the center line of the hypersonic tunnel

nozzle for the optical studies and additional pressure distribution measurements.

The Mach number along the center line of the nozzle is shown in Fig. 3. Since the nozzle was not contoured, a region of constant Mach number was not obtained and the tests are made in a region of Mach number gradient. The effects of this gradient will be discussed later. The diffuser, Fig. 2, is a straight tube with a central body sting support. This arrangement is probably not an optimum, but gave the best results of the limited varieties which were examined.

Experimental Study

A test program was undertaken to study the flow about the forepart of a flat plate at high Mach number. If only the adiabatic case is considered, there are three parameters which might influence the flow. These parameters are the Mach number, the Reynolds number, and the geometry. In the case of the semi-infinite flat plate, the only geometric parameter is the distance scale based on leading edge thickness.

The experimental model could only approach a semi-infinite plate since it had finite boundaries. In general, it would be expected that the effects of the tips and trailing edges would be limited to small regions and would not propagate over the entire plate. It would be expected that there should be considerable area which behaved as a semi-infinite plate. Again judging by lower speed data, the effect of the leading edge would be expected to be limited to a few leading edge thicknesses. Therefore, a sharp flat plate of reasonable aspect ratio might be expected to behave much like an infinitely sharp semi-infinite flat plate. (This is the model treated by several theoretical investigators (1) to (11)).

The experimental study undertaken was an analysis of the flow over a flat plate at variable leading edge thicknesses, Reynolds number, and Mach number. The effects of the tips and trailing edge were investigated in order to find a region which was free of these effects. The study was carried out by measurements of the shock shape and the surface pressure distributions. In order to study the effect of the leading edge thickness it was necessary to vary this thickness over a wide range. The leading edge thickness and stagnation pressures were varied over the widest ranges possible. The leading edge range was limited by the requirement that the leading edge had to be thick enough to remain unchanged during the run and could not be so thick that the tunnel was stalled. The stagnation pressure was varied between 1400 and 800 psia giving a Reynolds number per inch range of 1.15 to 0.65 million. To obtain sharp leading edges, a simple model with no pressure taps near the leading edge was used. This model could be hardened and honed on both surfaces. The model is shown in Fig. 4. Interferograms were taken of the model at Mach 12.7 at varying leading edge thicknesses and stagnation pressures. The leading edge thickness was varied from 0.17 to 59.5 thousandths of an inch. The blunting was accomplished by cutting off the leading edge perpendicular to the top surface. The measurement of the leading edge thickness was made with a microscope and calibrated eyepiece. A typical range of interferograms is presented in Fig. 5: "a" is for a thin leading edge, "b" a medium edge, and "c" for a thick leading edge. "a" shows a shock wave starting at or very close to the leading edge and a pronounced boundary layer indicated by the large fringe shift between the shock wave and surface. "c" shows a strong detached shock and almost no indication of a boundary layer. "b" is an intermediate position showing a blending together of the features found in "a" and "c." "a" shows the fringes approaching the plate perpendicularly. This does not mean that the flow is separated, but only that the density is so low at this point that the interferometer has not sufficient sensitivity to show the density changes in this region. A similar situation exists in "c." In this case, the density has been reduced to such a level outside of the boundary layer by the entropy changes through the strong shocks that the interferogram does not show the additional density changes through the boundary layer. These interferograms can be used only as qualitative indications of the density since the

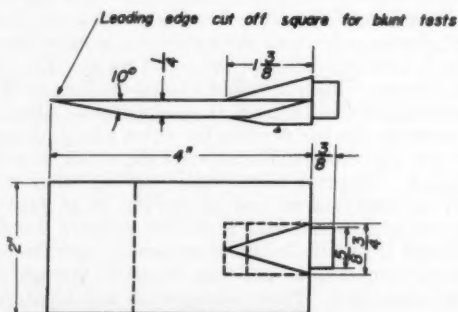


Fig. 4 Flat plate model

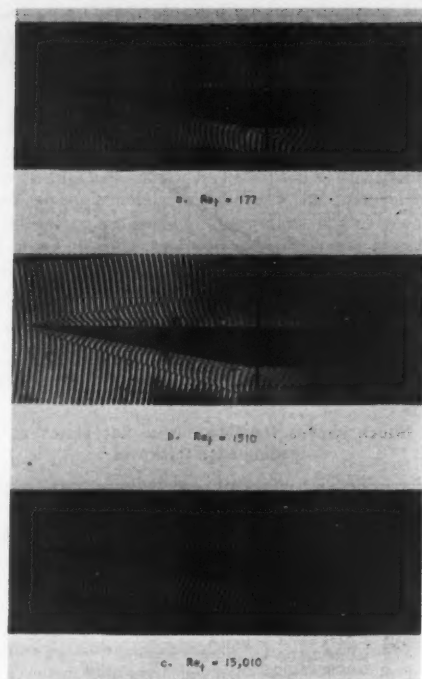


Fig. 5 Interferograms of flat plate mode. $M = 1.27$

flow field is not completely two-dimensional (the model does not span the tunnel) and the fringe shifts are too small to be accurately determined. Only the position of the shock can be determined and quantitatively analyzed.

Surface pressures were measured for the thicker leading edges. Pressure measurements were made on leading edge thicknesses between 1 and 43.8 thousandths of an inch. These measurements were made in two series, the first series at 0.001, 0.004, 0.007 inches leading edge thickness were made in the first nozzle at $M = 10.75$ and 11.8 and P_o of 800, 1000, and 1400 psia. The leading edges were not measured with the microscope and are not known with the same exactness as in the other tests. The second series of tests were for thicknesses between 0.0176 and 0.0438 inches and were made in the second nozzle with the use of the microscope for leading edge measurements. Mach numbers of 11.4, 12.7, and 13.8 were run at $P_o = 800, 1000, \text{ and } 1400 \text{ psia}$.

The model used for these measurements was similar to the one shown in Fig. 4, but contained pressure orifices along its top surface. Several orifices were placed off center line to check the tip effects. The tip effects were found to be negligible over the central portion of the plate. A pressure rise was found near the back of the plate which could be traced to the forward propagation of the shocks around the sting support. Only the data which were not influenced by the finite dimensions of the plate are presented. For most of the tests a square leading edge shape was used. A few of the thicker tests were run with a rounded leading edge to find the effects of the detailed leading edge shape.

Analysis

The positions of the shock waves as shown by the interferograms were read on an optical comparator. These positions, reduced by the leading edge thickness, are shown in Fig. 6. This figure shows that the thicker leading edge shock shapes correlate very well on this plot while the thinner leading edge shapes show some deviation. The difference becomes pronounced below a Re of about 4000. These measurements were made in the Mach number gradient shown in Fig. 3. No correction was made to the shock shapes

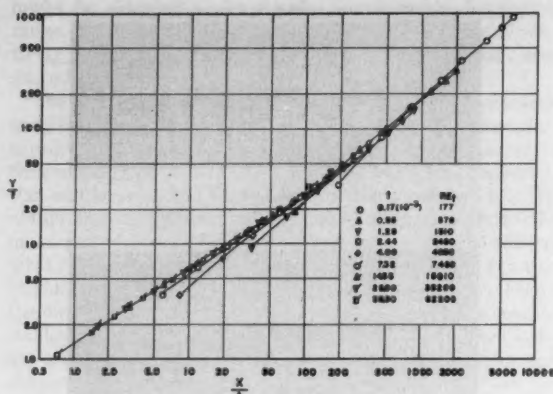


Fig. 6 Shock shapes for flow about flat plates at variable leading edge thickness

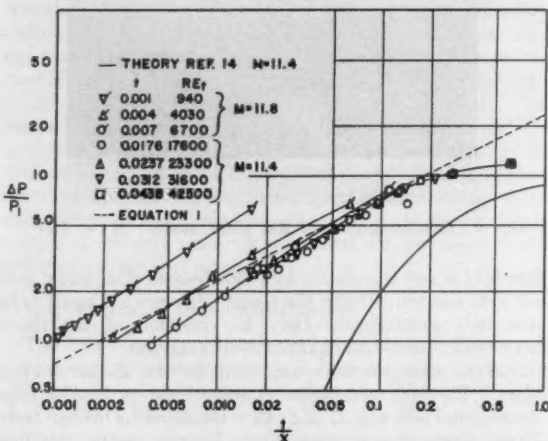


Fig. 7 Surface pressure increment for flow about a flat plate at variable Re_t

so that these should only be compared with each other and are not the shape for flow at constant Mach number. The pressure distributions have also been plotted as a function of t/x . These results have been corrected to a first order, for the Mach number gradient, by using the difference between the pressure on the plate surface and the tunnel empty static pressure at the same point. This nondimensionalized difference is plotted in Fig. 7 for $P_o = 1000$ psia and $M = 11.4$ and 11.8. Only these Mach numbers were used in this plot for the sake of clarity, but these results are typical of all the Mach numbers. No significant difference is found between the square and the round leading edge. From this figure it can be seen that all the pressure data, except for that of 0.001-in. leading edge, correlate quite well. This result could have been anticipated on the basis of the shock shape studies that showed correlation on the t/x basis down to Re_t of about 4000.

Leading edge thicknesses greater than Re_t of 4000 give a flow which is independent of Reynolds numbers. This flow is essentially inviscid and the boundary layer does not have a major influence. This conclusion is borne out by the interferograms which did not show the boundary layer for the thick leading edge, Fig. 5(c). At lower Reynolds number, this correlation no longer holds and boundary layer effects are more important. This result again checks with the interferograms which showed a pronounced boundary layer for thin leading edges, Fig. 5(a).

The shock shape and surface pressure distribution for the inviscid flow regime are caused by the interaction of the detached shock wave and expansion waves from around the

leading edge. The magnitude and downstream persistence of the leading edge effects is surprising. Maximum pressures of the order of 10 to 20 times free stream are reached at about 2 leading edge thicknesses from the leading edge followed by the pressure decreasing as $\sqrt{t/x}$ for $t/x < 0.25$. The following empirical relation has been fitted to the decreasing part of the curve.

$$\frac{\Delta p}{p_i} = 0.016 M^2 \sqrt{\frac{t}{x}} \quad (1)$$

This relation is based on the data at all Mach numbers and all P_o 's. It is shown plotted in Fig. 7.

There seems to be no available theoretical treatment of this problem. Most of the simplified techniques used to calculate hypersonic pressure distributions relate the pressure to the local slope of the body. Theories such as those based on Newtonian flow, shock plus expansion, or tangent-wedge are of this type. All such theories will predict constant pressure over the flat plate surface, so are entirely inadequate for this problem. This problem is an extension of the transonic problem to hypersonic velocities. For this reason it may be called a "tri-sonic" problem and a complete solution must involve the same considerations as the transonic problem complicated by the rotational terms introduced by the curved hypersonic shock wave.

In (14), Bertram has suggested a method for handling this problem. This approach was to use the model shown in Fig. 8. This model avoids the subsonic part of the problem by assuming an attached shock with $M = 1$ directly behind the shock. The results calculated for these assumptions are shown in Fig. 7. The numerical values and shape of the curve differ from the experiments, but at least the model predicts a varying pressure.

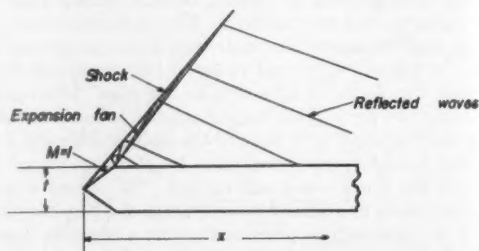


Fig. 8. Simplified flow model

A better understanding of the problem may be had by a study of the hodograph plane shown in Fig. 9 along with the same configuration on the physical plane. If the assumption is made that the flow becomes sonic just before the sharp corner, the contour A represents the flow along the solid boundary. A 90 deg expansion gives infinite Mach number for helium, so zero pressure would be expected just behind the corner. The conditions of the flow along the shock wave are given by the shock polar. The sonic point on the shock is the intersection of the shock polar and sonic circle. Some of the expansion waves from the corner will intersect the sonic line and some will intersect the shock wave. Those intersecting the sonic line will reflect as compressions, while those intersecting the shock will reflect as expansions. The limiting characteristic, the one dividing the waves which intersect the sonic line and those which intersect the shock, is given by contour B. Therefore all the waves starting before B would reflect as compressions and all beyond B as expansions. This reasoning would lead to surface pressure distribution that starts at zero behind the sharp corner, rises through the reflected compressions, and then decreases through the reflected expansions. These compressions and expansions are represented by the part of contour A along the 0 deg axis. The surface condition first moves toward the origin through

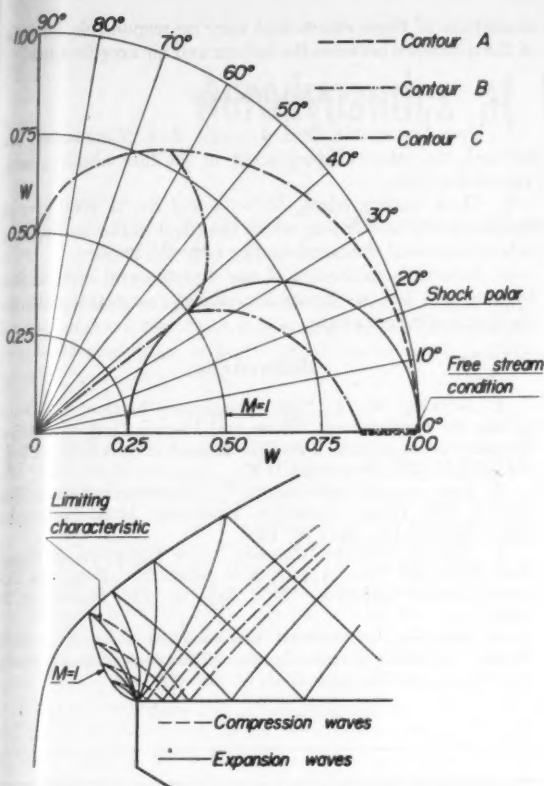


Fig. 9 Flow about a blunt flat plate in the physical hodograph plane

the compression and then away from the origin to the free stream condition. Qualitatively this agrees with the pressure measurements which show a peak value and then a decrease for high values of t/x .

It is interesting to note that the model suggested in (14) gives a considerably different picture on the hodograph plane. In this instance, the conditions on the surface are given by contour C. This model lacks the overexpansion and recompression from the sonic line found for the more correct case.

This description has neglected the vorticity of the flow behind the shock wave. The vorticity will introduce reflections of the expansion and compression waves from the vortex sheets. Therefore, Fig. 9 can be used only as a qualitative picture and an aid in understanding the flow.

Several attempts have been made to account for the effects of viscous forces near the leading edge of a sharp flat plate. All these theories—(1) to (11)—are for the case of an infinitely sharp leading edge. The general approach to this problem has been to take into account the effect on the external flow, and subsequent feedback into the boundary layer, of the change of effective body shape caused by boundary layer displacement thickness. The method used for a first approximation in (2) is relatively simple and shows the general method of attack. The boundary layer displacement thickness for free stream conditions on the surface of the plate is taken as

$$\frac{\delta^*}{x} = 2d_b \frac{M^2 \sqrt{C}}{\sqrt{Re_x}} \quad [2]$$

$$C = \frac{\mu_w/\mu_1}{T_w/T_1}$$

$$d_b = 0.865 \frac{T_w}{M_o^2} + 0.333 \left(\frac{\gamma - 1}{2} \right)$$

at Prandtl number of 1 for the adiabatic case $d_b = 0.599(\gamma - 1)$.

The slope of the boundary layer displacement thickness is

$$\frac{d\delta^*}{dx} = d_b \frac{M^2 \sqrt{C}}{\sqrt{Re_x}}$$

This slope is taken equal to the deflection of the free stream. The pressure-angle relation may now be taken from the Prandtl-Mayer or tangent-wedge relation for the free stream. Both of these relations give the same results for the first terms if expanded in series.

$$\frac{p}{p_1} = 1 + \gamma M_1^2 \frac{d\delta^*}{dx} + \dots \quad [3]$$

Substituting the relation for $d\delta^*/dx$ into Equation [3]

$$\frac{\Delta p}{p_1} = \frac{p - p_1}{p_1} = \gamma d_b \frac{M^2 \sqrt{C}}{\sqrt{Re_x}} \quad [4]$$

For the adiabatic case in helium, $\gamma = 5/3$

$$\frac{\Delta p}{p_1} = 0.599 (\gamma) (\gamma - 1) \frac{M^2 \sqrt{C}}{\sqrt{Re_x}} = 0.66 \frac{M^2 \sqrt{C}}{\sqrt{Re_x}}$$

If this expression is assumed to be correct for the infinitely thin leading edge plate, the correct expression for the finite leading edge plate must approach this solution for small Re_t and the inviscid expression for large Re_t . The simplest relation which meets these requirements is a linear combination of Equations [1] and [4].

$$\frac{\Delta p}{p_1} = 0.016 M^2 \sqrt{\frac{l}{x}} + 0.66 M^2 \sqrt{\frac{C}{Re_x}}$$

$$\frac{\Delta p}{p_1} = 0.016 M^2 \sqrt{\frac{l}{x}} \left(1 + 40 \sqrt{\frac{C}{Re_t}} \right) \quad [5]$$

This linear combination neglects the effects of the inviscid flow on the viscous flow, and vice versa. It should be expected to be fairly accurate at the two extremes where one term predominates. From this relation some idea of the relative magnitude of the two terms may be found. The value of Re_t at which both effects are equal is a function of $M(C \sim \bar{M}^{0.7})$. For Mach number of the order of 12, both effects are equal at $Re_t = 400$. All of the surface pressure measurements are at considerably higher Re_t . If the pressure data from the thinner leading edge cases, the only ones in which $\sqrt{C/Re_t}$ is significant, are reduced by the factor

$$\frac{1}{1 + 40 \sqrt{C/Re_t}}$$

and plotted against t/x , Fig. 10 results.

Fig. 10 shows that the 0.001-in. leading edge data correlate fairly well with Equation [5]. The data at 0.004 and 0.007-in. leading edge are overcorrected by Equation [5]. The viscous effect at 0.004 and 0.007-in. leading edge is overestimated

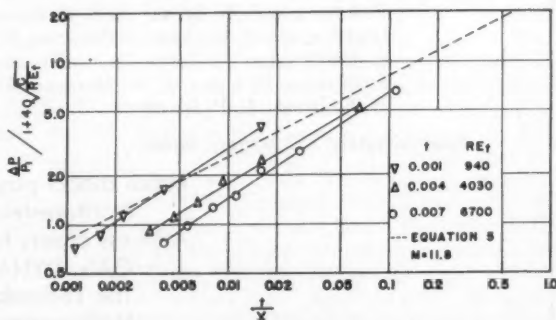


Fig. 10 Reduced surface pressure increment for flow about a flat plate at variable Re_t

by the viscous correction. This result is not unexpected since the Mach number near the surface for the thicker leading edge is much less than free stream. Therefore, the viscous theory, based on free stream Mach number, will overestimate the boundary layer buildup. The relative magnitudes of the viscous and inviscid effects are surprising. In most of the previous work on the leading edge effects on sharp bodies at hypersonic flow, the leading edge inviscid effect has not been recognized. If the Mach number dependence of C is substituted into the relation for surface pressures, the relation becomes

$$\frac{\Delta p}{p_1} = 0.016 M^2 \sqrt{\frac{t}{x}} \left(1 + \frac{1.45}{M^{0.35} \sqrt{Re_t}} \right) \dots \dots \dots [6]$$

This result indicates that the inviscid leading edge effect is the truly hypersonic one (predominant as $M \rightarrow \infty$) and the viscous effect seems to be significant at lower Mach numbers and very sharp leading edges. Because these results have only been derived from experiments over a limited range of Mach number, the accuracy of these extrapolations is open to question. However, the large effect on surface pressures of the leading edge thickness, even at distances greater than 1000 leading edge thicknesses, is most significant.

There are little other experimental data to compare with these results. Some data have been presented in (12) and (14) at Mach numbers of around 6 or 7 in air. These data appear to show much less leading edge inviscid effect than the data herein presented. This result confirms the idea that viscous effect is more important at intermediate speeds. The specific heat ratio probably has some effect on the relative

magnitude of these effects and may be responsible for some of the difference between the helium and air experiments.

Conclusions

1 Two hypersonic fluid dynamic flow phenomena, one inviscid, the other viscous, occur in the flow about a semi-infinite flat plate.

2 Thick leading edges, $M > 10$ and $Re_t > 4000$ give an essentially inviscid flow in which the effect of the leading edge is felt for several thousand leading edge thicknesses.

3 A linear combination of the experimental inviscid flow relation and viscous interaction theory correlates with the sharper leading edge data.

References

- 1 Bertram, M. H., "An Approximate Method for Determining the Displacement Effects and Viscous Drag of Laminar Boundary Layers in Two-Dimensional Hypersonic Flow," NACA TN 2773, September 1952.
- 2 Lees, L., and Probstein, R. F., "Hypersonic Viscous Flow Over a Flat Plate," Princeton University Aero. Engineering Dep., Rep. no. 195, April 20, 1952.
- 3 Lees, L., "On the Boundary Layer Equations in Hypersonic Flow and Their Approximate Solutions," Princeton University Aero. Engineering Dept. Rep. no. 212, September 20, 1952.
- 4 Lees, L., "Hypersonic Viscous Flow Over an Inclined Wedge," Reader's Forum, *Journal of the Aeronautical Sciences*, vol. 20, no. 11, November 1954, pp. 794-796.

(Continued on page 250)

Announcing the publication of the

PROCEEDINGS OF THE GAS DYNAMICS SYMPOSIUM on the theme AEROTHERMOCHEMISTRY

Held at The Technological Institute, Northwestern University
Evanston, Illinois August 1955

sponsored by the
American Rocket Society and Northwestern University
with the cooperation of the Air Research and Development Command (U.S.A.F.)

**25 original research papers on turbulent combustion, flame
stabilization, detonation, and thermodynamics, laminar flames,
and the combustion of condensed phases**

BY M. SUMMERFIELD; J. M. RICHARDSON; J. J. ZELINSKI, W. T. BAKER, L. J. MATHEWS,
E. C. BAGNALL; I. KIMURA AND S. KUMAGAI; E. E. ZUKOSKI AND F. E. MARBLE; A. A.
WESTENBERG, W. G. BERL, AND J. L. RICE; J. W. BJERKLIE; E. P. FRENCH; J. RUTKOWSKI
AND J. A. NICHOLLS; R. M. PATRICK AND A. KANTROWITZ; S. LEE AND J. F. LEE; H. N.
POWELL AND S. N. SUCIU; S. S. PENNER; E. MAYER AND H. CARUS; J. M. SINGER, J.
GRUMER, AND E. B. COOK; J. MANTON, B. B. MILLIKEN; C. F. MOZER, R. K. SHERBURNE;
L. CROCCO AND J. GREY; A. O. TISCHLER AND T. MALE; G. H. MARKSTEIN AND D.
SCHWARTZ; B. CHU; C. C. MIESSE; J. LORELL, H. WISE, R. S. CARR; S. L. SOO AND
H. K. IHRIG; G. P. WACHTELL.

Approximately 250 pages; bound

Price \$4.00

Make checks payable to:
Northwestern University

Address orders to:
GAS DYNAMICS SYMPOSIUM
The Technological Institute Library
Northwestern University
Evanston, Illinois

Aerodynamics at Very High Altitudes¹

S. A. SCHAAF²

University of California, Berkeley, Calif.

Research results in the Berkeley low density supersonic wind tunnel are described, covering a range of flow conditions corresponding to flight at altitudes up to eighty miles.

Introduction

AT VERY high altitudes, of the order of 20 miles or more, the earth's atmosphere becomes so rarefied that it no longer behaves as a continuous fluid. Proper account must be taken of the basic molecular structure of the air in the prediction of heat transfer and aerodynamic characteristics. The general field of rarefied gas dynamics, i.e., the mechanics of a gas so rarefied that mean free path effects become important, was discussed by Tsien (1).³ The terms "slip flow" and "free molecule flow" were introduced to characterize phenomena associated with moderate and extreme rarefaction respectively. A slip flow is a flow in which the mean free path is a small but not negligible fraction of the boundary layer thickness and thus corresponds to values of Mach number M and Reynolds number Re in the range $0.01 < M/\sqrt{Re} < 0.1$, since M/\sqrt{Re} is essentially the ratio of free mean path to boundary layer thickness. A free molecule flow is one in which the mean free path is large compared to the body size, and corresponds to $M/Re > 10$, i.e., to a ratio of mean free path to body dimension of approximately 10 or larger. The slip flow range would apply approximately to flight of a one-foot diameter missile, to take a specific example, at altitudes of the order to 20 to 50 miles, while free molecule flow would obtain at altitudes above 80 miles. Important applications to instrumentation occur at very much lower altitudes. The general regions of flow, together with the ranges of Mach and Reynolds covered by the various experimental programs described subsequently, are indicated in Fig 1.

Two experimental research groups—one at the Ames Laboratory of the NACA under the direction of Stalder and Goodwin, and one at Berkeley under the initial direction of Folsom and Kane—have been carrying on investigations in this area for the past nine years with particular emphasis on applications to high altitude, supersonic flight. Most of the work at Ames has been centered around problems of free molecule flow, while at Berkeley, most of the emphasis has been on the slip flow range. A fairly complete summary report, together with an extensive bibliography, of the progress of research in the field through the summer of 1952 is contained in (2). It is the purpose of this report to describe the principal results obtained at Berkeley during the period 1952-1955 which have application to high altitude aerodynamics. These investigations were carried out in the low density supersonic wind tunnel located at Berkeley and described in (2). Only those investigations which have not yet been published, or which have been published only in the form of project reports, will be discussed here. Other investigations during this period are listed in the bibliography of the present report.

Presented at the ARS 25th Anniversary Annual Meeting, Chicago, Ill., Nov. 14-16, 1955.

¹ This work was supported by the Office of Naval Research and the U. S. Air Force.

² Associate Professor of Engineering Science.

³ Numbers in parentheses indicate References at end of paper.

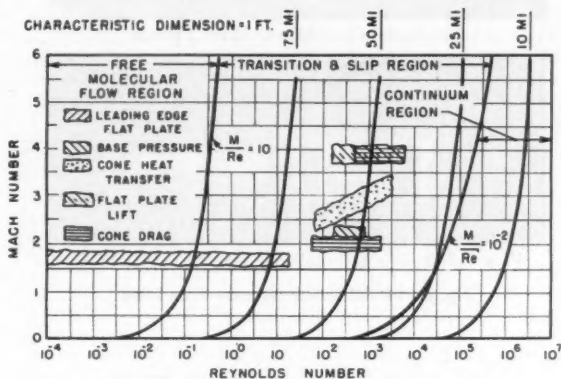


Fig. 1 Mach and Reynolds numbers covered by tests

Of these, special attention should be called to (3) and (4), which present data on the surface pressure distribution on slender cones at a Mach number of 4, and on the skin friction on flat plates at zero angle of attack over a range of Mach numbers from subsonic to 3.5.

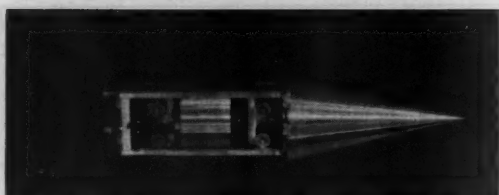
Cone Drag

In an inviscid supersonic flow, the surface pressure on a slender cone is constant, providing the Mach number is large enough to insure an attached bow shock wave. In a real viscous fluid, a boundary layer forms, which is particularly thick under the low Reynolds number conditions associated with slip flow. This boundary layer effectively increases the surface curvature of the cone, displacing the stream lines outward. It is to be expected that the surface pressure on a cone will thus be higher near the vertex and decrease along the slant surface, somewhat like the inviscid pressure distribution on an ogive.

In addition to producing a rise in the surface pressure, the thick boundary layer which forms on the surface of a cone under low density conditions also gives rise to a proportionately high skin friction. Ipsen (5, 6) has experimentally measured the total drag of the fore portion of 15 deg half-angle cones over the range $70 < Re < 1600$, $M \sim 2$; $500 < Re < 7000$, $M \sim 4$. Here M and Re are the Mach and Reynolds numbers based on the free stream flow and the cone slant length. A force-sensitive element mounted inside a 2-in. diam cone-cylinder housing was used to measure the total drag force on the floating fore portion of the cone, as indicated in Fig. 2. This total drag had components due to skin friction and also due to the surface pressure rise induced by the boundary layer. The technique did not permit separate evaluation of the two components. The results are presented in Fig. 3, in terms of the increment in the total drag coefficient over that corresponding to inviscid flow. The curves indicated in Fig. 3, are the theoretical predictions obtained by Probstein and Elliott (7), which take account of the induced effect due to the boundary layer. As will be noted, the agreement is quite good, except at the lowest Reynolds numbers where the effects of slip might be expected to begin to be of importance.



1-in. model in position in Mach 4 nozzle



View with balance removed from housing (1-in. model).

Fig. 2 Model set-up for cone-drag tests

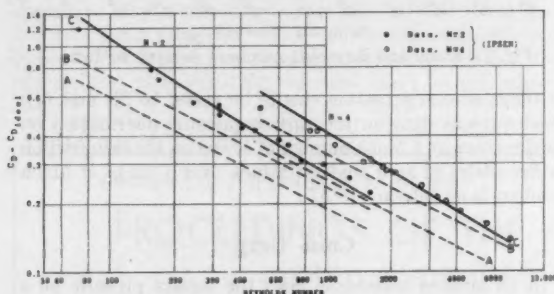


Fig. 3 Drag coefficients for cones with 15-deg semivertex angle

Flat Plate Lift

Normal forces on flat plates at angle of attack have been determined by Tellep (8). The experiments covered the range $228 < Re < 2412$, $2.42 < M < 3.69$ at angles of attack up to 8 deg. Re is the Reynolds number based on the free stream flow and on the length of the plate; M is the free stream Mach number. The results are presented in Fig. 4, in terms of a comparison with the theoretical pressure distribution to be expected on the basis of the hypersonic interaction theory of Lees and Probstein (9). It will be observed that the agreement between experiment and theory is good as regards trend, but that the theory in general underestimates the actual pres-

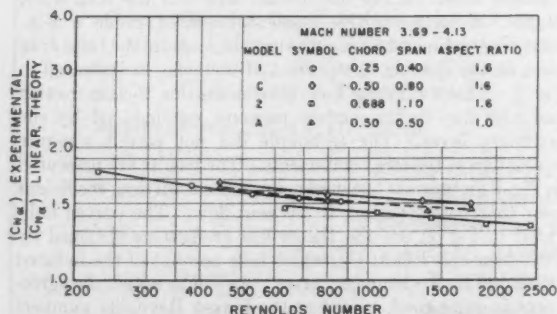


Fig. 4 Ratio of experimental normal force curve slope to theoretical normal force curve slope vs. Reynolds number

sure disturbance induced by the boundary layer. This is in accord with experiments at higher pressures conducted by Ferri (10).

As with the cone drag data of Ipsen, there is little indication of any slip effects. Both the cone and the flat plate are characterized by inviscid constant pressure distributions. To first order, therefore, the pressure gradient at the seam of the boundary layer is zero. Since the effect of slip to first order has been shown (11, 12) to be proportional to this pressure gradient, it is not surprising that slip effects are negligible for these two geometries. Experiments are now under way with a geometry for which the inviscid pressure gradient is not zero, with the expectation that slip effects will be more apparent.

Base Pressure on Cone Cylinders

The pressure on the base of typical cone-cylinder configurations in supersonic flow has been investigated in (13, 14) for the range $Re > 40,000$, where Re is the Reynolds number based on the free stream and the cone-cylinder length. Kavanau (15) has now extended these results to lower Reynolds numbers, $160 < Re < 800$, at $M \sim 2.10$ and $920 < Re < 7400$ for $M \sim 4.0$. He finds considerable variation in the pressure over the base, the pressure at the center being as much as twice as high as the pressure near the edges. His results, in terms of the area mean of the base pressure are presented in Fig. 5, together with the higher Reynolds number results indicated above. No adequate theory now exists for predicting the base pressure under these flow conditions. It is therefore difficult to determine the relative importance of slip-flow effects upon the observed values.

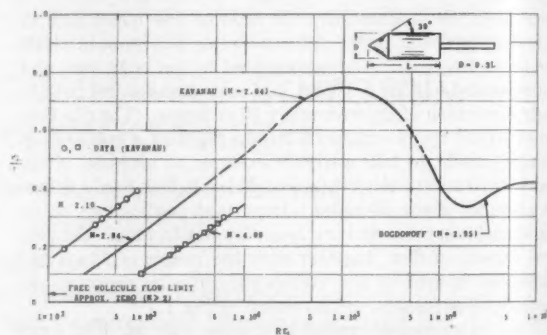


Fig. 5 Base pressure coefficient for cone-cylinder configuration

Cone Heat Transfer

The thermal characteristics of a series of cones at zero angle of attack have been determined in the slip flow range by Drake and Maslach (16). The data covered the ranges $87 < Re < 3270$, $2.16 < M < 3.54$, where M and Re are the Mach and Reynolds number based on free stream flow conditions and the cone slant length. The results are presented in Figs. 6 and 7 in terms of the recovery factor r and the Nusselt number Nu defined by

$$r = \frac{T_{eq} - T}{T_0 - T}$$

$$Nu = \frac{Q}{\rho U c_p A (T - T_{eq})}$$

where T , T_{eq} and T_0 are the stream temperature, the cone equilibrium temperature, and the adiabatic stagnation temperature, respectively, Q is the heat flux to the cone, ρ , U , and c_p free stream density, velocity and specific heat at constant pressure, and A is the cone surface area. The increase in the recovery factor with decreasing Reynolds number is interpreted as being due to the large dissipation of energy by friction.

is in
and by
indica-
are
To
of the
order
essure
le for
with
s not
more

gura-
) for
ased
anau
um-
D for
over
ce as
s of
to-
base
cult
pon

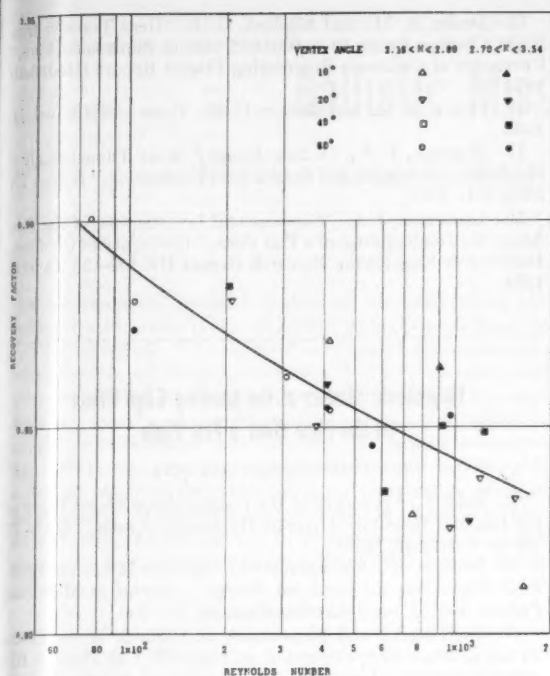


Fig. 6 Thermal recovery factors for cones in supersonic flow

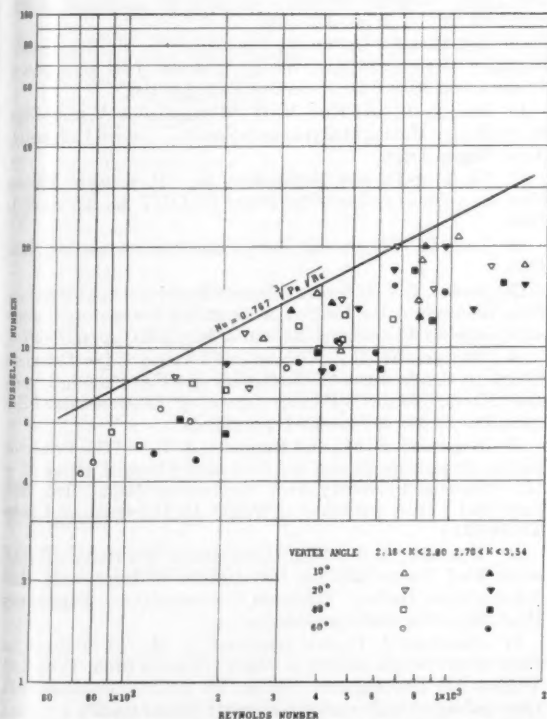


Fig. 7 Convective heat transfer coefficients for cones in supersonic flow

tion. The trend indicates a recovery factor greater than unity for somewhat lower pressures. Such values have been observed for spheres (17) and constitute an important effect for high altitude flight considerations. The heat transfer rate, on the other hand, decreases with increasing rarefaction. This is probably due to the effective thermal film resistance introduced by the temperature jump at the surface.

Survey of Boundary Layer Leading Edge Region

The thermal recovery factor of any convex body in free molecule flow is a rather sensitive function of the Mach number over the range $0.5 < M < 3.5$. The equilibrium temperature of a wire whose diameter is small compared to the mean free path and which is stretched across the test section of a wind tunnel thus depends on the Mach number and the local stagnation temperature. A "free molecule probe" of this sort has been used by Sherman (18) to determine the internal structure of a normal shock wave. The probe has been used by Laurmann (19), to explore the flow field in the immediate vicinity of a flat plate in supersonic flow. Only a qualitative picture can be obtained, since both the Mach number and the stagnation temperature vary in an interrelated way. How-

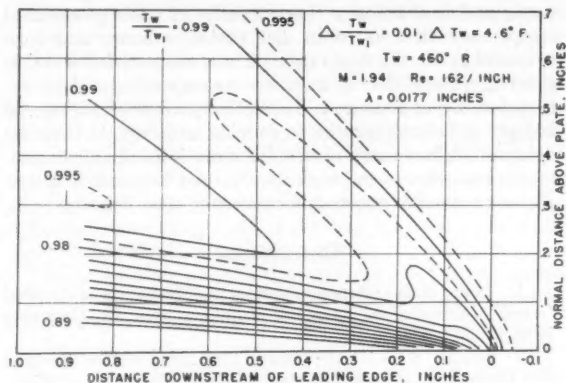


Fig. 8 Wire temperature isotherms $M \sim 2$, mean free path, $\lambda = 0.0177$ in.

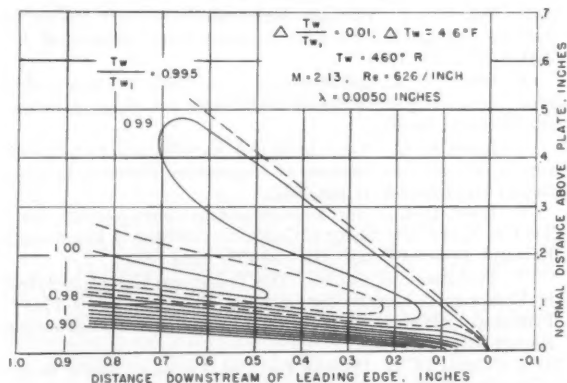


Fig. 9 Wire temperature isotherms $M \sim 2$, mean free path, $\lambda = 0.0050$ in.

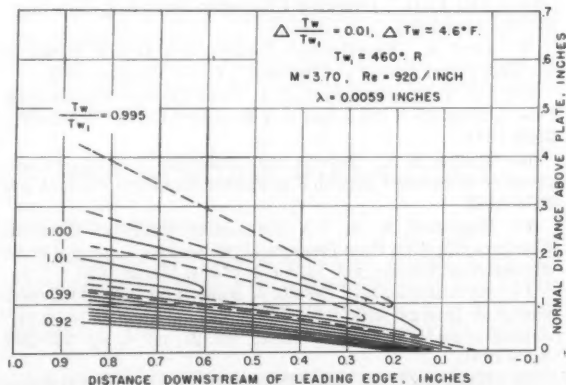


Fig. 10 Wire temperature isotherms $M \sim 4$, mean free path, $\lambda = 0.0059$ in.

ever, the general, over-all nature of the flow field can be inferred. A serious question for the hypersonic boundary layer interaction theory is the strength of the shock at the leading edge. The existence of a region of slip here could have a very great influence far downstream. The results are presented in Figs. 8, 9, and 10 in the form of contours through the flow field of constant wire temperature. These clearly show the shock and boundary layer regions. The possibility of slip at the higher Mach number is strongly suggested. These tests were carried out using "flat plates" in the form of ribbons only a small fraction of a mean free path thick. This work is now being extended to higher Mach numbers.

Conclusions

Empirical data are now available for predicting aerodynamic and heat transfer characteristics of basic geometrical components such as cones, flat plates, spheres, and cone cylinders in the slip flow range. These characteristics are, in general, quite different from the corresponding values obtained at higher pressures. Theoretical analyses, however, are not yet sufficiently precise to provide an adequate basis for determining how much of this difference is ascribable to non-continuum phenomena such as slip, and how much to low Reynolds number supersonic continuum flow behavior.

References

- 1 Tsien, H. S., "Superaerodynamics, Mechanics of Rarefied Gases," *Journal of the Aeronautical Sciences*, vol. 13, December 1946, pp. 643-664.
- 2 Schaaf, S. A., "Theoretical Considerations in Rarefied Gas Dynamics," chapter IX, Heat Transfer, University of Michigan Press, 1953, pp. 237-260. "Experimental Methods and Results in Rarefied Gas Dynamics," chapter X, Heat Transfer, University of Michigan Press, 1953, pp. 261-282.
- 3 Talbot, L., "Viscosity Corrections to Cone Probes in Rarefied Supersonic Flow at a Nominal Mach Number of 4," NACA TN 3219, 1954.
- 4 Schaaf, S. A., and Sherman, F. S., "Skin Friction in Slip Flow," *Journal of the Aeronautical Sciences*, vol. 21, no. 2, February 1954, pp. 85-90.
- 5 Ipsen, D. C., "Cone Drag in a Rarefied Gas Flow," University of California Institute of Engineering Research Projects Report HE-150-114, August 1953.
- 6 Ipsen, D. C., "New Experiments on Cone Drag in a Rarefied Gas Flow," University of California Institute of Engineering Research Projects Report HE-150-128, April 1955.
- 7 Probststein and Elliott, "The Transverse Curvature Effect in Compressible Axially Symmetrical Boundary-Layer Flow," Princeton University, Department of Aeronautical Engineering, Report 261, April 1954.
- 8 Tellep, D. M., "Lift on Flat Plates in Low Density Supersonic Flow," University of California Institute of Engineering Research Report HE-150-131, August 1955.
- 9 Lees, L., and Probststein, R. F., "Hypersonic Viscous Flow Over a Flat Plate," Princeton University Aero. Eng. Lab. Rep. no. 195, April 1952.
- 10 Ferri, A., "Experimental Results with Airfoils Tested in the High Speed Tunnel at Guidonia," NACA TM 946, 1940.
- 11 Lin, T. C., and Schaaf, S. A., "The Effect of Slip on Flow Near a Stagnation Point and in a Boundary Layer," NACA TN 2568, 1951.
- 12 Maslen, S. A., "Second Approximation to Laminar Compressible Boundary Layer on Flat Plate in Slip Flow," NACA TN 2818, 1952.
- 13 Bogdonoff, S. A., "A Preliminary Study of Reynolds Numbers Effect on Base Pressure at $M = 2.95$," *Journal of the Aeronautical Sciences*, vol. 19, no. 3, p. 201, March 1952.
- 14 Kavanau, L. L., "Results of Some Base Pressure Experiments at Intermediate Reynolds Numbers with $M = 2.84$," *Journal of the Aeronautical Sciences*, vol. 21, no. 4, pp. 257-260, April 1954.
- 15 Kavanau, L. L., "Base Pressure Studies in Rarefied Supersonic Gas Flows," University of California Engineering Project Report HE-150-125; also a Ph.D. Thesis, 1954.
- 16 Drake, R. M., and Maslach, G. J., "Heat Transfer from Right Circular Cones to a Rarefied Gas in Supersonic Flow," University of California Engineering Project Report HE-150-91, 1952.
- 17 Drake, R. M., and Backer, G. H., *Trans. ASME*, vol. 74, 1952.
- 18 Sherman, F. S., "A Low Density Wind Tunnel Study of Shock Wave Structure and Relaxation Phenomenon," NACA TN 3298, July 1955.
- 19 Laurmann, J. A., "Experimental Investigation of the Flow About the Leading Edge of a Flat Plate," University of California Institute of Engineering Research Report HE-150-126, October 1954.

Hypersonic Studies of the Leading Edge Effect on the Flow Over a Flat Plate

(Continued from page 248)

- 5 Lees, L., "Influence of the Leading Edge Shock Wave on the Laminar Boundary Layer at Hypersonic Speeds," GARCIT TR no. 1, July 15, 1954.
- 6 Shen, S. F., "An Estimate of Viscosity Effect in Hypersonic Flow Over an Insulated Wedge," *Journal of Math. and Physics*, vol. 31, no. 3, October 1952, pp. 192-205.
- 7 Li, Ting-Yi, and Nagamatsu, H., "Shock Wave Effects on the Laminar Skin Friction of an Insulated Flat Plate at Hypersonic Speeds," *Journal of the Aeronautical Sciences*, vol. 20, no. 5, May 1953, pp. 345-355.
- 8 Pai, Shih-I, "A Note on Hypersonic Viscous Flow Over a Flat Plate," Reader's Forum, *Journal of the Aeronautical Sciences*, vol. 20, no. 7, pp. 502-503.
- 9 Pai, Shih-I, "On Strong Interaction for the Hypersonic Boundary Layer on Inclined Wedge," *Journal of the Aeronautical Sciences*, vol. 20, no. 11, November 1953, pp. 796.
- 10 Pan, L. J., and Kuo, Y. H., "Compressible Viscous Flow Past a Wedge Moving at Hypersonic Speeds," Cornell University, Aero. Engng. Dept.
- 11 Li, Ting-Yi, and Nagamatsu, H., "Hypersonic Viscous Flow on a Non-Insulated Flat Plate," GARCIT no. 25, April 1, 1955.
- 12 Lees, L., "Hypersonic Flow," IAS Preprint no. 554, June 1955.
- 13 Becker, J. V., "Results in Recent Hypersonic and Unsteady Flow Research at the Langley Aeronautical Laboratory," *Journal of Applied Physics*, vol. 21, no. 7, July 1950, pp. 622-624.
- 14 Bertram, M. H., "Viscous and Leading Edge Thickness Effects on the Pressures on the Surface of a Flat Plate in Hypersonic Flows," Reader's Forum, *Journal of the Aeronautical Sciences*, vol. 21, no. 5, June 1954, pp. 430-431.
- 15 Bogdonoff, S. M., and Hammitt, A. G.: "The Princeton Helium Hypersonic Tunnel and Preliminary Results Above $M = 11$," Princeton University Aero. Engineering Dept., Rep. 260, June 1954. (Also published as Wright Air Development Center TR 54-124.)
- 16 Hammitt, A. G., "The Development of a Helium Hypersonic Wind Tunnel and the Investigation of Hypersonic Flow About Simple Bodies," Princeton University Aero. Engineering Dept. Rep. 253, January 1954.
- 17 Hammitt, A. G., and Bogdonoff, S. M., "A Study of the Flow About Simple Bodies at Mach Numbers From 11 to 15," Wright Air Development Center TR 54-257, October 1954. (Also published as Princeton University Report no. 277.)
- 18 Hammitt, A. G., Vas, I. E., and Bogdonoff, S. M., "Leading Edge Effects on the Flow Over a Flat Plate at Hypersonic Speeds," Princeton University Aero. Engineering Dept. Rep. 326, September 1955. (Also to be published as WADC TN 55-537.)
- 19 Hammitt, A. G., "A Preliminary Study of the Details of the Flow Field About a Flat Plate at Hypersonic Speeds," Princeton University Aero. Engineering Dept. Report 327, October 1955. (Also to be published as WADC TN 55-538.)
- 20 Bogdonoff, S. M., and Hammitt, A. G., "Fluid Dynamic Effects at Speeds from $M = 11$ to 15," *Journal of the Aeronautical Sciences*, vol. 23, no. 2, February 1956, pp. 108-117.

Ballistic Missile Performance¹

J. WILLIAM REECE,² R. DAVID JOSEPH,³ AND DOROTHY SHAFFER³

Cornell Aeronautical Laboratory, Inc., Buffalo, N. Y.

A semianalytic method is derived for calculating the range of one-stage, ballistic, rocket propelled, surface-to-surface missiles. The method consists of obtaining certain analytic solutions, supposing flight in vacuum, and then correcting these solutions for the effect of drag. Both the velocity at thrust cutoff and the range following cutoff are handled in this manner. An analog computer was used to compute the drag corrections and also the altitude and range at thrust cutoff for a large range of input parameters. The results are presented as working formulas and plots suitable for use in preliminary design studies of missiles having ranges of from 50 to 500 nautical miles.

Nomenclature

A	= area of cross section
a	= A/W_o
C_D	= drag coefficient based on area of cross section
C_D^*	= drag coefficient for $M = 2$
D	= drag
F	= function plotted in Fig. 5
G	= function plotted in Fig. 7
g	= acceleration due to gravity
h	= altitude
I	= τ/r = specific impulse
M	= Mach number
r	= $-(1/W_o) \cdot (dW/dt)$ = burning rate
R	= radius of the earth
t	= time
T	= thrust
V	= velocity
ΔV_D	= loss of cutoff velocity due to drag
W	= weight
X	= range after cutoff for vacuum trajectory over spherical nonrotating earth
ΔX_D	= range loss due to drag after cutoff
ψ	= angle shown in Fig. 2
θ	= flight path angle with local horizontal
ρ	= air density
τ	= W_o/W_{co}
τ	= T/W_o
ϕ	= $\cos \theta_{co} - \cos \theta_o$

Subscripts

- o refers to conditions at launching
- co refers to conditions at the end of burning

Introduction

ONE measure of the performance of a ballistic surface-to-surface missile is its maximum range with a given payload. A simple method for calculating this range has been devised. The type of missile considered is single stage and powered by a rocket motor.

The method is intended principally for use in preliminary design work. It should be of particular use in design comparison studies, economic studies, and investigation of the

Received Sept. 25, 1955. Presented at the 24th Annual Meeting of the Institute of the Aeronautical Sciences, ARS Rocket Propulsion session, New York, N. Y., January 24, 1956.

¹ This work was performed under the sponsorship of the Operations Research Office, The Johns Hopkins University.

² Engineer, Flight Research Dept.

³ Mathematician, Systems Research Dept.

trade-off between payload and range. In such applications the effect of changes in the missile parameters is of greater interest than the exact magnitude of the range itself. This calls for a simplified procedure for calculating range. In order to meet this objective, it is necessary to introduce several approximations into the work. Sufficient accuracy is to be maintained for the intended uses.

For the purpose of calculating range the missile may be described by a set of parameters. The basic parameters considered are: 1. thrust ratio, τ ; 2. mass ratio, r ; 3. specific impulse, I ; 4. area ratio, a ; 5. drag function, C_D vs. M .

The ballistic missile derives the major part of its range after thrust cutoff. For the case of trajectory in vacuum over spherical nonrotating earth, a solution in closed form is obtained for maximum range after cutoff.⁴

The range after cutoff is a function of the cutoff velocity and altitude. The dominating factor, cutoff velocity, can be solved analytically if drag is excluded.

The drag terms are not susceptible to analytic treatment. This difficulty was overcome by using an analog computer. The computer also provided cutoff altitude and range.

The ballistic trajectory following cutoff is considered first, in order to establish a certain boundary condition needed for programming the burning phase, which is the flight path angle at cutoff.

Assumptions

The following principal assumptions are made:

- 1 The earth is spherical and nonrotating.
- 2 Launching and impact are at sea level.
- 3 The missile follows a particle trajectory.
- 4 Thrust and burning rate are constant.
- 5 The missile is launched vertically, and during the burning phase $d\theta/dt = \text{const}$.
- 6 The drag corrections are small compared with the quantities to which they are applied.
- 7 Earth curvature may be ignored during the burning phase and also in obtaining the drag correction to range after cutoff.

Thrust and specific impulse, connected through the relation $I = \tau/r$, are to be represented by chosen mean values in recognition of the fact that rocket thrust varies somewhat with altitude. Any secondary propellants must be accounted for in τ , the total discharge rate, and consequently in the specific impulse as defined here.

Ballistic Trajectory Following Cutoff

Trajectory and Range

The vacuum trajectory of an object moving within the gravitational field of spherical nonrotating earth, and having less than the energy required for escape, is a Keplerian ellipse (3).⁵ One of the foci of the ellipse is at the center of

⁴ It has been brought to the attention of the authors that similar solutions have been obtained (1, 2) for the limiting condition $h_{co} = 0$.

⁵ Numbers in parentheses indicate References at end of paper.

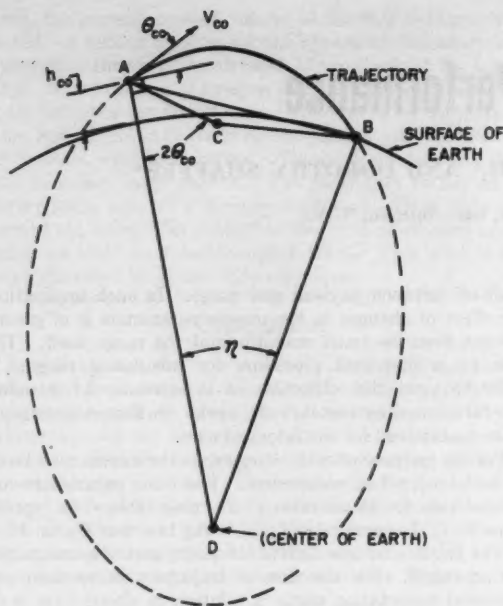


Fig. 1 Vacuum trajectory over spherical earth. Ellipse with foci at C and D

the earth (see Fig. 1). The length of the majorax is L is given by

$$L = \frac{gR^2}{gR - [1/2 V_{co}^2 + gh_{co}/(1 + h_{co}/R)]} \dots\dots\dots [1]$$

$$= \frac{R + h_{co}}{1 - (1 + h_{co}/R)V_{co}^2/2gR}$$

Let it be assigned to maximize the range following cutoff, $X = R\eta$, for particular values of V_{co} and h_{co} . This range is a maximum when the length AB (Fig. 1) is maximized. The sum of the focal radii AC and CB is given by

$$AC + CB = 2L - 2R - h_{co} \dots\dots\dots [2]$$

which is fixed for chosen values of V_{co} and h_{co} . This being so, the length AB is obviously a maximum when the second focus C lies on a line joining points A and B.

The three sides of the triangle ABD are now known for the condition of maximum range, and from the cosine law the angle η_{max} can be solved. The resulting equation can be written in the form

$$\eta_{max} = 2 \sin^{-1} \frac{c}{1 - c} \sqrt{1 + h_{co}/cR} \dots\dots\dots [3]$$

in which

$$c = \frac{V_{co}^2}{2gR} \left(1 + \frac{h_{co}}{R} \right) \dots\dots\dots [4]$$

Flight Path Angle at Cutoff

Through use of the property that the focal radii intersecting at a point on an ellipse make equal angles with the tangent at that point, it can be demonstrated that the angle DAC, Fig. 1, is equal to $2\theta_{co}$. The cosine law may be applied to the angle DAB to provide a solution for the optimum value of θ_{co} ; that is, the value that maximizes range for given V_{co} and h_{co} . The solution yields

$$\theta_{coopt} = \sin^{-1} \sqrt{\frac{c}{1 - c} \left[\frac{1 - c(2 + h_{co}/R)}{h_{co}/R + c(2 + h_{co}/R)} \right]} \dots\dots [5]$$

Approximations

For ranges not exceeding 500 nautical miles, $\eta/2 < 5$ deg, so that with sufficient accuracy, $\sin \eta/2 = \eta/2$ may be used to simplify Equation [3]. The maximum range following cutoff, for trajectory in vacuum, is then given with good accuracy by

$$X = \frac{2cR}{1 - c} \sqrt{1 + h_{co}/cR} \dots\dots\dots [6]$$

Furthermore, since $h_{co}/R \ll 1$, this term may be neglected in Equation [4] if desired.

Equation [5] may be approximated upon expanding the equation and ignoring terms of the order c^2 , $c(h_{co}/R)$, $(h_{co}/R)^2$ and higher. Then, since $h_{co}/R \ll 1$, c is replaced by $V_{co}^2/2gR$, with the result

$$\sin^2 \theta_{coopt} \approx \frac{1}{2} \left(1 - \frac{V_{co}^2}{2gR} - \frac{gh_{co}}{V_{co}^2} \right) \dots\dots\dots [7]$$

Equation [7] may be compared with the expansion of $\sin^2 \theta$ about $\pi/4$, retaining only the first order terms in the expansion, and it is seen that

$$\theta_{coopt} \approx \frac{\pi}{4} - \frac{V_{co}^2}{4gR} - \frac{gh_{co}}{2V_{co}^2} \dots\dots\dots [8]$$

An alternative form is as follows

$$\theta_{coopt} \approx \frac{\pi}{4} - \frac{X}{4R} - \frac{h_{co}}{2X} \dots\dots\dots [9]$$

These last equations put the desired cutoff angle at something less than 45 deg. In the cases covered by the work that follows it would fall between 39 deg and 43 deg. To facilitate the burning phase analysis a cutoff angle of 41 deg was chosen to handle all cases.

The remainder of the work will be directed toward the calculation of a sensible maximum total range. The calculation of a true maximum would involve extensive burning phase analysis plus the use of variational techniques. Such detailed analysis is not in line with, and would not contribute significantly to, the present objective.

The range X is to be calculated from Equation [6] regardless of the fact that the burning phase is assumed to be terminated in all cases at a flight path angle of 41 deg. If the total range is near maximum, the combined range-producing potential of V_{co} , h_{co} , and X_{co} is insensitive to minor changes in the burning phase history. An example of this statement can be seen in Fig. 2, which is discussed in the next section.

Burning Phase Trajectory

Programming

Since ballistic missiles are being dealt with, one would be inclined to assume a gravity turn path for the burning phase. However, this would complicate the analysis. For every set of missile parameters several trials would have to be made, each time varying the initial launch angle, in order to arrive at the prescribed boundary condition on flight path angle at cutoff. It was necessary to avoid this.

Instead, the missile is considered to be launched vertically, and caused to turn at a constant rate during the burning phase. The effect of this programming was checked against a maximum range gravity turn trajectory. The result, shown in Fig. 2, was obtained with an analog computer. Since the difference in range could not even be detected, the chosen programming is evidently a good compromise in so far as it simplifies the analysis.

It is intended that the total range to be calculated in the present method be understood to be essentially the maximum range of a missile following a zero lift, or ballistic, trajectory throughout flight.

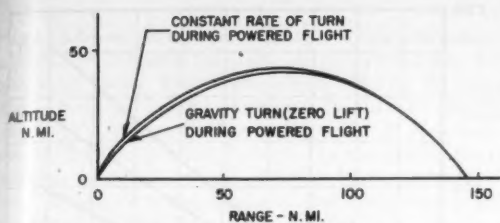


Fig. 2 Comparison of trajectories having different programming during powered flight

Cutoff Velocity

The cutoff velocity is obtained upon integrating the equation of motion over the time of burning. The equation of motion in the direction of flight is

$$T - D - W \sin \theta = (W/g)(dV/dt) \dots \dots \dots [10]$$

Under the assumptions that thrust, burning rate, and rate of turn are constant, the integration furnishes a formula for the cutoff velocity.

$$V_{co} = \frac{gT}{rW_o} \log \frac{W_o}{W_{co}} - \frac{\cos \theta_{co} - \cos \theta_o}{\theta_o - \theta_{co}} g t_{co} - \int_0^{t_{co}} \frac{g D dt}{W_o(1 - rt)} \dots \dots \dots [11]$$

$$= gI \log v - g\phi t_{co} - \Delta V_D \dots \dots \dots [12]$$

The burning time is obtained from

$$t_{co} = \frac{I}{\tau} \left(1 - \frac{1}{v} \right) \dots \dots \dots [13]$$

Computer Operations

The unsolved term in the equation for cutoff velocity must be solved. The cutoff range and altitude must be calculated. Finally, a correction for air resistance must be applied to the range after cutoff.

This was all done with the aid of an analog computer. The computer was wired to solve the complete trajectory of a ballistic missile in the presence of the earth's atmosphere. The curvature of the earth was neglected. The atmospheric functions, speed of sound and air density, were approximated as analytic functions of altitude, so that they could be generated using ordinary machine components.

The air density was represented by two third-degree polynomials in altitude. These were obtained as a least-squares fit to data for the NACA Standard Atmosphere. The first polynomial supplied the atmospheric density ratio from sea level to 100,000 ft. At 100,000 ft the second polynomial was switched in, supplying the density ratio between 100,000 ft and 200,000 ft. Above 200,000 ft the density was assumed zero.

The speed of sound was approximated as decreasing linearly with altitude, from a value of 1116 ft/sec at sea level to a value of 972 ft/sec at 35,000 ft above which it was assumed to remain constant.

Drag Function

A drag curve made up of analytic elements, as shown in Fig. 3, was assumed. This curve is believed to be a reasonable approximation to the typical drag curve of a cylindrical body with pointed nose and stabilizing fins.

Despite the arbitrarily assumed burning phase programming, neither lift forces nor drag due to lift were considered in the analog computer operations. Reasons for this were covered in the discussion of Fig. 2. The drag was computed through the equation

$$D = C_D^{1/2} \rho V^2 A \dots \dots \dots [14]$$

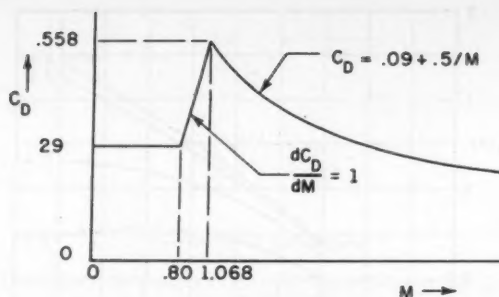


Fig. 3 Assumed variation of drag coefficient with Mach number

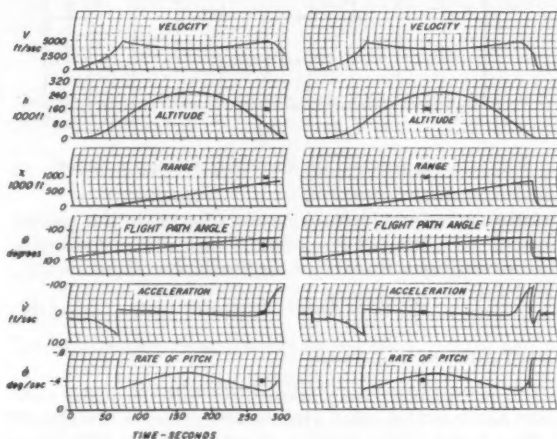


Fig. 4 Hand calculation (left) and REAC calculation (right) for flat earth performance of a hypothetical one-stage missile having the characteristics: $I = 235$ sec; $v = 2.71$; $\tau = 2.12$; $\alpha = 0.00082$ ft.²/lb.; C_D vs. M from Fig. 3.

As a check on the operations of the computer, Fig. 4 presents for comparison the results of an analog computer calculation and a hand calculation made using the same input parameters.

Parameter Bounds

Using the analog computer, a large number of runs were made covering the burning phase. The parameters that were varied, and their bounds, are

Thrust ratio	$1.5 \leq \tau \leq 4.0$
Mass ratio	$2.0 \leq v \leq 4.8$
Specific impulse	$200 \leq I \leq 235$ sec
Area ratio	$0.0005 \leq a \leq 0.0015$ ft ² /lb

Burning Phase Drag

The unsolved term, ΔV_D , in Equation [12], which is the decrease of cutoff velocity due to drag, is given by

$$\Delta V_D = \int_0^{t_{co}} \frac{g a C_D^{1/2} \rho V^2}{1 - rt} dt \dots \dots \dots [15]$$

The integral in Equation [15] was computed over a wide range of parameters. Function F , defined by

$$F = \frac{1}{C_D^*} \int_0^{t_{co}} \frac{g C_D^{1/2} \rho V^2}{1 - rt} dt \dots \dots \dots [16]$$

in which C_D^* is the drag coefficient for a Mach number of 2.0, can be plotted as a function of thrust ratio τ and mass ratio v alone, since the calculated results were found to be insensitive to changes in the remaining parameters. The C_D^* behaves as a mean value of drag coefficient, which was the desired effect.

The plot for function F is shown in Fig. 5. This and the re-

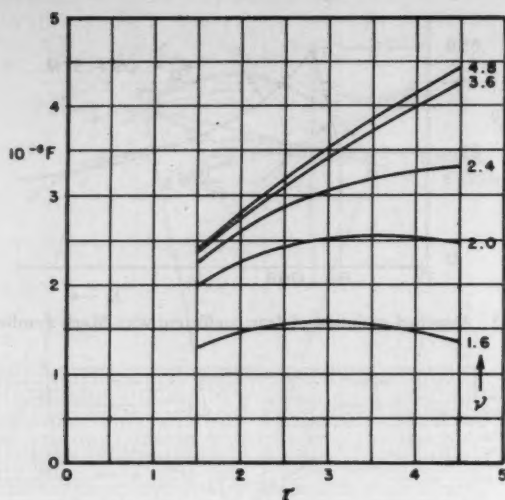


Fig. 5 Drag function for correcting velocity at cutoff

maining figures provide working plots for use in the present method. The value of F obtained from Fig. 5 is inserted in the following equation to solve the final term in Equation [12].

$$\Delta V_D \text{ (ft/sec)} = a C_D^* F \dots \dots \dots [17]$$

Cutoff Altitude and Range

The burning phase calculations made with the analog computer also provided cutoff altitude and range, shown plotted in Figs. 6 and 7 as a function of cutoff velocity for various

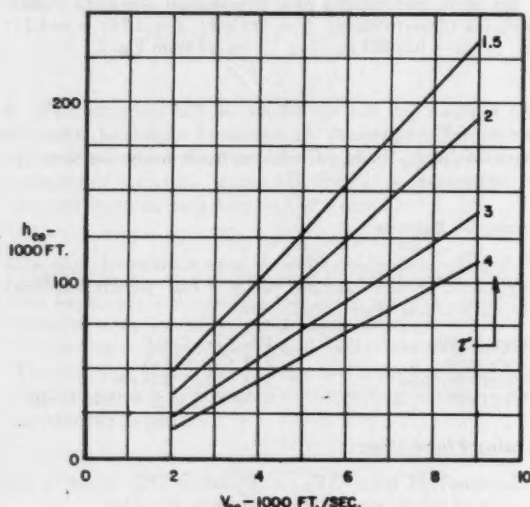


Fig. 6 Altitude at cutoff

values of parameter r . The plotted data were observed to be insensitive to changes of parameters ν and a . A further dependence of h_{co} and X_{co} on specific impulse is not reported in the plots, because of its rather small consequence. An approximate correction based on the original plotted data may be applied to the values of h_{co} and X_{co} read from Figs. 6 and 7, through the formula $\Delta h_{co}/h_{co} = \Delta X_{co}/X_{co} = 0.8 \Delta I/I_e$, in which $I_e \equiv 220$ sec.

Drag After Cutoff

It remains to correct the range following cutoff for the effect of air resistance. This was also done using the analog

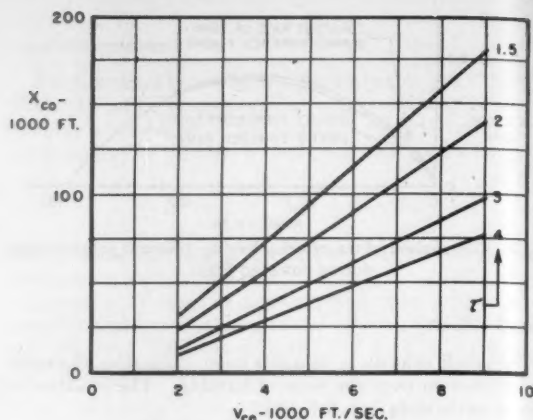


Fig. 7 Range at cutoff

computer. A method somewhat similar to that handling burning phase drag was employed. The range was computed, both in atmosphere and in vacuum, for a number of combinations of cutoff velocity and altitude, and three values of area-to-cutoff weight ratio, νa . It was observed that the difference between these range computations, which is the loss of range due to air resistance after cutoff, is proportional to νa . A further factor, drag coefficient just after cutoff, C_{Dco} , is introduced. The reason for this particular choice of drag coefficient is that the drag losses immediately following cutoff account for the greater part of the range reduction.

Function G was calculated through an inversion of the equation

$$\Delta X_D \text{ (ft)} = \nu a C_{Dco} G \dots \dots \dots [18]$$

and then plotted as shown in Fig. 8. The range correction can

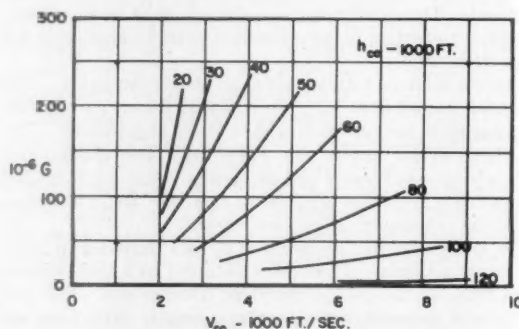


Fig. 8 Drag function for correcting range after cutoff

now be reconstructed upon inserting into Equation [18] the value of G obtained from Fig. 8. In determining C_D^* and C_{Dco} , account may be taken of any change in drag due to the application or termination of thrust.

Application and Evaluation

Parameter Flexibility

The range of specific impulse values admissible under this method is somewhat wider than the bounds that were shown above. The reason is that the primary effect of specific impulse is handled explicitly in the propulsion term of Equation [12]; secondary effects are unimportant.

There is also reason to believe that the procedure for handling drag permits the use of drag functions differing in detail from the curve shown in Fig. 3. This is found in the results of the burning phase calculations using various values

of the area-to-weight ratio, a . Changes in this area parameter cause similar changes in the drag. As the over-all drag level is changed, it causes the burning-phase histories of velocity, altitude, and thus dynamic pressure to be altered. The effect is similar to distorting the drag curve itself. It was observed, however, that the function F , needed to reconstruct the drag correction to cutoff velocity, remained insensitive to this effect. This leads to the conclusion that moderate changes in the shape of the drag curve can be tolerated.

Range Limits

At decreasing ranges the effect of drag rises in relative importance. If the major part of the drag loss occurs at transonic or especially subsonic speeds, the method as presently constituted cannot accurately predict the drag effects. For this reason caution should be used in applying this method to the calculation of ranges less than 50 miles.

For ranges exceeding 500 miles, the optimum cutoff angle begins to swing too far below 41 deg for the present results to be valid.

Accuracy

The original data have been examined to provide an idea of the accuracy of the method. Within the parameter bounds previously tabulated it is estimated that the errors contained in the values read from Figs. 5 to 8 will seldom exceed the following:

Function F , Fig. 5	$\pm 0.25 \times 10^6$ units error
h_{co} , Fig. 6	$\pm 5\%$ error (when corrected for I)
X_{co} , Fig. 7	$\pm 5\%$ error (when corrected for I)
Function G , Fig. 8	$\pm 10\%$ error

It is estimated that use of C_D^* as directed will not usually result in an error in excess of ± 10 per cent for drag curves other than that assumed here.

The total range is affected directly by errors in X_{co} and ΔX_D . The effect on range of errors in V_{co} and h_{co} can be determined by writing the first order approximation for Equation [6]

$$X \approx \frac{V_{co}^2}{g} + h_{co} \dots \dots \dots [19]$$

from which

$$dX = 2(V_{co}/g)dV_{co} + dh_{co} \dots \dots \dots [20]$$

The error in h_{co} thus produces an equal error in range, while the range error produced by error in V_{co} is $2V_{co}/g$ times the error in V_{co} .

Calculation Procedure

In making use of the present method the parameters τ , ν , I , a , and the function C_D vs. M must be known. The steps in calculating range are:

- 1 Calculation of velocity at thrust cutoff:

$$V_{co} \text{ (ft/sec)} = 32.2I \log \nu - 28.4 \frac{I}{\tau} \left(1 - \frac{1}{\nu} \right) - aC_D^*F \dots \dots [21]$$

- 2 Determination of altitude and range at cutoff. The values read from Figs. 6 and 7 can be rendered more accurate by correcting them for specific impulse, as previously noted.

- 3 Summation of the components of the range:

$$\text{total range} = X_{co} + \frac{2cR}{1-c} \sqrt{1 + h_{co}/cR} - \nu a C_{Dco} G \dots [22]$$

in which

$$c = \frac{V_{co}^2}{2gR} \left(1 + \frac{h_{co}}{R} \right)$$

Numerical Example

The hypothetical missile for which the parameters are given in Fig. 4 may be used to illustrate the application of the method. From Fig. 3, $C_D^* = 0.34$; and from Fig. 5, $F = 2.75 \times 10^6$. The cutoff velocity is now solved using Equation [21]:

$$V_{co} = 4780 \text{ ft/sec}$$

Using Figs. 6 and 7, and making corrections for specific impulse:

$$\begin{aligned} h_{co} &= 99,000 \text{ ft} \\ X_{co} &= 72,000 \text{ ft} \end{aligned}$$

The Mach number at cutoff is $4780/972 = 4.9$. Figs. 3 and 8 are entered to find $C_{Dco} = 0.19$; $G = 28 \times 10^6$.

Before calculating the range, the function c must be solved:

$$2cR = 714,000 \text{ ft}; \quad c = 0.0170$$

The total range is found from Equation [22]:

$$\text{Total range} = 882,000 \text{ ft or } 145 \text{ n.mi.}$$

The optimum value of flight path angle at cutoff is, from Equation [8], 41.0 deg.

The hand calculations for the performance of this missile yielded the following results:

$$\begin{aligned} V_{co} &= 4800 \text{ ft/sec} \\ h_{co} &= 100,800 \text{ ft} \\ X_{co} &= 69,400 \text{ ft} \end{aligned}$$

$$\text{Total range} = 146 \text{ n.mi. (corrected for earth curvature)}$$

The maximum expected errors in the example worked out above are as follows: V_{co} , 70 ft/sec; h_{co} , 5000 ft; X_{co} , 3600 ft; ΔX_D , 1200 ft. The range error produced by the 70 ft/sec error in V_{co} is 20,800 ft, which is here by far the most important error.

Under the conservative assumption that the errors in h_{co} and X_{co} are mutually consistent, the maximum expected total range error for the example, taken as the rms sum of 8600, 1200, and 20,800 ft, comes to 22,500 ft or 3.7 n.mi. Had an allowance for 10 per cent error in C_D^* been made to provide for different drag characteristics, the error in V_{co} would be $\sqrt{(70)^2 + (77)^2} = 104$ ft/sec, and the total expected range error would be increased to 5.3 n.mi.

References

- 1 Ivey, Bowen, and Oborny, "Introduction to the Problem of Rocket-Powered Aircraft Performance," NACA TN 1401, 1947.
- 2 G. A. Crocco, "La Barriera della Temperatura nei Missili Geodetici," *Atti della Accademia dei Lincei, Rendiconti di Scienze Fisiche, Matematiche e Naturali*, vol. X, Feb. 1951.
- 3 J. H. Jeans, "Theoretical Mechanics," Ginn and Co., Boston, 1935, p. 277.

Effect of Chemical Reactions in the Boundary Layer on Convective Heat Transfer¹

DAVID ALTMAN² and HENRY WISE³

Jet Propulsion Laboratory, California Institute of Technology, Pasadena, Calif.

An analysis is made of the relative change in heat-transfer rate resulting from chemical reactions in the boundary layer for either turbulent or laminar flow. Consideration is given to reactions both in the gas phase and on the wall. It is shown that, for gas phase reactions, if $D = \kappa$ (where D is molecular diffusivity and κ thermal diffusivity) or if reaction occurs in which both D and κ are much less than ϵ (the turbulent-exchange coefficient), the relative change in heat flux is given merely in terms of thermodynamic properties alone. For this case, the use of a "nondissociated" temperature representing the total enthalpy of the system is found to be useful.

Nomenclature

c	= isobaric specific heat
C	= isobaric molar heat capacity
D	= molecular diffusivity
F	= molar reaction rate per unit area of surface
M	= molecular weight
n	= molar concentration
N	= mole fraction
Pr	= Prandtl number
q	= heat flux per unit area
Q	= heat of reaction per mole of diffusing species ($-\Delta H$ of reaction)
\mathcal{R}	= molar reaction rate per unit volume
R	= universal gas constant
Sc	= Schmidt number
T	= temperature
y	= coordinate of heat flow
y^*	= dimensionless distance parameter = $(y/\nu)\sqrt{\tau/\rho}$
Z	= rate of molecular collisions per unit surface
α	= accommodation coefficient for surface reaction (cf. Eq. 14)
β	= dimensionless constant (cf. Eq. 15)
ϵ	= turbulent-exchange coefficient
κ	= thermal diffusivity
λ	= thermal conductivity
μ	= viscosity
ν	= kinematic viscosity
ρ	= density
τ	= shear stress
$()_0$	= wall ($y = 0$)
$()_1$	= edge of laminar sublayer ($y^* = 5$)
$()_2$	= outer edge of intermediate layer ($y^* = 30$)
$()_e$	= property including turbulent contribution
$()_i$	= diffusing species
$()_m$	= log mean of property in film
$()'$	= condition without chemical reaction
$(-)$	= average property in boundary layer
$()^0$	= fictitious free-stream property calculated in the absence of chemical dissociation

Received December 20, 1955.

¹ This paper presents the results of one phase of research carried out at Jet Propulsion Laboratory, California Institute of Technology, under Contract No. DA-04-495-Ord 18, sponsored by the Department of the Army, Ordnance Corps.

² Chief, Chemistry and Physics Section.

³ Present address: Stanford Research Institute.

⁴ Numbers in parentheses indicate References at end of paper.

I Introduction

IN THE combustion processes which yield a high concentration of chemically active species such as free radicals and atoms, the heat transfer between the free stream and the wall may be significantly altered by chemical reaction within the system. A simplified analysis is given of the relative change in heat flux from a hot moving gas stream to a cooled surface as a result of chemical reactions in the boundary layer and on the wall.

The assumptions and approximations incorporated in this treatment are as follows: (a) The gradients of the quantities considered along the flow line parallel to the wall are negligible with respect to gradients normal to the wall (y direction). (b) The coefficients of turbulent exchange for viscosity, diffusivity, and conductivity (eddy quantities) are equal. (c) The boundary layer thickness does not change significantly as a result of heat release; i.e., the Prandtl and Schmidt numbers remain essentially constant (1) and (2).⁴ (d) Steady state has been established, and pressure is uniform within the system. (e) The mole fraction of reactive species is low if more than one such species is considered. (f) The cold-wall temperature T_0 is fixed at a relatively low value by coolant flow. (g) Thermal diffusion of species is neglected. For species of equivalent molecular weight, this effect is known to be small. In the case of species with molecular weight much different from that of the mixture (such as H atoms) the inclusion of thermal diffusion would still act only as a correction in the present case and is therefore neglected to the degree of approximation employed in this paper. (h) Radiation effects are not considered.

II Derivation of Equations

Using von Kármán's treatment of the analogy between fluid friction and heat transfer (3), it is assumed that the boundary layer contains a laminar sublayer of thickness $y^* = 5$ and an intermediate layer (buffer layer) in the interval $5 < y^* < 30$. In the sublayer, the transport properties are given solely by the molecular quantities $\nu = \mu/\rho$, $\kappa = \lambda/c\rho$, and D . In the intermediate region, these quantities increase linearly with distance as a result of turbulence. The coefficient of turbulent exchange ϵ (3), also called exchange coefficient (4), represents the turbulent contribution to the transport quantities ν , κ , and D (Fig. 1). If the effective transport parameters are denoted by $\kappa_e = \kappa + \epsilon$ and $D_e = D + \epsilon$ to represent appropriate values in boundary layer, the conservation equations for heat and mass may be written as follows

$$\frac{d}{dy} \left(c\rho\kappa_e \frac{dT}{dy} \right) + Q\mathcal{R} = 0 \dots \dots \dots [1]$$

$$\frac{d}{dy} \left(\frac{D_e n}{1 - N_i} \frac{dN_i}{dy} \right) - \mathcal{R} = 0 \dots \dots \dots [2]$$

where Q is the heat released in the recombination of 1 mole of the labile species ($-\Delta H$ of reaction), \mathcal{R} is the reaction rate expressed in moles per unit volume per sec, ρ is the density, n

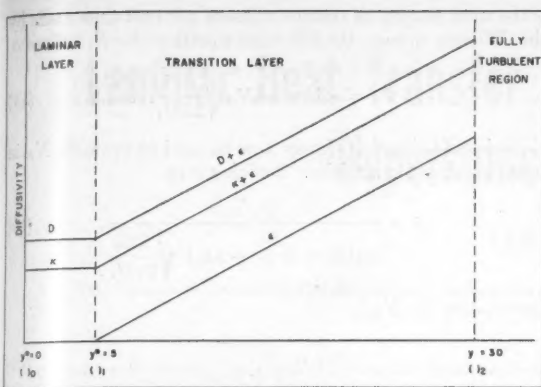


Fig. 1 Variation of exchange coefficient and effective diffusivities in the boundary layer

is the molar density, and N_i is the mole fraction of free radical. Elimination of α between Equations [1] and [2] results in

$$\frac{d}{dy} \left(c\rho\kappa \frac{dT}{dy} \right) + Q \frac{d}{dy} \left(\frac{D_i n}{1 - N_i} \frac{dN_i}{dy} \right) = 0 \dots [3]$$

Since the heat of reaction Q is essentially constant, a first integral of Equation [3] between the limits $y = 0$ and $y = y$, gives directly the heat-transfer rate per unit area of wall surface

$$q = c\rho\kappa \frac{dT}{dy} + \frac{Q D_i n}{1 - N_i} \frac{dN_i}{dy} \dots [4]$$

Division by $c\rho\kappa$ and integration between $y = 0$ and $y = y_2$ corresponding, respectively, to $T = T_0$ and $T = T_2$ and to $N_i = N_{i0}$ and $N_i = N_{i2}$ (cf. Fig. 1) yields

$$q \int_0^{y_2} \frac{dy}{c\rho\kappa} = T_2 - T_0 + Q \int_{N_{i0}}^{N_{i2}} \frac{D_i}{(1 - N_i) C \kappa} dN_i \dots [5]$$

where $c\rho/n = C$ is the average molar isobaric heat capacity of the gas mixture. If no chemical recombination occurs, Equation [5] reduces to the following equation, in which the primes denote appropriate values subject to the initial assumption of constant T_2 and T_0

$$q' \int_0^{y_2} \frac{dy}{c\rho\kappa} = T_2 - T_0 \dots [5']$$

Since, as was stated in Section I, chemical heat sources have only a small effect on the Prandtl number (2), the boundary layer thickness y_2' may be taken to be the same as y_2 . Furthermore, since the temperature limits over the boundary layer are the same, the integrals on the left-hand side of Equations [5] and [5'] may be equated within a reasonable approximation. The ratio of heat flux with and without recombination for identical boundary conditions in temperature is therefore

$$\frac{q}{q'} = 1 + \frac{Q}{T_2 - T_0} \int_{N_{i0}}^{N_{i2}} \frac{D_i + \epsilon}{(1 - N_i) C (\kappa + \epsilon)} dN_i \dots [6]$$

If more than one recombining species exists and if their combined mole fraction is low, Equation [6] can be easily generalized by summation of all the species i which react as follows

$$\frac{q}{q'} = 1 + \frac{1}{T_2 - T_0} \sum_{i=1}^j Q_i \int_{N_{i0}}^{N_{i2}} \frac{D_i + \epsilon}{(1 - N_i) C (\kappa + \epsilon)} dN_i \dots [6']$$

where $i = 1, 2, 3, \dots, j$. D_i is assumed to be an appropriate binary diffusion coefficient in the mixture.⁵ In the three cases of Equation [6] that follow, it is assumed that this generalization can be made.

A Reaction in Boundary Layer Where $D_i = \kappa_i$

In this first case a simplified expression for the relative change in heat flux is obtained if either of the following two conditions is satisfied:

1 $D = \kappa$ with reaction occurring anywhere in the entire boundary layer.

2 Reaction occurring only in the hot portion of the intermediate layer where D and κ are much less than ϵ .

In either case, Equation [6] can be integrated directly to yield

$$\frac{q}{q'} = 1 + \frac{Q(N_{i2} - N_{i0})}{N_m \bar{C}(T_2 - T_0)} \dots [7]$$

where N_m is the log-mean mole fraction of the remaining species. For the recombination of various labile species of low mole fraction

$$\frac{q}{q'} = 1 + \frac{\sum Q_i (N_{i2} - N_{i0}) / (1 - N_{im})}{\bar{C}(T_2 - T_0)} \dots [7']$$

where \bar{C} ($= \bar{c}M$) is the average molar heat capacity of the gas mixture in the temperature range of recombination.⁶ It is interesting that, in this case, the increase in heat transfer is no longer dependent on the transport properties but only on the ratio of recombination heat to sensible heat. Although N_{i2} and T_2 do not refer exactly to free-stream properties, such an identification can be made since, if the conditions of this first case hold, $D_i = \kappa_i$ beyond y_2 , and integration of Equation [6] can be made into the free stream.

If the recombination rate is fast, chemical equilibrium is closely approached in the boundary layer. Since the recombination heats for most of the free radicals are usually high (some 50 kcal/mole and higher), it follows that recombination occurs largely in the high-temperature region of the intermediate layer where $\epsilon \gg \kappa$. This condition is probably approached for many reactions at high flame temperatures. If T_0 is 1000 K or so less than T_2 , it is generally a good approximation to set N_{i0} equal to zero if chemical equilibrium is maintained, whereas N_{i2} and T_2 may be identified with equilibrium flame conditions. However, it is important to note that, regardless of whether or not chemical equilibrium is followed in the diffusion process, Equation [7] or [7'] is applicable. Hence the increase in heat transfer is independent of the manner or location of heat release except for the minor change of the molar heat capacity \bar{C} , which is averaged over the temperature range of chemical recombination.

Another simplification of Equation [7'] proves of practical utility for the case where N_{i0} is negligible. If T_2^0 denotes the calculated flame temperature for a combustion reaction where the products are assumed to be only those stable at ambient temperatures (i.e., CO_2 , H_2O , H_2 , CO , N_2 , etc.), then the energy-balance equation yields

$$\bar{C}^0(T_2^0 - T_2) = \sum Q_i N_{i2} \dots [8]$$

where \bar{C}^0 is the average molar heat capacity for the stable products between the temperatures T_2 and T_2^0 . At the high temperatures where chemical dissociation is important, equipartition of energy is closely obeyed, and \bar{C}^0 and \bar{C} differ only slightly, mainly as a result of a small composition difference and anharmonicity effects of the internal-energy states. Under the conditions that $\bar{C}^0 = \bar{C}$, that $N_{im} \ll 1$ [so that $1/(1 - N_{im}) \simeq 1 + N_{im}$], and that the N_{i0} values are

⁵ The accurate treatment for multicomponent parallel diffusion through a stagnant layer is quite intractable. Sherwood (5) has given a solution for two parallel diffusing species which was obtained by Gilliland. Wilke (6) has indicated an approximate method of obtaining D_i in multicomponent mixture which may be suitable for this case.

⁶ For recombination at or near chemical equilibrium, this average corresponds to a temperature close to T_2 because the degree of dissociation rises exponentially with temperature.

zero, Equation [8] may be incorporated into Equation [7'] to yield

$$\frac{q}{q'} = \frac{T_2^0 - T_0}{T_2 - T_0} + \frac{\Sigma Q_i N_{i2} N_{im}}{\bar{C}(T_2 - T_0)} \dots \dots \dots [9]$$

It may be noted that the second term in Equation [9] is small with respect to the first and may be neglected for approximate purposes. In using Equation [9], T_2^0 is calculated very simply by writing the energy balance between combustibles and stable products for the single net stoichiometric equation neglecting dissociation.

B Reaction Restricted to Surface

In the second case there are several types of reactions which are catalyzed by surfaces. Among such reactions are atomic and free-radical recombination, the endothermic dissociation of certain species such as ammonia, and certain chain reactions. The particular case of a reaction occurring solely on the surface can easily be treated in this scheme. Equations [1] through [6] are still valid in this second case, and if the restriction $D = \kappa$ quoted in the first case is satisfied, then Equation [7] can be employed. However, it is incorrect to employ Equation [7] if $\epsilon \gg D$ and κ and if $D \neq \kappa$, since the integral in Equation [6] extends over the entire boundary layer. In order to treat the general case of $D \neq \kappa$ (as occurs with H atoms, for instance), it is convenient to solve Equations [1] and [2] independently with $\alpha = 0$ since it is assumed that no reaction occurs in the bulk phase. In this treatment the heat liberated at the wall by surface reaction is entirely absorbed there by an appropriate coolant flow which holds the temperature T_0 fixed. This condition implies that the occurrence of surface reaction has a negligible effect on the temperature contour in the boundary layer and that therefore the convective flow of heat q' is the same with and without surface reaction. The second integral of Equation [1] can be expressed as

$$T_2 - T_0 = q' \int_0^{\nu} \frac{dy}{c\rho(\kappa + \epsilon)} \dots \dots \dots [10]$$

Denoting \bar{c} and $\bar{\rho}$ as the mean values in the film, the resulting integral can be solved according to the assumption given by von Kármán (3). The dimensionless distance $y^* = (y/\nu)(\sqrt{\tau/\rho})$ is employed in which it is assumed that $\epsilon = 0$ for $y^* < 5$ and $\epsilon/\nu = (y^*/5) - 1$ for $5 < y^* < 30$. Since $\nu/\kappa = Pr$, the result of the integration yields

$$q' = \lambda_0 \left(\frac{dT}{dy} \right)_0 = \frac{(T_2 - T_0)\bar{c}\bar{\rho}\sqrt{\tau/\bar{\rho}}}{5[Pr + \ln(1 + 5Pr)]} \dots \dots \dots [11]$$

A corresponding treatment can be made for solution of the conservation-of-mass equation (Equation [2]) with $\alpha = 0$. Let F_i be the rate at which the diffusing species reacts per unit wall surface; then it is easily shown that

$$F_i = \frac{Dn_i}{1 - N_i} \left(\frac{dN_i}{dy} \right)_0 = \frac{(N_{i2} - N_{i0})(\bar{n}/N_m)\sqrt{\tau/\bar{\rho}}}{5[Sc + \ln(1 + 5Sc)]} \dots \dots [12]$$

The relative heat flux is therefore

$$\frac{q}{q'} = \frac{q' + QF_i}{q'} = 1 + \frac{Q(N_{i2} - N_{i0})}{N_m \bar{C}(T_2 - T_0)} \left[\frac{Pr + \ln(1 + 5Pr)}{Sc + \ln(1 + 5Sc)} \right] \dots \dots \dots [13]$$

Clearly, if $D = \kappa(Sc = Pr)$, Equation [13] reduces directly to Equation [7] as just stated. However, the surface recombination of H atoms, for which the $Pr > Sc$, causes a magnification of the heat release effect since the diffusion of H atoms carrying recombination heat exceeds that of the remaining molecules-carrying thermal heat.

The remaining problem is the evaluation of N_{i0} in terms of the accommodation coefficient α , which is the fraction of molecular collisions with the wall leading to reaction. If Z_i

is the total number of surface collisions per unit time made by the diffusing species, the following equation⁷ for F_i defines α

$$F_i = \alpha Z_i = \alpha n_i N_{i0} \sqrt{\frac{RT_0}{2\pi M_i}} \dots \dots \dots [14]$$

Equations [12] and [14] may now be used to evaluate N_{i0} in terms of known quantities. Defining β as

$$\beta = \frac{\bar{n}\sqrt{\tau/\bar{\rho}}}{5n_i[Sc + \ln(1 + 5Sc)]} \sqrt{\frac{RT_0}{2\pi M_i}} \dots \dots \dots [15]$$

the solution for N_{i0} is

$$N_{i0} = \frac{(\beta/\alpha)N_{i2}}{1 + (\beta/\alpha)} \dots \dots \dots [16]$$

and Equation [13] reduces to

$$\frac{q}{q'} = 1 + \frac{QN_{i2}}{[1 + (\beta/\alpha)]N_m \bar{C}(T_2 - T_0)} \left[\frac{Pr + \ln(1 + 5Pr)}{Sc + \ln(1 + 5Sc)} \right] \dots \dots \dots [17]$$

For small values of β/α , $N_{i0} \rightarrow 0$, whereas for $\beta/\alpha \gg 1$, $N_{i0} \rightarrow N_{i2}$. As a typical example, consider a flame at 3000 K with a velocity of 100 fps at y_2 in a tube with the inner-wall temperature at 1000 K. With $Sc = 1$ and $M_i = 20$, the value of β is about 3.2×10^{-5} , and any value of $\alpha > 10^{-3}$ leads to $N_{i0} \simeq 0$; i.e., complete reaction at the surface.

C Reaction Restricted to Laminar Layer

In the third case, if reaction occurs only in the laminar layer where $\epsilon = 0$, Equation [6] can be integrated between the limits $N_i = N_{i0}$ and $N_i = N_{i1}$ provided $D/\kappa = Pr/Sc$ is independent of N_i and T as predicted by kinetic theory for rigid spherical molecules. Under these restrictions, the result is

$$\frac{q}{q'} = 1 + \frac{QPr}{\bar{C}Sc N_m} \left(\frac{N_{i1} - N_{i0}}{T_1 - T_0} \right) \dots \dots \dots [18]$$

For laminar flow where M_{i1} and T_1 are close to free stream properties, Equation [18] is useful for direct computation. For the general case including convective flow, an accurate solution can be obtained for N_i and T_1 by the separate solutions of Equations [1] and [2] in the regions $y^* < 5$ and $5 < y^* < 30$. In the sublayer where $y^* < 5$, Equations [1] and [2] must be solved using an appropriate expression for $\alpha = f(N_i, T)$. The unknown values T_1 and N_{i1} are then determined by matching with the solutions obtained from Equations [1] and [2] in the region $5 < y^* < 30$ where $\alpha = 0$. However, it may be noted that, if $D = \kappa$, the solution reduces to Equation [7] even though reaction occurs only in the laminar layer. Such a situation may occur in hot flames containing easily dissociated species such as Br or I atoms in low concentration.

III Specific Application

It may be of interest to examine the application of the equations derived to a specific flame system transferring heat to a cold wall. In most cases dealing with dissociated gases in high-temperature flames, the rates of chemical recombination are fast relative to the rate of transport through the boundary layer; thus, to a good approximation, the mole fraction of labile species at the wall may be considered negligible if the wall temperature is sufficiently low. The data represented in Tables 1 and 2 refer to the combustion products resulting from the reaction of liquid ammonia with gaseous oxygen at

(Continued on page 269)

⁷Strictly speaking, n_i , N_{i0} , and T_0 should be evaluated one mean free path from the wall. However, for most practical cases, the magnitude of one mean free path is much less than y_1 ; consequently the simplification employed is valid.

Laminar Heat Transfer Over Blunt-Nosed Bodies at Hypersonic Flight Speeds

LESTER LEES¹

The Ramo-Wooldridge Corporation, Los Angeles, and California Institute of Technology, Pasadena, Calif.

This paper deals with two limiting cases of laminar heat transfer over blunt-nosed bodies at hypersonic flight speeds, or high stagnation temperatures: (a) thermodynamic equilibrium, in which the chemical reaction rates are regarded as "very fast" compared to the rates of diffusion across streamlines; (b) diffusion as rate-governing, in which the volume recombination rates within the boundary layer are "very slow" compared to diffusion across streamlines. In either case the gas density near the surface of a blunt-nosed body is much higher than the density just outside the boundary layer, and the velocity and stagnation enthalpy profiles are much less sensitive to pressure gradient than in the more familiar case of moderate temperature differences. In fact, in case (a), the nondimensionalized enthalpy gradient at the surface is represented very accurately by the "classical" zero pressure gradient value, and the surface heat-transfer rate distribution is obtained directly in terms of the surface pressure distribution. In order to illustrate the method, this solution is applied to the special cases of an unyawed hemisphere and an unyawed, blunt cone capped by a spherical segment.

In the opposite limiting case where diffusion is rate-controlling the diffusion equation for each species is reduced to the same form as the low-speed energy equation, except that the Prandtl number is replaced by the Schmidt number. The simplifications introduced in case (a) are also applicable here, and the expression for surface heat transfer rate is similar; the maximum value of the ratio between the rate of heat transfer by diffusion alone and by heat conduction alone in the case of thermodynamic equilibrium is given by: $(\text{Prandtl no.}/\text{Schmidt no.})^{1/4}$. When the diffusion coefficient is estimated by taking a reasonable value of atom-molecule collision cross section this ratio is 1.30. Additional theoretical and (especially) experimental studies are clearly required before these simple results are accepted.

Nomenclature

The subscript w refers to gas properties evaluated at the local surface temperature, while the subscript e denotes quantities at the outer edge of the boundary layer, and the subscript ∞ refers to ambient properties just ahead of the bow shock wave. The subscripts i and j represent the i th and j th chemical species. The subscript o generally denotes quantities at the forward stagnation point. A prime denotes differentiation with respect to η .

- a = speed of sound
- C_i = concentration by weight of the i th species
- C_v, C_p = specific heats at constant volume and constant pressure, respectively, per unit mass ($\bar{C}_p = \sum C_i C_{p,i}$)
- $C(\eta)$ = $\rho\mu/\rho_{\infty}\mu_{\infty}$ Chapman-Rubens function
- D = diameter
- D_{ij} = coefficient of diffusion of species " i " into species " j "

- f = u/u_{∞}
- g = h_s/h_{s_s}
- h = static enthalpy
- h_i^o = standard enthalpy of formation
- h_s = total enthalpy
- k = coefficient of thermal conductivity
- M = Mach number u/a
- \bar{M} = molecular weight
- Nu = Nusselt number, hD/k , where $q_w = h/C_p(h_{s_s} - h_w)$
- p = static pressure
- Le = Lewis number, $\rho D_{12}\bar{C}_p/k$
- Sc = Schmidt number $\mu/\rho D_{12}$
- p_0' = stagnation pressure behind normal shock wave
- Pr = Prandtl number, $\bar{C}_p\mu/k$
- q = local heat transfer rate, per unit area, per unit time
- r_0 = radius of cross section of body of revolution
- r = distance between centers of two molecules or atoms
- R_0 = nose radius
- \mathcal{R}_0 = universal gas constant
- \mathcal{R} = \mathcal{R}_0/\bar{M}
- s = distance along body surface, measured from forward stagnation point
- \bar{s} = transformed coordinate along body surface (Eq. [7])
- T = absolute temperature
- T^* = kT/ϵ , where k is the Boltzmann const = 1.380×10^{-16} erg/°K
- u, v = components of velocity parallel and normal to surface
- w_i = net rate of production of i th species, gm/cm²/sec
- x = distance along body axis, measured from forward stagnation point
- y = distance normal to surface
- z_i = nondimensional concentration
- β = velocity gradient parameter, $(2\bar{s}/u_{\infty})(du_e/d\bar{s})$
- $\bar{\beta}$ = $(2\bar{s}/M_{\infty})(dM_{\infty}/d\bar{s})$
- γ = ratio of specific heats, C_p/C_v
- δ = boundary layer thickness
- δ^* = boundary layer displacement thickness, $\int_0^{\infty} [1 - (\rho/\rho_e)u/u_e] dy$
- ϵ = maximum attraction energy, erg
- η = nondimensional coordinate normal to body surface (Eq. [7])
- θ = angle between flight direction and radius vector from center of curvature of nose
- θ_s = angle of inclination of local surface element with respect to flight direction
- θ_c = cone half-angle
- μ = absolute viscosity
- ν = kinematic viscosity, μ/ρ
- ρ = gas density
- σ = zero-energy distance, or collision diameter
- $\varphi(r)$ = interaction potential for intermolecular force field
- ψ = stream function
- $\Omega_{ij}(l, m)^*(T^*)$ and $\Omega_i(l, m)^*(T^*)$, collision integrals
- ω_s = $\mu_s/\mathcal{R}_e T_s$

1 Introduction

AT HYPERSONIC flight speeds all bodies must be blunt-nosed to some extent in order to reduce the heat transfer rates to manageable proportions and to allow for internal heat conduction. Since the maximum local heat transfer rate in most cases will occur in the vicinity of the forward stag-

Received January 26, 1956.

¹ Consultant, and Professor of Aeronautics, Guggenheim Aeronautical Laboratory.

nation point, the fluid-mechanical problems associated with this region are of considerable practical, as well as theoretical, interest. Because of the strong falling pressure gradient and large heat transfer to the surface, the boundary layer in this region is expected to be laminar and therefore amenable to analytic treatment.

At hypersonic flight speeds the detached bow shock wave just ahead of a blunt-nosed body converts most of the kinetic energy associated with the flight velocity into thermal and chemical energy. At the "satellite escape speed" of 26,400 ft/sec, for example, this energy amounts to about 14,000 Btu per lb of air, which is sufficient to dissociate almost all of the nitrogen and oxygen molecules. The mechanism of heat transfer in the boundary layer under these conditions may differ markedly from the purely molecular heat conduction process of conventional fluid mechanics. For this reason it is desirable to examine certain limiting cases in order to become familiar with the relative importance of the various possible physical processes, and to provide a basis for comparison with experiment. Two important limiting cases are:

1 Complete thermodynamic equilibrium, in which the gas properties and concentrations of atoms, molecules, and ions are identical with their equilibrium values appropriate to the local temperature at every point of the flow. Here the chemical and electronic reaction rates are regarded as "very fast" in comparison with the rates of convection along streamlines, or the rates of diffusion across streamlines.

2 Diffusion as rate-governing for heat transfer. In this opposite limiting case the volume recombination rates within the boundary layer are "very slow" compared to diffusion across streamlines, because of the relatively low temperatures near the surface. Heat transfer from the boundary layer to the body surface is accomplished partly by ordinary heat conduction, and partly by the heat released by catalytic recombination of those atoms that manage to penetrate the screen of molecules diffusing away from the surface.²

The actual physical situation is expected to lie somewhere between these two limiting cases, at least at flight altitudes low enough so that the gas can still be regarded as a "continuum," and heat transfer to the body surface is still of major importance.

Even in these idealized limiting cases the laminar boundary layer problem is not simple, unless certain special approximations are introduced. Cohen and Reshotko (1)³ extended Thwaites' approximate momentum-integral method based on the "similar solutions" to compressible flows with constant specific heats. Also, S. Lal (2) developed straight-forward techniques for applying the momentum and energy integral methods to such flows. In a recent paper Hayes⁴ shows how the Stewartson-illingworth transformation, which reduces the problem to an equivalent low-speed flow, is generalized (at least approximately) to the case of an arbitrary imperfect gas. He also discusses the various methods and approximations available for solving the reduced problem. By following Hayes' approach, these methods could now be modified to include the case of temperature-dependent specific heats.

Fortunately, at hypersonic flight speeds, as we shall see in Section 2.2, the problem is simplified considerably by recognizing that the gas density near the surface of a blunt-nosed body is much higher than the density just outside the boundary layer. The ratio ρ_w/ρ_∞ is large, i. e. 10-20, not only because $T_w/T_\infty \ll 1$, but also because the molecular weight of the gas near the surface is roughly twice the average molecular weight just outside the boundary layer. Since the pressure gradient in the direction parallel to the surface depends on the "external" density, ρ_∞ , and is uniform across the boundary layer,

the velocity profile near the surface is much less sensitive to the pressure gradient than in the more familiar case of moderate temperature difference across the boundary layer. The stagnation enthalpy distribution is even less sensitive. In fact, for $\rho_w/\rho_\infty \gg 1$, we will show that an excellent first approximation is obtained by ignoring the direct effect of pressure gradient entirely in comparison with the influence of the local pressure on the gas density.⁵ The velocity profile is then identical with the Blasius distribution in properly transformed coordinates, and the heat transfer rate distribution over the surface of a blunt body is obtained directly in terms of the surface pressure distribution.

Since the nondimensionalized enthalpy gradient at the surface is independent of surface temperature in this approximation, the method is applicable to nonisothermal surfaces, so long as $\rho_w/\rho_\infty \gg 1$. The calculations are particularly simple when the modified Newtonian flow approximation is employed, and they can be carried out for a blunt-nosed cylindrical body as well as for a body of revolution. In Section 3 the heat transfer rate solution of the present paper is applied to the special cases of an unyawed hemisphere and an unyawed blunt cone capped by a spherical segment.

The methods developed here are also applicable to the second limiting case where diffusion is rate-controlling. The diffusion equation for each species is reduced to the same form as the low-speed energy equation, except that the Schmidt number $\mu/\rho D_{12}$ replaces the Prandtl number (Section 4). For $\rho_w/\rho_\infty \gg 1$, the maximum value of the ratio between the heat energy that would be transferred to the surface by diffusion alone, and by heat conduction alone is given by $(\rho D_{12} \bar{C}_p/k)^{1/2}$. When the diffusion coefficient D_{12} is estimated by taking reasonable values of atom-molecule collision cross section, this ratio is found to be 1.30. Additional theoretical and (especially) experimental studies of this problem are clearly required before these simple results can be accepted.

2 Laminar Boundary Layer Equations for an Atom-Molecule Mixture of Perfect Gases

2.1 Relative Magnitude of Heat Transfer by Diffusion and by Heat Conduction: The Parameter $(\rho D_{12} \bar{C}_p)/k$

Before examining the laminar boundary layer equations including diffusion in some detail, it is helpful to have some estimate of the relative magnitude of the rate of heat transfer by diffusion and by heat conduction. Because of the close similarity between the transport properties and atomic weights of oxygen and nitrogen, it is sufficient to treat the gas in the boundary layer as a binary mixture of atoms and molecules, so far as diffusion is concerned, in which case one deals with a single diffusion coefficient, D_{12} .⁶ Also the concentration of nitric oxide is generally low enough so that its contribution to the energy transfer is negligible. For the same reason one is justified in ignoring the presence of the ions and electrons in a discussion of boundary layer heat transfer at flight Mach numbers less than about 25.

With these simplifications the heat transfer rate is given by

$$\dot{q} = -k \frac{\partial T}{\partial y} + \sum \rho C_i V_i h_i = - \left[k \frac{\partial T}{\partial y} + \rho D_{12} \sum h_i \frac{\partial C_i}{\partial y} \right]$$

where V_i , the diffusion velocity, is equal to $-(D_{12}/C_i) (\partial C_i/\partial y)$ according to Fick's law, and

$$h_i = \int_0^T C_{pi} dT + h_{fi}$$

⁵ This approximation was first employed by the present author in treating the hypersonic boundary-layer shock-wave interaction problem (3), but it appears to be generally useful.

⁶ The author is indebted to Dr. S. S. Penner of the California Institute of Technology for this suggestion.

² The present paper does not consider the problem of radiative heat transfer from the hot gases outside the boundary layer to the surface.

³ Numbers in parentheses indicate References at end of paper.

⁴ Private communication.

where h_i^0 is the heat of formation of the i th species. Now, $dh = \bar{C}_p dT + \sum h_i dC_i$, where $\bar{C}_p = \sum C_i \bar{C}_{p,i}$, so that

$$\dot{q} = -\frac{k}{\bar{C}_p} \left[\left(\frac{\partial h}{\partial y} - \sum h_i \frac{\partial C_i}{\partial y} \right) + \frac{\rho D_{12} \bar{C}_p}{k} \sum h_i \frac{\partial C_i}{\partial y} \right]$$

In the limiting case of local thermodynamic equilibrium the atom concentration vanishes some distance away from the surface, provided the surface temperature is below the dissociation limit at the local pressure, p_s . At the surface

$$\left(\frac{\partial C_i}{\partial y} \right) = 0, \text{ and } \left(\frac{\partial h}{\partial y} \right)_w = \left(\frac{\partial h_s}{\partial y} \right)_w \sim \frac{h_{s,s} - h_w}{\delta}$$

so that

$$(q_w)_{\text{equil}} \sim \frac{1}{\delta} \frac{k_w}{\bar{C}_{p,w}} (h_{s,s} - h_w)$$

In the opposite limiting case where the volume recombination rates in the gas phase are slow compared to the diffusion rates

$$\left(\frac{\partial C_i}{\partial y} \right)_w \sim \frac{C_{i,s} - C_{i,w}}{\delta}$$

for the atoms, on the assumption that the atom concentration is zero at the surface, while for the molecules

$$\left(\frac{\partial C_i}{\partial y} \right)_w \sim \frac{C_{i,s} - C_{i,w}}{\delta}$$

Therefore

$$\dot{q}_w \sim \frac{1}{\delta} \frac{k_w}{\bar{C}_{p,w}} (h_{s,s} - h_w) \left[\left\{ 1 - \frac{\sum h_{i,w} (C_{i,s} - C_{i,w})}{(h_{s,s} - h_w)} \right\} + \frac{\text{conduction}}{\left(\frac{\rho D_{12} \bar{C}_p}{k} \right)_w \frac{\sum h_{i,w} (C_{i,s} - C_{i,w})}{(h_{s,s} - h_w)} \right] \text{diffusion}$$

In other words, the relative magnitude of the heat transferred by the two processes is governed by the parameters

$$\left(\frac{\rho D_{12} \bar{C}_p}{k} \right)_w \text{ and } \frac{\sum h_{i,w} (C_{i,s} - C_{i,w})}{(h_{s,s} - h_w)}$$

At sufficiently high flight speeds this last parameter is nearly unity, and diffusion is responsible for practically all of the heat transfer. In this case, the surface heat transfer rate at a given flight speed (given $h_{s,s}$) is larger than the value for thermodynamic equilibrium roughly by the factor $(\rho D_{12} \bar{C}_p / k)_w$. When $(\rho D_{12} \bar{C}_p / k)_w = 1$, the surface heat transfer rate is independent of the mechanism of heat transfer at any flight speed, and is exactly equal to the value for thermodynamic equilibrium.⁷

According to the kinetic theory of gases the quantity $\rho D_{12} \bar{C}_p / k$ is of the order of unity, where D_{12} is the coefficient of self-diffusion. In fact, for nitrogen molecules $\mu / \rho D_{12} = 0.74$ and $c_p \mu / k = 0.71$ at $T = 273^\circ \text{K}$ and $p = 1$ atm, so that $(\rho D_{12} \bar{C}_p / k) = 0.96$.⁸ But here we require the value of D_{12} , which involves atom-molecule collisions rather than collisions between molecules; an estimate of this coefficient is made in Section 4.2. One expects D_{12} to be larger than D_{11} if only because lighter and faster atomic particles are involved; therefore $(\rho D_{12} \bar{C}_p / k)_w > 1$. For this reason, it is desirable to obtain a somewhat closer estimate of the relative magnitude of the two modes of heat transfer by examining the boundary layer equations. Our procedure is to deal first with the case of thermodynamic equilibrium in some detail; many of the techniques developed here are immediately applicable to the case where diffusion is rate-controlling for heat transfer (Section 4).

⁷ A similar conclusion was reached by R. Bromberg using a different approach (private communication).

⁸ Table 1.2-3, page 16, Ref. (4).

In order to bring out the main features of the problem as simply as possible, consider the steady flow over an unyawed, blunt-nosed body of revolution (or a cylindrical body). The basic equations of laminar boundary layer flow are as follows

Continuity Equation

$$\frac{\partial}{\partial s} (\rho u r_0^k) + \frac{\partial}{\partial y} (\rho v r_0^k) = 0 \dots \dots \dots [1]$$

where $k = 0$ for a planar body and $k = 1$ for a body of revolution.⁹

Momentum Equation

$$\rho \left(u \frac{\partial u}{\partial s} + v \frac{\partial u}{\partial y} \right) = -\frac{dp_s}{ds} + \frac{\partial}{\partial y} \left(\mu \frac{\partial u}{\partial y} \right) \dots \dots \dots [2]$$

Energy Equation

$$\rho \left(u \frac{\partial h_s}{\partial s} + v \frac{\partial h_s}{\partial y} \right) = \frac{\partial}{\partial y} \left(\frac{\mu}{Pr} \frac{\partial h_s}{\partial y} \right) + \frac{\partial}{\partial y} \left\{ \mu \left(1 - \frac{1}{Pr} \right) \frac{\partial u^2}{\partial y} \right\} + \frac{\partial}{\partial y} \left\{ \rho D_{12} \left(1 - \frac{1}{Le} \right) \sum h_i \frac{\partial C_i}{\partial y} \right\} \dots \dots \dots [3]$$

Continuity Equation for Each Species

$$\rho u \frac{\partial C_i}{\partial s} + \rho v \frac{\partial C_i}{\partial y} - \frac{\partial}{\partial y} \left(\rho D_{12} \frac{\partial C_i}{\partial y} \right) = w_i \dots \dots \dots [4]^{10}$$

Equation of State

$$p = \rho \frac{R_0}{m} T, \text{ where } m = \left[\sum \frac{C_i}{m_i} \right]^{-1} \dots \dots \dots [5]$$

Since $h_s = \sum C_i h_i + u^2/2$, it includes the chemical enthalpy $\sum C_i h_i^0$.

Clearly there are two cases in which the energy equation takes the familiar form:

- 1 Lewis number = $\rho D_{12} \bar{C}_p / k = 1$.
- 2 C_i = constant across the boundary layer.

In the first case, as shown previously, the heat transfer rate is given by the expression

$$\dot{q} = -\frac{k}{\bar{C}_p} \frac{\partial h}{\partial y}$$

independently of the mechanism of heat transfer. In the second case, either the gas temperatures are low enough so that no dissociation has occurred, or no chemical reactions take place either in the gas phase or at the surface; i.e., the gas composition is "frozen."

Apart from these general remarks not much progress can be made until one finds the "similar solutions," or one-parameter family of velocity and total enthalpy profiles. In this respect the situation is not very different from the low-speed boundary layer problem.

2.2 Similarity Considerations for Thermodynamic Equilibrium: The Case of the Highly Cooled Surface

In the limiting case of thermodynamic equilibrium the concentration of each species is uniquely related to the local pressure and temperature, and the net rate of production of each species w_i is supposed to be large enough to balance the

⁹ For Reynolds numbers based on nose radius that are not "too low," $\delta/r_0 \ll 1$ and the continuity equation takes this reduced form. Also, $3\mathcal{C}\delta$ and $\delta^2 \partial \mathcal{C} / \partial s$ are assumed to be "small," where \mathcal{C} is body surface curvature. The boundary layer and shock wave are distinct when $\delta_0/\delta_s \sim (\rho_s/\rho_w)/\sqrt{u_w R_0/\nu_w} < 0.10$ (say), or roughly when $(u_w R_0/\nu_w) > 10^4$. (Here δ_s is the separation distance between the bow shock and the forward stagnation point.)

¹⁰ These equations are readily derived from the general equations given by Hirschfelder, et al. (Ref. 4). Thermal diffusion is considered to be negligible compared with mass diffusion.

convection and diffusion terms. In other words, Equation [4] is superfluous in this case. Also, tables or graphs of static enthalpy and molecular weight vs. temperature for air are either available or can be constructed by methods similar to those described in (5b).^{10a} By means of the relation $\rho/\rho_s = (T_s/T) (\pi/\pi_s)$ the density ratio is then uniquely determined by the enthalpy ratio h/h_s , for each value of h_s and the pressure p_s across the boundary layer.

Our procedure is to assume that "similarity" exists and then to determine the conditions (if any) under which this assumption is in fact justified. For this purpose the momentum and energy equations are reduced to the more convenient equivalent "low-speed" form by utilizing Levy's transformation (6), which he introduced for the special case of constant specific heats.¹¹ In order to simplify the discussion the Lewis number is taken to be unity; this restriction is not an essential one, and in no way affects the validity of the general arguments.

Let

$$\eta = \frac{\rho_s u_s}{(2s)^{1/2}} \int_0^s r_0^k \rho / \rho_s dy \quad \text{and} \quad \xi = \int_0^s \rho_s \mu_s u_s r_0^{2k} ds \quad \left. \begin{array}{l} \dots\dots\dots [6] \end{array} \right\}$$

The transformation from s, y coordinates to ξ, η coordinates is carried out by means of the relations

$$\left. \begin{array}{l} \frac{\partial}{\partial y} = \frac{\rho_s u_s r_0^k}{(2s)^{1/2}} \frac{\partial}{\partial \eta} \\ \frac{\partial}{\partial s} = \rho_s \mu_s u_s r_0^{2k} \left[\frac{\partial}{\partial \xi} + \frac{\partial}{\partial \eta} \frac{\partial \eta}{\partial s} \right] \end{array} \right\} \dots\dots\dots [7]$$

The over-all continuity equation is automatically satisfied by introducing the stream function ψ , which is defined by the usual relations

$$\rho u r_0^k = \frac{\partial \psi}{\partial y} \dots\dots\dots [8a]$$

and

$$\rho v r_0^k = - \frac{\partial \psi}{\partial s} \dots\dots\dots [8b]$$

Let $\psi(s, \eta) = (2s)^{1/2} f(\eta)$; then by Equations [7] and [8a], $u/u_s = f'(\eta)$, where the prime denotes differentiation with respect to η . Also define $h_s/h_\infty = g(\eta)$. The momentum equation then takes the form

$$(Cf'')' + ff'' + \frac{2s}{u_s} \frac{du_s}{ds} \left[\frac{\rho_s}{\rho} - (f')^2 \right] = 0 \dots\dots\dots [9]$$

and the energy equation is

$$\left(\frac{C}{Pr} g' \right)' + fg' + \frac{u_s^3}{2h_\infty} \left[2C \left(1 - \frac{1}{Pr} \right) f'f'' \right]' = 0 \dots\dots [10]$$

where

$$C = \frac{\rho \mu}{\rho_s \mu_s}$$

The boundary conditions are as follows:

$$\begin{aligned} f(0) = f'(0) = 0, \text{ and } f'(\eta) \rightarrow 1 \text{ as } \eta \rightarrow \infty; \\ g(0) = g_\infty(s), \text{ or } g'(0) = 0, \text{ while } g(\eta) \rightarrow 1 \text{ as } \eta \rightarrow \infty. \end{aligned}$$

For an isoenergetic flow outside the boundary layer the conditions for similarity are:

- (a) $(2s/u_s) (du_s/ds) [\rho_s/\rho - (f')^2] = F(\eta)$, or a const.
- (b) $C = C(\eta)$, or a const.

^{10a} Because the gas is treated as a binary mixture of atoms and molecules, the mass ratio of oxygen (atoms + molecules) to nitrogen is constant along every streamline and equal to the stoichiometric ratio for the standard atmosphere.

¹¹ Here we combine Levy's transformation with the Mangler transformation for bodies of revolution.

- (c) Either (a) $Pr = 1$ or (b) $Pr = Pr(\eta)$, or a const., while either $u_s^2/2h_\infty \ll 1$ (low local Mach number) or $u_s^2 \rightarrow 2h_\infty$ (high local Mach number).
- (d) $g_\infty(s) = \text{const.}$

Except for the special case of a uniform external flow, all of these conditions for similarity are never satisfied simultaneously at hypersonic flight Mach numbers, even if the surface temperature is uniform. The density ratio ρ_s/ρ , the Prandtl number, and the ratio $\rho \mu/\rho_s \mu_s$ are functions not only of h/h_s , but also of h_s itself, and of p_s through its effect on the composition of the gas. Of course it is always possible to find a "locally similar" solution in the neighborhood of the forward stagnation point that is "exact" so long as the boundary layer and bow shock are distinct. The boundary layer thickness δ , and p_s are all very nearly constant along the surface in this region, and the velocity and enthalpy ratios are functions of a single variable of the form Y/R_0

$\sqrt{u_\infty R_0/\nu_s}$, where $Y = \int_0^y (\rho/\rho_s) dy$. The question naturally arises as to whether one can obtain approximate solutions extending over most of the body surface. Such solutions can be developed in at least two cases of interest: (a) slowly varying external flow properties; (b) highly cooled surface, or $g_\infty \ll 1$.

In the first case the approximation of "local similarity" is employed, in which the velocity and enthalpy profiles at any station are supposed to be identical with the "similar profiles" corresponding to constant values of

$$\beta = \left(\frac{2s}{u_s} \frac{du_s}{ds} \right)_{\text{local}} \quad \text{and} \quad (u_s^2/2h_\infty)_{\text{local}}$$

all along the surface, and to the local relations between ρ_s/ρ , C , Pr , and the enthalpy ratio h/h_s . This approximation is utilized by Stine and Wanlass (7) (for example) in the special case of constant specific heats and ordinary stagnation temperatures, where $\rho_s/\rho = h/h_s$ and C and Pr are both practically constant.

In the second case, where the surface temperature is much lower than T_s , or $\rho_s/\rho_\infty \ll 1$, the influence of the pressure gradient term in Equation [9] should be small according to the qualitative physical argument in Section 1, and the problem is simplified considerably. This argument is supported in two ways: (a) rough estimates; (b) examination of known solutions for the special case of constant specific heats. At hypersonic flight speeds

$$\frac{\rho_s}{\rho} \cong \frac{h_s}{h_\infty} = g(\eta)$$

when the difference in molecular weight across the boundary layer is taken into account. Now

$$g \cong g_\infty + (1 - g_\infty) u/u_s \cong u/u_s = f'(\eta)$$

when $g_\infty \ll 1$.¹² Therefore, the term in brackets in Equation [9] is represented approximately by $[u/u_s - (u/u_s)^2]$, which is zero both at the surface and at the outer edge of the boundary layer, and has a maximum value of $1/4$ within the boundary layer. Thus, at most, the effect of the pressure gradient of the velocity profile is equivalent to the case of an isothermal low-speed flow with an "effective" value of $\beta = (2s/u_s) (du_s/ds)$ equal to one fourth of the actual value of this parameter.¹³

¹² This relation is "exact" when the pressure gradient is zero, and either $Pr = 1$, or $(u_s^2/2h_\infty) \ll 1$.

¹³ The first-order effect of the pressure gradient term on the skin friction, for example, is given by

$$\frac{(2s/u_s) (du_s/ds) \int_0^\infty e^{-\eta^2/d\eta} \left\{ \int_0^\eta e^{-\eta^2/d\eta} [\dots] d\eta \right\} d\eta}{\int_0^\infty e^{-\eta^2/d\eta} d\eta}$$

where $[\dots] = (\rho_s/\rho) - (f')^2 \cong u/u_s - (u/u_s)^2$ and $f(\eta)$ is the Blasius function.

At the forward stagnation point the parameter $(2s/u_*)$ (du_*/ds) is equal to $1/2$ for a body of revolution and unity for a cylinder. The maximum "effective" values of β when $\rho_e/\rho_w \ll 1$ are $1/8$ and $1/4$, respectively, and the influence of the pressure gradient on the velocity profile is much reduced, compared to the case of an insulated surface. But the effect of the pressure gradient on the heat transfer rate is even smaller, because the change in $g'(0)$ from its zero pressure gradient value depends upon an integral of the change in the velocity profile across the boundary layer. In fact

$$g'(0) \cong \frac{1 - g_w}{\int_0^\infty e^{-Pr \int_0^\eta d\eta} d\eta}$$

These conclusions are borne out by the results of the numerical calculations of Cohen and Reshotko (8) for the "similar solutions," with the particular assumption of constant specific heats and $Pr = 1$, $C = 1$. In that case

$$\rho_e/\rho = g + (\gamma - 1)/2 M_*^2 [g - (f')^2]$$

and Equations [9] and [10] become

$$f''' + ff'' + \beta [g - (f')^2] = 0$$

and

$$g'' + fg' = 0$$

with

$$\beta = (2s/M_*) (dM_*/ds) = \text{const}$$

The surface shear stress and heat transfer rate functions f_w'' and $g_w'/(1 - g_w) = -s_w'/s_w$ as calculated by Cohen and Reshotko (8) are shown as functions of β in Figs. 1a and 1b, for the cases $g(0) = h_w/h_{se} = 0, 0.20$, and 1.0 .¹⁴ Clearly the approximation that the direct influence of pressure gradient is negligibly small for $\rho_e/\rho_w \ll 1$ is highly accurate for the surface heat transfer rate, and somewhat less accurate for skin-friction.¹⁵ Similar conclusions can be drawn from the numerical results obtained by Levy (Fig. 10 of Ref. 6), and by Lal (Fig. 5 of Ref. 2).

With regard to the function $C(\eta)$ appearing in Equations [9] and [10], extrapolation of existing data on the viscosity of air by means of Sutherland's formula shows that at high enthalpy levels (30-100 times ordinary enthalpy), $\rho\mu \cong \rho_e\mu_e$ over a large portion of the boundary layer (see Ref. 5c, for example). Therefore so far as the heat transfer rate is concerned, it is sufficient to take $C = 1$, especially when we recall that C enters the problem as a square root. Also, in the present state of our knowledge, it seems reasonable to regard the Prandtl number as a constant, equal to some average value \bar{Pr} across the boundary layer (Section 4.2).

With regard to the energy equation (Sp. [10]), the solution can always be chosen so that the inhomogeneous last term does not contribute to the enthalpy gradient at the surface; in fact, this term determines the "recovery" enthalpy, or surface enthalpy for no heat transfer, as shown by Chapman and Rubesin (9). Of course this term vanishes at a stagnation point, in which case the recovery enthalpy is identical with h_{se} . In any event this term is numerically small on a blunt-nosed body at hypersonic flight speeds, where $(u_*^2/2h_{se})_{\max} \cong 1/2$ and $\bar{Pr} \cong 0.65-1.00$.

These considerations suggest that the nondimensionalized enthalpy gradient $g'(0)$ at the surface of a blunt-nosed body at hypersonic flight speeds is represented quite accurately by the zero pressure gradient value of $0.47 \bar{Pr}^{1/2}$, independently of surface temperature, local Mach number M_* , or pressure gradient, and is therefore applicable to a very general class of surfaces, whether isothermal or not, so long as $\rho_w/\rho_e \gg 1$.¹⁶

¹⁴ $g = 1 + s$.

¹⁵ From Figs. 1a and 1b it appears that the "effective" value of β is more nearly one sixth of the actual value.

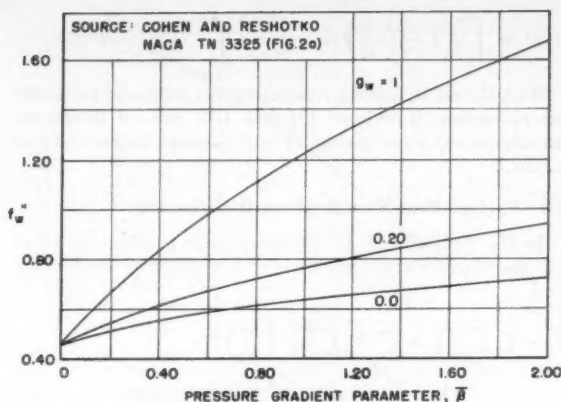


Fig. 1(a) Effect of pressure gradient and ratio of surface temperature to stagnation temperature on surface shear stress function, $Pr = 1$, $C = 1$

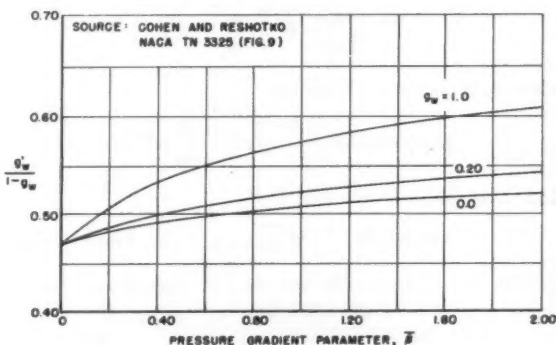


Fig. 1(b) Effect of pressure gradient and ratio of surface temperature to stagnation temperature on surface heat transfer rate function, $Pr = 1$, $C = 1$

If other quantities are required which depend more sensitively on the distribution of $\rho\mu$ and ρ across the boundary layer, they can be calculated by means of a straightforward iteration process. In the first step the stagnation enthalpy distribution $g^{(0)}(\eta)$ is obtained from Equation [10] by repeated quadratures, with $f^{(0)}(\eta)$ given by the Blasius function, $u_*^2/2h_{se}$ equal to its local value, $C = 1$ and $Pr = \bar{Pr}$. (Here the local similarity approximation is employed.) By substituting the corresponding density profile $\rho_e^{(0)}/\rho$ and the function

$$C^{(0)}(\eta) = \frac{\rho^{(0)} \mu^{(0)}}{\rho_e \mu_e}$$

into the momentum equation (Equation [9]), the next approximation $f^{(1)}(\eta)$ is calculated by numerical integration for the local value of

$$\beta = \frac{2s}{u_*} \frac{du_*}{ds}$$

and the process is repeated, if necessary. Finally, the actual distance normal to the surface is computed by means of the quadrature

$$y = \frac{(2s)^{1/2}}{r_0^h \rho_e u_*} \int_0^\eta \rho_e/\rho d\eta$$

and the displacement thickness (for example) is given by the expression

¹⁶ This approximation is clearly not applicable near boundary layer separation.

$$s^* = \int_0^\infty \left(1 - \frac{\rho}{\rho_s} \frac{u}{u_s}\right) dy = \frac{(2s)^{1/2}}{\tau_0^{1/2} \rho_s u_s} \int_0^\infty (\rho/\rho_s - u/u_s) d\eta$$

With the aid of modern computing machines and tabulated air properties, Equations [9] and [10] can be integrated simultaneously step-by-step for any constant values of β and $u_s^2/2h_{ss}$.

2.3 Surface Heat Transfer Rate Distribution

In the limiting case of thermodynamic equilibrium, all of the heat transfer at the surface is accomplished by conduction, and

$$\begin{aligned} \dot{q}_w &= k_w \left(\frac{\partial T}{\partial y} \right)_w = \frac{k_w}{C_{pw}} h_{ss} \left(\frac{dg}{d\eta} \right)_w \left(\frac{\partial \eta}{\partial y} \right)_w \\ &\cong \frac{k_w}{\mu_w C_{pw}} \frac{\mu_w \rho_w u_w \tau_0^{1/2}}{(2s)^{1/2}} h_{ss} (0.50 Pr^{1/2}) \dots [11] \end{aligned}$$

for $\rho_w/\rho_s \gg 1$, taking round numbers. Now $\rho_w \mu_w = \rho_s \mu_s$, to be consistent, and

$$\frac{\rho_s \mu_s}{(\rho_s \mu_s)_0} = \frac{p}{p_0} \frac{\omega_s}{\omega_{s0}}$$

where $\omega_s = \mu_s/\mathcal{R}_s T_s$. Therefore

$$2s = 2(\rho_s \mu_s)_0 u_\infty \int_0^\infty p/p_0' \frac{u_s}{u_\infty} \frac{\omega_s}{\omega_{s0}} \tau_0^{1/2} ds$$

and

$$\dot{q}_w \cong 0.50 (\overline{Pr})^{-1/2} \sqrt{(\rho_s \mu_s)_0} \sqrt{u_\infty} h_{ss} F(s) \dots [12]$$

where

$$F(s) = \frac{(1/\sqrt{2}) (p/p_0') (\omega_s/\omega_{s0}) (u_s/u_\infty) \tau_0^{1/2}}{\left[\int_0^s (p/p_0') (u_s/u_\infty) (\omega_s/\omega_{s0}) \tau_0^{1/2} ds \right]^{1/2}}$$

Here $k = 0$ for a planar body and $k = 1$ for a body of revolution, and \overline{Pr} is some average Prandtl number [see Section (4.2)]. In particular at the forward stagnation point

$$\dot{q}_w)_0 \cong 0.50 2^{k/2} (\overline{Pr})^{-1/2} \sqrt{(\rho_s \mu_s)_0} \sqrt{u_\infty} h_{ss} \frac{\sqrt{[(R/u_\infty) (du_s/ds)]_{s=0}}}{\sqrt{R_0}} \dots [12a]$$

Some years ago Squire (10) worked out the solution for the convective heat transfer near the forward stagnation point of a cylinder on the assumption of constant fluid properties (small temperature differences). More recently, Sibulkin (11) obtained an analogous solution near the forward stagnation point of a blunt body of revolution. Their results are expressed in the form

$$Nu_D = \frac{hD}{k_s} = 0.570 (Pr_2)^{0.4} (\sqrt{2})^k \sqrt{\left(\frac{D}{u_2} \frac{du_s}{ds} \right)_0} \sqrt{\frac{u_2 D}{\nu_2}}$$

where $\dot{q}_0 = h(T_{s0} - T_\infty)$, and the subscript 2 denotes quantities evaluated in the gas just behind the normal shock, following Sibulkin's suggestion.¹⁷ For purposes of comparison, define h in our case by the relation $(\dot{q}_w)_0 = (h/C_{pw}) (h_{ss} - h_w)$; then our result is expressed as

$$Nu_{D,s} = \frac{hD}{k_s} = (0.50) 2^{k/2} (\overline{Pr})^{1/2} \sqrt{\left(\frac{D}{u_2} \frac{du_s}{ds} \right)_0} \sqrt{\frac{u_2 D}{\nu_s}}$$

As expected, the present result has the same form as the

¹⁷ Cohen and Reshotko (12) have applied their similar solutions for a compressible fluid in the special case of constant specific heats and $C = Pr = 1$ to the forward stagnation point, with similar results. They also investigated the effect of fluid injection.

"low-speed," constant-property solutions, except that now the value of $[(D/u_2) \cdot (du_s/ds)]_0$ is obtained from the Newtonian flow approximation at hypersonic speeds, and not from the irrelevant low-speed potential flow over a cylinder or a sphere.

The expression for $Nu_{D,s}$ at the forward stagnation point is of the same form as the result obtained by Beckwith (13), who utilized the momentum and energy integral method, including an approximate density-enthalpy relation for dissociated air in thermodynamic equilibrium.

Also, R. Mark (14) worked out the differential equations for the similar solutions in the neighborhood of the forward stagnation point, and integrated these equations numerically, utilizing the equilibrium thermal properties of dissociated air given in (5c). (Lewis number = 1.) When his result for the stagnation point heat transfer rate is expressed in the same form as our Equation [12a], then his quantity λ [Eq. (14) and Fig. 5 of Ref. 14)], multiplied by $\rho_w \mu_w / \rho_s \mu_s$, should be compared with the numerical value $0.50 \sqrt{2} = 0.70$ (more precisely with $0.47 \sqrt{2} = 0.67$). For surface temperatures of 3000 and 5000 R, and over a range of values of stagnation enthalpy from 50–120 times the ordinary static enthalpy of air, the value of $\lambda(\rho_w \mu_w / \rho_s \mu_s)$ differs from 0.67 by 5 per cent at most. For $T_w = 1000$ R, the value of this quantity is about 10 per cent lower than 0.67. This result tends to justify the simplifying approximation $\rho \mu = \rho_s \mu_s$ utilized in this paper.

As discussed in Section 4 of (15), a careful examination of the experimental data on pressure distributions over hemisphere cylinders and blunt cones with spherical noses shows that the modified Newtonian law in the form $C_p/C_{pmax} = \sin^2 \theta_b$ is confirmed for $M_\infty > 2$ (approximately). Therefore, in Equation [12], $p/p_0' = \sin^2 \theta_b + (p_\infty/p_0') \cos^2 \theta_b$, and

$$\frac{u_s^2}{u_\infty^2} \cong \left(1 + \frac{2}{\gamma_\infty - 1} \frac{1}{M_\infty^2} \right) \left[1 - \left(\frac{p}{p_0'} \right)^{(\gamma-1)/\gamma} \right]$$

where γ is the mean ratio of specific heats behind the bow shock wave. (At high temperatures, $\gamma \cong 1.10$ –1.20.) Near the forward stagnation point $\sin^2 \theta_b = 1 - \sin^2 \theta$, so that

$$\frac{u_s}{u_\infty} \cong \sqrt{\frac{\gamma-1}{\gamma}} \sqrt{1 + \frac{2}{\gamma_\infty - 1} \frac{1}{M_\infty^2}} \sqrt{1 - \frac{1}{\gamma_\infty M_\infty^2}} \sin \theta + \dots$$

where $p_\infty/p_0' \cong 1/\gamma_\infty M_\infty^2$ and

$$\left(\frac{1}{u_\infty} \frac{du_s}{d\theta} \right)_{\theta=0} \cong \sqrt{\frac{\gamma-1}{\gamma}} \sqrt{1 + \frac{2}{\gamma_\infty - 1} \frac{1}{M_\infty^2}} \sqrt{1 - \frac{1}{\gamma_\infty M_\infty^2}}$$

The stagnation point heat transfer rate is then

$$(\dot{q}_w)_0 \cong \frac{0.50 2^{k/2} (\overline{Pr})^{-1/2} \sqrt{(\rho_s \mu_s)_0} \sqrt{u_\infty} h_{ss} G(M_\infty; \gamma, \gamma_\infty)}{\sqrt{R_0}} \dots [13]$$

where

$$G(M_\infty; \gamma, \gamma_\infty) = \left(\frac{\gamma-1}{\gamma} \right)^{1/4} \left(1 + \frac{2}{\gamma_\infty - 1} \frac{1}{M_\infty^2} \right)^{1/4} \left(1 - \frac{1}{\gamma_\infty M_\infty^2} \right)^{1/4}$$

In flight at hypersonic speeds $h_{ss} = u_\infty^2/2$; in the wind tunnel h_{ss} is usually the reservoir stagnation temperature; in the shock tube $h_{ss} = u_s^2$ for sufficiently strong shocks, where u_s is the velocity of the shock wave in the straight section.

¹⁸ This expression agrees with the experimental data (16) obtained on a hemisphere cylinder to within 3 per cent in the range $1.7 \leq M_\infty \leq 5$, with $\gamma = \gamma_\infty = 1.40$.

3 Surface Heat Transfer Rate Distribution over Unyawed Hemisphere and Blunt Cone

According to the modified Newtonian flow approximation, for the particular case of an unyawed body of revolution with a constant radius of curvature in the meridian plane, $p/p_0' = \cos^2 \theta + (1/\gamma_\infty M_\infty^2) \sin^2 \theta$, where θ is the angle between the radius vector and the flight direction. By retaining the second term in this last expression the heat transfer rate distribution obtained is quite accurate even for Mach numbers as low as 2.0, and joins smoothly with the distribution over an afterbody of arbitrary shape.

The velocity at the outer edge of the boundary layer can always be obtained from the isentropic flow relation with an effective γ . But the predicted velocity over a hemisphere varies very nearly linearly with θ up to $\theta = 80$ deg, and the experimental data for air in the range $1.97 < M_\infty < 5.8$ show a remarkable linearity (15, 16). In the present calculations, therefore, we take $u_e/u_\infty = (1/u_\infty) (du_e/d\theta)_{\theta=0} \theta$. On the conical skirt

$$u_e/u_\infty = \left(\frac{1}{u_\infty} \frac{du_e}{d\theta} \right)_{\theta=0} \cdot \left(\frac{\pi}{2} - \theta_c \right)$$

Because of the slow variation of the quantity $\omega_e = \mu_e/R_e T_e$ with enthalpy h_e at high enthalpy levels it is sufficient to take $\omega_e \approx \omega_\infty$. With this simplification the ratio of the local surface heat transfer rate to the heat transfer rate at the forward stagnation point is given by

$$\frac{\dot{q}_w}{(\dot{q}_w)_0} = \frac{(1/2) (p/p_0') (u_e/u_\infty) r_0}{\left[\int_0^\pi (p/p_0') (u_e/u_\infty) r_0^2 ds \right]^{1/2}} \times \frac{\sqrt{R_0}}{\sqrt{(1/u_\infty) (du_e/d\theta)_0}} \dots [14]$$

Case I Hemisphere:

For this body $ds = R_0 d\theta$, $r_0 = R_0 \sin \theta$; therefore

$$\frac{\dot{q}_w}{(\dot{q}_w)_0} = \frac{1/2 \sin \theta [\cos^2 \theta + (1/\gamma_\infty M_\infty^2) \sin^2 \theta]}{\left\{ \int_0^\pi \theta \sin^2 \theta [\cos^2 \theta + (1/\gamma_\infty M_\infty^2) \sin^2 \theta] d\theta \right\}^{1/2}}$$

or

$$\frac{\dot{q}_w}{(\dot{q}_w)_0} = \frac{20 \sin \theta [1 - (1/\gamma_\infty M_\infty^2) \cos^2 \theta + (1/\gamma_\infty M_\infty^2)]}{[D(\theta)]^{1/2}} \dots [15]$$

where

$$D(\theta) = \left(1 - \frac{1}{\gamma_\infty M_\infty^2} \right) \left(\theta^2 - \frac{\theta \sin 4\theta}{2} + \frac{1 - \cos 4\theta}{8} \right) + \frac{4}{\gamma_\infty M_\infty^2} \left(\theta^2 - \theta \sin 2\theta + \frac{1 - \cos 2\theta}{2} \right) \dots [15a]$$

Near the forward stagnation point

$$\frac{\dot{q}_w}{(\dot{q}_w)_0} = 1 - \left(0.722 - \frac{0.667}{\gamma_\infty M_\infty^2} \right) \theta^2 + \dots$$

In Fig. 2 the ratio $\dot{q}_w/(\dot{q}_w)_0$ is plotted as a function of θ for $M_\infty = 2, 3, 5, 10$, and ∞ , with $\gamma_\infty = 1.40$. The quantity $\sqrt{p/p_0'}$ for $M_\infty = 2$ is also shown in Fig. 3 for comparison. Evidently the heat transfer rate drops off somewhat faster than $\sqrt{p/p_0'} \sim \sqrt{\rho \mu}$. By dividing $\dot{q}_w/(\dot{q}_w)_0$ by $\sqrt{p/p_0'}$ we obtain a quantity proportional to the local heat transfer parameter

$$Nu/\sqrt{Re} = \frac{hx/k_s}{\sqrt{\rho_s u_s \mu_s}}$$

employed by Korobkin (16) and by Stine and Wanlass (7). For $M_\infty = 2$, the values of Nu/\sqrt{Re} calculated by the present method for $T_w/T_\infty \ll 1$ are about 12 to 15 per cent lower

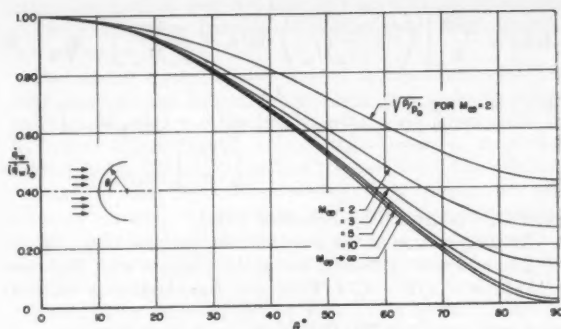


Fig. 2 Laminar heat transfer rate distribution over isothermal hemispherical nose, with $(T_w/T_e) \ll 1$

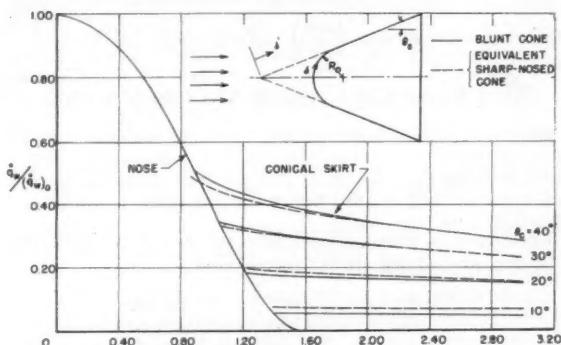


Fig. 3 Laminar heat transfer rate distribution over blunt cone, with $(T_w/T_e) \ll 1$, $M_\infty \sin \theta_c \gg 1$

than the theoretical values obtained by Stine and Wanlass for $T_w/T_\infty \approx 1$ (solid curve in Fig. 4b of Ref. 7). This difference is almost entirely accounted for by the fact that the nondimensionalized enthalpy gradient at the surface for $T_w/T_\infty \approx 1$ is 12 to 15 per cent higher than the Blasius value. (See Fig. 1b, $\beta = 1/2$; $g_w = 1$, for example.) Unfortunately, the scatter in the experimental data (7, 16) so far obtained is too great to permit any detailed comparisons to be made with the theoretical results.

Except for the portion of the hemisphere aft of $\theta = 60$ deg (approx.) the heat transfer rate distribution is close to the "frozen" hypersonic distribution when $M_\infty > 2$. For $M_\infty > 5$ the heat transfer rate is close to its hypersonic values over practically the entire hemisphere. Actually the static pressure is somewhat higher over the region near $\theta = 90^\circ$ than predicted by the Newtonian approximation, so the predicted values of $\dot{q}_w/(\dot{q}_w)_0$ there should be regarded mainly as indicative of relative magnitudes.

Case II Blunt Cone Capped by a Spherical Segment:

For this body the surface heat transfer rate distribution over the "nose" is of course identical with that found for the forward region of the hemisphere [$\theta \leq \pi/2 - \theta_c$, where θ_c is the cone half angle (see Fig. 3)]. On the conical skirt all physical quantities are regarded as constants, and $r_0 = s' \sin \theta_c$, where s' , the distance along the surface measured from the "virtual tip," is related to the actual distance s by the expression (Fig. 3)

$$\frac{s'}{R_0} = \cot \theta_c + \left[\frac{s}{R_0} - (\pi/2 - \theta_c) \right]$$

By substituting the expressions for p/p_0' , u_e/u_∞ , and r_0 into Equation [14], one obtains

$$\frac{\dot{q}_w}{(\dot{q}_w)_0} = A(\theta_c) \frac{s'/R_0}{[B(\theta_c) + (s'/R_0)^2]^{1/2}}$$

for $s'/R_0 \geq \cot \theta_c$, where

$$A(\theta_c) = \frac{\sqrt{3}}{2} \left[\left(1 - \frac{1}{\gamma_\infty M_\infty^2} \right) \sin^2 \theta_c + \frac{1}{\gamma_\infty M_\infty^2} \right]^{1/2} \sqrt{\frac{\pi}{2} - \theta_c}$$

$$B(\theta_c) = \frac{3/16}{\sin^2 \theta_c \{ [1 - (1/\gamma_\infty M_\infty^2)] \sin^2 \theta_c + (1/\gamma_\infty M_\infty^2) \}} \times \left[\frac{D(\theta)}{\theta} \right]_{\theta=(\pi/2)-\theta_c} - \cot^2 \theta_c$$

and $D(\theta)$ is defined by Equation [15a].

At the junction of the nose and the conical skirt, $s'/R_0 = \cot \theta_c$, and this expression for $\dot{q}_w/(\dot{q}_w)_0$ agrees with Equation [15] for $\theta = \pi/2 - \theta_c$. "Far" from the junction ($s'/R_0 \gg 1$)

$$\dot{q}_w \rightarrow \sqrt{3} (0.35) (\overline{Pr})^{-1/2} \sqrt{\rho_\infty \mu_\infty} \sqrt{u_\infty h_{\infty} (1/\sqrt{s'})}$$

which is exactly the value of the surface heat transfer rate on a sharp-nosed cone with an "equivalent velocity"

$$u_e = \left(\frac{d\mu_e}{d\theta} \right)_{\theta=0} (\pi/2 - \theta_c)$$

When $M_\infty \sin \theta_c \gg 1$, $A(\theta_c) \cong \sqrt{3/2} \sin \theta_c \cdot \sqrt{(\pi/2) - \theta_c}$

and

$$B(\theta_c) \cong 3/16 \frac{1}{\sin^4 \theta_c} \left[\frac{D(\theta)}{\theta} \right]_{\theta=\pi/2-\theta_c} - \cot^2 \theta_c$$

The numerical values of these functions for $\theta = 10$ deg, 20 deg, 30 deg, and 40 deg are tabulated below.

θ_c°	$A(\theta_c)$	$B(\theta_c)$
10	0.181	172.0
20	0.326	+4.2
30	0.443	-0.20
40	0.520	-0.26

Evidently for $\theta_c = 30$ deg and 40 deg the surface heat transfer rate distribution over the conical skirt is practically identical with the distribution for the "equivalent sharp-nosed cone." For slender cones, however, the heat transfer rate is smaller than the value for a sharp-nosed cone for a distance of several nose radii aft of the junction of nose and skirt. These conclusions are illustrated quantitatively in Fig. 3.

4 Diffusion as Rate Controlling for Heat Transfer

4.1 Surface Heat Transfer Rate

When the volume recombination rates in the boundary layer can be disregarded in comparison to the rate of diffusion across streamlines, the diffusion equation for each species takes the following form (Equation [4], Section 2.1, with $w_i = 0$):

$$\rho u \frac{\partial C_i}{\partial x} + \rho v \frac{\partial C_i}{\partial y} = \frac{\partial}{\partial y} \left(\rho D_{12} \frac{\partial C_i}{\partial y} \right) \dots \dots \dots [16]$$

By introducing the transformations of Equation [7], and defining $z_i(\eta) = C_i/C_{i\infty}$ for the atoms, and

$$z_i(\eta) = \frac{C_{i\infty} - C_i}{C_{i\infty} - C_{i0}}$$

for the molecules, Equation [16] is reduced to an equation for $z_i(\eta)$ of the same form as the energy equation (Equation [10]) with the term proportional to $u_e^2/2h_{\infty}$ suppressed, except that the Prandtl number is now replaced by the Schmidt number, or the parameter $\mu/\rho D_{12}$. By the arguments employed in Section 2.2, it follows that when $\rho_e/\rho_w \ll 1$, $z_i'(0) \cong 0.50 (\mu/\rho D_{12})_w^{1/2}$, and the rate of heat transfer to the surface by diffusion is

$$(\dot{q}_w)_{diff} = (\rho D_{12})_w \left(\frac{\partial \eta}{\partial y} \right)_w \left[\sum_i h_{i\infty} (C_{i\infty} - C_{i0}) \right] \cdot 0.50 \left(\frac{\mu}{\rho D_{12}} \right)_w^{1/2} \dots \dots \dots [17]$$

By comparing this expression with Equation [11], one obtains

$$\frac{(\dot{q}_w)_{diff}}{(\dot{q}_w)_{equil}} = \left(\frac{\rho D_{12} \bar{C}_p}{k} \right)_w \frac{\sum_i h_{i\infty} (C_{i\infty} - C_{i0})}{h_{\infty}}$$

where $(\dot{q}_w)_{equil}$ is the rate at which heat is transferred to the surface by conduction in the limiting case of thermodynamic equilibrium. In other words, at a given flight speed the maximum difference in surface heat transfer rate between two limiting cases is measured by the factor $(\rho D_{12} \bar{C}_p/k)_w^{1/2}$.

For the particular case in which the surface temperature is high enough so that all the C_{pi} 's are nearly the same (while $\rho_w/\rho_e \gg 1$), the enthalpy transferred by conduction can be treated separately from the full enthalpy transfer. The full static enthalpy equation for the laminar boundary layer is as follows:

$$\sum_i \frac{\partial}{\partial x} (\rho u C_i h_i) + \sum_i \frac{\partial}{\partial y} \rho (v + V_i) C_i h_i = \frac{\partial}{\partial y} \left(k \frac{\partial T}{\partial y} \right) + \mu \left(\frac{\partial u}{\partial y} \right)^2 + u \frac{dp_e}{dx} \dots \dots \dots [18]$$

By utilizing Equation [16] and the fact that $\sum \rho C_i V_i = 0$, Equation [18] is reduced to the familiar form

$$\rho u \bar{C}_p \frac{\partial T}{\partial x} + \rho v \bar{C}_p \frac{\partial T}{\partial y} = \frac{\partial}{\partial y} \left(k \frac{\partial T}{\partial y} \right) + \mu \left(\frac{\partial u}{\partial y} \right)^2 + u \frac{dp_e}{dx}$$

where

$$\bar{C}_p = \sum C_i C_{pi} \quad \text{and} \quad h_T = \int_0^T \bar{C}_p dT$$

Without going into details it is clear that in this case the surface heat transfer rate by conduction alone is given by

$$(\dot{q}_w)_{cond.} \cong 0.50 (Pr_w)^{1/2} \left(\frac{\partial \eta}{\partial y} \right)_w k_w [h_{\infty} - \sum h_{i\infty} (C_{i\infty} - C_{i0})]$$

and

$$\frac{(\dot{q}_w)_{cond.} + (\dot{q}_w)_{diff}}{(\dot{q}_w)_{equil}} \cong \left\{ \left[1 - \frac{\sum h_{i\infty} (C_{i\infty} - C_{i0})}{h_{\infty}} \right] + \left(\frac{\rho C_p D_{12}}{k} \right)_w^{1/2} \frac{\sum h_{i\infty} (C_{i\infty} - C_{i0})}{h_{\infty}} \right\} \dots \dots \dots [19]$$

In this particular case the differential equation for the partial enthalpy

$$\left(\frac{h_T + u^2/2}{h_{T\infty} + u_\infty^2/2} \right) = \theta_T(\eta)$$

is identical with Equation [10], and the temperature distribution is obtained by a method similar to that described in Section 2.2. The concentration profiles are obtained by numerically integrating the equation

$$z_i'' + \left(\frac{\mu}{\rho D_{12}} \right)_w f z_i' = 0 \quad \text{with} \quad f = f^{(0)} =$$

$$f_B(\eta) \text{ and } C^{(0)} = 1^{19}$$

and the boundary conditions $z_i(0) = 0$, $z_i(\eta) \rightarrow 1$ as $\eta \rightarrow \infty$. Once $z_i(\eta)$ is known, the density profile is obtained from the relation

$$\frac{\rho_e}{\rho} = \frac{m_e T}{m T_e}$$

where $m(\eta) = [\sum (C_i(\eta)/m_i)]^{-1}$. Of course iteration schemes similar to the method described at the end of Section 2.2 can be developed in this case also.

When the C_{pi} 's are not all nearly the same the problem is somewhat more complicated and the details will not be given

¹⁹ $f_B(\eta)$ is the Blasius function.

here. In any event the ratio of the total surface heat transfer rates in the two limiting cases considered will lie between the value given in Equation [19] and $(\rho D_{12} \bar{C}_p/k)^{1/2}$.

4.2 Estimate of the Diffusion Coefficient D_{12} and the Parameters $\mu/\rho D_{12}$ and $(\rho D_{12} \bar{C}_p/k)$ According to the Kinetic Theory of Gases

In recent years several different groups of investigators have been remarkably successful in predicting the transport properties of dilute, nonpolar gases²⁰ and gas mixtures with the aid of approximate interaction potentials for the intermolecular force field. Hirschfelder and co-workers have employed the two-parameter Lennard-Jones potential

$$\varphi(r) = 4\epsilon \left[\left(\frac{\sigma}{r} \right)^{12} - \left(\frac{\sigma}{r} \right)^6 \right]$$

where r is the distance between the centers of the two molecules, ϵ is the depth of the potential "well," or the maximum energy of attraction, and σ is the zero-energy distance, or separation distance at the point of closest approach for low-energy collisions ($\pi\sigma^2$ is the collision cross section). The inverse sixth-power term takes into account the long-range attractive forces, while the inverse twelfth-power term approximates the strong, short-range repulsive forces that are called into play when the electron clouds surrounding the two molecules begin to interpenetrate.²¹

For any potential function of the type $\varphi(r) = \epsilon f(r/\sigma)$ the first approximation to the diffusion coefficient of a binary mixture is given by

$$(D_{12})_1 = 0.002628 \sqrt{\frac{T^3(m_1 + m_2)}{2m_1 m_2}} \frac{1}{p \sigma_{12}^2 \Omega_{12}^{(1,1)*}(T_{12}^*)} \dots [20]$$

in cm²/sec, where p is the pressure in atmospheres; T is the absolute temperature in °K; m_1, m_2 are the molecular weights of species 1 and 2, respectively; $T_{12}^* = kT/\epsilon_{12}$, where k is the Boltzmann constant; $\sigma_{12}, \epsilon_{12}/k$ are the interaction parameters for collisions between species 1 and 2, in Å and °K, respectively, and $\Omega_{12}^{(1,1)*}(T_{12}^*)$ is the collision integral for mass transport; this integral is a measure of the departure from the rigid-sphere model, for which $\Omega_{12}^{(1,1)*} = 1.0$.²² The higher approximations to D_{12} are given by $(D_{12})_k = (D_{12})_1 f_{D_{12}}^{(k)}$, where $f_{D_{12}}^{(k)}$ depends on the mixture ratio, but for most binary mixtures $1.00 \leq f_{D_{12}}^{(2)} \leq 1.03$ for the Lennard-Jones potential. In other words, D_{12} is virtually independent of the mixture ratio.

For low energies [$T_{12}^* = 0(1)$] the collision integral for the Lennard-Jones potential is larger than unity, while for high energies $\Omega_{12}^{(1,1)*} < 1$. The Lennard-Jones molecule has a larger cross section than the rigid-sphere model at low energies, because of the importance of the attractive forces, and a smaller cross section at high energies to allow for the interpenetration against the repulsive forces. The function $\Omega_{12}^{(1,1)*}(T^*)$ is tabulated for $0.30 \leq T^* \leq 400$ in Table 1-M, pp. 1126-1127 of the Appendix to (4).

In principle, measurements of the diffusion coefficient provide the best source of information about interactions between unlike molecules, but such measurements are usually very limited. In general the interaction parameters σ_{12} and ϵ_{12} are approximated by the combining "rules" $\sigma_{12} = (\sigma_1 + \sigma_2)/2$ and $\epsilon_{12} = \sqrt{\epsilon_1 \epsilon_2}$, where $\sigma_1, \sigma_2, \epsilon_1$, and ϵ_2 are determined from measurements of the viscosity of the pure components of the binary mixture. As we shall see, the value of σ_{12} for atom-molecule diffusion determined in this manner is too low, be-

cause this method does not take into account the important physical differences between atom-atom and atom-molecule interactions.

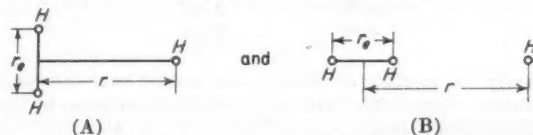
Fortunately a considerable amount of theoretical work has been done on the hydrogen atom-hydrogen molecule interaction, and also on the molecule-molecule interaction in hydrogen. Experimental data on the viscosity of molecular hydrogen provide a check on the theoretical results obtained for the second case. By studying these results for the simplest element, we are able to make a reasonable estimate of the difference between the known collision cross section for molecule-molecule interactions in air, and the required collision cross-section for atom-molecule interactions.

Even for the "simple" hydrogen molecule the calculation of the short-range repulsive forces in the H₂-H₂ interaction is so complicated that reasonable approximations must be introduced (see Ref. 4, pp. 1083-1092). Four possible orientations of the molecules are considered, as follows



When the spatial average of the potential over all four orientations is calculated, it is found that a Lennard-Jones function fits this potential very closely, provided $\sigma = 2.928$ Å and $\epsilon = 5.107 \times 10^{-15}$ erg. It is remarkable that these values agree to within 1 per cent with the values of σ and ϵ obtained from viscosity data on molecular hydrogen.

On the basis of rough physical considerations, one might expect that the "collision diameter," σ_{H-H_2} , would be smaller than $\sigma_{H_2-H_2}$ by a distance of the order of one half the equilibrium separation r_e of the atoms in H₂, or about 0.37 Å. Margenau (17) considered the atom-molecule configurations



He calculated the repulsive part of the potential in each case by a first-order perturbation method, while the attractive portion of the potential is approximated quite accurately by the sum of an inverse sixth-power and an inverse eighth-power term. For configuration A, $\sigma_{H-H_2} = 2.65$ Å and $\epsilon_{H-H_2} = 5 \times 10^{-6}$ erg; for B, $\sigma_{H-H_2} = 3.03$ Å and $\epsilon_{H-H_2} = 3.5 \times 10^{-15}$ erg. Configuration A appears to be much more probable, and the potential is surprisingly similar to the potential for configurations (b) and (c) in the H₂-H₂ interaction, at least in the range $2.50 \text{ Å} \leq r \leq 4.0 \text{ Å}$. Thus the collision diameter for atom-molecule interaction in hydrogen is about 0.28 Å smaller than $\sigma_{H_2-H_2}$, or $\sigma_{H-H_2} = \sigma_{H_2-H_2} - \sigma_{H-H_2} \cong 3/4 (r_e/2)$, while the maximum attraction energy in the two cases is virtually identical.

Now the best experimental value of the distance between the two nitrogen atoms in the N₂ molecule is about 1.1 Å. On the basis of the results of the study of the H-H₂ and H₂-H₂ interactions, it seems quite reasonable to suppose that the collision diameter for atom-molecule collisions in air is smaller than the value $\sigma = 3.69$ Å²³ for molecule-molecule interaction by about $3/4 (r_e/2)$, or about 0.4 Å. In other words, $\sigma_{12} \cong 3.69 \text{ Å} - 0.4 \text{ Å} = 3.3 \text{ Å}$. Also $\epsilon_{12}/k = \epsilon_{air}/k = 84$ K, at least for $300 \text{ K} < T < 1900 \text{ K}$. The diffusion coefficient D_{12} is to be obtained from Equation [20] with these values of σ_{12} and ϵ_{12}/k .²⁴

Suppose we consider first the viscosity and conductivity of the gas at the surface, where the concentration of atomic

²³ Table I-A, Appendix, Ref. (4).

²⁴ In Ref. (18) the value of σ_{12} is obtained from the rough approximation $\sigma_{12} = (\sigma_1 + \sigma_2)/2$, and σ_1 is taken as $1/2 \sigma_2$, i.e., $\sigma_{12} = 3/4 \sigma_2 \cong 2.77 \text{ Å}$. This value seems to be far too low. (Here the subscript "1" denotes the atomic and the subscript "2" denotes the molecular species.)

²⁰ Nonpolar molecules are those for which the potential function does not depend on the orientations of the two interacting molecules, but only on the distance between centers.

²¹ An excellent account of the whole modern development of the molecular theory of liquids and gases is given in (4).

²² For the rigid-sphere model $\varphi(r) = 0$ for $r > \sigma$, and $\varphi(r) = \infty$ for $r < \sigma$. Å $\equiv 1$ Ångström unit = 10^{-8} cm.

species is zero. Experimental data on the viscosity of molecular air are reproduced to within 1 per cent in the temperature range $300 \text{ K} < T < 1500 \text{ K}$, and to within 3 per cent in the temperature range $1500 \text{ K} < T < 1900 \text{ K}$, by the following expression based on the Lennard-Jones potential:

$$\mu \times 10^7 = 266.93 \frac{\sqrt{m_2 T}}{\sigma_2^2 \Omega_2^{(2,2)}(T_2^*)} \quad \text{in gm/cm-sec.} \quad [21]$$

where $\Omega_2^{(2,2)}(T_2^*)$ is the collision integral for momentum transport. By Equations [20] and [21] the Schmidt number for atom-molecule diffusion in air is

$$\left(\frac{\mu}{\rho D_{12}}\right)_\infty \cong 0.833 \frac{\sigma_{12}^2 \Omega_{12}^{(1,1)}(T_{12}^*)}{\sigma_2^2 \Omega_2^{(2,2)}(T_2^*)} \frac{1}{\sqrt{\frac{1}{2} [1 + m_2/m_1]}}$$

where 0.833 is the value of the Schmidt number for the idealized case of self-diffusion in a monatomic gas according to the rigid-sphere model. But $\epsilon_{12}/k \cong \epsilon_2/k = 84 \text{ K}$, so that $T_{12}^* = T_2^*$, and the ratio of the collision integrals $= 1/A^*(T^*)$, where $A^*(T^*)$ is a very slowly varying function of temperature given in Table 1-N, Appendix, Ref. (4). Also $m_2 = 2m_1$ and $\sigma_{12} = 3.3 \text{ \AA}$, while $\sigma_2 = 3.69 \text{ \AA}$, so that

$$\left(\frac{\mu}{\rho D_{12}}\right)_\infty \cong \frac{0.543}{A^*(T^*)}$$

A few calculated values of the Schmidt number are tabulated below:

T, °K	$(\mu/\rho D_{12})_\infty$
252	0.495
420	0.492
840	0.489
1680	0.485
3360	0.482

Clearly the variation in the Schmidt number over this temperature range is less than the probable inaccuracies in the estimated value itself.

For a monatomic gas or a mixture of such gases the thermal conductivity is predicted by the kinetic theory with the same accuracy as the viscosity coefficient. But for polyatomic gases the question of the exchange of energy between the translational and internal degrees of freedom enters the problem. For dry air the vibrational relaxation times for N_2 and O_2 are known to be long at temperatures below 1000 K ; thus, one might expect the thermal conductivity to behave as if only the translation and rotational degrees of freedom were involved. In other words the Prandtl number should be practically constant at its value for room temperature up to about $T = 1000 \text{ K}$. According to the NBS-NACA Tables (Table 2.44, Ref. (5a)) the Prandtl number for dry air based on the best fit to experimental values of μ and k , and spectroscopic data on $C_p^{(0)}$, varies from 0.708 at 300 K to a minimum of 0.680 for $500 \text{ K} \leq T \leq 600 \text{ K}$, and then rises again to 0.702 at $T = 1000 \text{ K}$. This variation in Prandtl number is less than the indicated scatter in the experimental data on thermal conductivity in Fig. 1, p. 5 of Table 2.42, Ref. (5a). Of course at somewhat higher temperatures the vibrational mode is much more readily excited, and the Prandtl number should increase gradually to the undissociated Eucken value of 0.783. Unfortunately no experimental data exist at temperatures above 1000 K , and the Eucken formula is known to give values of Prandtl number at $T = 300 \text{ K}$ that are about 5 per cent too high. For the present, we take $Pr = 0.71$.

Finally the parameter $(\rho D_{12} \bar{C}_p/k)_\infty$ governing the relative importance of heat transfer by atom-molecule diffusion and by thermal conduction is given by

$$\left(\frac{\rho D_{12} \bar{C}_p}{k}\right)_\infty = \frac{(\bar{C}_p \mu/k)_\infty}{(\mu/\rho D_{12})_\infty} \cong \frac{0.71}{0.49} \cong 1.45$$

and the maximum value of the ratio of the rate at which heat is transferred by diffusion and by heat conduction is $(1.45)^{1/2}$, or about 1.30.

In Sections 2.2 and 4.1 it was pointed out that the effect of the variation in Schmidt number, Prandtl number, and the quantity $C(\eta) = \rho \mu / \rho_{\text{air}} \mu_{\text{air}}$ across the boundary layer can be taken into account by means of straightforward iteration schemes, or by simultaneous integration of the equations of motion with the aid of computing machines. For the case of thermodynamic equilibrium the properties of air are given in (5c). However, the calculations of air properties in this report are based on values of atom-atom collision diameter $\cong 1.5 \text{ \AA}$, which are far too large. According to the quantum-mechanical treatment of the N-N interaction by Kopineck (19), the equilibrium separation distance is 1.109 \AA , which agrees very well with the experimental value of 1.095 \AA , while the collision diameter $\sigma_1 = 0.80 \text{ \AA}$. Also $\epsilon_1/k = 1.14 \times 10^4$. On the other hand the values of atom-molecule collision diameter utilized in (5c) and (18), namely $\sigma_{12} = (\sigma_1 + \sigma_2)/2 \cong 2.8 \text{ \AA}$, seem to be too small, if the estimate of the present paper is correct. While the effects on Prandtl number of the difference in these two sets of estimated values of σ_1 and σ_{12} is small, the effect on the Schmidt number and $C(\eta)$ may be significant.

For the second limiting case in which the volume recombination rates are regarded as negligible in comparison with the diffusion rates, the viscosity of the gas considered as a binary atom-molecule mixture is calculated from Equation 8.2-30, page 533 of (4), while the Prandtl number is obtained by the method described by Hansen (18), except that the correct values of σ_1 , σ_{12} , and σ_2 should be employed. The diffusion coefficient D_{12} is obtained from Equation [20] of the present paper. The following values are recommended for the interaction parameters.

$$\begin{aligned} \sigma_1 &= 0.80 \text{ \AA}, & \epsilon_1/k &= 1.14 \times 10^4 \text{ K} \\ \sigma_{12} &= 3.3 \text{ \AA}, & \epsilon_{12}/k &= \epsilon_2/k = 84 \text{ K} \\ \sigma_2 &= 3.69 \text{ \AA} \end{aligned}$$

References

- 1 Cohen, C. B., and Reshotko, E., "The Compressible Laminar Boundary Layer with Heat Transfer and Arbitrary Pressure Gradient," NACA TN 3326, 1955.
- 2 Lal, S., "Heat Transfer in Compressible Laminar Boundary Layers," Ph.D. Thesis, GALCIT, June 1955.
- 3 Lees, L., "On the Boundary Layer Equations in Hypersonic Flow and Their Approximate Solutions," *Journal of the Aeronautical Sciences*, vol. 20, no. 2, February 1953, pp. 143-145.
- 4 Hirschfelder, J. O., Curtiss, C. F., and Bird, R. B., "Molecular Theory of Gases and Liquids," John Wiley and Sons, Inc., New York, 1954.
- 5 (a) The NBS-NACA Tables of Thermal Properties of Gases, Heat and Power Div., NBS, Wash., D. C., February 1, 1951, and January 1, 1952.
(b) Wooley, H. W., "Effect of Dissociation on Thermodynamic Properties of Pure Diatomic Gases," NACA TN 3270, 1955.
(c) Romig, M. F., and Dore, F. J., "Solutions of the Compressible Laminar Boundary Layer Including the Case of a Dissociated Free-Stream," "Convair Report no. ZA-7-012, Aug. 4, 1954, San Diego, Calif.
- 6 Levy, S., "Effect of Large Temperature Changes (Including Viscous Heating) upon Laminar Boundary Layers with Variable Free-Stream Velocity," *Journal of the Aeronautical Sciences*, vol. 21, no. 7, July, 1954, pp. 459-474.
- 7 Stine, H. A., and Wanlass, K., "Theoretical and Experimental Investigation of Aerodynamic-Heating and Isothermal Heat-Transfer Parameters on a Hemispherical Nose with Laminar Boundary Layer at Supersonic Mach Numbers," NACA TN 3344, 1954.
- 8 Cohen, C. B., and Reshotko, E., "Similar Solutions for the Compressible Laminar Boundary Layer with Heat Transfer and Pressure Gradient," NACA TN 3325, 1955.

9 Chapman, D. R., and Rubesin, M. W., "Temperature and Velocity Profiles in the Compressible Laminar Boundary Layer with Arbitrary Distribution of Surface Temperature," *Journal of the Aeronautical Sciences*, vol. 16, no. 9, Sept. 1949, pp. 547-565.

10 Goldstein, S., "Modern Developments in Fluid Dynamics," Vol. 2, pp. 631-632.

11 Sibulkin, M. J., "Heat Transfer Near the Forward Stagnation Point of a Body of Revolution," *Journal of the Aeronautical Sciences*, vol. 19, no. 8, August 1952, pp. 570-671.

12 Reshotko, E., and Cohen, C. B., "Heat Transfer at the Forward Stagnation Point of Blunt Bodies," NACA TN 3513, 1955.

13 Beckwith, I. E., "The Effect of Dissociation in the Stagnation Region of a Blunt-Nosed Body," *Journal of the Aeronautical Sciences*, vol. 20, no. 9, Sept. 1953, pp. 645-646.

14 Mark, R., "Compressible Laminar Heat Transfer Near the Stagnation Point of Blunt Bodies of Revolution," Convair Report no. ZA-7-016, April 11, 1955, San Diego, Calif.

15 Lees, L., "Hypersonic Flow," paper presented at Fifth International Aeronautical Conference (IAS-R.AeS), Los Angeles, Calif., June 20-24, 1955. I.A.S. Preprint no. 554.

16 Korobkin, I., "Laminar Heat Transfer Characteristics of a Hemisphere for the Mach Number Range 1.9 to 4.9," U. S. Naval Ordnance Laboratory, White Oak, Md., NAVORD Report no. 3841, October 10, 1954.

17 Margenau, H., "The Forces Between a Hydrogen Molecule and a Hydrogen Atom," *Physical Review*, vol. 66, nos. 11 and 12, December 1 and 15, 1944, pp. 303-306.

18 Hansen, C. F., "Note on the Prandtl Number for Dissociated Air," *Journal of the Aeronautical Sciences*, vol. 20, no. 11, November 1953, pp. 789-790.

19 Kopineck, H.-J., "Quantentheorie des N_2 -Moleküls," *Zeitschrift für Naturforschung*, Teil a, Band 7a, 1952; part I, pp. 22-23; part II, pp. 314-324.

(Continued on page 274)

Effect of Chemical Reactions in the Boundary Layer on Convective Heat Transfer

(Continued from page 268)

stoichiometric mixture ratio and a total pressure of 20 atmospheres. Inasmuch as recombination is presumed to occur at equilibrium, the stoichiometry of the various reactions shown in Table 2 was arbitrarily chosen to yield stable end products, i.e., N_2 and H_2O . The total percentage increase in heat transfer calculated in Table 2 is 20.7 per cent. The use of the approximate simple formula given by Equation [9] employing a "nondissociated" flame temperature T_2^0 of 3555 K shows a heat transfer increase of 20.6 per cent, which is in good agreement with the more detailed analysis in Table 2. The small discrepancy is accounted for in the expansion $(1 - N_{im})^{-1} = 1 + N_{im}$.

The actual heat flux increase may be somewhat larger than shown in Table 2 since two of the reacting species, H and H_2 , occur at appreciable mole fractions and have values of $(D/\kappa) \gg 1$. Hence the chemical kinetics may not be sufficiently fast to maintain equilibrium for these species, and it is clear from Equation [6] that, if some of these species react where $D \approx \epsilon$, the heat flux should be increased somewhat. A detailed investigation of this correction can be made by solving Equations [1] and [2] with suitable expressions for the chemical reaction rates.

IV Conclusions

Heat transfer from flames to cooled surfaces generally can be expected to show an increase because of the heat release resulting from the recombination of dissociated species in the boundary layers and on the surface. For most chemical species the reaction tends to completion in the intermediate layer where D and κ are small with respect to ϵ . Thus, even if $D \neq \kappa$, $(D + \epsilon)/(\kappa + \epsilon) \approx 1$; and the chemical reaction rates are fast because of the high temperatures encountered

in this region. Under these conditions, a simplified expression may be used for the increase in heat flux which applies regardless of the location of the heat release as long as $D +$

Table 1 Equilibrium flame composition for representative system^a

Species	Mole fraction	$\Delta H_{\text{formation}}$ kcal/mole
H	0.0100	51.6
OH	0.0377	10.0
O	0.0039	58.6
N	0.0002	112.5
H_2	0.0582	0
NO	0.0080	21.5
O_2	0.0162	0

^a Ammonia (l)-oxygen (g) at 20 atm and stoichiometric mixture ratio.

Table 2 Theoretical increase in heat flux for representative system^a

Reaction ($A + B$ = products)	Mole fraction of reactants ^b		Heat release Q , kcal/mole	$\Delta q/q'$, %
	A	B		
H + OH =				
$H_2O(g)$	0.0100	0.0100	119.4	4.2
OH + $1/2 H_2$ =	0.0277	0.0139	67.8	6.7
$H_2O(g)$	0.0039	0.0039	58.6	0.8
O + H_2 = $H_2O(g)$				
NO + H_2 =				
$H_2O(g)$ + $1/2 N_2$	0.0080	0.0080	79.3	2.2
N + N = N_2	0.0002	0.0002	225	0.2
H_2 + $1/2 O_2$ =				
$H_2O(g)$	0.0324	0.0162	57.8	6.6
			Total 20.7	

^a Ammonia (l)-oxygen (g) at 20 atm and stoichiometric mixture ratio; flame temperature 3053 K; wall temperature 600 K; average heat capacity $11.7 \text{ cal mole}^{-1} \text{ } ^\circ\text{C}^{-1}$ at 2700 K.

^b Cf. Table 1.

$\epsilon \approx \kappa + \epsilon$. The theoretical analysis considers also the effect of surface reaction on heat transfer. In this case, certain reactions such as the heterogeneous dissociation of NH_3 may show a decrease in the heat-flux ratio due to the endothermic nature of the reaction.

For the usual case of heat transfer from flames, the concept of the "nondissociated" flame temperature T_2^0 is introduced since it permits a simple, yet reasonably accurate calculation of the change in heat transfer. This concept should be useful in predicting high-temperature, heat-transfer coefficients from low-temperature measurements.

References

- Moore, L. L., "A Solution of the Laminar Boundary-Layer Equations for a Compressible Fluid with Variable Properties, Including Dissociation," *Journal of the Aeronautical Sciences*, vol. 19, 1952, pp. 505-518.
- Hansen, C. F., "Note on the Prandtl Number for Dissociated Air," *Journal of the Aeronautical Sciences*, vol. 20, 1953, pp. 789-790.
- Von Kármán, Th., "The Analogy between Fluid Friction and Heat Transfer," *Transactions of The American Society of Mechanical Engineers*, vol. 61, 1939, pp. 705-710.
- Jakob, M., "Heat Transfer," New York, John Wiley and Sons, 1949.
- Sherwood, T. K., "Absorption and Extraction," New York, McGraw-Hill Book Co., Inc., 1937.
- Wilke, C. R., "Diffusional Properties of Multicomponent Gases," *Chemical Engineering Progress*, vol. 46, 1950, pp. 95-104.

On Laminar Boundary Layers With Heat Transfer

WALLACE D. HAYES¹

The Ramo-Wooldridge Corporation, Los Angeles, Calif.

In part I, a transformation is given which reduces the laminar boundary layer equations approximately to the incompressible form in the case of an imperfect gas. The transformation is related to the Stewartson-illingworth transformation, and involves fitting an approximate relation to the density profile. In part II, the problem of utilizing similar solutions in a momentum-integral method is treated with an approach in which the boundary layer thickness is characterized by a single function of distance along the boundary layer; the momentum, displacement, and enthalpy-defect thickness are expressed in dimensionless forms directly calculable from the similar solutions. It is noted that a basic inconsistency appears in the energy relation in that two different expressions for the heat transfer at the wall are obtained if the classic momentum-integral method is used. Various alternate methods are discussed.

Nomenclature

u, v	= velocity components
x, y	= Cartesian coordinates
\tilde{u}, \tilde{v}	= transformed velocity components
\tilde{x}, \tilde{y}	= transformed coordinates
ρ	= density
μ	= viscosity
h	= enthalpy
H	= total enthalpy
σ	= Prandtl number
$a(x)$	= transformation function
$N(y)$	= viscosity ratio function
κ, α	= dimensionless parameters
C_p	= specific heat at constant pressure
K	= coefficient of thermal expansion
T	= absolute temperature
$g(x)$	= boundary layer thickness function
β	= similarity parameter
f	= reduced stream function
η	= reduced normal coordinate
Δ	= dimensionless momentum thickness
δ	= dimensionless displacement thickness
Λ	= dimensionless enthalpy-defect thickness
A	= ratio of displacement to momentum thickness
Δ^*	= logarithmic derivative of Δ with respect to subscript
Λ^*	= logarithmic derivative of Λ with respect to subscript
β	= enthalpy similarity parameter
$\Gamma(x)$	= kinetic energy correction parameter
a_1, a_2	= vorticity parameters for exterior flow

Subscripts

- 1 = free-stream conditions
w = wall conditions

Received Feb. 28, 1956.

¹ Consultant. Also Associate Professor of Aeronautical Engineering, Princeton University, Princeton, N. J.

* Numbers in parentheses indicate References at end of paper.

I APPROXIMATE METHOD FOR AN IMPERFECT GAS

Introduction

ANALYTICAL methods for treating laminar boundary layers in a compressible fluid are generally based upon the assumption that the fluid is a perfect gas with constant ratio of specific heats. The first part of this paper presents an approximate method for treating the case of a gas which is not perfect; this method utilizes a velocity transformation similar to the Stewartson-illingworth transformation (1, 2).² The basic Howarth transformation which replaces normal distance by normal mass is included, of course.

The boundary layer equations are taken in their two-dimensional form; the modification required for the axisymmetric case is indicated later.

Basic Equations

The basic boundary-layer equations for a two-dimensional laminar boundary layer may be expressed

$$u \frac{\partial u}{\partial x} + v \frac{\partial u}{\partial y} = \frac{\rho_1}{\rho} u_1 \frac{du_1}{dx} + \frac{1}{\rho} \frac{\partial}{\partial y} \left[\mu \frac{\partial u}{\partial y} \right] \dots [I-1a]$$

$$u \frac{\partial H}{\partial x} + v \frac{\partial H}{\partial y} = \frac{1}{\rho} \frac{\partial}{\partial y} \left[\mu \left(\frac{\partial H}{\partial y} + \frac{\sigma - 1}{2} \frac{\partial u^2}{\partial y} \right) \right] \dots [I-1b]$$

$$\frac{\partial \rho u}{\partial x} + \frac{\partial \rho v}{\partial y} = 0 \dots [I-1c]$$

In these equations the total enthalpy H is given by

$$H = h + \frac{1}{2} u^2 \dots [I-2]$$

and the viscous shear and conductive heat transfer are $\mu(\partial u/\partial y)$ and $(\mu/\sigma)(\partial h/\partial y)$, respectively.

The quantity N is introduced, defined by

$$N = \frac{\rho \mu}{\rho_w \mu_w} \dots [I-3]$$

Using this terminology, the quantity $\rho_w \mu_w$ may be taken outside the derivative in the last terms of Equations [I-1a] and [I-1b].

A variant of the Stewartson-illingworth transformation is now introduced, through a function $a(x)$ which is as yet undetermined. A reduced longitudinal velocity component \tilde{u} is introduced

$$u = a \tilde{u} \dots [I-4]$$

in terms of which the basic equations are rewritten

$$\tilde{u} \frac{\partial \tilde{u}}{\partial x} + \frac{v}{a} \frac{\partial \tilde{u}}{\partial y} = \frac{\rho_1}{\rho} \frac{u_1}{a^2} \frac{du_1}{dx} - \frac{\tilde{u}^2}{a} \frac{da}{dx} + \frac{\rho_w \mu_w}{a \rho} \frac{\partial}{\partial y} \left[\frac{N}{\rho} \frac{\partial \tilde{u}}{\partial y} \right] \dots [I-5a]$$

$$\tilde{u} \frac{\partial H}{\partial x} + \frac{v}{a} \frac{\partial H}{\partial y} = \frac{\rho_w \mu_w}{a \rho} \frac{\partial}{\partial y} \left[\frac{N}{\sigma \rho} \left(\frac{\partial H}{\partial y} + \frac{(\sigma - 1)a^2}{2} \frac{\partial \tilde{u}^2}{\partial y} \right) \right] \dots [I-5b]$$

$$\frac{\partial \rho \tilde{u}}{\partial x} + \frac{\partial \rho v}{\partial y} = 0 \dots [I-5c]$$

The quantity κ is now defined, relating the functions $u_1(x)$ and $a(x)$

$$\kappa = \frac{u_1}{\bar{u}_1} \frac{d\bar{u}_1}{du_1} = 1 - \frac{u_1}{a} \frac{da}{du_1} \dots [I-6]$$

The quantity κ is a function of x , in general. A dimensionless variable θ is introduced to replace H , through a parameter α which will be assumed to be constant

$$\frac{H}{H_1} = \alpha + (1 - \alpha)\theta \dots [I-7]$$

It may be noted that $\theta_1 = 1$.

An approximate relation connecting the density ratio and the variable θ is now postulated

$$\frac{\rho_1}{\rho} + (\kappa - 1) \frac{u^2}{u_1^2} = \kappa\theta \dots [I-8]$$

From Equations [I-6], [I-7], and [I-8] may be obtained the relation

$$\frac{\rho_1}{\rho} \frac{u_1}{a^2} \frac{du_1}{dx} - \frac{a^2}{a} \frac{da}{dx} = \theta \bar{u}_1 \frac{d\bar{u}_1}{dx} \dots [I-9]$$

The transformation is now completed with the introduction of the transformed quantities

$$\bar{x} = \int a \rho_w \mu_w dx \dots [I-10a]$$

$$\bar{y} = a \int \rho dy \dots [I-10b]$$

$$\bar{v} = \frac{1}{a \rho_w \mu_w} \left(\rho v + \bar{u} \int \frac{d a \rho}{dx} dy \right) \dots [I-10c]$$

The basic equations now take the form

$$\bar{u} \frac{\partial \bar{u}}{\partial \bar{x}} + \bar{v} \frac{\partial \bar{u}}{\partial \bar{y}} = \theta \bar{u}_1 \frac{d\bar{u}_1}{d\bar{x}} + \frac{\partial}{\partial \bar{y}} \left[N \frac{\partial \bar{u}}{\partial \bar{y}} \right] \dots [I-11a]$$

$$\bar{u} \frac{\partial \theta}{\partial \bar{x}} + \bar{v} \frac{\partial \theta}{\partial \bar{y}} = \frac{\partial}{\partial \bar{y}} \left[\frac{N}{\sigma} \left(\frac{\partial \theta}{\partial \bar{y}} + \frac{(\sigma - 1)a^2}{2(1 - \alpha)H_1} \frac{\partial \bar{u}^2}{\partial \bar{y}} \right) \right] \dots [I-11b]$$

$$\frac{\partial \bar{u}}{\partial \bar{x}} + \frac{\partial \bar{v}}{\partial \bar{y}} = 0 \dots [I-11c]$$

Except for the term in $(\sigma - 1)$ in Equation [I-11b], these equations are now in the low-velocity form for a perfect gas.

Fitting the Density Ratio

The application of the foregoing transformation requires the establishment of the approximate validity of Equation [I-8]. This relation is automatically satisfied under free-stream conditions. It is now required that it be satisfied at the wall and in its first derivative at the wall.

Using Equation [I-7], the condition at the wall is expressed

$$\frac{h_w}{H_1} = \alpha + \frac{(1 - \alpha)}{\kappa} \frac{\rho_1}{\rho_w} \dots [I-12]$$

The coefficient of thermal expansion K is introduced

$$K = \rho \left[\frac{\partial(1/\rho)}{\partial T} \right]_p \dots [I-13]$$

in terms of which the condition on the derivative is expressed

$$\frac{C_{pw}}{H_1} = \frac{(1 - \alpha)}{\kappa} \frac{\rho_1}{\rho_w} K_w \dots [I-14]$$

Eliminating κ yields

$$\alpha = \frac{h_w - \frac{C_{pw}}{K_w}}{H_1} \dots [I-15]$$

whence κ may be expressed

$$\kappa = \frac{\rho_1}{\rho_w} \left[1 + \frac{H_1 - h_w}{C_{pw}/K_w} \right] \dots [I-16]$$

It is presumed that α as given by Equation [I-15] is approximately constant. If this is not so, a suitable value must be chosen and the fitting accomplished by obtaining κ from Equation [I-12].

An important special case is that for which the gas is imperfect in general, but under the conditions at and near the wall behaves like a perfect gas with constant ratio of specific heats. For such a perfect gas $K = T^{-1}$, and $C_p/K = h$. In this case the parameter α as derived from Equation [I-15] is zero, and

$$\kappa = \frac{\rho_1}{\rho_w} \frac{H_1}{h_w}; \quad \alpha = 0 \dots [I-17]$$

The case for which the gas is perfect throughout serves as a check on these results. In this case $\kappa = H_1/h_1$, and Equation [I-6] may be integrated to give a proportional to $h_1^{1/2}$. The transformation in this case is identical with that of Stewartson (1) and Illingworth (2), for which Equation [I-8] is exact.

Axisymmetric Case

For a body of revolution at zero incidence for which the body curvatures times boundary-layer thickness are small, the well-known Mangler transformation may be used to reduce the equations to the two-dimensional form.

A shape function $r(x)$ appears as a factor within the differentials of the continuity equation Equations [I-1c], [I-5c]. The Mangler transformation may be included in the transformation of Equations [I-10] by replacing a by ar , $\rho_w \mu_w$ by $\rho_w \mu_w r$, and v by vr in those equations. The set of Equations [I-11] then follow from the altered set Equations [I-5].

Forward Stagnation Point

The density ratio only plays a part in determining the boundary layer solution if the pressure gradient is different from zero. To exemplify the method presented here, the case of a forward stagnation point is considered. The function g and the parameter β are defined

$$g^2 = 2 \int \bar{u}_1 d\bar{x}_1 \dots [I-18a]$$

$$\beta = \frac{g^2}{\bar{u}_1^2} \frac{d\bar{u}_1}{d\bar{x}} \dots [I-18b]$$

and a stream function gf and a reduced normal coordinate η are introduced such that

$$\frac{\partial gf}{\partial \bar{y}} = \bar{u} \dots [I-19a]$$

$$\eta = \frac{\bar{u}_1}{g} \bar{y} \dots [I-19b]$$

The $(\sigma - 1)$ term of Equation [I-11b] is dropped, β and θ_w are assumed to be constant, and N and σ are assumed to be functions of η alone. Under these conditions, similar boundary layer profiles may be obtained, corresponding to the solution of the ordinary differential equations

$$(Nf_{\eta\eta})_{\eta} + ff_{\eta\eta} + \beta(\theta - f_{\eta}^2) = 0 \dots [I-20a]$$

$$\left(\frac{N}{\sigma} \theta_{\eta} \right)_{\eta} + f\theta_{\eta} = 0 \dots [I-20b]$$

These are essentially the similar solutions found by Stewartson (1) and treated in detail with extensive calculations for the

case ($\sigma = 1, N = 1$) by Cohen and Reshotko (3). These solutions have also been studied by Li and Nagamatsu (4) and by Levy (5). Cohen's quantity S is equal to $\theta - 1$ here.

In the vicinity of a forward stagnation point the quantity κ may be assumed constant and the relations

$$\bar{u}_1 \propto u_1^\kappa \dots \dots \dots [\text{I-21a}]$$

$$\bar{x} \propto x^{2-\kappa} \dots \dots \dots [\text{I-21b}]$$

established locally. The resulting similar profile is one for which

$$\beta = \kappa \dots \dots \dots [\text{I-22}]$$

instead of $\beta = 1$, as in the perfect-gas case.

In the axisymmetric case the influence of the Mangler transformation with $r \propto x$ is to change Equation [I-21b] to

$$\bar{x} \propto x^{4-\kappa} \dots \dots \dots [\text{I-23}]$$

leading to the value $\beta = \kappa/2 \dots \dots \dots [\text{I-24}]$

in place of $\beta = 1/2$, as in the perfect-gas case.

In either the two-dimensional or the axisymmetric case, then, the fact that the gas is imperfect may be approximately taken into account for a forward stagnation point through a change in the similarity parameter β of the boundary-layer profile.

Shear Stress and Heat Transfer

In order to reconnect the physical quantities of interest with the analysis presented, the shear stress $\mu(\partial u/\partial y)$ and the heat transfer $(\mu/\sigma)(\partial h/\partial y)$ are expressed in terms of the quantities introduced. The shear stress is given

$$\mu \frac{\partial u}{\partial y} = \rho \mu a^2 \frac{\partial \bar{u}}{\partial \bar{y}} = \frac{\rho \mu u_1^2}{g} f_{\eta\eta} \dots \dots \dots [\text{I-25a}]$$

$$\left(\mu \frac{\partial u}{\partial y} \right)_w = \rho_w \mu_w a^2 \left(\frac{\partial \bar{u}}{\partial \bar{y}} \right)_w = \frac{\rho_w \mu_w u_{1w}^2}{g} f_{\eta\eta_w} \dots \dots \dots [\text{I-25b}]$$

The heat transfer is given

$$\frac{\mu}{\sigma} \frac{\partial h}{\partial y} + \frac{u}{\sigma} \left(\mu \frac{\partial u}{\partial y} \right) = \frac{\rho \mu H_1 (1 - \alpha) a}{\sigma} \frac{\partial \theta}{\partial \bar{y}} = \frac{\rho \mu H_1 (1 - \alpha) u_1}{\sigma g} \theta_\eta \dots \dots \dots [\text{I-26a}]$$

$$\left(\frac{\mu}{\sigma} \frac{\partial h}{\partial y} \right)_w = \frac{\rho_w \mu_w H_{1w} (1 - \alpha_w) a}{\sigma_w} \left(\frac{\partial \theta}{\partial \bar{y}} \right)_w = \frac{\rho_w \mu_w H_{1w} (1 - \alpha_w) u_{1w}}{\sigma_w g} \theta_{\eta_w} \dots \dots \dots [\text{I-26b}]$$

In the axisymmetric case the factor r appears in these equations.

II MOMENTUM-INTEGRAL METHODS

Introduction

The calculation of laminar boundary layers with an arbitrary pressure distribution is generally carried out with one of various assumptions as to the profiles which may be present, utilizing equations involving integrals taken across the boundary layer. The primary equation considered is that derived from the momentum equation which involves the momentum and displacement thicknesses. It is convenient to assume that the boundary layer profiles at any point are the same as those for one of a family of similar solutions for which separate calculations are available. This second part of the paper presents a modification of the classical momentum-integral method in which the various integral thicknesses are used in the dimensionless forms which arise naturally from the similar solutions.

Application of similar solutions to calculations with arbitrary pressure distributions was first made by Falkner and Skan (6) in a method which did not use the momentum-inte-

gral concept. The two concepts were combined by Thwaites (7) who assumed a correlation connecting the shear stress at the wall, the local pressure gradient, and the ratio of displacement to momentum thickness, and whose selection of a particular correlation was influenced by available calculations of similar solutions. The approach of Thwaites has been extended by Rott and Crabtree (8) who treated in particular the case $\sigma = 1, \theta_w = 1$, and by Cohen and Reshotko (9) who treated in particular the case $\sigma = 1, \theta_w = \text{const}$. For detailed discussion and extensive references, the reader is referred to the authors cited.

The approach of this note is similar in many respects to the Thwaite approach; it differs in that the basic boundary layer thickness used as a reference value is a function $g(x)$ appearing in the separation-of-variables procedure underlying the similar solution analysis rather than the related quantity of Thwaites defined in terms of the momentum thickness.

Basic Equations

The laminar boundary layer equations will be considered in their fully reduced form, as given in Equations [I-11]. The bars have been dropped here, so that the fact that u, v, x , and y are reduced quantities must be kept in mind.

$$u \frac{\partial u}{\partial x} + v \frac{\partial u}{\partial y} = \theta u_1 \frac{du_1}{dx} + \frac{\partial}{\partial y} \left[N \frac{\partial u}{\partial y} \right] \dots \dots [\text{II-1a}]$$

$$u \frac{\partial \theta}{\partial x} + v \frac{\partial \theta}{\partial y} = \frac{\partial}{\partial y} \left[\frac{N}{\sigma} \left(\frac{\partial \theta}{\partial y} + \frac{\sigma - 1}{2u_1^2} \Gamma \frac{\partial u^2}{\partial y} \right) \right] \dots [\text{II-1b}]$$

$$\frac{\partial u}{\partial x} + \frac{\partial v}{\partial y} = 0 \dots \dots \dots [\text{II-1c}]$$

$$\text{where} \quad \Gamma(x) = \frac{u_1^2 a^2}{(1 - \alpha) H_1} \dots \dots \dots [\text{II-2}]$$

is a parameter equal to twice the ratio of kinetic energy to total enthalpy in the free stream. The boundary conditions are

$$y = 0: \quad u = v = 0, \quad \theta = \theta_w(x), \quad (N = 1) \dots [\text{II-3a}]$$

$$y = \infty: \quad u = u_1(x), \quad \theta = 1 \dots \dots \dots [\text{II-3b}]$$

A function $g(x)$ which is as yet undetermined is introduced, together with a stream function for Equation [II-1c] equal to gf . The variable y is replaced by a variable η defined by

$$\eta = \frac{u_1}{g} y \dots \dots \dots [\text{II-4}]$$

With these quantities Equations [II-1] become

$$(N f_{\eta\eta})_\eta + \frac{g'g}{u_1} f f_{\eta\eta} + \frac{g^2 u_1'}{u_1^2} (\theta - f_\eta^2) = \frac{g^2}{u_1} (f_\eta f_{\eta x} - f_{\eta\eta} f_x) \dots \dots [\text{II-5a}]$$

$$\left(\frac{N}{\sigma} \theta_\eta \right)_\eta + \frac{g'g}{u_1} f \theta_\eta = \frac{g^2}{u_1} (f_\eta \theta_x - \theta_\eta f_x) - \left(\frac{\sigma - 1}{\sigma} N \Gamma f_\eta f_{\eta\eta} \right)_\eta \dots \dots [\text{II-5b}]$$

under the boundary conditions

$$\eta = 0: \quad f = 0, \quad f_\eta = 0, \quad \theta = \theta_w(x), \quad (N = 1) \dots \dots [\text{II-6a}]$$

$$\eta = \infty: \quad f_\eta = 1, \quad \theta = 1 \dots \dots \dots [\text{II-6b}]$$

An integral of Equations [II-5] from $\eta = 0$ to ∞ is now taken, giving

$$-f_{\eta\eta_w} + \left(\frac{g'g}{u_1} + \frac{g^2 u_1'}{u_1^2} \right) \Delta + \frac{g^2 u_1'}{u_1^2} \delta = -\frac{g^2}{u_1} \frac{d\Delta}{dx} \dots [\text{II-7a}]$$

$$-\frac{1}{\sigma_w} \theta_{\eta_w} + \frac{g'g}{u_1} \Delta = -\frac{g^2}{u_1} \frac{d\Delta}{dx} \dots \dots \dots [\text{II-7b}]$$

$$\Delta = \int_0^\infty f_\eta(1 - f_\eta) d\eta \dots \dots \dots [\text{II-8a}]$$

$$\delta = \int_0^\infty (\theta - f_\eta) d\eta = A\Delta \dots \dots \dots [\text{II-8b}]$$

$$\Lambda = \int_0^\infty f_\eta(1 - \theta) d\eta \dots \dots \dots [\text{II-8c}]$$

are dimensionless momentum, displacement, and enthalpy-defect thicknesses, respectively. Equations [II-7] may be re-written

$$\frac{g^2}{u_1} \frac{d\Delta}{dx} + \left[\frac{g'g}{u_1} + (1 + A) \frac{g^2 u_1'}{u_1^2} \right] \Delta = f_{\eta\eta_w} \dots [\text{II-9a}]$$

$$\frac{g^2}{u_1} \frac{d\Lambda}{dx} + \left(\frac{g'g}{u_1} \right) \Lambda = \frac{1}{\sigma_w} \theta_{\eta_w} \dots \dots \dots [\text{II-9b}]$$

Similar Solutions

A solution to the set of equations

$$(Nf_{\eta\eta})_\eta + ff_{\eta\eta} + \beta(\theta - f_\eta^2) = 0 \dots \dots [\text{II-10a}]$$

$$\left(\frac{N}{\sigma} \theta_\eta \right)_\eta + f\theta_\eta + \left(\frac{\sigma - 1}{\sigma} N\Gamma f_{\eta\eta} \right)_\eta = 0 \dots [\text{II-10b}]$$

considered as ordinary equations in η is here defined as a similar solution. Such a solution corresponds to a physically realizable similar solution which is an x -independent solution to the boundary layer equations only if N and σ are functions of η alone and Γ is constant or $\sigma = 1$. It is now assumed that the variables Δ , A , and $f_{\eta\eta_w}$ in Equation [II-9a] and Λ and θ_{η_w} in Equation [II-9b] are the same as they would be if the actual solution were a similar one with the local values of θ_w and Γ and with a suitable value of β . This is the underlying assumption of this method and corresponds to Thwaites' correlation assumption. With this assumption, the relations

$$[1 + (1 + A)\beta]\Delta = f_{\eta\eta_w} \dots \dots \dots [\text{II-11a}]$$

$$\Lambda = \frac{1}{\sigma_w} \theta_{\eta_w} \dots \dots \dots [\text{II-11b}]$$

are valid, and Equations [II-9] may be put in the form

$$\frac{g^2}{u_1 \Delta} \frac{d\Delta}{dx} + \frac{g'g}{u_1} - 1 + (1 + A(\beta)) \left(\frac{g^2 u_1'}{u_1^2} - \beta \right) = 0 \dots [\text{II-12a}]$$

$$\frac{g^2}{u_1 \Lambda} \frac{d\Lambda}{dx} + \frac{g'g}{u_1} - 1 = 0 \dots \dots \dots [\text{II-12b}]$$

The quantities Δ and Λ are now considered to be functions of β and θ_w alone, for the purpose of simplifying the analysis. Dependence upon Γ or σ_w may be treated in the same way as dependence upon θ_w , while variations in $N(\eta)$ or in σ/σ_w with x would entail some additional complication. Logarithmic partial derivatives are defined

$$\Delta^*_\beta = \frac{\beta}{\Delta} \frac{\partial \Delta}{\partial \beta}; \quad \Delta^*_{\theta_w} = \frac{\theta_w}{\Delta} \frac{\partial \Delta}{\partial \theta_w} \dots \dots \dots [\text{II-13a}]$$

$$\Lambda^*_\beta = \frac{\beta}{\Lambda} \frac{\partial \Lambda}{\partial \beta}; \quad \Lambda^*_{\theta_w} = \frac{\theta_w}{\Lambda} \frac{\partial \Lambda}{\partial \theta_w} \dots \dots \dots [\text{II-13b}]$$

with respect to β and θ_w ; similar notation may be used with respect to Γ and σ_w . Equations [II-12] now becomes

$$\frac{g^2}{u_1} \left(\frac{\beta'}{\beta} \Delta^*_\beta + \frac{\theta_w'}{\theta_w} \Delta^*_{\theta_w} \right) + \frac{g'g}{u_1} - 1 + (1 + A) \left(\frac{g^2 u_1'}{u_1^2} - \beta \right) = 0 \dots [\text{II-14a}]$$

$$\frac{g^2}{u_1} \left(\frac{\beta'}{\beta} \Lambda^*_\beta + \frac{\theta_w'}{\theta_w} \Lambda^*_{\theta_w} \right) + \frac{g'g}{u_1} - 1 = 0 \dots [\text{II-14b}]$$

The functions $u_1(x)$ and $\theta_w(x)$ are known functions, while $g(x)$ and $\beta(x)$ are as yet unknown. Some latitude is available in the manner in which g and β are determined.

The Classical Method

In the classical method of applying the momentum-integral method, the enthalpy equation is ignored and an assumption is made regarding the relation between the basic parameter and the velocity gradient. As interpreted here, Equation [II-14b] is ignored and β is determined by the relation

$$\beta = \frac{g^2 u_1'}{u_1^2} \dots \dots \dots [\text{II-15}]$$

Equation [II-14a] gives the differential equation for g

$$\frac{g'g}{u_1} (1 + 2\Delta^*_\beta) - \beta \left(2 - \frac{u_1 u_1'}{u_1'^2} \right) \Delta^*_\beta - 1 + \frac{g^2}{u_1} \frac{\theta_w'}{\theta_w} \Delta^*_{\theta_w} = 0 \dots \dots [\text{II-16}]$$

or the equivalent differential equation for β

$$\frac{\beta'}{\beta} (1 + 2\Delta^*_\beta) - 2 \frac{(1 - \beta)}{\beta} \frac{u_1'}{u_1} - \frac{u_1''}{u_1'} + 2 \frac{\theta_w'}{\theta_w} \Delta^*_{\theta_w} = 0 \dots \dots [\text{II-17}]$$

Either of these equations may be integrated numerically to obtain the quantities g and β .

The heat transfer may be calculated from the momentum solution in two different ways. The relation Equation [II-11b] may be used, corresponding to the slope of the assumed local enthalpy profile corresponding to the velocity profile; or, the relation Equation [II-9b] may be used, corresponding to the heat transfer necessary to maintain the assumed corresponding enthalpy profile. These give the heat transfer equations

$$\theta_{\eta_w} = \sigma_w \Lambda \dots \dots \dots [\text{II-18a}]$$

$$\theta_{\eta_w} = \sigma_w \Lambda \left[1 - \frac{g^2}{u_1} \frac{\beta'}{\beta} (\Delta^*_\beta - \Lambda^*_\beta) - \frac{g^2}{u_1} \frac{\theta_w'}{\theta_w} (\Delta^*_{\theta_w} - \Lambda^*_{\theta_w}) \right] \dots \dots [\text{II-18b}]$$

These equations cannot be consistent in general unless Δ equals a constant times Λ over the entire range of the parameters. It is not completely clear which of Equations [II-18] should be preferable, although it appears to the writer that the simpler form Equation [II-18a] should be more trustworthy.

A basic inconsistency in the calculation of heat transfer from the enthalpy profile corresponding to the assumed velocity profile thus appears. That this is so is not surprising in light of the fact that the upstream temperature profile has no effect on the heat transfer calculated by this method, except in so far as it may affect the velocity profile.

Alternate Methods

A. In this method the relation Equation [II-15] connecting β and g is dropped, and Equations [II-14] are to be solved as a pair of simultaneous equations for determining both β and g . The derivatives of β and g may be separated, giving the equations

$$\frac{g^2 \beta'}{u_1 \beta} (\Delta^*_\beta - \Lambda^*_\beta) + \frac{g^2 \theta_w'}{u_1 \theta_w} (\Delta^*_{\theta_w} - \Lambda^*_{\theta_w}) + (1 + A) \left(\frac{g^2 u_1'}{u_1^2} - \beta \right) = 0 \dots [\text{II-19a}]$$

$$\left(\frac{g'g}{u_1} - 1 \right) (\Delta^*_\beta - \Lambda^*_\beta) + \frac{g^2 \theta_w'}{u_1 \theta_w} (\Delta^*_\beta \Lambda^*_{\theta_w} - \Lambda^*_\beta \Delta^*_{\theta_w}) - (1 + A) \left(\frac{g^2 u_1'}{u_1^2} - \beta \right) \Lambda^*_\beta = 0 \dots [\text{II-19b}]$$

This set of equations may pose difficulties of a mathematical nature, particularly with regard to the question of stability. An approximate statement of a stability condition may be formulated, that

$$\Delta^* \beta - \Lambda^* \beta < 0. \dots \dots \dots [\text{II-20}]$$

This method gives a simultaneous solution for the skin friction and the wall heat transfer, in a self-consistent form, provided that a mathematically unobjectionable solution can be found.

B. The classical method as just described may be followed except for the computation of heat transfer properties. The enthalpy profile is now assumed to be a similar one with the appropriate values of θ_w and Γ with the function $g(x)$ computed for the momentum equation, but with a different value of the fundamental parameter β , corresponding to a different value of $\bar{\Lambda}$. This gives the equation for β in place of Equation [II-14b]

$$\begin{aligned} \frac{\beta'}{\beta} \frac{\Lambda^*}{\beta} + \frac{\theta_w'}{\theta_w} \frac{\Lambda^*}{\theta_w} &= \frac{u_1}{g^2} \left(1 - \frac{\theta' g}{u_1} \right) \\ &= \frac{\beta'}{\beta} \Delta^* \beta + \frac{\theta_w'}{\theta_w} \Delta^* \theta_w \dots \dots [\text{II-21}] \end{aligned}$$

The heat transfer is given directly in terms of $\bar{\Lambda}$. This method may be expected to give reasonably trustworthy results if the difference between β and $\bar{\beta}$ does not become too great.

C. For a very rough estimate all the derivatives of Δ and Λ in Equations [II-14] may be neglected, giving the relation Equation [II-15] for β in terms of g , and the relation

$$g^2 = 2 \int u_1 dx \dots \dots \dots [\text{II-22}]$$

Although rather crude, this method should give an estimate of the heat transfer from Equation [II-11b] which is about as accurate as that given by the classical method.

D. The solution obtained by method C may be used to calculate the Δ and Λ derivative terms in Equations [II-14] for use in an algebraic calculation of second approximation. Such a successive approximation scheme, although not strictly convergent, may have semiconvergent properties that make it useful if $|\Delta^* \beta - \Lambda^* \beta|$ is small. This should give essentially the solution of method A by an easier method.

External Rotational Flow

One of the basic boundary layer assumptions is that the layer is so thin that the structure of the external flow does not affect the structure of the boundary layer except through the single function $u_1(x)$. It is possible that in certain cases, if the vorticity in the external flow is sufficiently large, that this vorticity may influence the boundary layer structure even though the layer is quite thin. For a similar boundary layer profile similarity conditions must be imposed on the external vorticity which are, in general, inconsistent with the steady-flow conditions on the inviscid exterior flow. However, the case of the neighborhood of the stagnation point on a blunt body of revolution is one in which finite vorticity at the wall does follow the similarity condition. With the type of use of similar profiles of this note the requirement of the similarity condition on the vorticity is not essential.

The inviscid profile (no boundary layer present) is assumed to be of the form

$$f_\eta = 1 + a_1 \eta + a_2 \eta^2 + \dots \dots \dots [\text{II-26}]$$

The procedure to be followed is first to form the inviscid expression for f

$$f = \eta + \frac{1}{2} a_1 \eta^2 + \frac{1}{6} a_2 \eta^3 + \dots \dots \dots [\text{II-27}]$$

and then eliminate η between Equations [II-26] and [II-27]. The resultant relation connecting f_η and f then replaces the boundary condition $f_\eta = 1$ of Equation [II-6b]. With only the quantity a_1 present or important, this relation is

$$f_\eta^2 = 1 + 2a_1 f \dots \dots \dots [\text{II-28}]$$

The absolute magnitude of the parameter a_1 serves as a measure of its importance in affecting the boundary layer profile. Unless a_1 is negligibly small, it should be added as a parameter determining the boundary layer solution.

References

- 1 Stewartson, K., "Correlated Incompressible and Compressible Boundary Layers," *Proceedings of the Royal Society of London*, ser. A, vol. 200, 1949, pp. 84-100.
- 2 Illingworth, C. R., "Steady flow in the Laminar Boundary Layer of a Gas," *Proceedings of the Royal Society of London*, ser. A, vol. 199, 1949, pp. 533-558.
- 3 Cohen, C. B., and Reshotko, E., "Similar Solutions for the Compressible Laminar Boundary Layer with Heat Transfer and Pressure Gradient," NACA TN 3325, 1955. Also Cohen, C. B., Ph.D. Thesis, Princeton University, 1954.
- 4 Li, T.-Y., and Nagamatsu, H. T., "Similar Solutions of Compressible Boundary Layer Equations," Heat Transfer and Fluid Mechanics Institute, 1954, pp. 143-157, California Book Co., Berkeley. Also *Journal of the Aeronautical Sciences*, vol. 20, no. 9, 1953, pp. 653-655.
- 5 Levy, S., "Effect of Large Temperature Changes upon Laminar Boundary Layers with Variable Free-Stream Velocity," *Journal of the Aeronautical Sciences*, vol. 21, no. 7, 1954, pp. 459-474. Also, with Seban, R. A., *Journal of Applied Mechanics*, vol. 20, 1953, pp. 415-421.
- 6 Goldstein, S., "Modern Developments in Fluid Dynamics," vol. I, Oxford, 1938, pp. 178-180.
- 7 Thwaites, B., "Approximate Calculation of the Laminar Boundary Layer," *Aeronautical Quarterly*, vol. 1, 1949, pp. 245-280.
- 8 Rott, N., and Crabtree, L. F., "Simplified Laminar Boundary-Layer Calculations for Bodies of Revolution and for Yawed Wings," *Journal of the Aeronautical Sciences*, vol. 19, no. 8, 1952, pp. 553-565.
- 9 Cohen, C. B., and Reshotko, E., "The Compressible Laminar Boundary Layer with Heat Transfer and Arbitrary Pressure Gradient," NACA TN 3326, 1955. Also Cohen, C. B., Ph.D. Thesis, Princeton University, 1954.

Laminar Heat Transfer Over Blunt-Nosed Bodies

(Continued from page 269)

SUPPLEMENTARY REFERENCES

Gas Properties

- Hilsenrath, J., and Beckett, C. W., "Thermodynamic Properties of Argon-Free air to 15,000°K," National Bureau of Standards Rep. no. 3991, April 1, 1955.
- Gilmore, F. R., "Equilibrium Composition and Thermodynamic Properties of Air to 24,000°K," RAND Corporation Res. Mem. no. 1543, August 24, 1955 (Santa Monica, Calif.).
- Bond, J. W., Jr., "Equilibrium Conditions Behind a Normal Shock Front in the Atmosphere," Lockheed Aircraft Corp., Missile Systems Div., Rep. no. 1456, December 20, 1955 (Van Nuys, Calif.).
- Bond, J. W., Jr., and Dyer, J. N., "Equilibrium Composition of Air at Various Densities and Temperatures," Lockheed Aircraft Corp., Missile Systems Div., Rep. no. 1487, December 30, 1955.
- Logan, J., "Thermodynamic Properties of Argon-Free Air (2000°K to 15,000°K)," Cornell Aeronautical Laboratory Memo., 1955 (preliminary).

Boundary Layer Equations

- Fay, J. A., "The Laminar Boundary Layer in a Dissociating Gas," AVCO Manufacturing Corp., Research Laboratories Rep. TM-13, June 22, 1955 (revised July 8, 1955). Also, Fay, J. A., and Riddell, F. R.; and Penner, S. S., and Litvak, M. M., AVCO Summary Rep. (unclassified portions), October 1955 (Everett, Mass.).
- Hall, N. H., "Flow Equations for Multicomponent Fluid Systems. Part I. General Equations. Part II. Binary Boundary Layer Equations (zero pressure gradient)," University of Minnesota Inst. Technol., Mechanical Engng. Dept., Tech. Rep. no. 2, August 22, 1955.

Technical Notes

Sun-Follower for High Altitude Sounding Rocket

D. D. TERWILLIGER¹ and G. J. GRANROS²

Aircraft Armaments, Inc., Cockeysville, Md.

A PROGRAM of upper atmosphere research has required the direct measurement of solar radiation below 3100 Ångstroms and atmospheric absorption of this radiation. Units have been designed, built, and flown which house a spectrograph and direct the solar radiation into this spectrograph. These units, known as Sun-Followers, are mounted on high altitude sounding rockets. In order to obtain sufficient exposure times at the shorter wave lengths, sunlight is directed into the spectrograph regardless of the spin and precession of the rocket. In the latest equipment this is accomplished by means of a two-axis tracker, design and performance of which are described in this report.

The present design of the Sun-Follower has been developed as a result of the experience gained on several previous units built and tested. The first units were single axis units, tracking the sun in azimuth only, and were mounted on a V-2 and on an Aerobee. A subsequent pair of units was designed to mount on a Viking rocket and an Aerobee. These units were also single axis types but incorporated design improvements.

In order to obtain more intense spectra the latest units track the sun in both axes. This is accomplished by two-axis control of a mirror which reflects the sunlight down the longitudinal axis of the rocket, on which the spectrograph is fixed. An azimuth drive corrects for rocket roll motion and an elevation drive corrects for rocket pitch and yaw motion. Photoelectric cells mounted on the line of sight are used to sense angular pointing errors and, by means of servo systems, the error is kept to a minimum.

Figs. 1, 2, and 3 show some of the construction details of the latest Sun-Followers. A block diagram of the control system is shown in Fig. 4.

Photoelectric Cells

For control of elevation and azimuth axes, two pairs of photoelectric cells are employed; one pair being used for coarse control to search for the sun, lock on, and to bring the Sun-Follower approximately in line with the sun, the second pair of photoelectric cells to keep the Sun-Follower accurately on the sun to within ± 0.25 deg. A special switching circuit is used to remove the supply voltage to the coarse photoelectric cells when the Sun-Follower is operating on the fine eye system.

The coarse eyes for azimuth control are mounted on the azimuth ring as shown in Fig. 3. The fine azimuth and fine and coarse elevation eyes are mounted in an eye block which is driven by the elevation servo to the line of sight (Fig. 3). The mirror is geared directly to this eye block but is driven at one-half speed in order to obtain the reflection on the longitudinal axis.

Each photoelectric cell is followed by a cathode follower, and the pointing errors are obtained as the differential out-

Presented at the ARS 25th Anniversary Annual Meeting, Chicago, Ill., Nov. 14-18, 1955.

¹ Chief Electromechanical Engineer.

² Design Engineer.

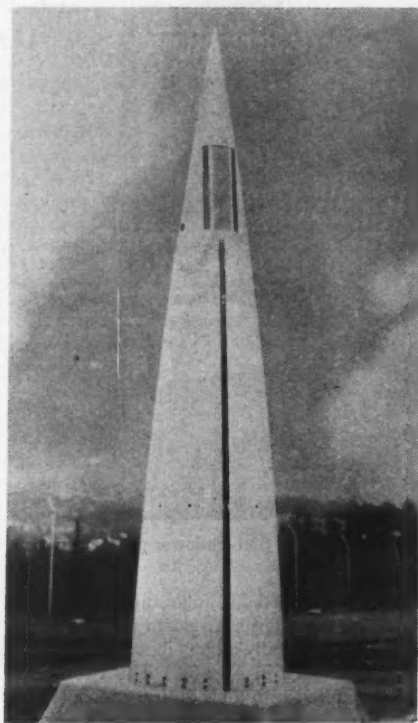


Fig. 1 Assembly of Sun-Follower including rocket skin sections

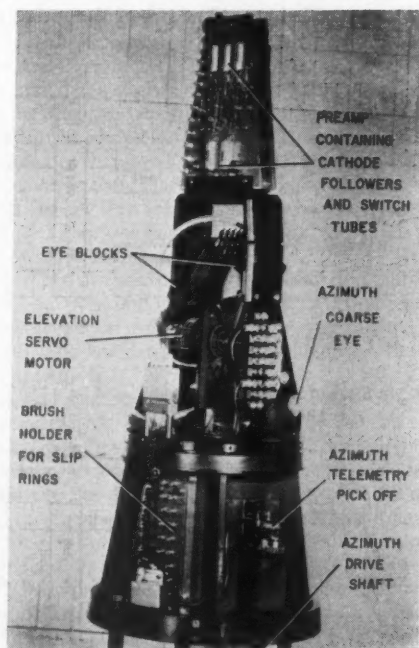


Fig. 2 Internal details of Sun-Follower

EDITOR'S NOTE: This section of JET PROPULSION is open to short manuscripts describing new developments or offering comments on papers previously published. Such manuscripts are published without editorial review, usually within two months of the date of receipt. Requirements as to style are the same as for regular contributions (see first page of this issue).

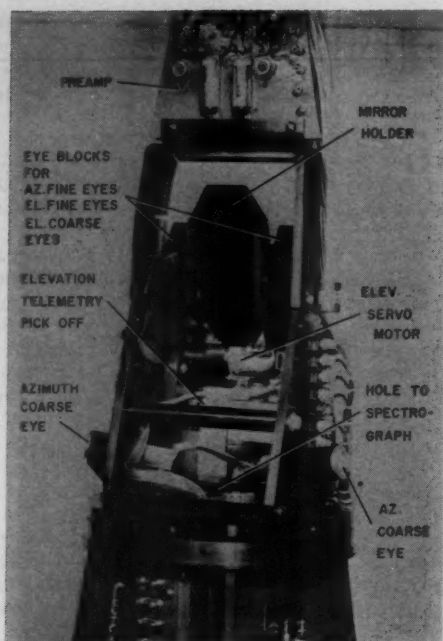


Fig. 3 Details of Sun-Follower photoelectric eyes

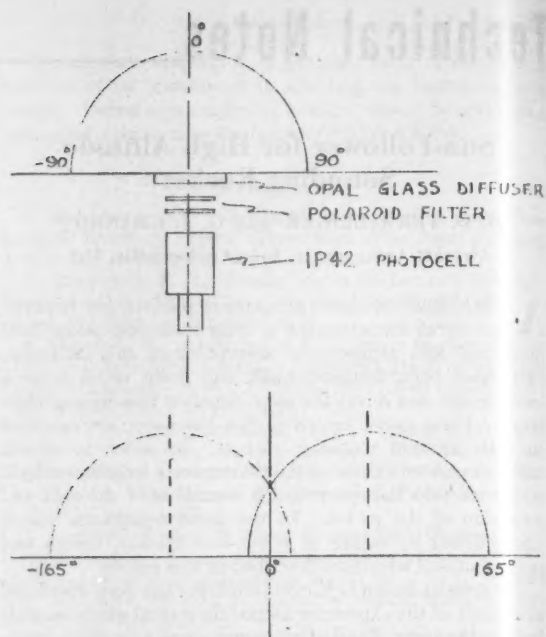


Fig. 5a, b Coarse eye assembly and pickup patterns

puts of the pairs of cathode followers. The coarse photoelectric cells use an optical system to produce a pickup pattern which is essentially a half sinusoid with the maximum dead ahead, as shown in Fig. 5a. The two coarse eyes in azimuth are mounted with their optical axes located ± 75 deg from the boresight line. In this manner a composite error curve as shown in Fig. 5b is obtained.

This permits a proper servo-error signal to be obtained from $+165$ deg to -165 deg. The remaining 30 deg directly opposite from the sun is not covered, but unbalance of the servo system, stray light, or slow roll of the rocket should

bring the system out of this possible dead zone. The elevation coarse eyes are boresighted along the line-of-sight. A blinder for each eye is provided to distort the pickup pattern to give a large signal on either side of dead ahead. This results in a relatively broad null but the fine eyes are capable of controlling the Sun-Follower in this region. As elevation coverage is only required to be ± 45 deg, no dead zone exists.

The fine photoelectric cells use an optical system to obtain a pickup pattern as shown in Fig. 6. The design of the fine and coarse eye assemblies and the eyes used on this model Sun-Follower were supplied by the University of Colorado.

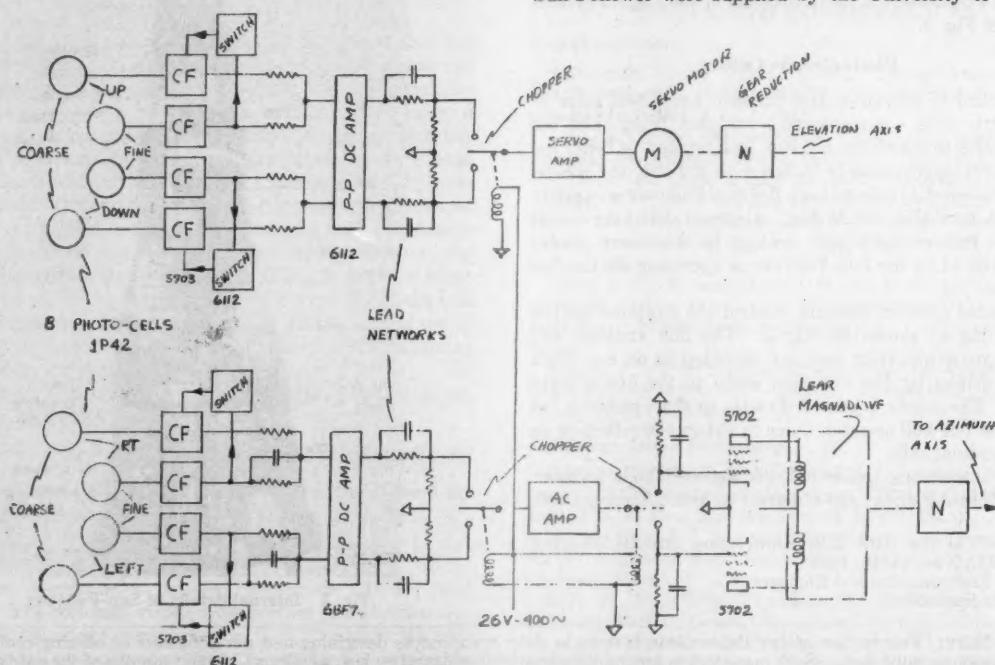


Fig. 4 Block diagram of control circuitry

These eyes were developed by them for use on their Biaxial Pointing Control System (Special Report No. 7, "Photoelectric Eyes for a Solar Pointing Control"). These are arranged so that one photoelectric cell has a pattern as shown by the solid line, to the right of center, and the other photo-

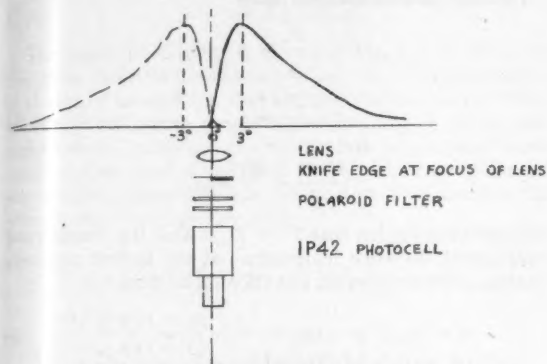


Fig. 6 Fine eye assembly and pickup pattern

electric cell of the pair has the mirror image on the left of center as shown by the dashed line. Similarly, for elevation, the fine eye pair is arranged above and below center. The combination of lens and knife edge at the focal point of the lens gives the sharp cutoff on the unwanted side of center, and the steep linear rise on the other.

Coarse to Fine Switching Circuitry

A special switching circuit was developed to perform two important functions. The first was to switch from coarse to fine eye control. The second was to disable the coarse eyes once the fine eyes were functioning. This is required in order to prevent coercion of the fine data during tracking.

The possibility of coercion exists because the coarse azimuth eyes are mounted on the azimuth axis while the fine eyes are mounted on the line of sight or deflection axis. Any misalignment of the coarse eyes as a function of elevation will cause a coercive error. Also extraneous sources of light such as reflections from the earth or clouds may cause errors in the coarse system. In one of the previous rocket firings, the telemetered data indicated that this actually happened.

In the present switching circuitry, the fine eye photoelectric cell cathode follower outputs go to the grids of a dual triode, the plates of which are tied together. If either of the fine eye photoelectric cells are illuminated, the grids of the switch tube are driven sufficiently positive to saturate the tube and to bring its plate potential to a low value. The coarse eye photoelectric cell anodes are connected to the switch tube plates, so that when the fine eyes are illuminated, the coarse eye photoelectric cell anode potential drops to a sufficiently low value that the coarse eyes are inoperative regardless of the illumination on these cells.

The outputs of the coarse and fine systems are mixed as shown in Fig. 4, by means of adding resistors, with only one system operative at any one time.

Servo Amplifier

Following the mixing network, the differential signals are amplified, passed through a lead network for stabilization of the servo loop, and modulated by means of a 400 cps chopper. In the elevation system, this a-c error signal is amplified to drive the elevation servo motor which in turn drives the elevation axis. In the azimuth system, the a-c error signal is amplified, demodulated by a synchronous chopper, and fed to the grids of pentode tubes which control the current in the clutch coils of a Lear Magnadrive. This Magnadrive in turn drives the azimuth axis of the Sun-Follower.

Additional stabilization for the azimuth axis was found to be necessary due to the high azimuth inertia and extremely high lock-on rates. This was accomplished by inserting a small condenser across the coarse eye adding resistors, to provide a small additional amount of lead. In this manner it was possible to make the system capable of searching and locking on the sun while traveling at azimuth rates in excess of 720 deg/sec, and following with an accuracy of less than ± 0.25 deg. No additional stabilization was required for the elevation servo system due to its relatively small inertia. Elevation tracking accuracy also is ± 0.25 deg.

The 400 cps power required for the synchronous choppers, and the fixed phase of the 2-phase induction motor in the elevation servo were obtained from a separate oscillator and power amplifier. Anode voltages for the circuitry were obtained from a dynamotor and vacuum tube voltage regulator circuit.

In order to permit conventional electronic circuitry to be used on equipment exposed to very high altitudes, the entire electronic package is placed in a pressurized container. No special precautions are taken to insure that the container is airtight. It is ground tested at 15 psig and sealed so that leakage does not exceed 1 psi per 10 min. As the maximum flight times are less than 5 min, this is considered adequate.

All circuits not pressurized are limited to 27 volts on any exposed contacts.

Telemetry

In order to obtain a continuous check of the operation of the circuitry, various data are telemetered to ground receivers in the vicinity of the rocket launching site. These data are: Plate voltage, 26.5 volt battery supply voltage, Sun-Follower azimuth and elevation pointing angles, azimuth and elevation pointing error signals, azimuth magnadrive clutch currents. An FM-FM telemetering system using a single sub-carrier oscillator together with a commutator is used to transmit the required data.

Results of Flight Tests to Date

The history of the previous four Sun-Follower flights show a steady increase in over-all performance and in data gathered by the spectrograph.

The first flight started out with a bang; that is, the V-2 rocket on which the instruments were mounted blew up and was destroyed completely at take-off.

An Aerobee was used to carry the second Sun-Follower. The telemetry records for this flight indicated that the single azimuth sensing eye was pointing away from the sun, although the servo system was nulled. No data were obtained on the spectrograph camera.

An Aerobee was used again to carry the third Sun-Follower. Usable data were obtained on the spectrograph camera, although the servo system was oscillating about the null position. The oscillation apparently reduced the spectrograph exposure time.

A Viking rocket was used to carry the fourth Sun-Follower. Telemetry records indicated that at 120 sec after take-off the rocket began to roll and accelerated to 180 rpm at approximately 140 sec after take-off. This roll rate appreciably exceeded the Sun-Follower design roll rate of 120 rpm. At 200 sec the Sun-Follower finally lost track of the sun because of the high roll rate. There was little usable spectrographic data before 120 sec, due to the atmosphere; however, from 120 to 200 sec the Sun-Follower tracked sufficiently well to obtain the best data of the series so far.

The fifth and sixth Sun-Followers have been built, tested, and delivered by Aircraft Armaments Inc., to the Naval Research Laboratory where they are undergoing installation and check-out tests. The present schedule calls for the fifth and sixth Sun-Follower to be fired on an Aerobee rocket at White Sands Proving Ground about May 22, 1956.

Heat-Up Time of Wire Glow Plugs

S. K. CLARK¹

University of Michigan, Ann Arbor, Mich.

Nomenclature

- P = power input, units per unit time, based on the average resistance of the wire over the temperature range to be encountered
- A = specific heat of glow plug material \times weight of glow plug
- T_w = absolute temperature of glow plug wire at any time
- t = time
- B = emissivity \times surface area of glow plug wire \times Stefan-Boltzmann constant
- T_0 = absolute temperature of chamber walls to which glow plug loses heat by radiation
- T^1 = absolute temperature of plug wire at start of heating, i. e., $t = 0$
- $C = P + BT_0^4$
- $\gamma = (C/B)^{1/4}$
- $\alpha = 4B\gamma^4/A = 4Cl/A\gamma$
- $\beta = T_w/\gamma$
- $\lambda = T^1/\gamma$

THE time-temperature relationship in a wire resistance glow plug, used as a heat source starter in a reaction chamber, can be obtained with a considerable degree of accuracy by assuming that the primary heat loss of the wire is due to radiation effects. This assumption is justified in many respects since the chamber walls are usually quite close to the wire and almost completely surround it, and since the air remaining inside the system under actual starting conditions is usually stagnant or of negligible velocity. Knowledge of the time-temperature relationship allows the fuel injection to take place at the proper prescheduled time (temperature) after the power input to the glow plug has begun. Alternatively, if the time delay of fuel injection is fixed, solution to the problem enables the proper glow plug to be chosen for a specified set of conditions, such as a desired wire temperature at the time of fuel injection.

Neglecting convection and conduction, the differential equation governing temperature is

$$P = A \frac{dT_w}{dt} + B(T_w^4 - T_0^4) \dots [1]$$

where T_0 is assumed to remain a constant since the chamber mass is almost invariably many times larger than that of the glow plug. Equation [1] may also be written

$$\left(\frac{A}{B}\right) \frac{dT_w}{dt} + T_w^4 = \gamma^4 \dots [1a]$$

The solution of this differential equation can be obtained by direct integration of Equation [1a], written in the form

$$\int_0^t dt = - \left(\frac{A}{B}\right) \int_{T^1}^{T_w} \frac{dT_w}{(T_w^4 - \gamma^4)} \dots [1b]$$

by noting that

$$\left(\frac{1}{T_w^4 - \gamma^4}\right) = \left(\frac{1}{2\gamma^4}\right) \left(\frac{1}{T_w^2 - \gamma^2}\right) - \left(\frac{1}{2\gamma^4}\right) \left(\frac{1}{T_w^2 + \gamma^2}\right) \dots [2]$$

by expansion by partial fractions. The result is

$$t = \frac{A}{4B\gamma^3} \left[2 \left(\tan^{-1} \frac{T_w}{\gamma} - \tan^{-1} \frac{T^1}{\gamma} \right) - \ln \frac{(T_w - \gamma)(T^1 + \gamma)}{(T_w + \gamma)(T^1 - \gamma)} \right] \dots [3]$$

This may be conveniently reduced to dimensionless form by

Received January 10, 1956.

¹ Assistant Professor, Department of Engineering Mechanics.

noting that the constant γ is the equilibrium or steady state temperature of the wire, since from Equation [1]

$$(T_w) \frac{dT_w}{dt} = [P/B + T_0^4]^{1/4} = \gamma \dots [4]$$

Defining the dimensionless ratios

$$\frac{T_w}{\gamma} = \beta$$

$$\frac{T^1}{\gamma} = \lambda \dots [5]$$

$$\frac{4B\gamma^4}{A} = \frac{4Ct}{A\gamma} = \alpha$$

and assuming further that $T^1 = T_0$, or that the chamber and plug are at the same temperature at the instant resistance heating of the plug begins, Equation [3] becomes

$$\alpha = 2(\tan^{-1}\beta - \tan^{-1}\lambda) - \ln \frac{(\beta - 1)(\lambda + 1)}{(\beta + 1)(\lambda - 1)} \dots [6]$$

where the limits on the variables λ and β are

$$0 \leq \lambda \leq 1$$

$$\lambda \leq \beta \leq 1$$

Equation [6] may be shown clearly by a plot of α vs. β for various fixed values of λ . This is illustrated in Fig. 1. It is, of course, possible to solve this problem by numerical step-by-step integration, in which case the actual change in resistance with temperature of the glow plug wire may be used, again on a step-by-step basis. Comparison of results obtained by the use of Equation [3], using the average resistance of the wire over the temperature range encountered, with step-by-step calculations shows agreement to within 2 per cent on time to rise to a given temperature.

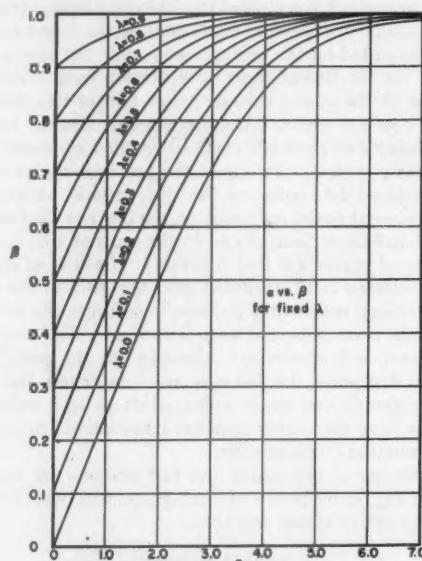


Fig. 1 α vs. β for fixed λ

As an example of the use of Fig. 1, assume the following specific wire plug:

Calculated equilibrium temperature = 1800 F

Fixed starting temperature = $T_0 = T^1 = 190$ F

Calculated $4C/A\gamma = 0.5$

To find: Time for wire to reach 1650 F

Calculate:

$$\lambda = 650/2260 = 0.287$$

$$\beta = 2110/2260 = 0.934$$

By interpolation, follow along the $\lambda = 0.287$ curve until reaching $\beta = 0.934$, at which point $\alpha \approx 3.8$. Then

$$\frac{4C}{A\gamma} t = \alpha = 0.5t \approx 3.8$$

$$t \approx 7.6 \text{ sec}$$

The largest uncertainty in the use of Fig. 1 or Equation [3] lies in the choice of the effective emissivity. In regard to this it should be pointed out that a single test in which all other constants are known except emissivity, and in which wire temperature is measured at a specific time before steady-state conditions are reached and again after steady-state conditions are reached, gives sufficient information to determine the average effective emissivity, since

$$B = \frac{A}{4t\gamma^3} \left[2(\tan^{-1}\beta - \tan^{-1}\lambda) - \ln \frac{(\beta - 1)(\lambda + 1)}{(\beta + 1)(\lambda - 1)} \right]$$

Comments on "Manifolds for Solid Propellant Rocket Motors"

HENRI VERDIER¹

Société d'Étude de la Propulsion par Réaction, Villejuif (Seine), Paris, France

Introduction

IN HIS paper "Manifolds for Solid Propellant Rocket Motors," Mr. Geckler gives a very interesting theory for computing the adequate size of manifold connecting two similar solid propellant rockets. However, the author says he does not know of any experimental tests verifying the validity of his equations.

Many static and flight tests have been conducted by SEPR with manifolds for double-base solid propellant boosters. In static tests, the mechanical and thermal behavior of the manifold was experimented by using nozzles with different throat areas in each rocket motor. Thus, an important mass flow rate of propellant gas was obtained in the manifold. From the results of those tests, experimental values of the factor CY used in Mr. Geckler's theory can be deduced as stated below.

Method for Determining CY

For two rocket motors having the same nozzle throat area A_n , interconnected by a manifold of cross-sectional area A_M , Mr. Geckler writes

$$A_M = A_n \frac{\Gamma(1-n)(\Delta p_i - \Delta p_f)}{2CY\sqrt{2p_{2f}\Delta p_f}} \dots [1]$$

where

$$\Gamma = \sqrt{\gamma} \left(\frac{2}{\gamma + 1} \right)^{\frac{\gamma + 1}{2(\gamma - 1)}}$$

$\gamma = C_p/C_v$ = ratio of specific heats
 n = pressure exponent in the burning rate rule
 CY = factor in the mass flow rate rule for the manifold

$\Delta p_i = p_{1i} - p_{2i}$ = pressure difference between the two chambers, without manifold

$\Delta p_f = p_{1f} - p_{2f}$ = pressure difference between the two chambers, with manifold

For two rocket motors having different nozzle throat

areas, A_{n1} and A_{n2} we can substitute for Equation [1] the following equation

$$A_M = \frac{\Gamma(1-n)[(A_{n1}p_{1i} - A_{n2}p_{2i}) - (A_{n1}p_{1f} - A_{n2}p_{2f})]}{2CY\sqrt{2p_{2f}(p_{1f} - p_{2f})}} \dots [2]$$

The factor CY is given by

$$CY = \frac{\Gamma(1-n)}{2\sqrt{2}} \times \frac{\alpha_1(p_{1i} - p_{1f}) - \alpha_2(p_{2i} - p_{2f})}{\sqrt{p_{2f}(p_{1f} - p_{2f})}} \dots [3]$$

where $\alpha = A_i/A_M \dots [4]$

The ballistic properties of the double base solid propellant used are known

$$\gamma = 1.26 \quad \Gamma = 0.66$$

$$n = 0.68 \quad 1 - n = 0.32$$

Besides $p_i = f(A_p/A_i, \theta) \dots [5]$

where A_p = propellant burning area
 θ = propellant temperature

For each test, the different terms of Equation [3] are known

$$\Gamma(1-n)/2\sqrt{2} = 0.074$$

A_{p1} , A_{p2} , A_{n1} , A_{n2} , and A_M are given; θ is measured; p_{1i} and p_{2i} are deduced from Equation [5]; p_{1f} and p_{2f} are measured; α_1 and α_2 are deduced from Equation [4]; we can then obtain numerical values for CY .

Experimental Results

Experimental results were obtained for values of: $\Delta p_f/p_{2f} = (p_{1f} - p_{2f})/p_{2f}$ varying between 1.5 per cent and 6 per cent.

The precision on numerical values of CY is small because $(p_{1f} - p_{2f})$ is not directly measured, but obtained as the difference between p_{1f} and p_{2f} with an important incertitude. Nevertheless, all the results with the type of manifold represented on Fig. 1 have given values of CY between 0.38 and 0.59

$$0.38 \leq CY \leq 0.59$$

$$CY = 0.48 \pm 0.11$$

Moreover, static tests have shown other advantages of manifolds than pressure equilibrium. Particularly, the simultaneity of ignition is very good (difference inferior to 0.01 s) and so is the simultaneity of extinction.

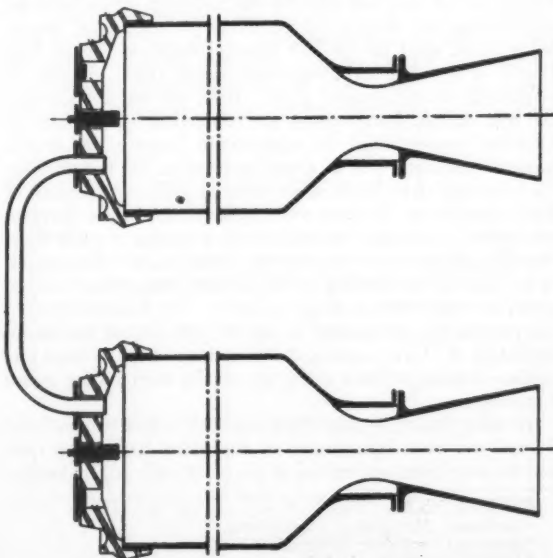


Fig. 1 Type of manifold used on SEPR boosters

Received Feb. 28, 1956.

¹ "Manifolds for Solid Propellant Rocket Motors," by Richard D. Geckler, *JET PROPULSION*, vol. 25, Oct. 1955, pp. 540-541.

² Engineer, Solid Propellant Rocket Department.

Measurement of Total Emissivity of Porous Materials in Use for Transpiration Cooling

E. R. G. ECKERT,¹ J. P. HARTNETT,² and T. F. IRVINE, JR.³

University of Minnesota, Minneapolis, Minn.

Introduction

TRANSPIRATION or porous-wall cooling is one of the more promising proposals for the maintenance of tolerable temperatures on surfaces subjected to intensive heating. The use of such transpiration cooling has been advocated for cooling combustion chamber walls, gas turbine blades, and external surfaces of high-speed aircraft subjected to aerodynamic heating. The equilibrium temperature of such transpiration-cooled surfaces is determined by a balance between the convective, conductive, and radiative heat transfer. In view of this, the knowledge of the radiative characteristics of porous surfaces is of considerable engineering importance. Such a study is currently under way at the Heat Transfer Laboratory of the University of Minnesota. The purpose of this note is to present a description of the test apparatus that is being used for the determination of the total normal emissivity values of a number of porous materials and to discuss its theory. In addition, total emissivity data are presented for a sintered bronze material. A more comprehensive report covering a number of porous materials will be presented at a later date.

Description of Apparatus

The test arrangement used in the present emissivity measurements is essentially the same as that first described by E. Schmidt (1, 2).⁴ It is illustrated in Figs. 1 and 2. The principal piece of equipment is the radiometer which is so designed that the radiant energy entering the opening (a) is collected by a 5-in.-diam gold surface mirror (b) and directed to the receiving surface of a thermopile (c) (Kipp and Zonen Microthermopile, E-3). The amount of radiant energy striking the thermopile is controlled by two orifices located in front of the thermopile. The deflection of a sensitive galvanometer attached to the thermopile gives a measure of the energy impinging on the thermopile surface. A black body or ideal radiator (d) constructed of copper and heated electrically serves as a reference for the radiation measurements. The porous test sample (e) is held in a balsa wood frame, balsa being used for its low thermal conductivity of 0.03 Btu/hr ft²F. The porous specimen is held tightly against an electrically heated copper plate. Both the black body and the test sample temperatures are controlled by varying the electrical power input to appropriate heaters. A double walled container (f) is arranged in front of the test sample. Its inner and outer surfaces are painted black with a paint of high absorptivity for long wave radiation and these surfaces are kept at a constant temperature by a stream of water flowing through the space between the double walls. Its purpose is to create a surrounding of well-defined temperature and to avoid any reflection of stray radiation. Its cylindrical opening permits the radiometer to see the test sample and an indentation of 1 1/4 in. diam and 4 1/2 in. long in the surrounding surface creates a black body (g) at the surrounding guard temperature.

In using this equipment the thermopile is first removed and is replaced by a light source of the same size. The radiometer may then be directed at the black body (d) by looking

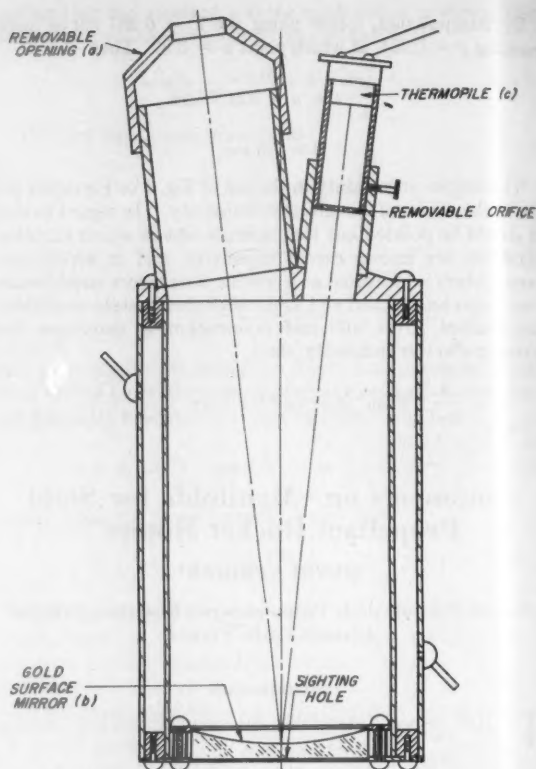


Fig. 1 Emissivity apparatus

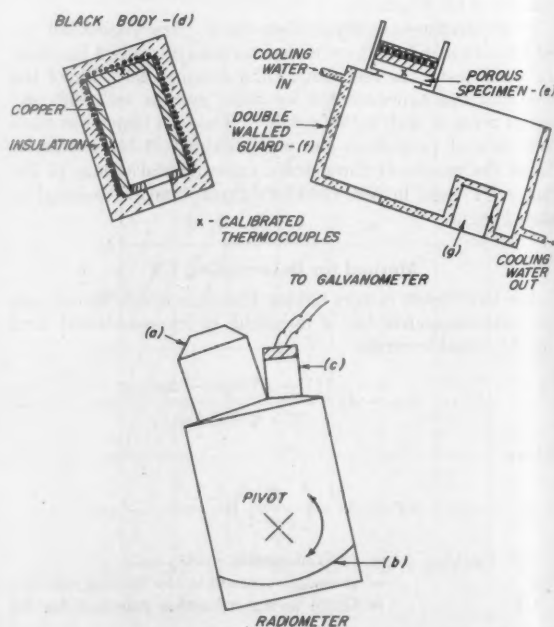


Fig. 2 Schematic of emissivity apparatus

through a sighting hole in the back of the radiometer. The unit is in proper adjustment when the light bundle, after reflection from the gold mirror, goes on through the opening in the black body without hitting the adjacent front walls. Similar checks are made on the sample and on the guard black body (g). The light is then removed and replaced by the thermopile. Then the galvanometer deflections oc-

Received Feb. 26, 1956.

¹ Professor, Mechanical Engineering.

² Assistant Professor, Mechanical Engineering.

³ Instructor, Mechanical Engineering.

⁴ Numbers in parentheses indicate References at end of paper.

carring when the radiometer points toward the porous surface (e) and the two black bodies (d) and (g) are recorded. These readings, in conjunction with the corresponding temperature measurements, allow the calculation of the emissivity of the sample.

Analysis of Data

The radiative energy flux leaving the black body at temperature T_s and arriving on a unit area of the thermopile is determined by the solid angle intercepted by the two diaphragms ahead of the thermopile and may be designated as G_1 .

$$G_1 = F\sigma T_s^4 \dots \dots \dots [1]$$

F is an angle factor determined by the geometry and position of the two diaphragms and σ is Boltzmann's constant.

Since the sample at temperature T_s is completely surrounded by a black container at a temperature T_g , the energy flux G_2 leaving its surface and arriving on a unit area of the thermopile is composed of the emitted radiation and the reflected radiation

$$G_2 = F\sigma[\epsilon_s T_s^4 + \rho_s T_g^4] \dots \dots \dots [2]$$

with ϵ_s indicating the emissivity and ρ_s the reflectivity of the test specimen.

With the assumption $\epsilon_s = 1 - \rho_s$, the following result is obtained from Equation [2]

$$G_2 = F\sigma[\epsilon_s(T_s^4 - T_g^4) - T_g^4] \dots \dots \dots [2a]$$

The radiant energy flux leaving the small black body in the guard surface at temperature T_g and arriving on a unit area of the thermopile is

$$G_3 = F\sigma T_g^4 \dots \dots \dots [3]$$

Subtracting Equation [3] from Equations [1] and [2a] and rearranging results in the following expression for the emissivity

$$\epsilon_s = \left(\frac{T_s^4 - T_g^4}{T_s^4 - T_g^4} \right) \left(\frac{G_2 - G_3}{G_1 - G_3} \right) \dots \dots \dots [4]$$

The assumption $\epsilon_s = 1 - \rho_s$ requires that the sample is sufficiently thick so that none of the impinging radiation leaves it through the back surface and strictly that the emissivity does not depend on wavelength. Equation [2a] is a good approximation even when the last condition is not fulfilled provided T_g is considerably smaller than T_s , or when both temperatures are nearly equal. The possible error on the end result of a variation of the emissivity with wavelengths has to be decided from case to case.

It now remains to relate the radiation fluxes, G , to the thermopile deflection, Δ . A heat balance may be written on the front face of the thermopile for the condition that it is irradiated by energy coming from the black body

$$C_1 G_1 = \sigma \epsilon_i T_{f1}^4 - q_{rad} + q_{loss} \dots \dots \dots [5]$$

where

c = loss factor accounting for absorption of energy by CO_2 and water vapor in air and by the gold surface mirror

ϵ_i = emissivity of thermopile

T_{f1} = temperature of exposed surface of thermopile

q_{rad} = radiant energy, absorbed by thermopile, originating from surrounding walls

q_{loss} = losses from thermopiles by convection and conduction

We may write similar expressions when the thermopile is subjected to radiation from the sample, and from the guard black body.

$$C_2 G_2 = \sigma \epsilon_i T_{f1}^4 - q_{rad} + q_{loss} \dots \dots \dots [6]$$

$$C_3 G_3 = \sigma \epsilon_i T_{f1}^4 - q_{rad} + q_{loss} \dots \dots \dots [7]$$

If the assumption is made that the decrease in intensity is equal in all cases ($C_1 = C_2 = C_3$), and that the environment radiation to the thermopile and the conduction and convection losses remain the same, we may write, on combining Equations [5], [6], and [7]

$$\frac{G_2 - G_3}{G_1 - G_3} = \frac{T_{f1}^4 - T_{f2}^4}{T_{f1}^4 - T_{f3}^4} = \frac{4T_{f1}^3(T_{f1} - T_{f2})}{4T_{f1}^3(T_{f1} - T_{f3})} \dots \dots \dots [8]$$

The error introduced in Equation [8] by writing it in the form on the right is quite small, with the numerator being in error approximately by the amount $1.5(T_{f1} - T_{f2})/T_{f1}$ and the denominator by $1.5(T_{f1} - T_{f3})/T_{f1}$. The value $T_{f1} - T_{f3}$ is of the order of 1 to 2 degrees, thereby giving an error of the order of 1/2 per cent in the numerator and denominator. The error in the quotient is probably less than this amount.

The assumption $C_1 = C_2 = C_3$ may not be admissible in all cases since the absorption of carbon dioxide and water vapor depends strongly on wave length. Provision is, therefore, made to flush the radiometer with a nonabsorbing gas.

The thermopile indication Δ is directly proportional to the differential between the front side temperature, T_{f1} , of the thermopile and the unexposed back side temperature, T^* .

Therefore, when the radiometer is sighted on the black body, the indication is

$$\Delta_1 = k(T_{f1} - T^*) \dots \dots \dots [9]$$

The thermopile is so constructed that T^* remains constant when the radiometer is directed toward the other surfaces, yielding the following relations

$$\Delta_2 = k(T_{f2} - T^*) \dots \dots \dots [10]$$

$$\Delta_3 = k(T_{f3} - T^*) \dots \dots \dots [11]$$

Substituting Equations [9], [10], and [11] in Equation [8], and combining with Equation [4], we arrive at the final relationship for ϵ_s

$$\epsilon_s = \left(\frac{T_s^4 - T_g^4}{T_s^4 - T_g^4} \right) \left(\frac{\Delta_2 - \Delta_3}{\Delta_1 - \Delta_3} \right) \dots \dots \dots [12]$$

Thus the knowledge of the three temperatures and the deflections $\Delta_2 - \Delta_3$ and $\Delta_1 - \Delta_3$ allows the calculation of the emissivity of the porous sample.

Total Emissivity Values for Porous Bronze

Data were obtained for a sintered bronze material currently used for transpiration cooling experiments. The test sample of 4 in. sq was removed from a large plate 14 in. wide and 72 in. long \times 1/8 in. thick. Its porosity is such that an 8 psi differential across the plate allows an air flow of 0.55 lb per sq ft per sec. It was fabricated by Powdercraft, of Spartanburg, South Carolina. The surface roughness of the plate

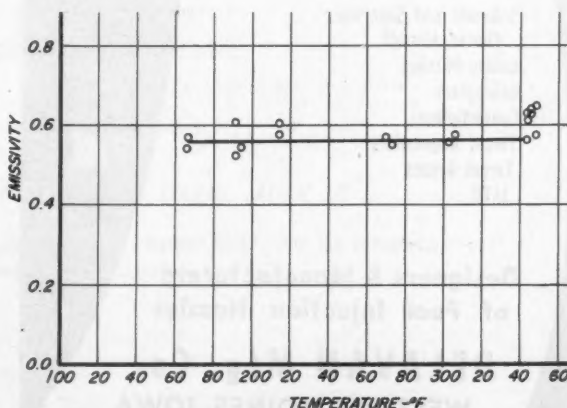


Fig. 3 Total normal emissivity of porous bronze

delavan NOZZLES

FOR:

Liquid Propellant Rockets
Ramjets
Pulsejets
Turbojets
Turboprops

POWERING:

Subsonic and Supersonic
Piloted Aircraft
Guided Missiles
Helicopters
Convertiplanes
Thrust Augmenters
Target Drones
JATO

Designers & Manufacturers
of Fuel Injection Nozzles
DELAVAN Mfg. Co.
WEST DES MOINES, IOWA

was found to have an absolute average roughness value of 0.0005 in. when it was measured with a Brush Surfindicator having a stylus with a tip radius of 0.0005 in.

The test results are presented in Fig. 3 and cover a temperature range of 160 F to 350 F. The emissivity value found for this material is 0.57 ± 0.04 . At 350 F the sintered bronze rapidly oxidized which resulted in an increase in the emissivity value to 0.63.

The emissivity value of the solid bronze surface obtained by grinding the porous test specimen to close the openings was measured and found to be 0.04 at 150 F. This is an order of magnitude lower than the value for the porous surface and emphasizes the possible error involved if emissivity values for solid surfaces are used to predict the radiative heat transfer from porous materials.

Acknowledgments

The authors acknowledge the able assistance of R. Eichhorn and Richard Birkebak in the design of the radiometer and, in addition, wish to express appreciation to F. J. Bradac for his skillful construction of the radiometer.

References

- 1 Schmidt, E., "Bericht über Messungen der Gesamt-Strahlung von Aluminiumflächen," *Hauszeitschrift der VAW u.d. Erftwerk A. G. für Aluminium*, vol. 2, 1930, p. 91.
- 2 Schmidt, E., "Messung der Gesamtstrahlung des Wasserdampfes bei Temperaturen bis 1000°C," *Forschung Geb. Ingenieurwesen*, vol. 3, 1933, p. 57.

The Near-Constancy of Full-Power Duration for Unboosted Rocket Vehicles

WILLARD P. BERGGREN¹

University of Bridgeport, Bridgeport, Conn.

THE firing duration (at constant thrust) of a rocket engine which constitutes the sole propulsion system of a piloted craft or single-stage missile may conveniently be expressed in terms of the initial thrust-weight ratio F/W_0 , the mass ratio ζ , and the specific impulse I_{sp} ,

$$T = I_{sp} \zeta W_0 / F \dots \dots \dots [1]$$

One example of magnitudes, for a piloted aircraft, might be $I_{sp} = 220$ sec, $\zeta = 0.5$, $F/W_0 = 1.0$, for which combination $T = 110$ sec. Thus, a rocket-propelled fighter of moderately high performance might operate less than two minutes at full throttle.

A second typical set of magnitudes for insertion into Equation [1] would apply to a missile of advanced design where $I_{sp} = 250$, $\zeta = 0.9$, $F/W_0 = 3.0$; giving a duration $T = 75$ sec. This vehicle would, if launched vertically, reach a speed of the order of Mach 2.5 at 15,000-ft altitude and an acceleration of 30 g's at burnout. These conditions might be intolerable because of drag and stress, respectively, and a 25 per cent reduction of design thrust ($F/W_0 = 2.25$) would result in $T = 100$ sec.

It is rather striking to find this latter figure so near to the full-throttle duration of the piloted aircraft considered in the first example. This near-constancy of full-powered operating time for unboosted vehicles of widely varying designs has been recognized for some time; however, the elementary Equation [1] may be an aid to quick visualization of the influence of basic design parameters in this regard.

Power plant design questions of a most fundamental sort, such as pressurization and cooling, depend upon firing duration. Because of the near-constancy of duration often found, these questions may have unexpectedly similar answers for widely different applications.

Received Dec. 29, 1955.

¹ Director of Engineering.

THE AMERICAN ROCKET SOCIETY 1956 ROSTER

Will Carry Your Advertising Message
for the Next

**TWELVE IMPORTANT MONTHS
TO MORE THAN 5000 ARS MEMBERS**

The titles of these members suggest the influence they have in their field. Some of these titles, taken from the listings of typical organizations in last year's Roster, are shown below:

One Missile Firm

Supervisor, Propulsion Division
Director, Aerophysics Department
Manager, Rocket Engine Field Laboratory
Group Leader, Instrumentation and Equipment
Group Leader, Flight Test

Senior Design Engineer
Instrumentation Design Specialist
Supervisor, Rocket Engine Facility
Research Engineer-in-Charge of Turbojet Test Lab and
Hot Fuel Test Lab
Supervisor, Preliminary Design

One Missile Proving Ground

Chief, Solid Propellant Section
Chief, Engineering Division
Chief, Propulsion Branch
Chief, Instrumentation and Standards Branch
Chief, Microwave Branch
Chief, Analog Simulation Section
Chief, Systems Evaluation Branch

Chief, Design and Preparation Section
Chief, Range Facilities Control
Chief, Instrumentation Engineer
Commander
Executive Operations Officer
Assistant Chief, Missile Flight Safety Office
Chief, Communicating and Instrumentation Branch

One Government Arsenal

Chief, Guidance Design Section
Chief, Missile Firing Laboratory
Chief, Reliability Office
Chief, Fuselage Design Section
Chief, Test and Evaluation Branch
Chief, Structures and Mechanics Branch
Technical Advisor to Chief, National Procurement
Division

Chief, Internal Ballistics Section
Chief, Technical and Engineering Division
Deputy Chief, Ammunition Division
Chief, Interior Ballistics Section
Chief, Combustion and Fuel Laboratory
Chief, Guided Missile Development Division
Chief, Propulsion Meas. Laboratory

One University Jet Propulsion Research Center

Senior Development Engineer
Section Chief, Guidance Systems Section
Senior Research Engineer
Propulsion Supervisor
Section Chief, Solid Rockets

Chief, Design and Development Section
Division Chief, Guided Engineering
Chief, Propulsion Section
Research Instrumentation Engineer
Senior Resident Engineer

One Government Flight Research Center

Head, Machine Design
Head, Rocket Thermodynamics Section
Head, Rocket Combustion Section

Chief, Fuels and Combustion Research Division
Associate Director
Chief, Rocket Branch

CLOSING DATE: JUNE 15 PUBLISHING DATE: JULY 10

Make space reservations now, at advertising rates applicable to JET PROPULSION, with the advertising representatives listed on page 225, or directly to:

1956 Roster
American Rocket Society
500 Fifth Avenue
New York 36, New York

Jet Propulsion News

Alfred J. Zashringer, American Rocket Company, Associate Editor

Norman L. Baker, Indiana Technical College, Contributor

Jet Aircraft, Engines

TRANSPORTS. New version of the Boeing 707 jet transport is called the Intercontinental (*photo*). The plane will gross 290,000 lb and will carry 124 or 145 passengers. The range will be over 4000 miles. Power will come from four P&W JT4 turbojets. Specifications include: length, 146 ft, 8 in; span 141½ ft; payload will be 36,500 lb; fuel capacity is 21,200 gal. All models will be equipped with the new Boeing-developed combined sound suppressor and engine thrust reversers. Pan American World Airways has ordered 12 jets for delivery in August, 1959. Other orders include: 4 for Continental Air Lines; Air France, 10; Sabena Belgian World Airlines, 3; and 5 for Braniff Airways.



Boeing

Intercontinental jet transport

- Orders for the Douglas DC-8 jet are also rolling in. Eastern Airlines has ordered 26, Scandinavian Airlines 7. Orders now total 95. Douglas has stated that although the J-57 turbojet is presently provided for in the DC-8, use of the Rolls-Royce Conway bypass engine is also under consideration for foreign use.

- Other jet transports have also been making news. The Comet 3 on a round-the-world flight is expected to cover 30,000 miles in a flight time of about 68 hours. The Comet 3 is a prototype of the Comet 4 which goes into public service in 1959. Comet 4 will carry 60-76 passengers over stage lengths of 2700-3000 miles. Optimum cruising speed is Mach 0.74 (about 500 mph). Maximum takeoff weight will be around 152,000 lb.

- Deliveries of the Britannia, Britain's latest turboprop transport, will be made in 1957 to Canadian Pacific Airlines. The Britannia carries 100 passengers at 400 mph and at ranges up to 6000 miles.

- Douglas Aircraft Co. has announced that 25 DC-8 jet airliners were sold to Pan American World Airways. The Pan Am purchases, first for the DC-8, were in excess of \$160 million. Deliveries are scheduled for 1959. Another order for 30 DC-8's was placed by United Airlines. Deliveries are also scheduled in 1959. It is expected that flight times in the U. S. will be materially reduced. For example, the Chicago-New York run will be around 1½ hr (about 1 hr less than best existing times) while the Los Angeles-New York trip will be around 4½ hr (about 3 hr better than existing runs).

- The Air Force has ordered the Convair B-58 supersonic bomber into initial production and the building stage is near at Fort Worth, Texas.

JET ENGINES. The 500th gas turbine engine was completed by Boeing. The engine was one of the 502-7 series. The latest production engines weigh 320 lb complete with accessories and oil. It produces 270 hp maximum and 240 hp on a continuous basis. Specific fuel consumption is about 1 lb/hp/hr. Time between overhauls will be about 1000 hours. An automobile equipped with a similar gas turbine engine, for example, would travel at over 100 mph and would travel over 100,000 miles without engine overhaul. It is anticipated that by 1957, the fuel consumption of these engines can be expected to drop to about 0.7 lb/hp/hr and making it competitive with gasoline engines of the same power output. A 175-hp engine was successfully used to propel a 24-ft Navy personnel boat (*photo*).



Boeing

Gas turbine afloat

- Precision forging of titanium jet turbine blades was announced by the Canadian Steel Improvement, Ltd. Secret of the process lies in protecting the titanium during forging and heat treatment. The process was developed for Orenda Engines in Malton, Ontario. The blades are to be used on turbojets now being produced for the Avro CF-100.



deHavilland

Static test of SUPER SPRITE

FIGHTERS. New drag chutes were recently installed on the F-84F jet planes and have given landings in only 2400 ft. This is 1000 ft shorter than the normal landing without chute. The chute is 16 ft in diameter and trails 35 ft behind the craft. At 130 knots, the drag of the chute is about 8000 lb. The equipment is being installed on present production equipment.

- First flight of the F-105A, the USAF-Republic supersonic fighter-bomber has been completed at Edwards AFB, Calif. The model is powered by a P&W J-57 turbojet engine of 10,000-lb thrust. The craft has short, very thin swept wings, a long cylindrical fuselage, wing-root air scoops, and a one-piece flying tail that sets low on the aft fuselage section. Unusual feature of the ship is a vertical fin on the bottom aft fuselage section for lateral stability. Classed as a weapons system, the F-105A can carry nuclear weapons, as well as conventional bombs and rockets.

- Crusader, the F8U-1 jet fighter by Chance Vought is to be produced under a \$100 million production order. The carrier based Navy fighter has flown supersonically in level flight and gets its thrust from a P&W J-57-P-12.

- Two light fighters have been in the news. The British Folland Gnat has hit close to Mach 0.95 in flight tests. Ceiling of the small 7000 lb craft is above 50,000 ft. Powered by a Bristol Orpheus turbojet of about 4000 lb thrust, specs are: span, 22 ft, 2 in; length, 29 ft, 9 in. The French Dassault Mystere 22 is a NATO fighter grossing 12,000 lb. With a 45-deg sweepback, the craft is powered by two Turbomeca jets of 2200 lb thrust each. Armament is expected to be 30-mm cannon, rockets, and external stores.

- The Soviets have disclosed that their twin-jet medium bomber has a range of about 3000 miles. The bomber has also been modified for use as an airliner.

Facilities

- DuMont has consolidated its missile work in a new Missiles Engineering Department. Los Angeles may be the site for this group.

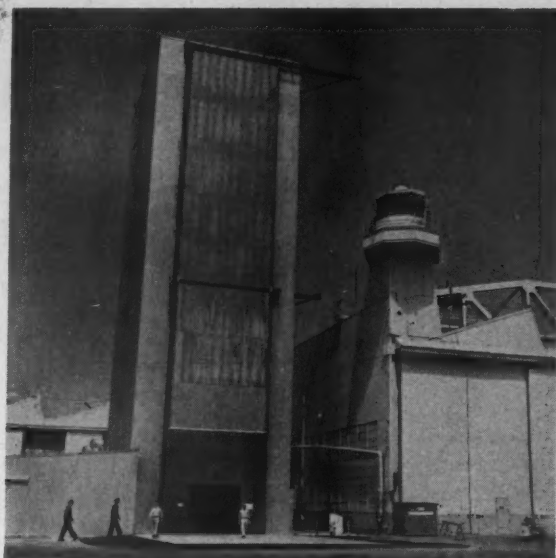
- Sperry Rand Corp. is locating its new Air Division in Phoenix, Ariz., and will include work on drones and pilotless aircraft.

- Steel RATO sub-assemblies will be made by the Norris-Thermador Corp. in a new \$2 million plant at Waco, Tex. Work will be concerned with the new T-60 RATO being produced by Phillips Petroleum at McGregor, Tex.

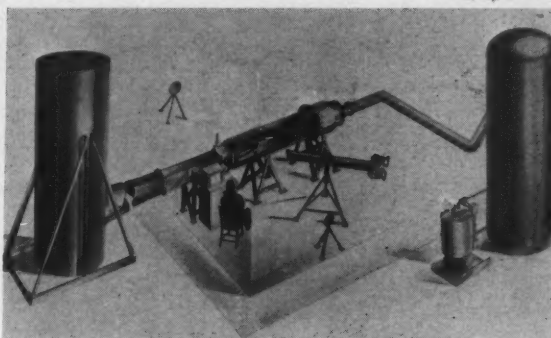
- Philadelphia has been selected as the new headquarters of the Special Defense Projects Department of General Electric. The department is currently engaged in research and development work on several large weapons systems in the guided missile field. The move from Schenectady will take place in mid-1956 and total employment will be about 1000 personnel.

- Rocketdyne is the name of the rocket division of North America Aviation. Headquarters of the \$9.5 million establishment is taking shape at Canoga Park in the San Fernando Valley of Calif. Rocketdyne will be responsible for the design, development, manufacture, and tests of rocket power plants for aircraft and missiles and for the design and development of small caliber aircraft rockets. The division supplies the ATO rocket for SM-64 NAVAHO and rocket power plants for ATLAS and REDSTONE. Downey Division is now working on SM-64 (photo). All large rockets, however, are static tested at the Simi Hills Field Test Laboratory in the Santa Susana Mountains.

- Two new supersonic wind tunnels were announced by industry. Republic Aviation is to build a Mach 4 tunnel costing \$12 million at its Farmingdale, N. Y., facility. Boeing is putting the finishing touches on its 9 x 9-in. tunnel at Wichita, Kan. This tunnel is also of Mach 4 design (photo).



Simulation tower for flight loads on NAVAHO
North American

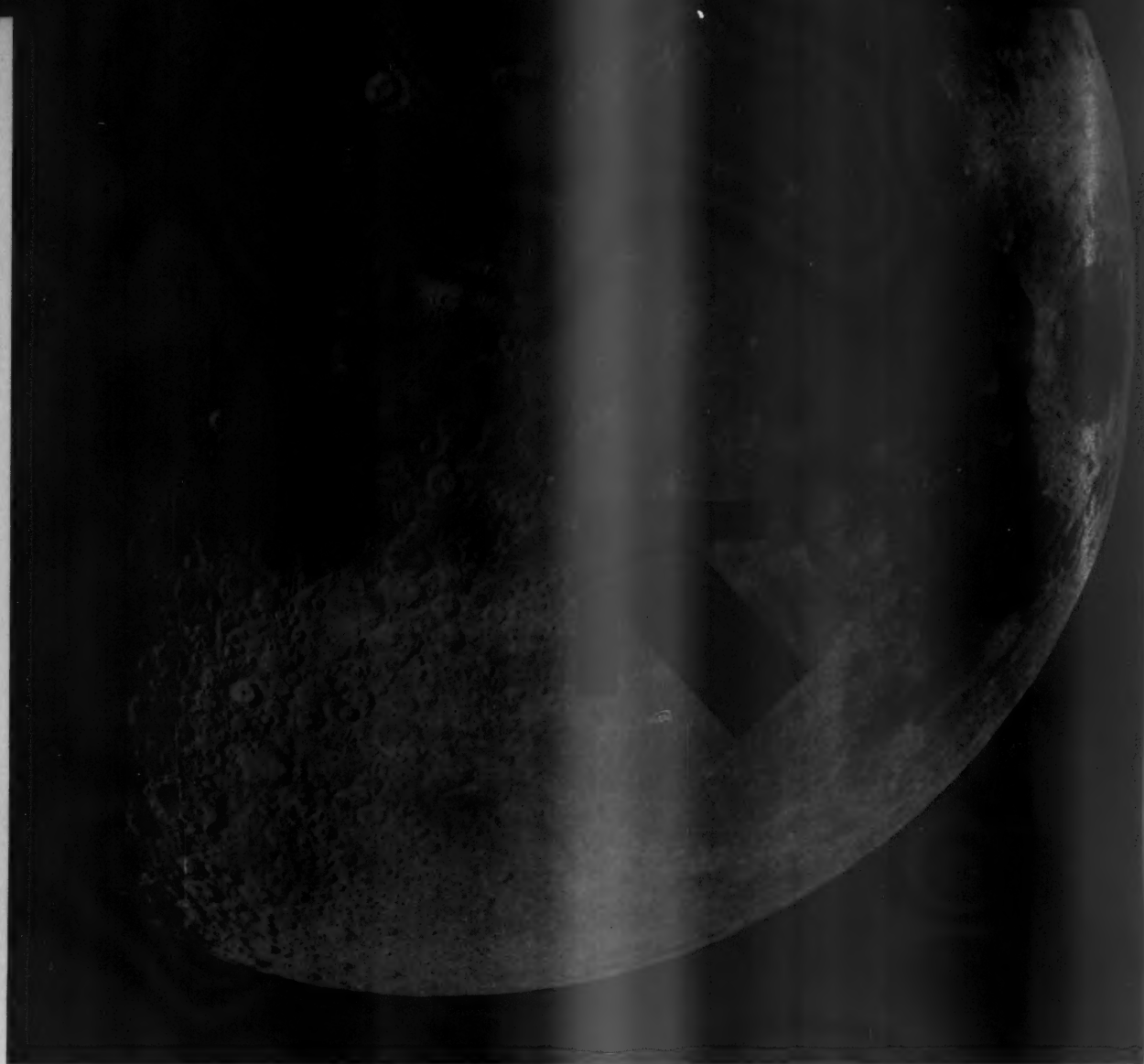


Supersonic wind tunnel. Compressed air stored in tower at left passes instrumented test section (center) and expanded and discharged through tower at right
Boeing



ARS Regular Feature on Detroit T. V.

"Rocket Digest" is a regular Friday night ARS program on Detroit Station WTVS. Featured on the show is Alfred J. Zaehring (left), Associate Editor of JET PROPULSION. Recently a live firing was made of one of Zaehring's medium size gas generator units—the smokeless, odorless, variety. The half-hour program is moderated by ARS member Donald J. Kenney (right), a member of the faculty at the University of Detroit.



NEW FRONTIER

"If we had to put a man on the moon, we could do it."

—Overheard at an Institute of Aeronautical Sciences luncheon

This impromptu statement was not a matter of idle conjecture. It was a statement of a positive and scientific fact — as provable as if he'd said the Aleutian Islands — and contingent only upon three prime requisites: enough time, money, and necessity. And by "we" he meant today's mindpower and facilities oper-

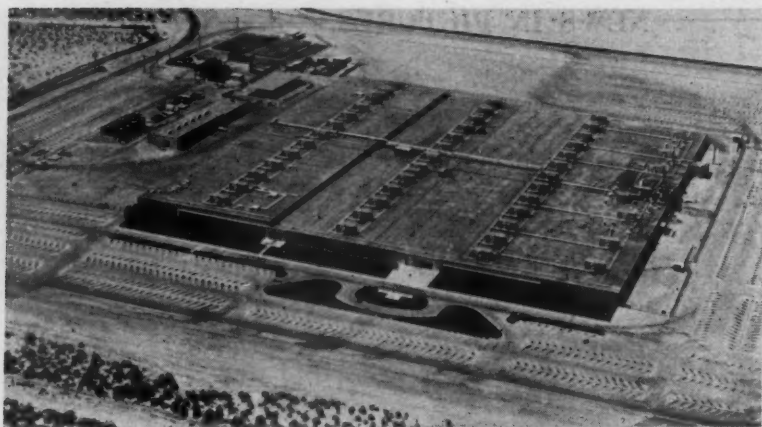
ating under the most advanced concepts of research and development.

Those concepts as practiced at Martin today would be essential to the fastest possible solution of any complex flight systems problem now within the capacity of man to solve.

It is this that has established Martin as one of the prime forces in the coming conquest of the new frontier — Space itself.

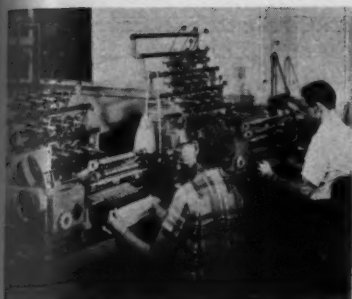
MARTIN
BALTIMORE

Modern Falconry



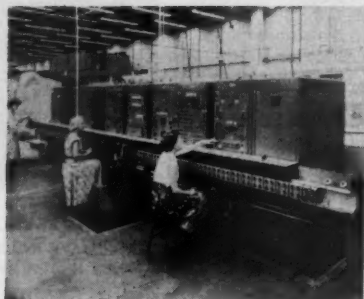
Hughes

Falcon Nest... Home of the FALCON is at the Tucson, Arizona, plant of Hughes Aircraft Co. Designed for the GAR-1 production, the plant, with 12 acres under one roof, was constructed in 1952 at a cost of \$8 million. It contains over \$6 million of production equipment and \$15 million of special test equipment



Hughes

Missile Bobbins... FALCON's "innards" are fashioned on these multiple-coil winding machines each winding 12 coils of copper wire. Coils will be used in electromagnets for control system. Entire plant is air conditioned at higher than atmospheric pressure to guard against dust



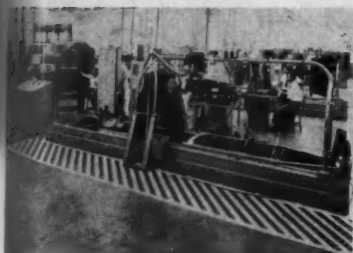
Hughes

Tube Tester... Capable of testing over 600 vacuum tubes per hour, this automatic machine is loaded at left. Shock and vibration are among some of the tests simulated



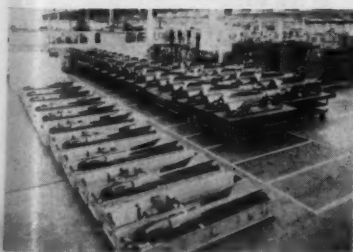
Hughes

Shaping Up... Forward sections, magnesium shells, begin to take shape on this sheet metal assembly line



Hughes

Cradled... FALCON is about to undergo vibration tests suspended in this cradle. Shock tests are conducted in the bottom of the cradle. Note altitude test chamber in background



Hughes

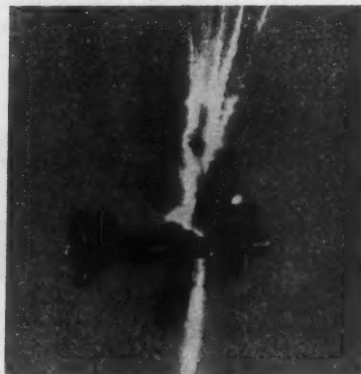
Missile Row... Final assembly and testing completed, the birds are boxed for shipment to the Air Force



(Left)

Hughes

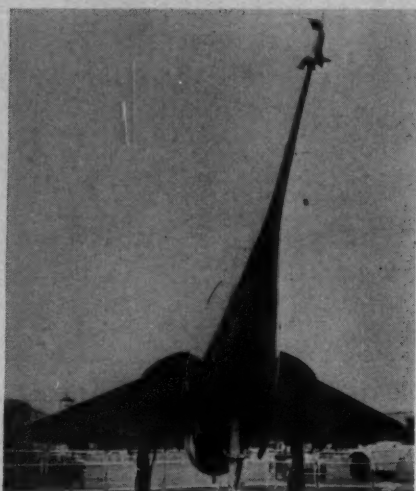
Bird in Hand... Smallest guided missile in production, the GAR-1 tips the scale at over 100 lb. Power comes from a Thiokol solid propellant rocket motor. Although having a typical canard layout with small forward fins and large aft supporting surfaces, the forward wings are fixed and steering is accomplished by control surfaces hinged to the trailing edge of the stabilizers. A round nose fairing into the cylindrical fuselage which terminates in a boat-tail housing rocket exhaust nozzle



Thiokol

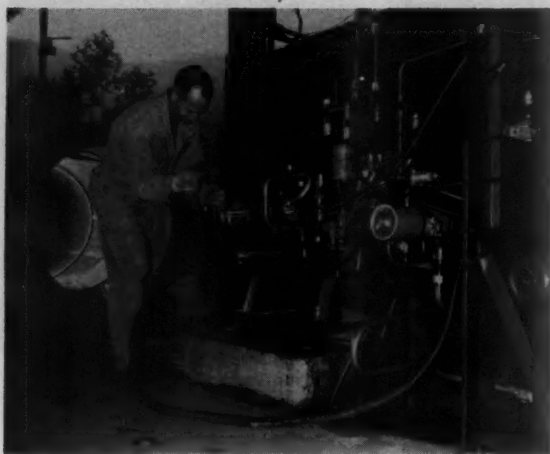
Falcon Strikes... Makes direct hit on target drone aircraft in tests

NEWS IN PICTURES



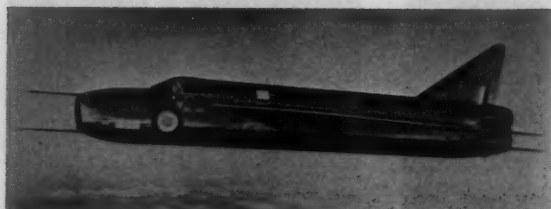
British Information Services

DROOP-SNOOT. . . Second British aircraft capable of supersonic speed in level flight is this Fairey Delta 2, single-seat craft with an elongated nose that can be lowered like a drawbridge to give pilot better vision for landing, take-off, and taxiing. Wing span is 26 ft, 10 in; length is 52 ft, 3 in.



JPL

PLUMBERS NIGHTMARE. . . Technician finishes hooking up a liquid rocket motor for test. Note observation window in center, armor plate at right protecting vital components, exhaust silencer at left



British Information Services

BUGLIKE. . . English Electric P-1 interceptor was the first British plane to hit sonic speed in level flight. It has been flying since 1954 and has made over 100 flights. 20 preproduction models have been ordered by the RAF



British Information Services

GROUND LEVEL EJECTION. . . British ejection seat has successfully worked at ground level and speeds of 130 mph. Top, dummy is fired from aircraft. Bottom, it parachutes to safety



University of Michigan

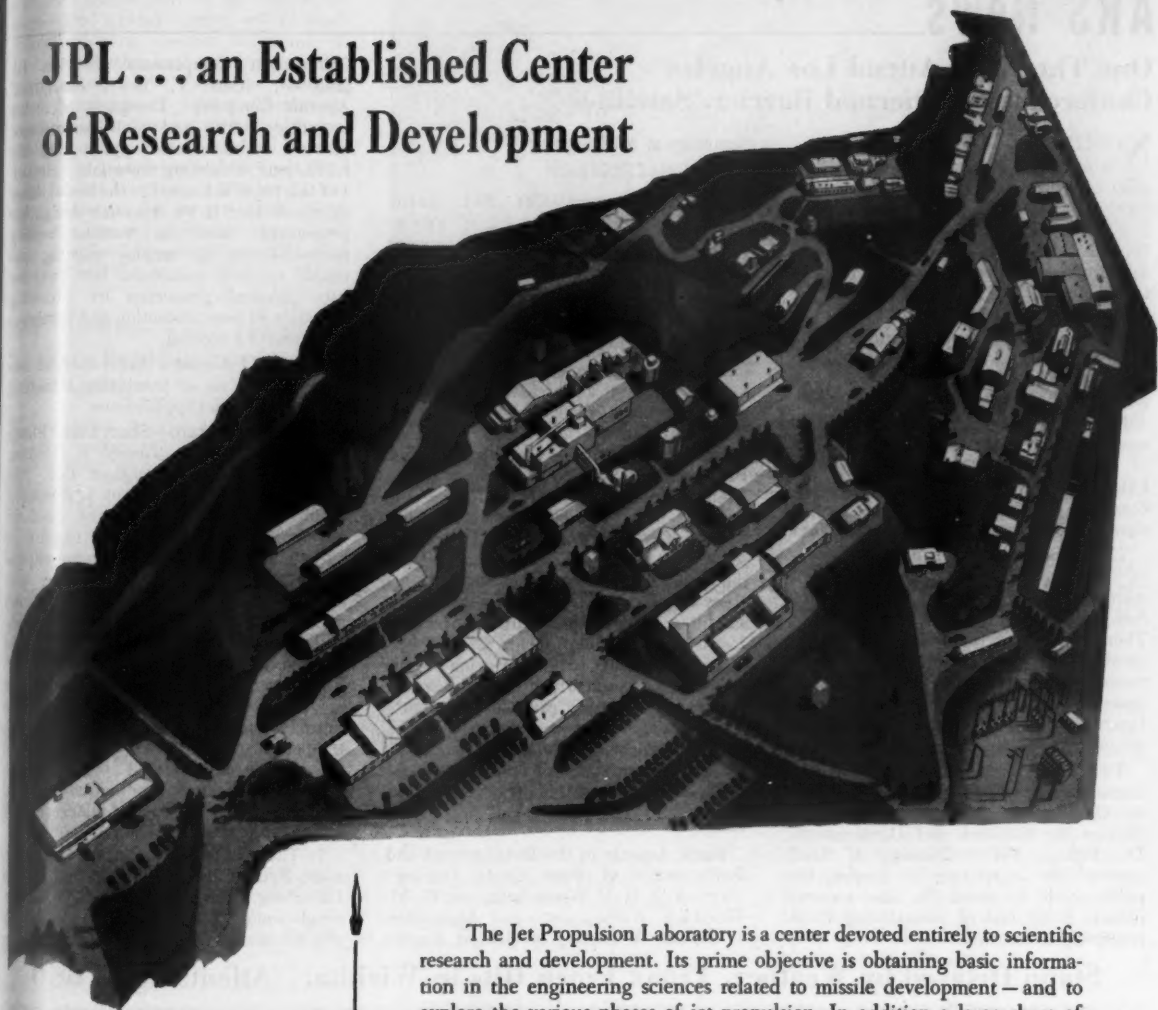
HOT CAN. . . Observers watch progress on J-47 turbojet burner in test stand



Aerojet-General

AND AWAY WE GO. . . PV-1 airplane equipped with internally mounted rocket engines makes take-off. Two 15KS-1000 units are being used here

JPL... an Established Center of Research and Development



★ At this time we are particularly interested in interviewing graduate engineers and scientists in the fields of aerodynamics, aircraft structures, mechanical engineering, chemistry, chemical engineering, heat transfer, electronics, systems analysis, electro-mechanical instrument design, instrumentation, metallurgy, nuclear physics and solid state physics.

These men should be definitely interested in scientific research and development relating to the problems of the future.

The Jet Propulsion Laboratory is a center devoted entirely to scientific research and development. Its prime objective is obtaining basic information in the engineering sciences related to missile development — and to explore the various phases of jet propulsion. In addition a large share of its program is devoted to fundamental research in practically all of the physical sciences.

The Laboratory extends over more than 80 acres in the foothills of the San Gabriel mountains north of Pasadena. It is staffed entirely by personnel employed by the California Institute of Technology and conducts its many projects under contracts with the U.S. Government.

Exceptional opportunity for original research coupled with ideal facilities and working conditions have naturally drawn scientists and engineers of a very high caliber. These men, working in harmony, are building a very effective task force for scientific attack on the problems of the future.

An unusual atmosphere of friendliness and cooperation is apparent at the "Lab" and newcomers soon sense the warmth of their acceptance. New advanced projects are now providing some challenging problems — and good jobs for new people.

If you would like to develop your skill and knowledge at the "Lab" and, at the same time, help us solve some of our problems — write us today.

CALTECH

jpl

JET PROPULSION LABORATORY

A DIVISION OF CALIFORNIA INSTITUTE OF TECHNOLOGY
PASADENA, CALIFORNIA

ARS News

One Thousand Attend Los Angeles Conference on Thermal Barrier, Satellites

NINETEEN SESSIONS—including one ARS session which was conducted twice in order to accommodate demand—featured the March 14-16 ARS-ASME Aviation Division Conference at the Hotel Statler, Los Angeles. Cosponsors were the ASME Instruments and Regulators Division and the Institute of the Aeronautical Sciences.

Two sessions were run under ARS sponsorship. One of them, on Earth Satellites, attracted a total of some 600 people in two repeat sessions.

David Shoner of Aerophysics Development Corporation was ARS chairman of the meeting. The ASME Aviation Division Chairman, George T. Hayes, Stanford Research Institute, announced that total registration approached 1000.

The Aviation Division offered sessions on Air Cargo (market analysis, commercial applications, military research forecast, military applications); on the Thermal Thicket (human factors, structural materials, optimum airframe structures, accessory drives, factor of safety concepts, propulsion, controls) and the Instruments and Regulators Division on aircraft instrumentation.

Two luncheons were held and the featured speaker at the banquet was C. C. Furnas, Assistant Secretary of Defense for Research and Development. Dr. Furnas, Fellow Member of ARS, stressed the importance of keeping the public well informed on the nation's defense setup and of maintaining U. S. leadership in research.

Summary of ARS papers:

EARTH SATELLITES

Project Vanguard—The IGY Earth Satellite (289-56), F. R. Furth, Farnsworth Electronics Company. Successful construction and launching of the satellite will demand going to the present limits—or beyond—our engineering knowledge in many fields. Admiral Furth discusses the problems involved, the techniques to be followed, and the roles to be assigned to various military and scientific organizations concerned with implementing the three-year project.

Scientific Aspects of the Satellite Program (288-56), W. H. Pickering, Jet Propulsion Laboratory, California Institute of Technology. Observations made in the field of upper-atmosphere research are briefly reviewed, followed by a discussion of the actual scientific observations which can be taken from the earth satellite. Many experiments can be performed with no instruments aboard, but other experiments require carrying instruments of a type in which the data can be sent to the earth by radio. First flights will certainly carry experiments to measure the kind of environment existing on the satellite because this factor will affect the operation of instruments.

HIGH TEMPERATURE MATERIALS

Some Aspects in the Development and Performance of Pure Oxide Coating: (Section 1), R. V. Westerholm and W. M. Wheildon, Norton Co.; and **Application of Rokide A Coating to Ramjet Engine**

Combustion Components (Section II) (295-56), Alan V. Levy, Marquardt Aircraft Company. Designers of rocket propulsion units and high performance aircraft turbines are approaching the limitations of existing materials. Section 1 of this paper is limited to the broad line of approach that if we discount design improvement (such as various cooling methods) we can employ existing materials to their maximum low temperature physical properties by providing adequate surface protection and insulation by means of a coating.

Section II discusses flame-sprayed alumina coating as an insulating refractory coating for ramjet applications.

High Temperature—Short Lived Plastic Laminates (292-56), Gerald E. Dodson, H. I. Thompson Fiberglass Co. New design concepts and higher performance requirements have shown the need for developing plastic laminates capable of withstanding extremely high temperatures (2000 to 5000 F). Temperature span includes the melting points of most metals and is far beyond the long time temperature resistance of any plastic material (including the irradiated materials). There are three families of plastic resins in use that are suitable both costwise and reproducibility-wise for use in the high temperature ranges. These resin families are discussed in detail together with general manufacturing techniques designed to utilize the best physical characteristics of the laminates.

Is There a Thermal Barrier for Supersonic Ramjet Tailpipes? (293-56), Walter Unterberg, Marquardt Aircraft Company, Single-walled metal tailpipes, internally ceramic-coated where necessary, encounter

Stapp Delayed by Weather, Truax Pinch Hits in Wichita. Attendance: 660



(Wichita Eagle)

HE PINCH HIT

Commander Robert C. Truax, national Vice President of ARS, was slated only to present the charter to the newly formed Wichita Section on Jan. 27. On his arrival, however, he found that the scheduled speaker, Lt. Col. John P. Stapp, renowned aeromedical scientist, had been delayed by weather, and 460 dinner guests were present to hear him speak. Commander Truax, again demonstrating the stuff of which old time rocket men are made, went "on" and regaled his audience with the "old days" in the liquid propellant field. He is shown above (third from left) with John P. Gaty, Vice President of Beech Aircraft; James F. Reagan, Beech's manager of missile engi-



HE WENT ON ANYWAY

neering and President of the Section; and Brig. Gen. L. C. Coddington, Commander of McConnell Air Force Base.

On the following day, Col. Stapp did arrive and 200 "second nighters" appeared at McConnell Air Force Base to hear his lecture on his rocket sled experiments. Above photo shows Col. Stapp (left) with Lawrence J. McMurtrey, power plant staff engineer at Boeing Airplane Co., and Vice President of the Section; and Dr. Reagan. They are inspecting a model space vehicle designed and built by David Henderson, an aeronautical engineering student at the University of Wichita and member of the Section's board of directors.

a thermal barrier only in the high Mach number-low altitude region where more complex cooling means are required. A high-performance variable-geometry "paper" ramjet was chosen as example, with internal gases at 4000 F throughout, near the maximum obtainable from hydrocarbon-air combustion. Graphs show how the tailpipe metal temperature at thermally critical locations is affected by the major variables of steady state flight conditions, ground and air launch transients, tail-pipe exit geometry, wall thickness, and wall material.

New Mexico-West Texas Section Establishes Scholarship

TO stimulate interest in rocketry and provide assistance to a qualifying junior student during his senior year at New Mexico College of Agriculture and Mechanic Arts, a \$200 scholarship will be given by the New Mexico-West Texas Section. The award will be made at the June Commencement for the best paper on a subject related to the field of rocketry. Papers must be submitted for certification of standing and classification through the dean of the appropriate school and received by the Section by May 1, 1956.

More Student Chapters Forming

FOUR more student groups have submitted by-laws and petitions to become chartered as student chapters of ARS. The University of Michigan student chapter was first to be chartered, on December 8, 1955.

The new units and their officers are as follows:

Academy of Aeronautics, Flushing, N. Y.

President, Alex Havriliak
Vice President-Treasurer, Anthony Varvaro
Secretary, Norman Lange
Faculty Advisor, Ralph Hautau

New York University, Bronx, N. Y.

President, Ned Greenberg
Vice President, Bertram Kramer
Secretary, Larry Gottlieb
Treasurer, Andrew Dapuzzo
Faculty Advisor, Michael Maccarone

Polytechnic Institute of Brooklyn, Brooklyn, N. Y.

President, Donald Morin '57
Vice President, Mario Cardullo '57
Secretary, Bernard Shatz '57
Treasurer, J. Codispoti '58
Faculty Sponsor, T. P. Torda, Department of Mechanical Engineering

Under the guidance of Professor Torda, the group is developing a liquid-fueled motor. Project coordinator is William Peschke. Design group members include R. Mootchnik (injector systems), Morin (chamber configurations), I. Reba and P. Schuyler (exhaust nozzles), Cardullo (propellants) and Peschke (feed systems). It will have a pressure feed system and is being designed for 250 lb thrust.



Charter Presented to North Texas Section

George P. Sutton of North American's Rocketdyne Div., national director and membership chairman of ARS, presented the charter for the newly formed North Texas Section on Feb. 17. Accepting the charter on behalf of the Section was George H. Craig of Convair, Fort Worth, president.

Shown at the ceremony are (left to right) Jim Nolan, Convair, program chairman; John Kerr, Convair, director-at-large; Jack Wurts, Chance Vought, secretary; Sutton; Harry Graham, Chance Vought, vice president; and Craig. Charles F. Crabtree, Convair, treasurer, was not present when picture was taken.

Cardullo is editing a newsletter for the group, entitled "Rocket Study."

On February 24 a meeting was addressed by C. C. Miesse of Aerojet-General's liquid engine division on combustion instability.

Saint Louis University, (Parks College), East Saint Louis, Ill.

President, James M. Llewellyn, Jr.
Vice President, Dale Anderson
Secretary, Frank Brown
Treasurer, Joe Kelly
Technical Activities Chairman, Pete Butkewicz
Faculty Sponsor, Franz Hug



Donald J. Morin, President, Polytechnic Institute of Brooklyn Chapter

Niagara Frontier Elects Smith of Bell

WILLIAM M. SMITH, chief rocket engineer at Bell Aircraft Corp., Buffalo, has been elected president of the Niagara Frontier Section for 1956. He succeeds Tommie Zannes, also of Bell.

Following are the other officers named: Stanley F. Lewinski, Bell, vice president;

John H. Keefe, Becco Chemical Div., Food Machinery & Chem. Corp., treasurer; Daniel Y. Sing, Bell, treasurer; Walter J. Zebrowski, Convair, recording secretary.

Directors include, for two-year terms: Harry Ferullo, John van Lonkhuyzen, and Zannes, all of Bell; and D. E. Morrison, Orenda Engines, Ltd. Serving for one-year terms will be H. O. Kauffman, Becco; John Blanton, Bell; George Markstein, Cornell Aeronautical Laboratory; and Delbert D. Thomas, Olin-Mathieson Chemical Corp.

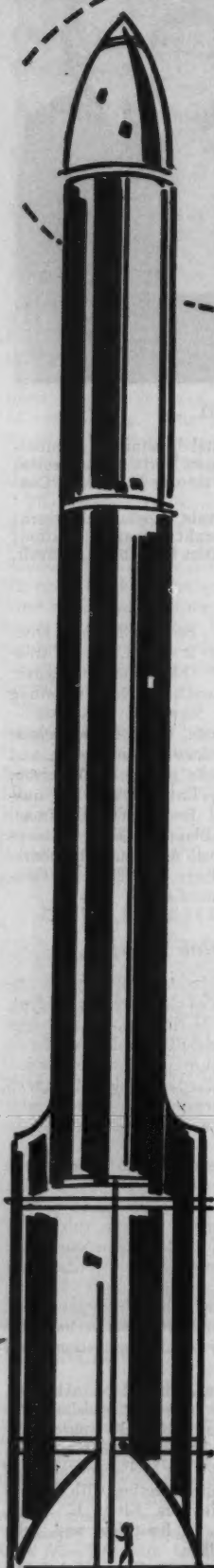
Section Doings

Arizona. A March 7 meeting, at the Tucson residence of C. J. Green, president, featured James J. Harford, ARS Executive Secretary, who discussed the Society's history and future plans. The Section members also talked over plans to launch an educational program on rockets in local high schools, as well as a Section publication.

California Desert. A meeting at the Naval Ordnance Test Station, China Lake, was attended by some 66 people. Heinz Haber spoke on the subject of Space Medicine, followed by a tour of the station. Richard Schmidt, Assistant Chief, Rocket Engine Test Station, Edwards AFB, is in charge of organization of this Section, and prospective members in this area may obtain application forms by writing him.

Central Texas. James J. Harford, ARS executive secretary, visited the Section on March 6. He toured the plant of the Phillips Petroleum Co., Rocket Fuels Div., in McGregor, and had an informal dinner meeting with Section officers and directors Elton E. Rush, Fred Sauls, A. C. Keathley, and John Alden, all of Phillips.

Chicago. Local Sections of the IAS



**Even for the special
"out of this world"
wiring problem...
a down-to-earth
solution —
Continental Wire**

Whether it's a rocket to the moon or a radio for a room—chances are you'll find Continental ready to serve your wiring needs exactly—with both speed and efficiency.

With many quality insulations of Asbestos... Glass... Nylon... Varnished Cambric... Polyethylene... Polyvinyl... Teflon... Zytel, among others, Continental also offers a wide range of wire sizes—in stock and on special order. For instance, Continental's **ELECTRONIC HOOK-UP WIRE**. This nylon-insulated, hook-up wire saves **TIME... LABOR... and GUESS-WORK** in assembly. Resistance to abrasion, acids, alkalis and petroleum solvents—and temperatures ranging from -50°C to $+125^{\circ}\text{C}$ —assures dependability plus versatility. Available in **AWG SIZES 18 to 32**.

One source for your many wiring requirements—Continental. Write today for Continental's complete catalog of heat-resistant, moisture-resistant wires, cables and cords. Serving 600-5000 volts. Sizes, 18 AWG—2,000,000 CM.

Continental's industrial wire and cable specialists are available to serve you at any time.

Contact: Continental Sales, Box 363,
Wallingford, Conn., Phone COlony 9-7718

Continental
WIRE CORPORATION
WALLINGFORD, CONNECTICUT • YORK, PENNSYLVANIA

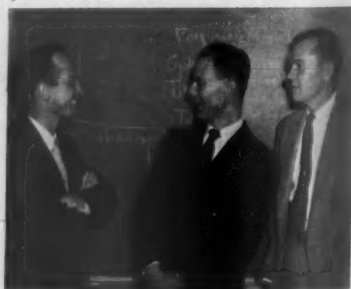
and ARS joined forces for the first time at the February meeting at Illinois Institute of Technology. A pre-meeting dinner was held at the IIT Student Union. Speaker was Emerson W. Smith of North American Aviation, who discussed the practical aspects of aircraft power plant installation testing. Several charts and photos were used to illustrate his talk.

Columbus. A brief discussion on proposed by-laws preceded the February meeting addressed by A. N. Tifford, Aeronautical Engineering Dept., Ohio State Univ. His lecture on escape from earth was followed by a motion picture on rockets.

Indiana. S. V. Gunn of the Rocketdyne Div., North American Aviation, Inc., spoke to approximately 75 persons at the February meeting. Dr. Gunn's subject included a discussion of problems associated with the development of large thrust rocket engines. He also discussed the activities of the newly formed Rocketdyne Div., and briefly described the test facilities located at the Santa Susana Test Station.

Maryland. Sixty members and guests attended the February meeting held at Johns Hopkins University. Guest speaker was Kurt Stehling whose subject was "Winged Rockets." He showed slides and films of the Bell X-1A and X-2 research aircraft.

New Mexico-West Texas. Invitations in the form of perforated strips of "Space tour" tickets were issued by the Section in connection with their "Annual Solar System Soirée" in March. The tickets were "good for passage for two" from the White Sands Proving Ground Navy Officers BOQ, stops at a space station and six planets, and return to Earth. Each portion of the ticket featured an appropriate symbol of the planet named. "In-flight" punch was served to the "space travelers."



Commander L. I. Stecher (center) who addressed the New Mexico-West Texas Section recently on "The Inter-Range Instrumentation Group." Left, program chairman R. Gilbert Moore, and right, section president R. K. Sherburne.

New York. At the February 10th meeting at IBM World Headquarters, Gilbert Parker of IBM discussed the field of scientific computing with specific emphasis upon large electronic computing equipment. A film was shown ("Piercing the Unknown") in which the use of computing equipment was demonstrated in modern aeronautical and rocket applications. Mr. Parker discussed general types of modern computers and how they can assist the engineer and scientist in

time at
stitute
ner was
Speaker
Ameri-
practi-
installa-
photos

on on
bruary
Tifford,
Ohio
e from
picture

etdyne
Inc.,
at the
subject
associ-
thrust
ed the
etdyne
facili-
a Test

guests
eld at
peaker
t was
slides
X-2

ations
Space
ection
Solar
ickets
m the
Navy
n and
Each
ropri-
"In-
space

who
exas
ange
gram
sec-

10th
ters,
field
specific
uting
rcing
com-
d in
lica-
neral
they
t in

ION

Airborne Mule Skinner for today's Defense

Now to the service of supply comes a new idea in military logistics—air transports that rival the train in ton-mile cost. Newest and largest, now on the way, is the turbo-prop Douglas C-133.

About to undergo flight tests, C-133 packs the load of *five freight cars* into its huge hull, loads 96% of military or construction equipment—fully assembled and ready for action—through an adjustable platform ramp in its tail section.

Speed and range are still secret but C-133's ability to shuttle back and forth across oceans gives it the cargo potential of a 7000-ton ship. Cost drops drastically because C-133 gets material into action in hours, rather than weeks or months.

Biggest cargo transport—the Douglas C-133A

Development of the Douglas C-133 shrinks supply lines and bolsters America's armed strength. But the core of that strength is the personnel manning posts and aircraft. Ask your local recruiting officer about the opportunities in the U. S. Air Force.

Depend on **DOUGLAS**



First in Aviation

missile engineers

CONTROL
GUIDANCE
SERVO
COMPUTERS
RECORDING
OPTICAL
RELIABILITY
ELECTRO-MECHANICAL
TELEMETERING

With 16 years leadership in the vital field of missile research and development, Northrop Aircraft offers unusual opportunities for advancement in the categories listed below. Where better could you be, and grow, than with a pioneer? There's an interesting position for you in one of the following groups:

Guidance and Controls, encompassing research and development of advance automatic guidance and flight control systems for both missiles and piloted aircraft. Specific areas of development include: radio and radar systems, flight control systems, inertial guidance systems, instrument servo systems, digital computer and magnetic tape recording systems, airborne analog computer systems, optical and mechanical systems, and systems test and analyzer equipment. Within these areas activities include: original circuit development, electronic and electro-mechanical design, laboratory and field evaluation of systems under development, and reliability analysis both at a system and component level.

Flight Test Engineering Section, which plans the missile test programs and establishes test data requirements in support of the programs. The data requirements are predicated on the test information required by the Engineering analytical and design groups to develop and demonstrate the final missile design, and are the basis from which the instrumentation requirements are formulated.

The analysis work performed consists of aerodynamic, missile systems, dynamics, flight control, propulsion and guidance evaluation. The Flight Test Engineering Section is also responsible for the field test program of the ground support equipment required for the missile.

Flight Test Instrumentation Section, which includes a Systems Engineering Group responsible for the system design concept; a Development Laboratory where electronic and electro-mechanical systems and components are developed; an Instrumentation Design Group for the detail design of test instrumentation components and systems; a Mechanic Laboratory where the instrumentation hardware is fabricated; and a Calibration and Test Group where the various instrumentation items and systems are calibrated and tested.

There are now a number of openings available for engineers in each of these groups at all experience levels.

If you qualify for any of these challenging opportunities, we invite you to contact Engineering Industrial Relations, Plant 2, Gate 3B, Broadway & Prairie, Northrop Aircraft, Inc., Hawthorne, California; or write Manager of Engineering Industrial Relations, Northrop Aircraft, Inc., 1021 East Broadway, Hawthorne, Calif.

NORTHROP AIRCRAFT, INC.

PIONEERS IN ALL WEATHER AND PILOTLESS FLIGHT

Producers of Scorpion F-89 Long-Range Interceptors and Snark SM-62 Intercontinental Missiles.



5-A-55

calculating problems associated with rocketry. The talk was followed by a demonstration of computers operated at the data processing center.

Southern California. Homer E. Newell, Jr., acting superintendent of the Atmosphere and Astrophysics Division of the Naval Research Laboratory, was the speaker at the February meeting in Pasadena. His subject was the use of rockets and satellites for geophysical research. Dr. Newell has specialized in upper atmosphere research at NRL for nearly ten years.

Wichita. About 100 members and guests attended a March 1 meeting at the Beech Employees Club which featured the appearance of James J. Harford, ARS executive secretary, as speaker. A film program followed.

Five Companies Join ARS

TWO Michigan organizations, two from California, and one eastern company are recent applicants for Corporate Membership in ARS. The firms, their fields of interest, and their Corporate representatives are:

Accessory Products Corporation, Whittier, California. Valves, regulators, filters and allied equipment for control of fluids. Research on high flow fuel, high and low pressure pneumatics and environmental test equipment for aircraft, rockets and missiles. Robert G. Rogers, President; Robert L. Maple, Executive Vice President; William M. Smith, Vice President, Chief Engineer; Orville A. Cordes, Sales Manager; William P. Taylor, Project Engineer.

Chrysler Corporation—Missile Operations, Detroit, Mich. Producer of U. S. Army's Redstone Missile. Aerodynamics, ballistics, guidance and control, handling, launching, propulsion of missiles. C. A. Brady, Operating Manager; J. P. Butterfield, Chief Engineer; B. J. Meldrum, Business Manager; C. W. Williams, Manager, Fabrication and Assembly; R. M. Graham, Manager, Quality Control.

Consolidated Western Steel Division, United States Steel Corporation, Los Angeles, Calif. Maker of motor cases for various rocket and missile programs. Charles E. Fife, contracting Engineer; Charles R. Fenninger, Contracting Engineer; J. Greer Thompson, Assistant Vice President, Sales; George E. Boyd, Contracting Manager, General Sales; M. P. Klick, Chief Engineer.

Electro-Mechanical Products Company, Garden City, Mich. Manufacturer of guided missile components, flight simulators, propulsion controls, optics, and varied electro-mechanical devices. Jack M. Beauchamp, President; George T. Spencer, Sales Manager; Chester C. Quantz, Chief Engineer; Wallace H. Franklin, Staff Engineer; Frank W. Beauchamp, Executive Vice President.

Norden-Kelay Corporation, New York, N. Y. Airborne automatic control systems and components. G. D. Butler, Director of Sales; B. Levine, Director of Design and Application Engineering; C. F. Schaeffer, Technical Director, Norden Laboratories Division; R. Seymour, Chief Engineer, Instrument and Systems Division; R. Porter, Chief Engineer, Precision Components Division.

NOW-SPERRY ENGINEERS

*project a proud past
into a new realm of*
**ENGINEERING OPPORTUNITY
FOR YOU!**

THE MISSILES SYSTEMS DIVISION

Drawing on a 50-year history of engineering accomplishment, Sperry now adds a Missiles Systems Division to its ever-expanding organization.

"Firsts," of course, are an old story with Sperry engineers. From the installation of the first gyro-compass aboard a Navy warship, back in 1911, to a myriad of electronic wonders today, Sperry has been busy marking milestones of progress. And Sperry Engineers are eminently qualified to embark on their newest project. Their vast experience with missiles and associated systems make them intimately acquainted in this field. As a matter of record, way back in 1918 Sperry engineers successfully developed the first radio-controlled "guided missile."

What all this means to engineers in search of a rewarding life work should be clear. In Sperry's new Missiles Systems Division, major opportunities are unfolding. Not only can you now tap the tremendous potential in the field of missiles and pilotless air-borne devices, but you can do so from the well-established base of a stable organization. Over 1500 employees have been employed by Sperry for more than 15 years. And, as Sperry grows, you will grow . . . in professional stature and in personal gain.

Consider These Exceptional Openings For Engineers in the Following Fields:

- Feed Back Control Systems
- Magnetic Amplifier Circuitry
- Digital Computers
- Radar Systems
- Stable Platforms
- Telemetering
- Aerodynamics
- Systems Analysis
- Environmental Test
- Reliability

RELOCATION ALLOWANCES • LIBERAL EMPLOYEE BENEFITS

AMPLE HOUSING in Beautiful Suburban Country Type Area

TUITION REFUND PROGRAM (9 graduate schools in area of plant)

MODERN PLANT with Latest Technical Facilities

ASSOCIATION WITH OUTSTANDING PROFESSIONAL PERSONNEL

APPLY IN PERSON

Daily (Including Sat.). Also Wed. Eves.

OR SUBMIT RESUME

to Mr. J. W. Dwyer

Engineering Employment Supervisor

OR PHONE FOR APPPOINTMENT

Fieldstone 7-3600, Ext. 2605 or 8238

SPERRY

GYROSCOPE COMPANY

Division of Sperry Rand Corp.

GREAT NECK, LONG ISLAND, NEW YORK

unusual
career
opportunity
at IBM's

AIRBORNE COMPUTER LABORATORY

At IBM's Vestal*, New York, Laboratory is gathered a group of computer engineers whose entire efforts are devoted exclusively to the development and perfection of airborne computers.

In support of these engineers are the finest IBM engineering facilities, experienced staffs of logicians, mathematicians and other specialists, and an engineering know-how accumulated during 42 years of building the world's finest mechanical, electrical and electronic computing equipment.

At the Vestal Laboratory, you'll work in a climate of creativeness with stimulating associates on today's most advanced projects.

If you are an engineer with experience in any of the following fields, we'd like to tell you more about this unusual opportunity and outline other advantages of working with IBM: **digital and analog computer circuitry and design—transistor circuitry—electronic display systems—microwave theory and wave guide design—component application and evaluation—electronic packaging—power supply design—servo and servo-control systems—optics—systems analysis and operations research—instrumentation theory and design—field engineering.**

Write, outlining your interests and qualifications to: A. N. Hurst, Room 4504, International Business Machines Corp., Endicott, New York

*near Binghamton and Endicott, N.Y.

IBM

Producer of electronic data processing machines, electric typewriters, and electronic time equipment.

ARS SECTIONS AND PRESIDENTS

Alabama

Conrad Swanson, Redstone Arsenal

Arizona

Charles J. Green, Hughes Aircraft Co.

Central Texas

Elton Rush (acting), Phillips Petroleum Co.

Chicago

Gerald M. Platz, Armour Research Foundation

Cleveland-Akron

Walter T. Olson, Lewis Flight Propulsion Laboratory, NACA

Connecticut Valley

Charles H. King, Jr., United Aircraft Corp.

Detroit

Fred Klemach, Nat'l Des. & Res. Corp.

Florida

R. S. Mitchell, Pan American World Airways

Fort Wayne

Lloyd Wadekamper, Indiana Tech. College

Holloman-Alamogordo Group

John P. Stapp, Holloman Air Development Center

Indiana

Philip M. Diamond, Purdue University

Maryland

William A. Webb, Aircraft Armaments, Inc.

National Capital

J. D. Gilchrist, Aerojet-General Corp.

New England

Joseph Kelley, Allied Research Assoc., Inc.

Niagara Frontier

W. M. Smith, Bell Aircraft Corp.

New Mexico-West Texas

Russell K. Sherburne, New Mexico College of A.&M.A.

New York

Charles J. Marsel, New York University

North Texas

George Craig, Convair

Northeastern New York

A. H. Fox, Union College

Northern California

M. A. Pino, California Research Corp.

Pacific Northwest

Jim C. Drury, Boeing Airplane Co.

Princeton Group

J. Preston Layton, Princeton Univ.

St. Louis

J. J. Mazzoni (acting), McDonnell Aircraft Corp.

Southern California

Richard D. Geckler, Aerojet-General Corp.

Southern Ohio

W. C. Cooley, General Electric (ANP Dept.)

Twin Cities

T. F. Irvine (acting), University of Minnesota

Wichita

J. F. Reagan, Beech Aircraft Corp.

RCA'S MISSILE TEST PROJECT

**is attracting Creative Engineers
and Scientists who are bound
toward success**



*Specific fields
include:*

**TELEMETRY
RADAR
TIMING
COMMUNICATIONS
DATA PROCESSING
OPTICS**

● **Request Your Interview NOW...**
*RCA Engineering management
will arrange an interview at the
time and place you find most
convenient. Please send complete
resume of education and
experience to:*

**Mr. H. N. Ashby, Technical Employment
Missile Test Project, Dept. N-7D
RCA Service Company, Inc., P.O. Box 1226
Melbourne, Florida**

MTP... the Missile Test Project of the RCA Service Company, Inc. . . . at the Air Force Long Range Missile Test Center . . . is the largest missile-testing range and laboratory in the world! The responsibility for providing precision instrumentation for advanced stage missiles with a vast range of performance characteristics means new engineering and planning organizations and—real opportunity for rapid individual growth.

Here you will encounter instrumentation problems that challenge the state of the art and stimulate your creative ability in Aero, Ballistic and Space techniques.

Your rewards will include all the fascination, excitement and satisfaction of achievement in new frontiers of scientific knowledge . . . plus top salary.

What's more, you'll enjoy the pleasant climate and ideal living on Florida's central east coast, where Patrick Air Force Base, site of the MTP, is located.

RCA offers many additional advantages: Complete facilities . . . Planned advancement program . . . Professional recognition . . . Liberal program of company-paid benefits . . . Relocation assistance. You should have a Bachelor's or advanced degree in EE, ME, Physics or Mathematics and two or more years' experience.



Tmks. ©

RADIO CORPORATION of AMERICA



Potentiometer type transducers for use at temperatures between -60°C . and $+120^{\circ}\text{C}$.

Designs available permit single or multiple range linear output from non-linear input function, and operation over wide ranges of environmental conditions.

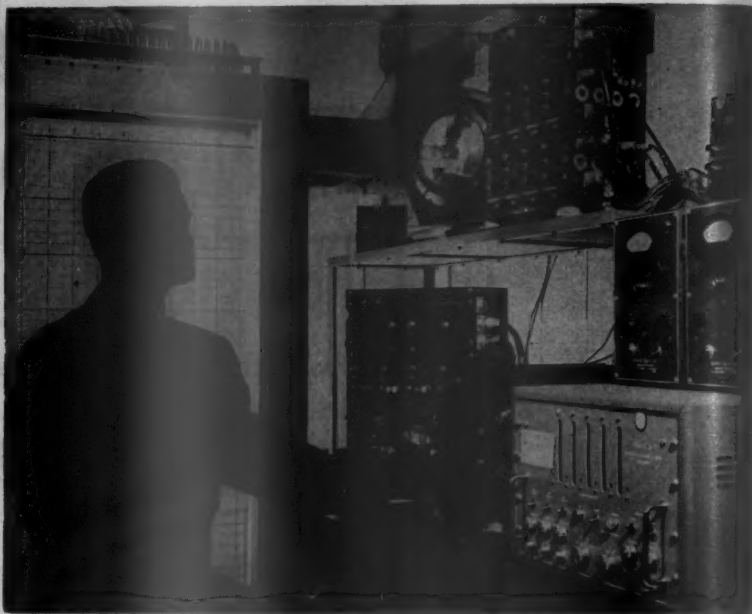
Designs available for operation to 160°C .

Special instruments for use with corrosive oxidants and fuels are available.

Specifications available on request.

RAHM
INSTRUMENTS, INC.
12 WEST BROADWAY
NEW YORK 7, N. Y.

TO THE FINE ENGINEERING MIND
SEEKING THE CHALLENGING PROJECTS IN



ROCKET PROPULSION ENGINEERING

ROCKET PROPULSION ENGINEERS are offered unusual career opportunities now at Convair in beautiful, San Diego, California, including: *Design Engineers* for design and analysis of advanced high performance rocket engine systems and components including propellant systems, lubrication systems, control systems, mounting structure, and auxiliary power plants; *Development Engineers* for liaison with Engineering Test Laboratories and Test Stations in the planning, analysis, and coordination of rocket engine system and component tests; *Development Engineers* for coordination with Rocket Engine Manufacturers in the installation design, performance analysis, and development tests in conjunction with Convair missile programs. Professional engineering experience in rocket missiles and aircraft propulsion system development will qualify you for an exceptional opportunity.

CONVAIR offers you an imaginative, explorative, energetic engineering department... truly the "engineer's" engineering department to challenge your mind, your skills, your abilities in solving the complex problems of vital, new, long-range programs. You will find salaries, facilities, engineering policies, educational opportunities and personal advantages excellent.

Generous travel allowances to engineers who are accepted. Write at once enclosing full resume to:

H. T. Brooks, Engineering Personnel, Dept. 1416

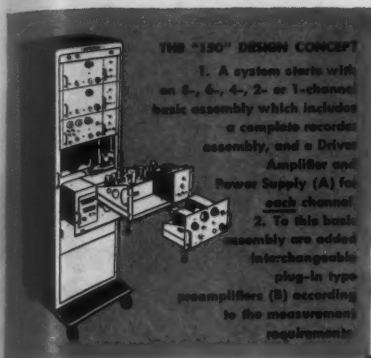
CONVAIR

A Division of General Dynamics Corporation

3302 PACIFIC HIGHWAY

SAN DIEGO, CALIFORNIA

SMOG-FREE SAN DIEGO, lovely, sunny city on the coast of Southern California, offers you and your family a wonderful, new way of life... a way of life judged by most as the Nation's finest for climate, natural beauty and easy (indoor-outdoor) living. Housing is plentiful and reasonable.



HERE'S REAL DEMONSTRATED AT
BOOTHS 455 AND 457
OSCILLOGRAPHICS AVENUE
N.E. SHOW
RECORDING VERSATILITY

A Sanborn "150 Series" System can be set up to record any of these inputs in any of the channels.

AC or DC Signals,



AC-DC Preamp

balanced or single-ended, with sensitivity of 1 mv to 2 v/cm (AC), 1 mv to 2 v/mm (DC).

Low Level Signals,



STABILIZED DC Preamp

with extreme stability, high gain, and greater bandwidth than with 150-1500 Low Level Preamplifier.

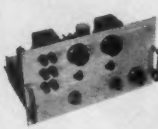
Magnitude and Direction of Physical Variables,



CARRIER Preamp

with variable resistance, differential transformer or variable reluctance transducers.

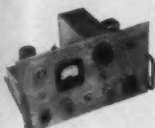
Average Value of AC Watts in a Circuit,



AC WATTMETER Preamp

in ranges from 25 volts x 40 ma to 250 volts x 2 amps. (with internal multipliers and shunts which can handle up to 4 amps).

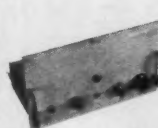
AC Voltage Components



SERVO MONITOR Preamp

in phase or 180° out of phase with a reference voltage (e.g., servo error signal).

Higher Level Signals



INPUT COUPLING NETWORK

where maximum sensitivity of 1 v/cm, and input impedance of about 200,000 ohms are adequate.

DC Signals



DC COUPLING Preamp

(push-pull, single-ended or difference between two). Basic sensitivity 50 mv/cm to 50 v/cm.

RMS Values of AC Voltages, Currents,



VOLT/AMMETER Preamp

from 25-250 volts, 50 ma — 1 amp.

Voltage Levels Recorded Logarithmically



LOG-AUDIO Preamp

Audio signals (20 cycles to 20 KC) or DC voltages recorded in logarithmic fashion on 50 decibel chart.

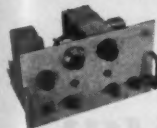
Symmetric or Asymmetric Waveform Inputs,



FREQUENCY DEVIATION Preamp

in 350-450 cycles (2 cycles/mm) and 375-425 cycles (1 cycle/mm) ranges.

Extremely Low Voltages and Currents,



LOW LEVEL Preamp

at sensitivities of 100 μ v and 1 μ a per cm. (with external shunt of 100 ohms), by means of DC chopper circuit.

BASIC "150" design features include: inkless recording in true rectangular coordinates, improved overall linearity, numerous paper travel speeds, and a choice of mobile-cabinet or portable-case packaging in 2-, 4-, 6-, and 8-channel systems.

Sanborn Representatives will be glad to help you select the equipment best suited to your needs. Complete catalog available.

SANBORN COMPANY, Cambridge 35, Mass.



world's largest
turbine-powered
transport helicopter

...designed
and built by

asecki

...uses
Statham
Accelerometers
to gather
invaluable
test data

Statham
LABORATORIES



THE Y-4 PERISCOPE BOMBSIGHT used in B-47 Stratojets has 3,433 parts, nearly 2,000 of them in this head-end assembly alone. General Mills manufactures this precision instrument in quantity under a USAF prime contract.

No need to swamp your staff with piece part and assembly problems...

Let General Mills supply the whole package

Eliminate the thousands of detail problems involved in turning out complete electro-mechanical assemblies—and save money, too!

The Mechanical Division of General Mills is ready to manufacture or purchase component parts, assemble to your requirements, and deliver assemblies performance-tested to rigid Government standards—on time. We have the experience and

equipment required to take over the complete job. The highest precision standards are maintained in engineering, manufacture, quality control, packaging and accounting.

LET US BID on your requirements. Write, wire or phone: Dept. JP-2, Mechanical Division of General Mills, Inc., 1620 Central Ave., Minneapolis 13, Minn. STerling 9-8811.

Job opportunities available for creative engineers. Work closely with outstanding men on interesting projects.

MECHANICAL DIVISION OF General Mills

New Equipment and Processes

Equipment

Electrical, Electronic

Missile Alternator. For short-time operation, weighs 15 lb; 400 cycle, 12,000 rpm. Can be rated to 2000 va., 3-phase 115 v. Specialty Component Motor Div., General Electric Co., Schenectady 5, N. Y.

Line Pressure Transducer. Rated at 250 psig at differential pressures up to 250 psid. Statham Laboratories, 12401 W. Olympic Blvd., Los Angeles 64, Calif.

Missile Heating Element. Neoprene coated, can be used as rocket-tube heater where only moderate heat is required. Higher temperatures available. Safeway Heat Elements, Inc., Middletown, Conn.

Direct-Reading Pre-Amplifier. Model 2014 is a probe type for piezoelectric pickups. With VTVM can read acceleration, pressure, force. Endeavor Corp., 180 E. California St., Pasadena 1, Calif.

Teledyne Strain Gage. New pressure transducer, 2 1/2-in. diam and 3 1/2 in. long available in eight ranges up to 10,000 psi. Tubor Instrument Corp., Section 36, 111 Goundry St., N. Tonawanda, N. Y.

Miniature Blower. Motor and blower in 1-in. cube moves 3 cu ft of air per min. Weight, 1 oz, power 4 watts. For aircraft and missiles. Sanders Associates, Inc., Nashua, N. H.

Subminiature Relay. Length 1 1/8 in., diam 1 3/4. Wt. 0.225 lb, 2 amps at 26.5 VDC or 115 VAC. 4 pdt. Will take 50 G. U.S. Relay, 1744 Albion St., Los Angeles, Calif.

Silicon Diode. Model 1N23D is designed for X-band mixer at low noise (7.5 db). Normal and reversed polarity models. Bomac Laboratories, Inc., Beverly, Mass.

Klystron Radar Transmitter. 50 kw peak, 1 kw average power for MTI applications. Power required is 40 amps per phase for 208 v 50/60 cps, 3-phase supply. Levinthal Electronic Products, 2910 Fair Oaks Ave., Redwood City, Calif.

Signal Simulator. 400 cycle suppressed carrier modulated signal generator for checking aircraft or missile autopilots. Micro Gee Products Inc., 6100 W. Slauson Ave., Culver City, Calif.

Sub-Miniature Rate Gyro. Weighing 4 oz, measures 2 1/2 in. long and 1 in. diam. Rate range of 10-500 deg/sec. Frequencies of 8-75 cps. Robey Rotor Div., J. B. Rea Co., 1723 Cloverfield Blvd., Santa Monica, Calif.

High Temp Pressure Switch. Kilotrol switch allows operation to 800 F, burst pressure 10,000 psi; operating pressure of 3100 psi at 800 F. SPST 1/4 amp at 28 VDC contacts. Cook Electric Co., 2700 Southport Ave., Chicago 14, Ill.

Compact Power Rectifier. 30 W liquid-cooled germanium rectifier occupies volume of 190 cu. in. Current outputs of 540-750 maps. Input voltages of 26 v to 66 v rms. International Rectifier Corp., 1521 E. Grand Ave., El Segundo, Calif.

Materials

Metals

No Bead Tubing. Internal welding bead eliminated from tubing by new

reverse process. Smooth and flawless interior. Crucible Steel Co. of America, Oliver Bldg., Pittsburgh 30, Pa.

Small Self-Locking Fasteners. Size ranges of 0-80 and 4-48. Standard Pressed Steel Co., Jenkintown, Pa.

Ni-SpanC. Nickel-chromium-iron-titanium alloy retains uniform elasticity at elevated temperatures. H. A. Wilsom Co., Union, N. J.

Safety Well. Type 304 stainless steel protects thermocouple elements to 3000 psi and -300 F to +1850 F. Conax Corp., 7811 Sheridan Drive, Buffalo 21, N. Y.

JAN Shield Insert. Corrugated cadmium-plated brass insert conducts heat away from tubes. Inserts fit all 5 1/2 and 6 1/2 miniature envelopes. Bircher Corp., 4371 Valley Blvd., Los Angeles 32, Calif.

Thermocouple Connector. Kit features interchangeability with various materials. Merlin Manufacturing Corp., 12410 Triskett Road, Cleveland 11, Ohio.

Plastics

Fuming Nitric Acid Filter. Woven Teflon housed in stainless steel. Pore sizes of 150 x 300 microns and 25 x 40 microns. Porous Plastic Filter Co., 30 Sea Cliff Ave., Glen Cove, N. Y.

Acid Resistant Hose. Fluorinated inner tube permits acid resistant operation from -100 to +500 F. Aeroquip Corp., 303 S. East St., Jackson, Mich.

Resistant Tubing. Fiberglass-epoxy tubing in lengths up to 9 ft and diameters down to 1/16 in. ID. Withstands temps to 350 F. Lamtex Industries, 51 State St., Westbury, L. I., N. Y.

Stripper for Epoxies and Polyesters. Solvent Monastrip EP for reclaiming pottings and castings. Mona Industries, Paterson 4, N. J.

Vinyl Chloride. Pliovic AO in organosols. Chemical Div., Goodyear Tire & Rubber Co., 1144 E. Market St., Akron 16, Ohio.

Plastic Patch Kit. Epoxy welds metals, nonmetals. Temperature and acid resistant. Amchem Corp., 823 Tuxedo, Highland Park 3, Mich.

Formica Tooling. Sheet S-52 for stretch forming, metal spinning and die forming. Formica Co., 4614 Spring Grove Ave., Cincinnati 32, Ohio.

Polyester Resin. Solid Atlac 382 resin for laminates, molding permits monomer to be added in desired amount. Atlas Powder Co., Wilmington 99, Del.

Miscellaneous

Silicone Polymers. New silicones are available with water solubility. For rubber, plastics, and lubricants. Linde Air Products Co., 30 E. 42nd St., New York 17, N. Y.

Thixotroping Agent. Cabo-O-Sil, a finely divided silicon dioxide permits lay-up with sharp corners, etc., in polyester-glass reinforced plastics. Godfrey L. Cabot, 77 Franklin St., Boston 10, Mass.



As designers of America's finest aircraft instruments, Kollsman can provide excellent opportunity for professional growth. And the congenial atmosphere, the modern facilities contribute to an environment in which a man can do his best work. Please submit resumes to T. A. De Luca. Confidential interviews will be arranged.



kollsman INSTRUMENT CORPORATION

90-08 40th AVENUE, ELMHURST, NEW YORK • SUBSIDIARY OF Standard COIL PRODUCTS CO. INC.

SYSTEMS ENGINEERS

For development, testing and field service of airborne navigational systems. Some experience with servos utilizing electronic and electro-mechanical components desirable.

ELECTRICAL ENGINEERS

Experience in small electro-mechanical devices, motors, synchros and induction pick-offs.

FIELD SERVICE ENGINEERS

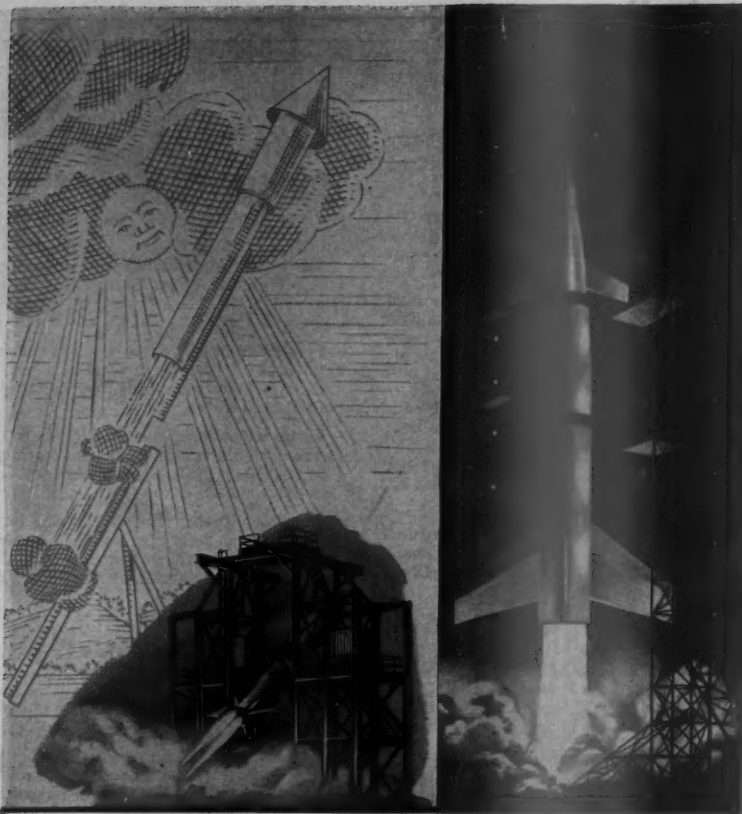
For work associated with airborne navigational equipment. Should be versed in electronic circuitry and mechanical repairs. Entails some travel.

DESIGNERS

Electronic, Electro-mechanical, Mechanical

1. Electronic and electrical packaging. Knowledge of sub-miniaturized techniques. Work is associated with servos, amplifiers and components.

2. Mechanical or electro-mechanical packaging of precision flight instruments.



ONE OF A SERIES — depicting Rocketry — "Yesterday, Today and Tomorrow"

from the tartar wall to the moon

The Battle of Kai-fung-fu in 1232 . . . Ft. McHenry in 1814 . . . Goddard's experiments in 1920 . . . the supersonic Bell X-1 in 1947 . . . these were milestones in rocketry. Slowly evolving into today's potent weapon, the rocket is still more than a weapon . . . it is man's escape route into space.

Before this frontier can be achieved, tremendously complex problems must be solved. Intriguing problems that challenge the ingenuity of even the most creative engineer. These problems are being solved every day by Bell Aircraft's engineering teams.

Bell's rocket engine division has designed and built numerous successful rocket engines for different Army, Navy and Air Force projects, including the Nike and Rascal guided missiles. In a continuing research program complete facilities are available, including 44 test cells capable of conducting over 400 test runs a month.

For the imaginative engineer with a sincere interest in his professional future and a wide choice in career opportunities, contact . . .

MANAGER, ENGINEERING PERSONNEL

- RESEARCH ENGINEER — heat transfer and fluid mechanics
- GROUP ENGINEER — heat transfer and fluid mechanics
- AERONAUTICAL AND MECHANICAL ENGINEERS
- ROCKET TEST ENGINEERS



DEPT. 20N • P. O. BOX 1 • BUFFALO, N. Y.

Sintered Metal Oxides. Alite aluminum oxide features high strength, high temperature and chemical resistance. U. S. Stoneware Co., Box 350, Akron, Ohio.

Silicone Adhesives. C-269 and C-274 pressure sensitive adhesive can be used over temperature range of -80 F to +500 F. Dow Corning Corp., Midland, Mich.

Casting and Laminating Resin. SC-55-73 provides technical data on new low-viscosity epoxy resin, Epon 815. Shell Chemical Corp., 380 Madison, New York 17, N. Y.

Plastics Equipment. Spiral flow intensive mixers, presses, and calendars. Stewart Bolling & Co., 3190 E. 65th St., Cleveland 27, Ohio.

Care and Maintenance of Acrylic Plastics in Aircraft. Folder no. PL-24. Rohm & Haas Co., Washington Square, Philadelphia 5, Pa.

Sub-Miniature Galvanometers. Series M galvanometers. Fluid and electromagnetic damping. Flat frequency responses of 0-3000 and 0-240 cps. Bulletin 301, Heiland Instruments, 5200 E. Evans Ave., Denver 22, Colo.

Product List. Alloys and compounds of boron, columbium, hafnium, lithium, selenium, tantalum, tungsten, titanium, and zirconium. Kawecki Chemical Co., 220 E. 42nd St., New York 17, N. Y.

Engineering Hand-Book. Data on Bakelite laminated, vulcanized fibre, and plastics. Manne-Knowlton Insulation Co., 416 W. 13th St., New York 14, N. Y.

Commercial Aluminum Alloys. Folder describes properties, fabricating applications, and sizes. Peter A. Frasse & Co., 17 Grand St., New York 13, N. Y.

Titanium. Bulletin lists chemistry and metallurgy, properties, heat-treat, forging and welding of MST-6A1-4V titanium alloy. Mallory-Sharon Titanium Corp., Niles, Ohio.

Flexible Metal Hose. Reference Manual on bronze, monel, nickel, carbon, and stainless steel hose. Universal Metal Hose Co., 2133 S. Kedzie Ave., Chicago 23, Ill.

Arc-Cast Moly. 72-page book compiles technical data. Climax Molybdenum Co., 500 Fifth Avenue, New York 36, N. Y.

Small Gas Turbines. GE Brochure GED-2600 covers history of gas turbines for small aircraft. General Electric Co., Schenectady 5, N. Y.

Shaped Tubing. Data Memo No. 17 illustrates various shapes available for aircraft and special work. Superior Tube Co., 1505 Germantown Ave., Norristown, Pa.

High Heat Treat Steel. Manufacturing and engineering forum report. Lockheed Aircraft Corp., 2555 N. Hollywood Way, Burbank, Calif.

Aluminum Coated Steel. Folder tells how to protect steel from corrosion and oxidation with Alumincoat. Arthur Tickle Engineering Works, 21 Delavan St., Brooklyn 31, N. Y.

PLEASE NOTE: In the March issue, p. 205, middle column, the manufacturer's name for the Liquid Oxygen Storage model was regrettably omitted. It is: Ronan and Kunsal, Inc., Marshall, Mich.

JET PROPULSION

Alite strength, high resistance
O, Akron
and C-374
to be used
F to +600
nd, Mich.
SC-55
new low
5. Shel
New York

flow is
calenders
65th St.

Acrylic
PL-24
Square

Series
electro-
ency re-
Bulletin
C. Evans

mpounds
lithium,
titanium,
ical Co.,
Y.

ata on
ore, and
sulation
N. Y.

Folder
applica-
& Co.,

try and
orging
titanium
Corp.

e Man-
on, and
Metal
Chicago

com-
Molyb-
v York

ochure
urbines
ic Co.

No. 17
le for
Tube
estown,

turing
kheed
Way,

r tells
n and
Tinkle
St.

issue,
urer's
model
n and

SION



The Chance Vought F8U-1 Crusader, newest of the Navy's jet fighters, is equipped with a Marquardt ram-air emergency power package. In case of engine failure the unit pops into the air stream and supplies A-C, D-C, and hydraulic power sufficient to maintain flight control and communication through all speeds down to safe landing.



Lifesaver... WHEN POWER FAILS

Marquardt Aircraft, the West's largest jet engine research and development center, is an important contributor to the OMAR Joint Technical Committee. With Reaction Motors, first in the American rocket industry, and Olin Mathieson Chemical, a leading producer of chemicals, explosives, metals, Marquardt adds

greatly to a continuous joint technical effort to achieve improved rocket and ramjet engines and special fuels. Exemplifying the weapons systems concept in action, the OMAR Committee combines for the first time both chemical and mechanical experience applicable to high-energy power generation.

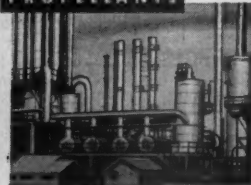
Engineers, chemists, physicists, production and tool specialists... a wide variety of fascinating careers await you on this weapons systems team. For information write OMAR Employment Officer at the company nearest you.

RAMJETS



Marquardt Aircraft Company
Van Nuys, California

PROPELLANTS



Olin Mathieson Chemical Corp.
New York, New York

ROCKETS



Reaction Motors, Inc.
Denville, New Jersey

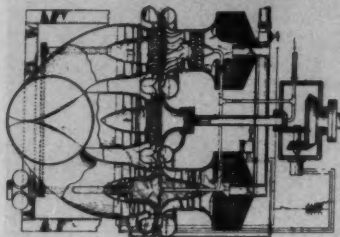
MARQUARDT AIRCRAFT
OLIN MATHIESON CHEMICAL
REACTION MOTORS



New Patents

Electric ignition control in starting devices for turboengines (2,730,862). Rene L. Lamy, Paris, France, assignor to Société du Carburateur Zenith.

Means responsive to the speed of a turbo-engine during the starting period whereby a switch in the ignition circuit is closed as the speed reaches a value enabling the engine to run by its own power.



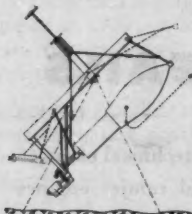
2,730,863

Gaseous fuel turbine power plant having parallel connected compressors (2,730,863). Nathan C. Price, St. Helena, Calif., assignor to Lockheed Aircraft Corp.

Plurality of parallel units each including a compressor, a turbine and a load-driving turbine. A combustion chamber is in receiving relation to the outlets of the compressor, and delivers combustion gases to drive the load-driving turbines.

Circuit for measuring the average intensity of disturbances (2,730,896). Desolde R. de Boisblanc, Bartlesville, Okla., assignor to Phillips Petroleum Co.

System for determining combustion instability in a jet engine: An electromagnetic detector picks up acoustical noise from the burner and measures the output of an integrating circuit.



2,730,927

Launching device for self-propelled missiles (2,730,927). Louis Marie E. Bourguard, Courbevoie, France, assignor to Société d'Exploitation des Matériaux Hispano-Suiza.

Support for holding a rocket missile in the direction of firing. When the support is retracted simultaneously from all points of contact, the missile drops with its axis parallel to direction, and the propelling charge is immediately ignited.

Exhaust gas temperature responsive fuel system for gas turbine power plant (2,731,974). Bruce N. Torrell, Wethersfield, Conn., assignor to United Aircraft Corp.

Fuel flow metered as a function of exhaust gas temperature. System includes rotor driven by exhaust gases and system for maintaining a constant pressure ratio

across the rotor which actuates the fuel metering means.

Acoustic pulses jet engine with acoustic air intake system (2,731,795). Albert G. Bodine, Jr., Van Nuys, Calif.

Standing wave established within a resonant sonic column. An air-induction pipe has a length corresponding to one-quarter of the wave length of the wave pattern in the fluid column. The pipe resonates with the fluid column and the end of the pipe furthest from the combustion zone represents a zone of minimum pressure variation.

Gas turbine plant comprising a rotary regenerative heat exchanger (2,731,798). R. J. Welsh and R. D. van Millingen, Rugby, England, assignors to the English Electric Co., Ltd.

Process of operating a turbine plant with a fuel mixture of air and a methane concentration below 1 percent. Mechanical energy extracted from heated and compressed elastic fluid is used partly for compressing the fluid and partly for driving an external load.



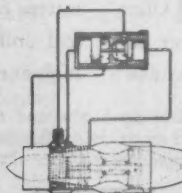
2,731,885

Rocket stowage and launching mechanism (2,731,885). Auldin D. Nolan, Palos Verdes, Calif., assignor to Northrop Aircraft, Inc.

Cylindrical streamlined shell containing 19 rockets and mounted on a wing. Rockets stowed at the center of the shell are conveyed on pivotally mounted launching arms to external positions as the shell doors are swung open.

Control valve apparatus for turbojet engine (2,731,983). Leighton Lee II, Rocky Hill, Conn., assignor to Pratt & Whitney, Inc.

Spool valve with barometric control for increasing compressor pressure differential moves. A valve in the system is subject to tailpipe temperature. Lifting of a piston in the system permits increasing the torque.



2,732,125

Differential area compressor bleed control (2,732,125). Lowell E. Ruby, Marlborough, Conn., assignor to United Aircraft Corp.

Multistage axial flow compressor in which the intermediate stage is bled to

George F. McLaughlin, Contributor

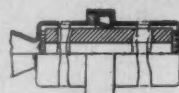
move a piston as a function of compressor pressure ratio. Discharge pressure is admitted to the flow regulating means to control compressor bleeding.

Rocket sight for aircraft (2,733,006). Horace W. Babcock, Pasadena, Calif., assignor to the U. S. Navy.

Fire control sight with motor coupled sighting member and computer. A potentiometer with a sliding contact is mechanically coupled so that incremental movements of the sight are followed by corresponding movements of the contact.

Ejectable aircraft seat capsule (2,733,027). Doane R. Gero, Akron, Ohio, assignor to Goodyear Aircraft Corp.

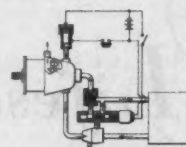
One piece shell, completely open at front, on launching rails. A lower and upper door completely closing the shell are operated by gas power located within the capsule.



2,733,568

Solid propellant jet reaction motor (2,733,568). Lionel A. Dickinson, Aylesbury, England, assignor to the British Government.

Propellant grain within a casing providing an annular space between its outer surface and the inside surface of the casing. The space communicates with the inside of the grain at both ends and an annular resilient sealing washer prevents the longitudinal flow of gas through the space in a rearward direction.



2,733,569

System for supplying liquid fuel to a combustion chamber (2,733,569). David R. Trowbridge, Horncchurch, England, assignor to the Plessey Co., Ltd.

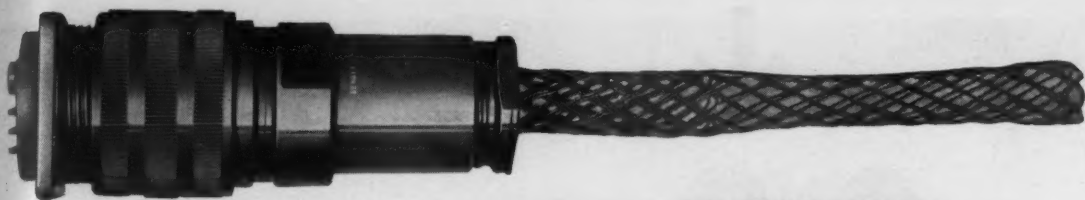
Pressurized exhaust gases are initially supplied to the combustion chamber from a cartridge firing device. A regulating valve conducts the flow of low pressure fuel from the turbopump to the chamber. **Jet engine power regulator (2,734,340).** Cyrus F. Wood, Swarthmore, Pa., assignor to Westinghouse Electric Co.

A normally balanced electrical network operated in response to engine speed and temperature is used for varying the fuel input and the area of a jet nozzle.

Gas turbine engine with means for reheating turbine exhaust gases (2,734,341). Alfred Cyril Lovesey, Derby, England, assignor to Rolls-Royce Ltd.

Closed end casing structure in the exhaust duct with a restriction maintaining the combustion chamber pressure approximately at that within the main combustion equipment.

EDITOR'S NOTE: The patents listed above were selected from recent issues of the Official Gazette of the U. S. Patent Office. Printed copies of patents may be obtained at a cost of 25 cents each, from the Commissioner of Patents, Washington 25, D. C.



Presenting the New **QWL** **Bendix** ELECTRICAL CONNECTOR

A HEAVY-DUTY WATERPROOF POWER AND CONTROL CONNECTOR FOR USE WITH MULTI-CONDUCTOR CABLE

This new QWL Bendix* Electrical Connector was designed for and is being used principally on ground-launching equipment for missiles and ground radar equipment.

Obviously, for this important type of service only the highest standards of design and materials are acceptable.

That's why it will pay you to specify the Bendix QWL Electrical Connector for any job that requires exceptional performance over long periods of time.

QWL outstanding features:

1. It combines the strength advantages of machined bar stock aluminum with the shock-resistant qualities of a resilient insert.
2. A modified, double stub thread provides for speed and convenience in mating and disconnecting and the special tapered cross-section thread design resists loosening under vibration. The threads can be easily hand cleaned if contaminated by a substance such as mud or sand.
3. An Alumilite 225 hard anodic finish is used which gives a case hardening to the aluminum surface. This finish offers outstanding resistance to corrosion and abrasion.

4. The cable-compressing gland used within the cable accessory accomplishes both a firm anchoring of the cable and effective waterproofing for multi-conductor cables. Neoprene sealing gaskets are used at every joint to insure a watertight connector assembly.

5. The cable accessory is designed to accommodate a Kellogg stainless steel wire strain relief grip for additional cable locking.

6. A left-hand thread is used on the cable accessory to prevent inadvertent loosening.

7. High-grade copper alloy contacts are used which provide for high current capacity and low voltage drop. The famous Bendix closed-entry socket is used for contacts sizes 12 and 16.

*TRADEMARK

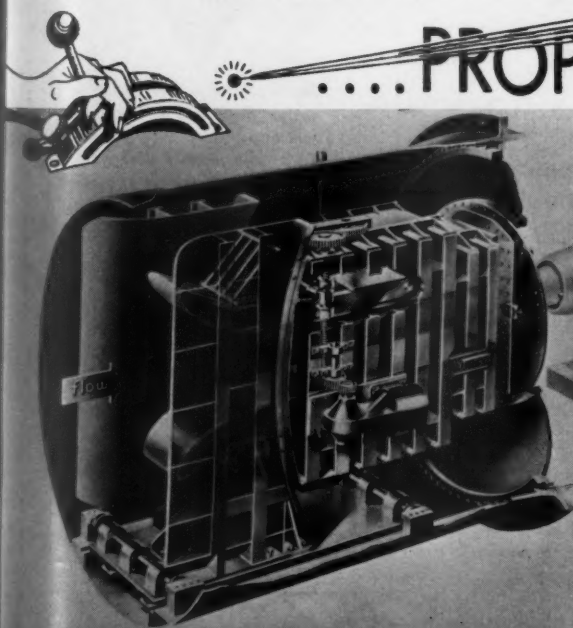


SCINTILLA DIVISION OF
SIDNEY, NEW YORK



Export Sales and Service: Bendix International Division, 205 East 42nd St., New York 17, N.Y.
Canadian Representatives: Aviation Electric Ltd., 200 Laurentien Blvd., St. Laurent, Montreal 9, Quebec

NEW DIMENSIONS forPROPULSION TESTING



Realistic simulation of flight trajectories for supersonic ramjet engines is now possible with a "VARIABLE SUPERSONIC NOZZLE" developed by several engineers of ARO, INC., operating contractor for the U.S. Air Force's ARNOLD ENGINEERING DEVELOPMENT CENTER... typical of contributions to aeronautical progress by engineers staffing the advanced research and development facilities of this \$250 million wind tunnel center.

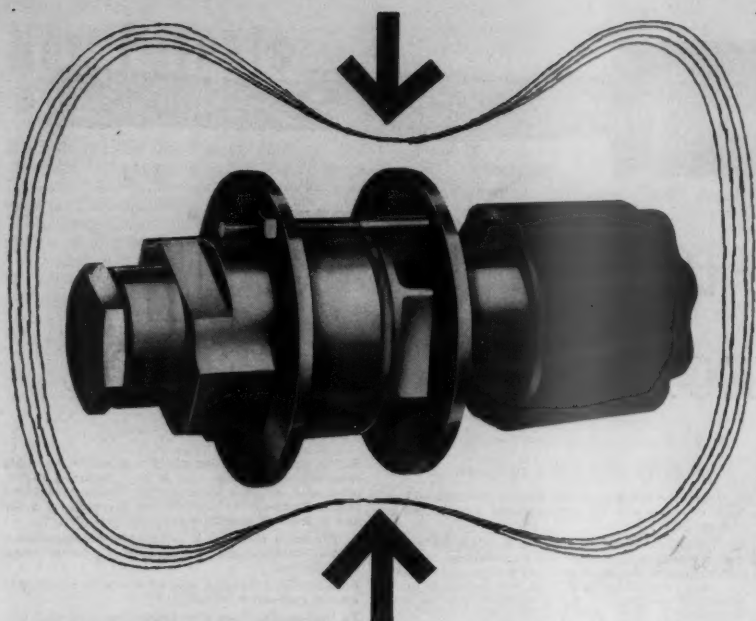
Current vacancies: TURBOJET and RAMJET PERFORMANCE ANALYSTS . . . EXPERIMENTAL RESEARCH THERMODYNAMICISTS . . . SENIOR TEST PROGRAMMERS . . . SUPERSONIC AERODYNAMICISTS.

write -- Lee C. Kelley

ARO, INC., TULLAHOMA, TENNESSEE

A subsidiary of Sverdrup & Parcel Inc., St. Louis, Missouri

ARNOLD ENGINEERING DEVELOPMENT CENTER



REVOLUTIONARY, NEW HIGH PRESSURE REGULATOR

Look at these outstanding new developments:

- Widest adjustment range available for manual regulation due to greater sensitivity created by a new engineering innovation!
- 1/4" tube straight thread gasket seal bosses per AND10050!
- Maximum inlet pressure of 4500 psi!
- Internal relief valve and filter!
- Internal valve and filter are removable without disturbing spring, diaphragm structure!

Catalog Number	Adjustable Range Outlet Pressure PSI
110100-2	5/150
110100-4	15/300
110100-6	30/750
110100-8	150/1500
110100-10	400/3000

Write today for new engineering data sheet and catalog covering our complete range of regulators.

APCO

ACCESSORY PRODUCTS CORP.

Dept. - J-4 616 W. Whittier Blvd.
Whittier, Calif. • Phone: OXford 3-3747

**SQUIB
SPECIALISTS**



ELECTRIC
PRIMERS

EXPLOSIVE POWER
CARTRIDGES

GAS-GENERATING
CANISTERS

M-48 Power
Cartridge
2700 psi
into 20 cc

An organization specializing in the design, development, and manufacture of explosive ordnance, McCormick Selph places first emphasis on dependability. The entire group is located in a 60,000-sq-ft plant on a 200-acre site having perhaps the most complete facilities of its kind in existence.

Your procurement and reliability problems in specialized explosives* can probably be solved at McCormick Selph — either with standard items, tried and proved, or with units produced to meet your specific need.

Send for data
or submit your
problems to:

* Ignition
Actuation
Ejection
Fracturing



**MCCORMICK SELPH
ASSOCIATES**
HOLLISTER 2, CALIFORNIA

JPL

CORPORAL

MARTIN

MATADOR

NORTH
AMERICAN

NAVAHO

REDSTONE
ARSENAL

REDSTONE

CHANCE
VOUGHT

REGULUS

NORTHROP

SNARK

AND THE LATEST
INTERCONTINENTAL MISSILES



ALL these
great guided missiles carry vital
electronic equipment protected by

ROBINSON

ALL-METAL SHOCK and VIBRATION MOUNTS

Decisions by design groups to specify Robinson stand on exacting performance tests. These tests compared every available shock and vibration mount to prove which had superior characteristics and which could best stand the terrific punishment of guided missile operation. We invite you to submit your problem of maximum protection and optimum functioning of airborne electronic equipment.

VIBRATION CONTROL IS RELIABILITY CONTROL

ROBINSON AVIATION INC.

TETERBORO, NEW JERSEY

Vibration Control Engineers

AIRBORNE DIVISION

SEND FOR BULLETIN No. 800—
Robinson Vibration and Shock Mounts for
Guided Missiles, Rockets, and Jet Aircraft

Book Reviews

Ali Bulent Cambel, Northwestern University, Associate Editor

Mathematics of Engineering Systems, by Derek F. Lawden, M. A., Methuen, London; John Wiley, New York; 1954, viii + 380 pages. \$5.75.

Reviewed by JOHN J. MARTIN
Bendix Products Division
Bendix Aviation Corporation

"Mathematics of Engineering Systems" will serve as an excellent primer for the young engineer beginning in the dynamic analysis of physical systems, and will in addition be the ready reference, for the most part, for the practitioner of the art. The physical systems considered range through electronic amplifiers and oscillators, electric circuits, servomechanisms and regulators, and other mechanical and electrical systems. The book will be a blow to the feelings of some undergraduates who hold that their courses in mathematics and mechanics are needless complications to receiving a baccalaureate degree.

The book begins with a concise as well as complete introduction to fundamentals, including the definition of the function concept, limits and derivatives, integrals, and complex numbers. For the person without the mathematical background to take Chap. 1 in stride, further study would be indicated before the latter chapters are taken on. For the most part, Chap. 1 will serve as a sufficient review for the above average graduate engineer.

Chap. 2, without much ado, gets into the practice of solving linear differential equations with constant coefficients by classical methods, and applies these to the solution of practical problems. As the next obvious step, the chapter considers simultaneous differential equations of the type mentioned and brings this consideration to useful fruition in the study of the stability of linear systems in general, and of some common systems in particular.

Chap. 3 extends the work of Chap. 2 on linear differential equations with constant coefficients from the point of view of modern methods. For the most part, the introduction and use of the operational calculus are the substance of the chapter, and this is applied to linear systems. The chapter is concluded by the generalization of the Heaviside operational calculus to the method of the Laplace transform.

Chap. 4 deals with Fourier analysis and is a standard treatment beginning with the trigonometric series representation of periodic functions, continuing with a study of how the coefficients of this series are obtained, and giving some useful applications. These practical applications include those relating to the band width of an R.F. amplifier and to the servomechanism. After this, some of the advantages of the Fourier analysis are presented, and the chapter is concluded with a consideration of the Fourier integral in the infinite interval. Hence the text treats the operational calculus from Heaviside to the generalizations named for Laplace and Fourier.

In the final chapter, Chap. 5, some modern work applying to nonlinear differential equations is given and these range over the same problems treated earlier in the text. If the subject of the last chapter becomes of considerable interest to the reader, other texts on nonlinear mechanics may be of interest. Two good ones are "Non-Linear Mechanics" by Minorsky and "Introduction to Non-Linear Mechanics" by Kryloff and Bogoliuboff.

Running through the text are problems, the solutions for which are given in the back of the book. In addition, a short table of common Laplace transforms is included. In general, the book is highly recommended for those entering or engaged in systems analysis work.

A History of Mechanical Inventions, by Abbott Payson Usher, Harvard University Press, Rev. Ed., 1954, 450 pp. \$9.

Reviewed by R. S. HARTENBERG
Northwestern University

Recent discoveries in physics, reduced to practice by advances in technology, have somewhat shaken the world. Just where and how these things will find their place in the future remains to be seen. The new horizons are only relative, however, for the past has had its technological and other impacts, too—a fascinating story unknown to many. An outline of this story is presented in this "History of Mechanical Inventions."

History, the study of past events, is, contrary to a generally held belief, neither static nor well defined, for it is the study of man's unrest. Knowledge derived from newly found archeological evidence, mislaid documents and the enlightened collation of old materials adds continuously to the story of how it was. This edition, a revision that covers a span of 25 years, reflects the winnings of those years.

Abbott Payson Usher, Professor of Economics (Emeritus) at Harvard University, has an interest and understanding that goes beyond mechanical devices. The interplay of the forces of nature and their economic implications has been the author's concern in four other volumes: it is from this matrix of ideas that the present volume is justly derived. One may not agree with all points of Professor Usher's thesis, but one will find each thought-provoking.

Since mechanical inventions are many, and perhaps even impossible to list completely, a consideration of the chapter headings is necessary to show the scope of the over 400 pages of text. They are: I, The Place of Technology in Economic History; II, Historical Analysis of Social Change; III, The Particular System of Events; IV, The Emergence of Novelty in Thought and Action; V, The Early History of the Pure Applied Mechanical Sciences; VI, The Mechanical Equipment of Pre-Christian Antiquity; VII,

The Development of Water Wheels and Windmills; 150 B.C.-A.D. 1500; VIII, Water Clocks and Mechanical Clocks; 16 B.C.-A.D. 1500; IX, Leonardo da Vinci: Engineer and Inventor; X, The Invention of Printing; XI, Machinery of the Textile Industries; 100-1800; XII, The Development of Clocks and Watches into Instruments of Precision; 1500-1800; XIII, The Production and Application of Power; 1500-1830; XIV, Machine Tools and Quantity Production; 1450-1850; XV, The Production and Distribution of Power Since 1832.

The first four chapters are entirely new to this revision. Here a theory of invention and a concept of social evolution are presented. Gestalt psychology forms the basis of the argument; according to this, the mark of man's behavior is the manifestation or striving to achieve an end, where the solution to the problem is reached by an act of insight, a grasp of the logical significance of the whole situation, instead of by only the blundering tactics of trial and error.

The remainder of the book is in the form of a critical narrative, concerned in large part with the production of power. Necessarily the interdependence of industry and power, of mechanism and machine, are studied.

It is inevitable that a reader will find that he has questions that are left unanswered. In justice to this fine single volume he must realize that there was space for only selected topics, and that even these could not always be discussed in ultimate detail. The Notes and Bibliography are extensive; they show not only the tremendous wealth of source material but also the great diversification of sources.

This book is well worth reading, for it is not often that one finds the story of how the particular is imbedded in a total pattern, i.e., the relation of a part to the whole.

HALEY ELECTED CHAIRMAN OF ARS BOARD

At a meeting of the ARS Board of Directors in New York City on January 24, 1956, Mr. Andrew G. Haley, a Director of the Society, and Past President of the ARS, was elected Chairman of the Board of Directors, to serve in that capacity until the return to active duty of President Noah S. Davis, Jr. Mr. Davis is currently unable to serve as Chairman of the Board because of illness, although his return to this capacity is expected in the near future. This election was conducted in accordance with the provisions of Article VII, Section 4, of the ARS by-laws.

Mr. Haley was also named, at the last meeting, to membership on the ARS Space Flight Committee.

AIRCRAFT-TYPE hydraulic POWER UNITS ...

To supply dependable hydraulic power for critical applications, Eastern units are engineered to perform under extreme conditions. Compact design and varying motor sizes make them unique power sources, especially desirable for airborne use. The equipment illustrated in detail presents a typical Eastern Power Unit designed for one application. Many other requirements can be satisfied with designs of this general type.

Unit consists of: positive-displacement pump, electric motor drive, oil reservoir, expansion chamber, porous bronze ten-micron filter, pressure regulating valve, filter relief valve, and expansion relief valve.

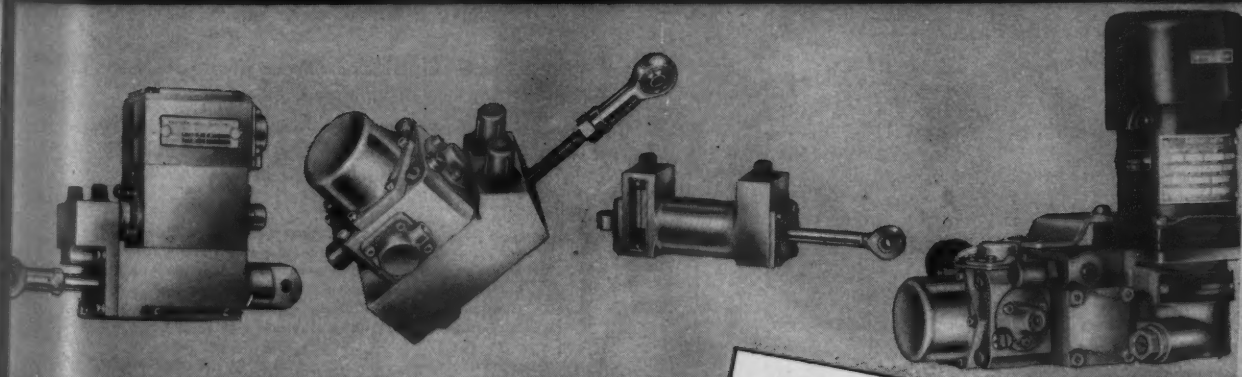
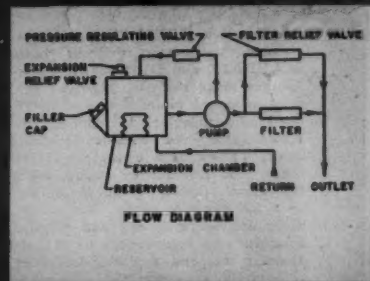
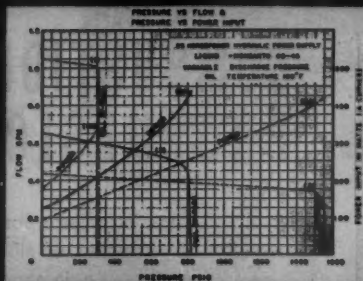
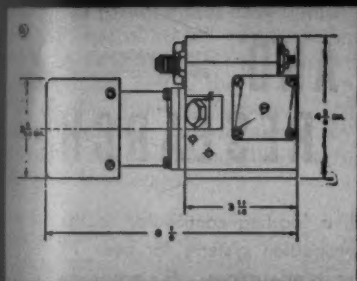
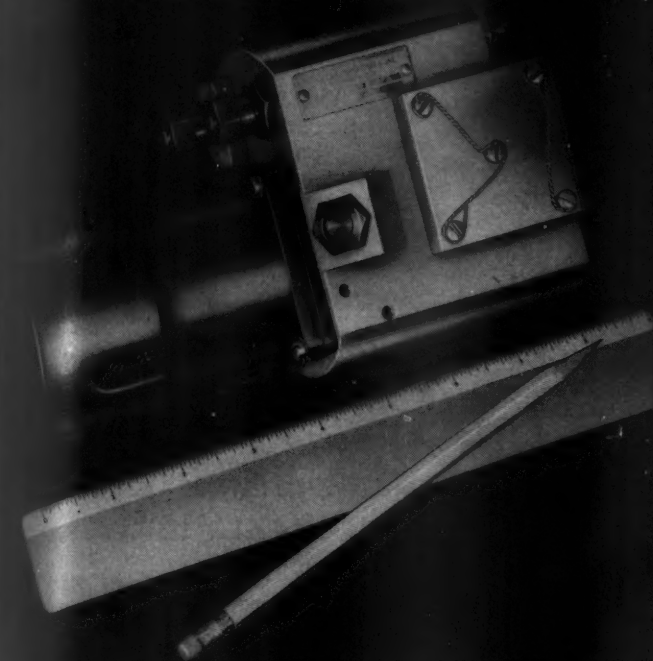
SPECIAL UNITS to be built into Servo Systems and specialized projects are available. As illustrated below, Actuators combined Servo-valve and Actuator, and Servo-valve Hydraulic System combinations are being produced by Eastern for custom-specified jobs. If your project involves equipment of this type, write to us for further information.

Specifications:

Available with either $\frac{1}{8}$, $\frac{1}{4}$, or $\frac{1}{2}$ horsepower motor, in 28 V. D.C. or 400 Cycles 3 Phase power.

Available with various pump characteristics. Under certain operating conditions, units can be made self-cooling. Example: $\frac{1}{4}$ H.P. Unit has a continuous-duty oil-temperature rise above ambient of approximately 60 F. at sea level. Pressure range from 0 to 1500 PSIG with compatible flow.

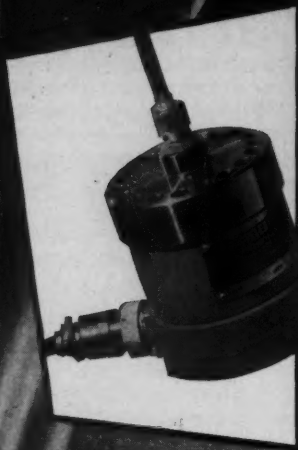
Anodized aluminum body contains all components except motor.



Write for Aviation
Products Catalog 340



Teledyne BONDED STRAIN GAGE ELECTRICAL PRESSURE TRANSMITTER



...research and testing on
rockets, pulse jets, and turbo jets.
...range, 0-10,000 P.S.I.

Research and test personnel engaged in projects on rockets, pulse jets and turbo jets can control higher pressures with the new TELEDYNE electrical pressure transmitter that is both **ACCURATE** and **DURABLE**. These features make the new Teledyne the most advanced piece of equipment of its kind available: 15 ranges (0-10,000 PSI) for wide application. Bonded strain gage construction (insensitive to vibration or shock). High frequency response. Linear output over full pressure range. Easily disassembled for clean-out and repairs. Insensitive to accelerations in 2 horizontal planes and vertically less than .3% of full scale per "G". Temperature compensated for zero shift and sensitivity change.

Courtesy LEEDS & NORTHRUP

The Model S shown becomes a part of the **TABER** Teledyne system for Indicating, Recording and Controlling pressures, both liquid and gas. Model S has integral control unit for proportioning type control.



Write for Illustrated Literature

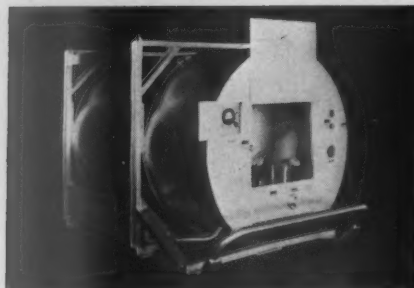


TABER INSTRUMENT CORPORATION
SECTION 211

111 Goundry St., N. Tonawanda, N.Y.

The **SAFE-EFFICIENT** EQUIPMENT for **HANDLING**

Liquefied Oxygen and Nitrogen



MODEL
LOX 150
●
150 GALLON
CAPACITY

VACUUM INSULATED STORAGE AND TRANSPORT CONTAINERS

produced by

CRYOGENIC DIVISION
RONAN AND KUNZL, INC.
MARSHALL, MICHIGAN

ILLUSTRATED LITERATURE IS AVAILABLE. WE INVITE YOUR INQUIRY.

COMBUSTION AND PROPULSION RESEARCH

Experiment Incorporated, a leading contributor to the development of missile propulsion systems for over 11 years, is again expanding its operations. Ei's programs cover a broad range of activities from fundamental research to design and fabrication of engines.

ENGINEERS and SCIENTISTS with experience are needed for challenging and responsible positions in:

- Air-Turborocket Development
- Engine Component Design
- Rocket Design and Testing
- Propellant Development
- Fundamental Combustion Research



Located in suburban Richmond for over a decade, the company offers completely modern facilities, attractive working conditions and opportunity for individual responsibility. Living is pleasant in Richmond and the company maintains competitive salaries with liberal benefit programs. A relocation allowance is provided new employees.

For descriptive brochure, address inquiries to Personnel Manager.

EXPERIMENT INCORPORATED
RICHMOND 2, VIRGINIA
RESEARCH • DEVELOPMENT • ENGINEERING • PRODUCTION

THE RV-A-10 MISSILE

**powered by a
"THIOKOL"
solid propellant
rocket motor**

The RV-A-10 missile, developed jointly by the Army Ordnance Corps, General Electric, and Thiokol Chemical Corporation, is an example of technical progress in solid propellant rocketry. The rocket motor for this missile was designed and developed by the Thiokol Chemical Corporation. Its successful flight tests definitely established the feasibility of "Thiokol" solid propellant power plants for use in large, long range and high altitude missiles.

Development of the power plant for the RV-A-10 stems largely from Thiokol's "systems" concept of rocket motor development. Under this concept of rocket motor design, all of the requirements of the missile are taken into consideration before the propulsion unit is put on the drawing boards. The motor's thrust, duration, size and shape are all governed by the specific application for which the unit is intended.

Close coordination is conducted with the missile prime contractor to consider problems such as aerodynamic stability, center of gravity requirements, guidance system impact and vibration resistance, wing and fin attachments, and other over-all missile problems.

Engineers and Chemists — become a member of Thiokol's rocket development and manufacturing team. We welcome inquiries from mechanical engineers, chemical engineers and chemists interested in the rocket field.

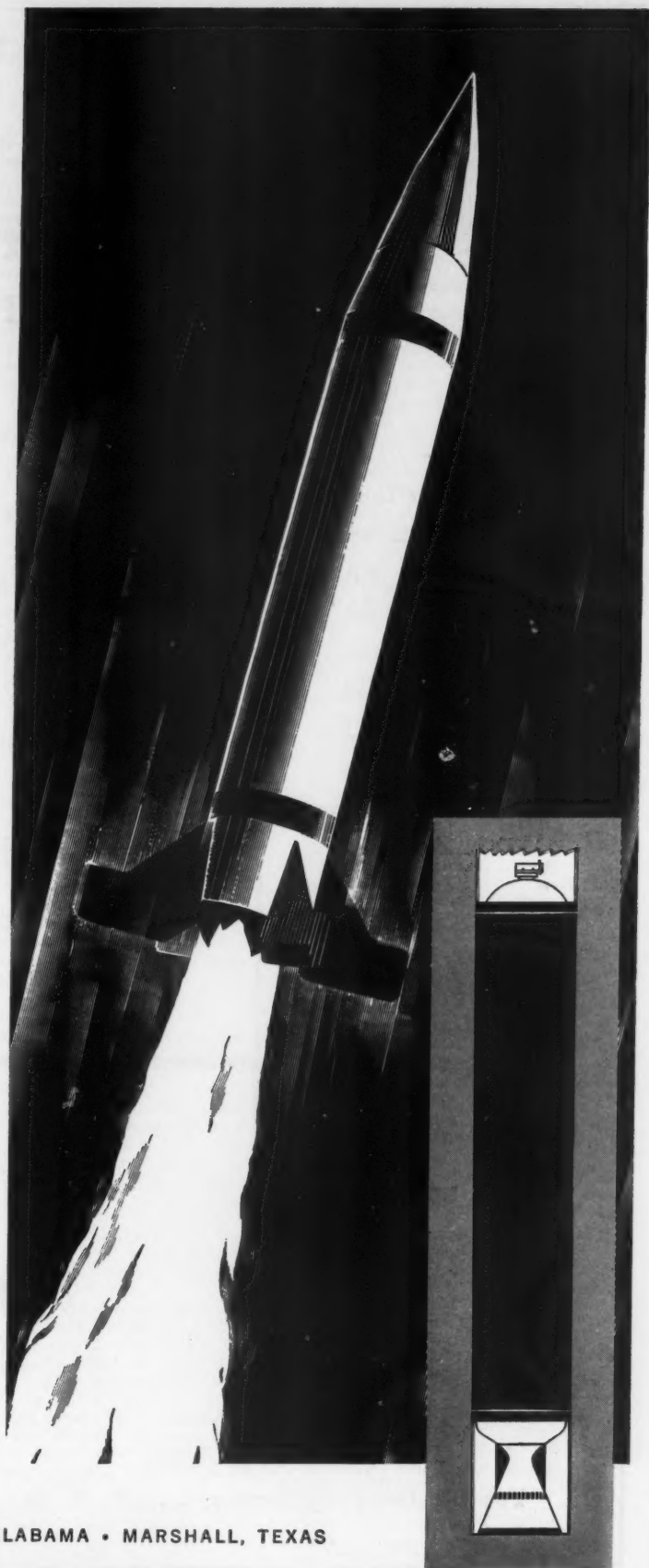
THIOKOL CHEMICAL CORPORATION

780 North Clinton Avenue,
Trenton 7, N. J.

Thiokol®
CHEMICAL CORPORATION

ROCKET DIVISIONS AT

ELKTON, MARYLAND • HUNTSVILLE, ALABAMA • MARSHALL, TEXAS



EMPLOYMENT OPPORTUNITIES

for
Engineers . . Scientists
Experienced Technical
Specialists and Trainees

to
Work and Live in
Smog - Free Redlands

For Your
Invitation
To Join
Our Team
Of Solid
Propellant
ROCKET
Specialists
Call
PYramid 4-6775
Ask for
Mr. Graber

ROCKETS

BOOSTERS

**MISSILE
POWER
PLANTS**

**SPECIAL
DEVICES**



For Challenging Careers . . . P. O. Box 111, Redlands, California

Technical Literature Digest

M. H. Smith, Associate Editor, and M. H. Fisher, Contributor
The James Forrestal Research Center, Princeton University

Jet Propulsion Engines

Effects of Variation in Fuel Pressure on Combustion Performance of Rectangular Ramjet, by Wesley E. Messing and Dugald O. Black, *NACA RM E8T28*, Nov. 1948, 26 pp. (Declassified from Confidential, Dec. 2, 1955.)

The Supercharged and Intercooled Free-Piston and Turbine-Compound Engine, a Cycle Analysis, by A. L. London, *ASME Paper* no. 55-A-147, Nov. 1955, 8 pp.

Some Design Aspects of the Free Piston Gas Generator Turbine Plant. Part I, Thermodynamic and Component Characteristics, by S. L. Soo and W. A. Morain. Part II, Control and Accessories, by W. A. Morain and S. L. Soo, *ASME Papers* no. 55-A-146 and A-55-155, Nov. 1955, 30 and 20 pp.

The Slotted Blade Axial Flow Blower, by H. E. Sheets, *ASME Paper* no. 55-A-156 Nov. 1955, 11 pp.

Closed Systems for Testing Compressors, by R. M. Johnson, *ASME Paper* no. 55-A-157, Nov. 1955, 9 pp.

Tests on a Typical Whittle Compressor, by A. Simons and C. K. Roberts, *Gt. Brit. Aeron. Res. Coun. Rep. and Mem.* no. 2913, 1955, 10 pp.

The Gyrone—Most Powerful Jet Engine in the World; Announcement of the Gyrone Junior, *De Havilland Gazette*, no. 89, Oct. 1955, pp. 132-133.

Heat Transfer and Fuel Flow

An Experimental Investigation of Two-Dimensional Turbulent Mixing of Parallel Compressible Jets at Large Temperature Differences and Approximately Equal Mach Numbers, by Ronald E. Walker, *Bumblebee Rep.* no. 232, May 1955, 78 pp. (The Johns Hopkins Univ., Appl. Phys. Lab.)

The Viscosity of Steam, Heavy Water Vapor and Argon at Atmospheric Temperature Up to High Temperatures, by C. F. Bonilla, S. J. Wang, and H. Weiner, *ASME Paper* no. 55-A-6, Nov. 1955, 4 pp.

Momentum Diffusion from a Slow Jet into a Moving Secondary, by A. S. Weinstein, J. F. Osterle, and W. Forstall, *ASME Paper* no. 55-A-60, Nov. 1955, 7 pp.

Liquid Droplet Heating and Evaporation in a High Temperature Gas Stream, by J. W. Rizika, *ASME Paper* no. 55-A-154, Nov. 1955, 25 pp.

The Thermodynamics of Cooled Turbines, by W. R. Hawthorne. Part I, The Turbine Stage; Part II, The Multi-stage Turbine, *ASME Papers* no. 55-A-186 and 55-A-191, Nov. 1955, 25 and 11 pp.

Application of Internal Liquid Cooling to Gas Turbine Rotors, by Sumner Alpert, Ralph E. Grey, and Delson D. Drake, *ASME Paper* no. 55-A-202, Nov. 1955, 21 pp.

An Experimental Investigation of Flow Separation in Nozzle at High Mach Numbers and Low Density, by Norman B. Tucker, *Toronto Univ. Inst. of Aerophys. Rep.* no. 33, Aug. 1955, 33 pp.

Tables for Quasi-Exponential Decay of Explosive Shock in Air, by G. F. Kinney, *Naval Postgrad. School, Res. Rep.* no. 8, Nov. 1955, 10 pp.

Engineering Relations for Heat Transfer and Friction in High Velocity Laminar and Turbulent Boundary Layer Flow Over Surfaces with Constant Pressure and Temperature, by E. R. G. Eckert, *ASME Paper* no. 55-A-31, Nov. 1955, 11 pp.

Calculation of a Cascade for a Distribution of Subsonic Mach Numbers Given as a Potential Function, by Robert Legendre, *Recherche Aeron.* no. 47, Sept.-Oct. 1955, pp. 3-9 (in French).

Combustion

Sampling Studies of Cool Flames, by K. G. Williams, J. E. Johnson, and H. W. Carhard, *Indust. Engng. Chem.*, vol. 47, Dec. 1955, pp. 2528-2532.

Pulsating, Pressure Generating Combustion Systems for Gas Turbines, by F. H. Reynst, *ASME Paper* no. 55-A-56, Nov. 1955, 12 pp.

The Temperature Stability of the Laminar Combustion Wave, by J. F. Wehner, *Princeton Univ. Chem. Kinetics Project, TN 24 (Off. Sci. Res. TN-55-426)*, July 1955, 13 pp.

The Explosive Reaction of Carbon Monoxide and Oxygen at the Second Explosion Limit in Quartz Vessels, by Alvin S. Gordon and R. H. Knipe, *J. Phys. Chem.*, vol. 59, Nov. 1955, pp. 1160-1165.

Spectrum of Carbon-Monoxide Oxygen Explosion. I. The Visible Spectrum, by R. H. Knipe, and Alvin S. Gordon, *J. Chem. Phys.*, vol. 23, Nov. 1955, pp. 2097-2101.

On the Origin of the Electronically Excited C_2 Radical in Hydrocarbon Flames, by R. E. Ferguson, *J. Chem. Phys.*, vol. 23, Nov. 1955, pp. 2085-2089.

Experimenting with Rocket System Stabilizers, by Y. C. Lee, A. M. Pickles, and C. C. Miesse, *Aviation Age*, vol. 25, Jan. 1956, pp. 110-115.

Burning Velocities of Hydrogen-Air Flames, by Herman Burwasser and Robert N. Pease, *J. Amer. Chem. Soc.*, vol. 77, Nov. 20, 1955, pp. 5806-5808.

Integration of a Simplified Kinetic Model for a Hydrogen Bromine Flame, by Edwin S. James, *Wisconsin Univ. Naval Res. Lab. CM-849*, July 1955, 82 pp.

An Investigation of High-Frequency Combustion Oscillations in Liquid-Propellant Rocket Engines, by Adelbert O. Tischler, Rudolph V. Massa, and Raymond L. Mantler, *NACA RM E53B27*, June 1953, 37 pp. (Declassified from Confidential, Dec. 2, 1955.)

The Effect of Structure on Combustion Stability of Liquid Propellant Rockets During Flight and During Static Test Stand Firings, by Robert S. Wick, *Calif. Inst. of Tech. Jet Propulsion Lab. Prog. Rep.* 20-274, July 1955, 36 pp.

Combustion Instability in Liquid Propellant Rocket Motors, *Princeton Univ. Dept. Aeron. Engng., Rep.* 216-M (13th Quart. Prog. Rep.), May 1-July 31, 1955, 23 pp.

Spectrographic Study of a Combustion Wave in the Laminar Regime, by S. Barrère, *Recherche Aeron.*, no. 46, July-Aug. 1955, pp. 15-24 (in French).

Burning Rate Studies. II. Variation of Temperature Distribution with Consumption Rate for Burning Liquid Systems, by D. L. Hildenbrand and A. Greenville Whittaker, *J. Phys. Chem.*, vol. 59, Oct. 1955, pp. 1024-1028.

Fuels, Propellants, and Materials

Vapor- and Liquid-Phase Reactions Between Nitrogen Dioxide and Water, by M. S. Peters and J. L. Holman, *Indust. Engng. Chem.*, vol. 47, Dec. 1955, pp. 2536-2539.

Nitric Acid-Nitrogen Dioxide-Water System, by Anderson B. McKeown and Frank E. Belles, *Indust. Engng. Chem.*, vol. 47, Dec. 1955, pp. 2540-2543.

Stability of Dilute Alkaline Solutions of Hydrogen Peroxide, by W. D. Nicoll and A. F. Smith, *Indust. Engng. Chem.*, vol. 47, Dec. 1955, pp. 2548-2554.

Corrosion of Metal Rods by the Products of Combustion of Perchlorate Propellants, by Robert W. Geene, *Aberdeen Prov. Ground, Ballistic Res. Labs. Mem. Rep.* no. 928, Sept. 1955, 10 pp.

The Development of Cermets as Structural Materials, by J. T. Norton, *ASME Paper* no. 55-A-196, Nov. 1955, 9 pp.

A Report on Jet Fuel Stability Studies by C. M. Barringer and others, *SAE J.*, vol. 63, Dec. 1955, pp. 39-44.

Oxidant Resistant Coatings for Molybdenum, by J. R. Blanchard, *Wright Air Dev. Center, TR* no. 55-205, June 1955, 36 pp.

Effect of Dissolved Oxygen on the Filterability of Jet Fuels for Temperatures Between 300° and 400° F., by Anderson B. McKeown and Robert R. Hibbard, *NACA RM* no. E55I18, Dec. 1955, 22 pp.

Research on the Safety Characteristics of Normal Propyl Nitrate, *Bur. Mines, Div. Explosives Tech. Prog. Rep.* no. 1, Sept. 14-Oct. 31, 1955, 10 pp.

Studies on Boron Hydrides, Ninth Annual Report of Investigations on Water Reactive Chemical Compounds, by Anton B. Burg, *Univ. Southern Calif. Dept. Chem.*, Nov. 1955, 28 pp.

Which Alloys for Jet Hot Spots, by S. G. Demirjian, *Materials and Methods*, vol. 42, Oct. 1955, pp. 116-118.

Jet and Rocket Applications of the "New" Metals, by Gerald D. Johnson, *J. Space Flight*, vol. 7, Nov. 1955, pp. 1-4.

Physical Properties of Fourteen API Research Hydrocarbons, C_9 to C_{15} , by David L. Camin and Frederick D. Rossini, *J. Phys. Chem.*, vol. 59, Nov. 1955, pp. 1173-1179.

Instrumentation and Experimental Techniques

A Method of Telemetering Temperature Data, by R. S. Weil, *J. Instrum. Soc. Amer.*, vol. 2, Nov. 1955, pp. 502-504.

Note on a Convenient Recording Technique for Rapid Changes (in Temperature), by A. D. Misner, *Can. J. Tech.*, vol. 34, Jan. 1955, pp. 41-43.

Guide to Instrumentation Literature, by W. G. Brombacher, Julian F. Smith, and

An Invitation to Scientists and Engineers:

SPEND FIVE MINUTES EXPLORING YOUR FUTURE

There is a dynamic future ahead in the controls field. Automatic controls and instrumentation are playing an increasingly more important role in the development of our air defenses. No other field offers greater challenges to capture your interests and to fully utilize your creative capabilities. No other area of endeavor affords the scientist and engineer greater opportunity for professional and economic growth.

The Aeronautical Division of Robertshaw-Fulton Controls Company—engaged in a broad and expanding program of research, development, engineering and production of control devices for aircraft, missiles and ordnance equipment—invites you to explore the unprecedented career opportunities now open in this field of steadily increasing importance.

Robertshaw-Fulton's Aeronautical Division is one of the newest and best equipped research and development facilities in Southern California. Here you will find unusual diversity, blended with the stability afforded by a company that has been a leader in its field for more than half a century. Here, you would be associated with a small, broadly competent, carefully selected staff.

In this stimulating yet practical atmosphere, you will know the widest possible scope of interests and professional satisfactions, the greatest personal achievement, responsibility and recognition.

Southern California's Orange County is considered by many as an ideal working environment. Here you will find the best in suburban living...excellent housing, schools, relaxed community life and a superb year-around climate...close proximity to the sea, mountains and metropolitan cultural activities.

Selective senior positions, as well as openings for junior engineers and technicians, exist in these fields:

Electronics
Mathematics
Metallurgy

Research Study

Nuclear Physics
Thermodynamics
Chemistry

If you want the satisfactions of doing an absorbing and highly important job, with unlimited opportunity for personal achievement and growth, you will be investing wisely by taking a few minutes of your time to learn more about the challenging future—your future—in the fast growing controls field. Send your resume to Dr. W. M. Roberds, Chairman of Research Department, at the address below.



"Mr. Controls"®

Aeronautical Division
Robertshaw-Fulton

CONTROLS COMPANY
ANAHEIM, CALIFORNIA

Lyman F. Van der Pyl, *Nat. Bur. Stand. Circ. no. 567*, Dec. 1955, 156 pp.

Fuel Cut-Off Control for Guided Missiles, by Gerald L. Zomber and Donald MacMillan, *Electronics*, vol. 29, Jan. 1956, pp. 126-127.

A Practical Pulsation Threshold for Flowmeters, by V. P. Head, *ASME Paper no. 55-A-188*, Nov. 1955, 13 pp.

Pulsation Errors in Manometer Gages, by T. J. Williams, *ASME Paper no. 55-A-92*, Nov. 1955, 17 pp.

Turbine Supervisory Instruments, by J. C. Spahr and R. L. Richards, *ASME Paper no. 55-A-62*, Nov. 1955, 9 pp.

Optical Characteristics of Laminated Camera Windows, by A. C. Marchant and B. M. Mathieson, *Gl. Brit. Aeron. Res. Coun. Curr. Paper no. 210*, 1955, 8 pp.

Turbulence Measurements with the Hot Wire Anemometer, by Ralph D. Cooper and Marshall P. Tulin, *NATO, Advis. Group Aeron. Res. Dev. AGARDograph no. 12*, Aug. 1955, 58 pp.

Ultrasonic Flowmeter, by Jack Kritt, *Instrum. and Automation*, vol. 28, Nov. 1955, pp. 1912-1913.

Ultrasonic Gas Analyzer, by Michael Kniazuk and F. Robert Prediger, *Instrum. and Automation*, vol. 28, Nov. 1955, pp. 1916-1917.

Photo-Eye Sees Red to Detect Rocket Fires, by Henry P. Steier, *Amer. Aviation*, vol. 19, Oct. 10, 1955, p. 42.

Terrestrial Flight, Vehicle Design

Soviet Missile Progress, by Alfred J. Zaehring, *Aero. Digest*, vol. 71, Dec. 1955, pp. 48-51.

Proof Test of Corporal Servicing Platform, XM-280E1, USA No. 5171012, White Sands Proving Ground, Tech. Pub. no. 276, Dec. 1955, 28 pp.

Controlling Ballistic Missile Powerplants During Static Firing and Airborne Operations, by Rudolf H. Reichel, *Aero Digest*, vol. 71, Dec. 1955, pp. 22-27.

Talos Integrates Terrier Frame, Ramjet, by David A. Anderton, *Aviation Week*, vol. 64, Jan. 16, 1956, pp. 37-38.

Atomic Energy

Design Comparison of Reactors for Research, by L. B. Borst, *Ann. Revs. Nuclear Sci.*, Stanford, Calif., 1955, vol. 5 1955, pp. 179-196.

Recent Developments in the Technology of Ceramic Materials for Nuclear Energy Service, by J. M. Warde and J. R. Johnson, *J. Franklin Inst.*, vol. 260, Dec. 1955, pp. 455-466.

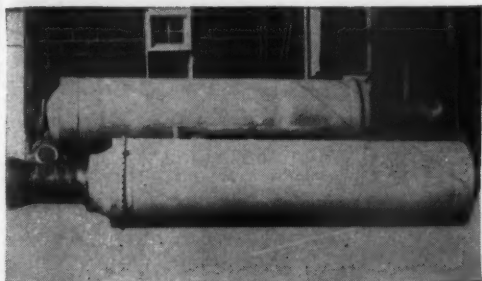
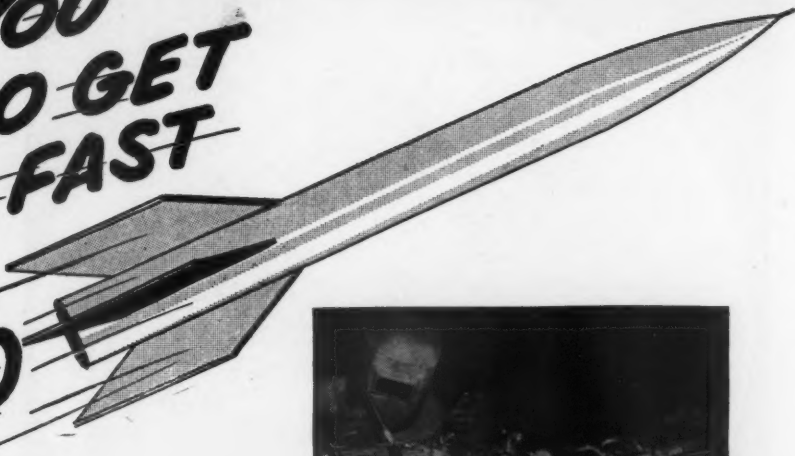
Reactor Handbook, vol. 1, Physics; vol. 2, Engineering; vol. 3, Materials, *Atomic Energy Comm. AECD-3645*, 3466, and 3647, March-May 1955, 790, 1073, and 610 pp., Washington, D. C., U. S. Govt. Print. Off.

Aspects of Nuclear Power Application for Jet Propulsion, Part II, by Norman V. Peterson, *Astronautics*, vol. 2, Fall 1955, pp. 111-118.

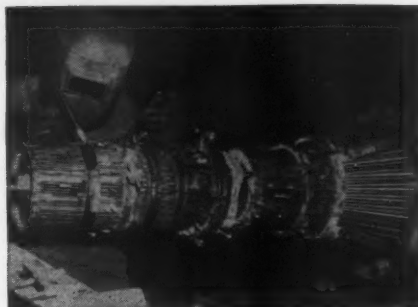
Reactor Engineering Lectures, by Stuart McLain, *Atomic Energy Comm., Argonne Nat. Lab., ANL-5424*, March 1955, 353 pp.

Functional Requirements and Design Criteria for the Air Force Nuclear Engineering Test Facility at Wright Air Development Center, *Wright Air Dev.*

**WHEN YOU
HAVE TO GET
GOING FAST
CALL
EXCELCO**



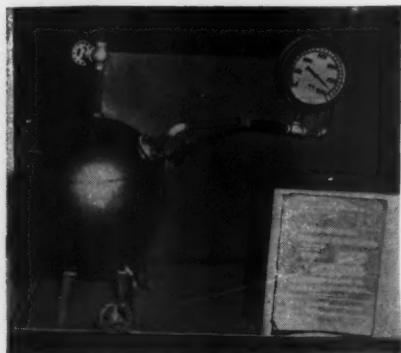
**SOLID PROPELLANT POWER PLANTS
THIN OR HEAVY WALLED
PRECISION MACHINED NOZZLES
& MOTOR CASES ALSO
LIQUID PROPELLANT MOTOR COMPONENTS**



**EXPERIMENTAL WORK
NO JOB TOO TOUGH**



**MOCK UP OR COMPLETE
MODELS**



**HIGH PRESSURE SPHERES EXPERIENCED
IN ALL MATERIALS X4130
HEAT TREATED, STAINLESS,
ALUMINUM ALLOY, INCONEL X ETC.**

**A DIVERSIFIED, EXPERIENCED
ORGANIZATION GEARED TO MOVE QUICKLY
ON YOUR PRELIMINARY PRODUCTION
PROBLEMS; ONE ABLE TO ABSORB YOUR
INITIAL ENGINEERING CHANGES AND PUT
THEM INTO EFFECT WITHOUT DELAY.**

**A LETTER OR PHONE CALL WILL BRING
OUR REPRESENTATIVE**

**EXCELCO DEVELOPMENTS INC.
SILVER CREEK, NEW YORK
PHONE 101**



the sky is our world

From advanced research into the fundamental forces of the universe—gravity, nucleonics, astrophysics—to the launching of man's first stepping stones into space itself, Martin engineering activities are among the most exciting in the aircraft industry today.

The sky is our world, and outer space is the next frontier!

If you are interested in learning the story of a great engineering adventure, which includes some of the most advanced projects now in the research and development stage, contact J. M. Hollyday, Dept. JP-04, The Martin Company, Baltimore 3, Maryland.

MARTIN
BALTIMORE

Center, TN-55-S469, NAA-AER-1495, Oct. 1955, 157 pp.

A Bibliography of Available Digital Computer Codes for Nuclear Reactor Problems, by A. Radkowsky and R. Brodsky, *Atomic Energy Comm. AECU*, 3078, Oct. 14, 1955, 102 pp.

Metallurgical Problems in Design of Nuclear Power Reactors, by Vincent P. Calkins, *Metal Prog.*, vol. 68, Dec. 1955, pp. 73-76.

Preparation of Metal Powders for Nuclear Reactors, by P. Chiotti and H. Wilhelm, *Metal Prog.*, vol. 68, Dec. 1955, pp. 77-80.

An Introduction to Reactor Physics, by George Leppert, *J. Amer. Soc. Naval Engrs.*, vol. 67, Nov. 1955, pp. 855-874.

Powder Metallurgy—Its Role in the Design of Nuclear-Power Reactors, by H. H. Hausner and M. C. Kells, *J. Amer. Soc. Naval Engrs.*, vol. 67, Nov. 1955, pp. 875-882.

Thermonuclear Power Reactors—Are They Feasible? by Hans Thirring, *Nucleonics*, vol. 13, Nov. 1955, pp. 62-65.

Highlights of Reactor Technology, 1942-1955, by M. C. Leverett, *Gen. Elec. Rev.*, vol. 58, Nov. 1955, pp. 23-26.

Materials for Atomic Plants, by Blair R. Elder, *Gen. Elec. Rev.*, vol. 58, Nov. 1955, pp. 38-41.

How to Control a Boiling Reactor, by John Macphree, *Nucleonics*, vol. 13, Dec. 1955, pp. 42-45.

Structural Materials for Heat Transfer in Nuclear Reactors, Part I—Selecting Materials for Liquid Sodium Systems, by R. F. Koenig and E. G. Brush, *Materials and Methods*, vol. 42, Dec. 1955, pp. 110-114.

Astrophysics, Aerophysics, Space Flight

Astronautics, by Eugene Sanger, *Aero Digest*, vol. 71, Dec. 1955, p. 21.

The Satellite Vehicle for Communications and Navigation, by Hayward E. Canney, Jr., *Aero Digest*, vol. 71, Dec. 1955, pp. 40-46.

Interplanetary Magnetic Fields and Cosmic Rays, by Levett Davis, Jr., *Phys. Rev.*, vol. 100, Dec. 1, 1955, pp. 1440-1444.

Radio Observations of the Ionosphere at Oblique Incidence, by J. H. Chapman, Kenneth Davies, and C. A. Littlewood, *Can. J. Phys.*, vol. 33, Dec. 1955, pp. 713-722.

Cosmic-Ray Experiments with a Proton Velocity Selector, by K. W. Ogilvie, *Can. J. Phys.*, vol. 33, Dec. 1955, pp. 746-750.

Studies of Small Scale Turbulent Diffusion in the Atmosphere, by F. N. Frenkiel and I. Katz, *The Johns Hopkins Univ. Appl. Phys. Lab. CM-852*, Aug. 1955, 30 pp.

Circulation in the Upper Atmosphere, by P. S. Pant, *New York Univ. Coll. Engng. Sci. Rep.* no. 1, May 1955, 43 pp. (AF Cambr. Res. Center, TN no. 55-651).

A Method of Sealing and Gas-Conditioning an Orbital Duty Survival Suit, by M. C. Paul, *J. Brit. Interplan. Soc.*, vol. 14, Nov.-Dec. 1955, pp. 300-306.

The Radio Exploration of Space, by R. C. Jennison, *J. Brit. Interplan. Soc.*, vol. 14, Nov.-Dec. 1955, pp. 307-314.

The Volcanic Theory of Martian Green Areas, by A. E. Slatter, *J. Brit. Interplan. Soc.*, vol. 14, Nov.-Dec. 1955, pp. 319-323.

Orbit Lifetimes of the U.S. Artificial Satellites, by Harold Ketchum, *J. Space Flight*, vol. 7, Oct. 1955, pp. 1-5.

JET PROPULSION

495, Oct.
 Digital
 Reactor
 and R.
 AECT.
 Design of
 Vincent P.
 Dec. 1955.
 ders for
 and H.
 Dec. 1955.
 ysics, by
 Naval
 5-874.
 in the
 s, by H.
 Amer.
 1955, pp.
 rs—Are
 ing, Nu-
 -65.
 y, 1942-
 ec. Rev.,
 Blair R.
 v. 1955,
 ctor, by
 3, Dec.
 1
 transfer
 electing
 ems, by
 ials and
 0-114.
 ysics,
 Aero
 nica-
 ard E.
 , Dec.
 s and
 s, Jr.,
 5, pp.
 sphere
 pman,
 ewood,
 713-
 Proton
 , Can.
 6-750.
 t Dif-
 F. N.
 pkins
 Aug.
 sphere,
 Coll.
 13 pp.
 351).
 Condi-
 it, by
 , vol.
 e, by
 Soc.,
 Green
 plan.
 -323.
 ficial
 Space



AIR-TO-GROUND TV SYSTEM

Transmits Combat Pictures on FM

Airborne military television crams a self-contained transmitting station into a small reconnaissance plane, then flies this ever-moving station over unpredictable terrain. Taking these adverse conditions into account, Admiral developed an extremely compact television system which uses FM transmission for the picture. It is now in production for the U.S. Army Signal Corps. Even under difficult conditions, this equipment provides excellent definition.

The transmitting plane, flying at approximately 1,000 feet, would have a line-of-sight range of 25 or 30 miles. This would enable a battle commander aided by a panel of TV screens, each screen showing a different sector, to coordinate military operations over a wide area.

In addition, a mobile ground-to-ground TV system is under development. Inquire about Admiral's exceptional capabilities in the field of military electronics. Address inquiries to:

Admiral.

CORPORATION

Government Laboratories Division, Chicago 47

**LOOK TO Admiral FOR
RESEARCH • DEVELOPMENT • PRODUCTION
IN THE FIELDS OF:**

COMMUNICATIONS UHF AND VHF • MILITARY TELEVISION
RADAR • RADAR BEACONS AND IFF • RADIAC
TELEMETERING • DISTANCE MEASURING
MISSILE GUIDANCE • CODERS AND DECODERS
CONSTANT DELAY LINES • TEST EQUIPMENT

Facilities Brochure describing
Admiral plants, equipment and ex-
perience sent on request.



ENGINEERS: The wide scope of work in progress at
Admiral creates challenging opportunities in the field of
your choice. Write Director of Engineering and Research,
Admiral Corporation, Chicago 47, Illinois.

Note: NEW COLOR SOUND FILM on Admiral Automation available for showing to technical or business groups. Address Public Relations Director, Admiral Corporation, Chicago 47.

GASDYNAMICS RESEARCH ENGINEER

needed to supervise and formulate research programs related to high energy gas-dynamic equipment such as shock tube and rotating wave machines. Duties will also include the design and construction of test apparatus and the preparation of reports.

Experimental equipment includes a hypersonic shock tunnel, propulsion test stands, shock tubes, transonic or supersonic wind tunnels and associated instrumentation.

An especially attractive feature of employment at C.A.L. is the system of "internal research" wherein promising research ideas of engineers and scientists are sponsored and supported by the Laboratory.



**CORNELL
AERONAUTICAL**
Laboratory, Inc.

2300 SENeca ST., BUFFALO, N. Y.

ENGINEER

Design

Engine Units

for Nuclear Powered Flight

ME
or
AE

The next big advance in aviation is nuclear powered flight, a field which offers exceptional possibilities for professional achievement. General Electric now has a position open in this new field.

Qualifications include 2 to 6 years' experience in thermodynamics and aerodynamic development. Work involves thermodynamics and fluid flow aspects of turbine type aircraft engines and components.

Openings in Cincinnati, Ohio and Idaho Falls, Idaho.

Address replies to location you prefer

Aircraft Nuclear Propulsion Dept.

GENERAL ELECTRIC

Att: Mr. W. J. Kelly • Att: Mr. L. A. Munther
P. O. Box 132 • P. O. Box 535
Cincinnati, O. • Idaho Falls, Idaho

Index to Advertisers

ACCESSORY PRODUCTS CORPORATION.....	306
Anderson-McConnell Advertising Agency, Inc., Hollywood, Calif.	
ADMIRAL CORPORATION, Crutenden and Eger Associates, Chicago, Ill.....	317
AEROJET-GENERAL CORPORATION, D'Arcy Advertising Co., St. Louis Mo.	Back Cover
AIR PRODUCTS, INCORPORATED.....	235
Thoma and Gill, East Orange, N. J.	
ARO, INCORPORATED.....	305
BARBER-COLMAN COMPANY.....	238
Howard H. Monk and Associates, Inc., Rockford, Ill.	
BELL AIRCRAFT CORPORATION.....	302
Comstock and Co., Buffalo, N. Y.	
BENDIX AVIATION CORPORATION, SCINTILLA DIVISION.....	305
MacManus, John and Adams, Inc., Bloomfield Hills, Mich.	
CALIFORNIA INSTITUTE OF TECHNOLOGY, JET PROPULSION LABORATORY.....	289
Frank Barrett Cole Advertising, Pasadena, Calif.	
CLARY CORPORATION.....	229
Erwin, Wasey and Co., Ltd., Los Angeles, Calif.	
CONTINENTAL WIRE CORPORATION.....	292
The Taylor and Greenough Co., Wethersfield, Conn.	
CONVAIR, A Division of General Dynamics Corporation.....	298, Third Cover
Barnes Chass Company, San Diego, Calif.	
Buchanan and Company, Inc., Los Angeles, Calif.	
CORNELL AERONAUTICAL LABORATORY, INCORPORATED.....	318
Melvin F. Hall Advertising Agency, Inc., Buffalo, N. Y.	
DEHAVAN MANUFACTURING COMPANY.....	282
Fairall and Company, Des Moines, Iowa	
DOUGLAS AIRCRAFT COMPANY, INCORPORATED.....	232, 293
J. Walter Thompson Co., Los Angeles, Calif.	
DU PONT DE NEMOURS, E. I., AND COMPANY.....	320
Batten, Barton, Durstine and Osborn, New York, N. Y.	
EASTERN INDUSTRIES, INCORPORATED.....	309
Remsen Advertising Agency, Inc., New Haven, Conn.	
EXCELCO DEVELOPMENTS, INCORPORATED.....	315
EXPERIMENT, INCORPORATED.....	310
Eastern Associates, Richmond, Virginia	
FAIRCHILD ENGINE AND AIRPLANE CORPORATION, ENGINE DIVISION.....	239
Gaynor Colman Prentiss and Varley, Inc., New York, N. Y.	
FORD INSTRUMENT COMPANY, A Division of Sperry Rand Corporation ..	233
G. M. Basford Co., New York, N. Y.	
GENERAL ELECTRIC COMPANY (Aircraft Products Department)	319
Deutsch and Shea, New York, N. Y.	
GENERAL ELECTRIC COMPANY (Aircraft Nuclear Propulsion Department) ..	318
Deutsch and Shea, New York, N. Y.	
GENERAL ELECTRIC COMPANY, AGT DIVISION.....	226
Deutsch and Shea, New York, N. Y.	
GENERAL MILLS, INCORPORATED.....	300
Batten, Barton, Durstine and Osborn, Minneapolis, Minn.	
GENERAL PRECISION EQUIPMENT CORPORATION.....	236, 237
Geer, DuBois and Co., Inc., New York, N. Y.	
GIANNINI, G. M., AND COMPANY, INCORPORATED.....	228
Western Advertising Agency, Inc., Los Angeles, Calif.	
GRAND CENTRAL ROCKET COMPANY.....	312
INTERNATIONAL BUSINESS MACHINES CORPORATION.....	296
Benton and Bowles, Inc., New York, N. Y.	
KOLLSMAN INSTRUMENT CORPORATION.....	301
Deutsch and Shea, Inc., New York, N. Y.	
LOCKHEED AIRCRAFT CORPORATION, MISSILE SYSTEMS DIVISION.....	231
Hal Stebbins, Inc., Los Angeles, Calif.	
MANNING, MAXWELL AND MOORE, INCORPORATED	319
Fuller and Smith and Ross, Inc., New York, N. Y.	
MARQUARDT AIRCRAFT COMPANY.....	303
Doyle, Kitchen and McCormick, Inc., New York, N. Y.	
MARTIN, THE GLENN L., COMPANY.....	286, 316
Vansant, Dugdale and Company, Baltimore, Md.	
MCCORMICK SELPH ASSOCIATES.....	306
Gerth-Pacific Advertising Agency, San Francisco, Calif.	
MCDONNELL AIRCRAFT CORPORATION.....	230
MINIATURE PRECISION BEARINGS, INCORPORATED.....	319
Henry A. Loudon, Advertising, Inc., Boston, Mass.	
NEW YORK AIRBRAKE COMPANY.....	227
Humbert and Jones, Advertising, New York, N. Y.	
NORTH AMERICAN INSTRUMENTS, INCORPORATED.....	319
Heints and Company, Inc., Los Angeles, Calif.	
NORTHROP AIRCRAFT, INCORPORATED.....	294
West-Marquis, Inc., Los Angeles, Calif.	
OLIN MATHIESON CHEMICAL CORPORATION.....	303
Doyle, Kitchen and McCormick, Inc., New York, N. Y.	
RADIO CORPORATION OF AMERICA.....	297
Al Paul Lefton Company, Inc., Philadelphia, Penna.	
RAHM INSTRUMENTS, INCORPORATED.....	298
Herbert W. Cohen Co., New York, N. Y.	
REACTION MOTORS, INCORPORATED.....	Second Cover, 303
J. Wheelock Associates, New York, N. Y.	
Doyle, Kitchen and McCormick, Inc., New York, N. Y.	
ROBERTSHAW-FULTON CONTROLS COMPANY.....	314
Bozell and Jacobs, Inc., Beverly Hills, Calif.	
ROBINSON AVIATION, INCORPORATED.....	307
Platt, Dyson and O'Donnell, Inc., New York, N. Y.	
ROCKETDYNE, A Division of North American Aviation, Incorporated.....	234
Batten, Barton, Durstine and Osborn, Los Angeles, Calif.	
RONAN and KUNZL, INCORPORATED.....	310
SANBORN COMPANY, Meissner and Culver, Inc., Boston, Mass.....	299
SPEERY GYROSCOPE COMPANY, A Division of Sperry Rand Corporation.....	295
Equity Advertising Agency, New York, N. Y.	
STATHAM LABORATORIES, INCORPORATED.....	299
Western Advertising Agency, Inc., Los Angeles, Calif.	
STURTEVANT, P. A., COMPANY.....	319
Ross Llewellyn, Inc., Chicago, Ill.	
TABER INSTRUMENT CORPORATION.....	310
The Purcell Company, Buffalo, N. Y.	
THIOLKOL CHEMICAL CORPORATION.....	311
Grant Advertising, Inc., New York, N. Y.	
WATERTOWN DIVISION, THE NEW YORK AIR BRAKE COMPANY.....	227
Humbert and Jones, Advertising, New York, N. Y.	
WESTVACO CHLOR-ALKALI DIVISION, Food Machinery and Chemical Corp....	240
James J. McMahon, Inc., New York, N. Y.	

"TORQUE WRENCH" MANUAL

TORQUE MANUAL



SENT UPON REQUEST

Applications

Engineering Data

Screw Torque Data

Adapter Problems

General Principles

PA. **STURTEVANT CO.**
ADDISON QUALITY ILLINOIS

Manufacturers of over 85% of the torque wrenches used in industry



Stuck?

Got problems in design miniaturization that remind you of this? Send for the inside info on how over 500 types and sizes of M.P.B.'s*



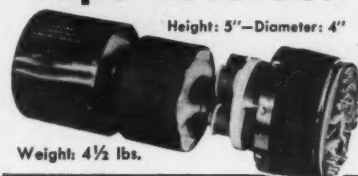
BALL BEARINGS ACTUAL SIZE

such as these will help to make things easier and easier.

*
MINIATURE PRECISION BEARINGS, INC.
20 Precision Park, Keene, N. H.

NORTHAM

Miniature Magnetic Tape Recorder



Height: 5" — Diameter: 4"

Weight: 4½ lbs.

Eight channels of information can be applied simultaneously to a ½-inch tape in the Model MR-1 Recorder (illustrated). This self-contained unit includes transistor timing oscillator and battery power source and operates under axial accelerations up to 500 g. A pre-record carrier system permits direct coupling with D.C. devices such as thermocouples and strain gauge transducers.

MODEL MR-1 SPECIFICATIONS:

Accuracy: ±5% full scale
Sensitivity:28 millivolts D.C. full scale across 40 ohms impedance
Frequency Bandwidth: 0-250 cps
Timing: 1000 cps transistor oscillator
Running Time: 45 seconds
Applications: Running time, number of channels and recording characteristics are adaptable to meet requirements of applications—including rocket and aircraft flight testing, oil well logging and atmospheric studies.

WRITE FOR BULLETIN NO. ... JP-104

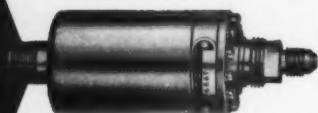
NORTHAM PRODUCTS INCLUDE ...

Transducers for pressure, acceleration and displacement measurement and auxiliary electronic equipment for complete systems.

NORTH AMERICAN INSTRUMENTS, INC.
2420 North Lake Avenue • Altadena, Calif.

PRESSURE ACTUATED SWITCH

TYPE 6867



Accurate operation under vibration. Withstands rocket fuels. Small: 4.750" L. x 1.520" Dia. overall — Light: 6 oz.

DIAPHRAGM MATERIAL	Stainless steel.
OPERATING MEDIA	Standard aircraft fuels, oil, water-alcohol solutions, nitric acids, hydrogen peroxide, and all other commonly used rocket fuels or products of combustion.
OPERATING RANGES	Adjustable from 30-200, 200-500 psig.
OPERATING TOLERANCES	Approximately 5% of control point setting.
PROOF PRESSURE	2000 psi.
BURST PRESSURE	4000 psi.
AMBIENT TEMPERATURE	—65° F. to +250° F.
VIBRATION	Up to 2000 cps at 20 g.
CONTACTS	SPDT—SPST (normal-open or normal-closed)—DPST.
PRESSURE CONNECTION	7/16-20 per AND 10050, 5/16-24 per AND 10050 (optional).
MOUNTING	Bulkhead
ELECTRICAL CONNECTOR	Hermetically-sealed type receptacle (mates with standard AN units).

The Manning, Maxwell & Moore Type 6867 switch is designed for use in aircraft systems to control electrical circuits by pressure of a liquid or gas. Reliable, accurate operation under vibration makes the unit particularly attractive for rocket applications. Our complete line of airborne pressure switches covers operation from inches of water through 4000 psi. We believe our long experience and extensive facilities for developing, manufacturing and testing pressure switches for modern aircraft can be helpful to you. Our engineering counsel is at your service. Write for details about our pressure switches, including Type 6867.

ASK FOR DATA SHEETS



MANNING, MAXWELL & MOORE, INC.

AIRCRAFT PRODUCTS DIVISION, Danbury, Conn.

Our Aircraft Products include: Turbjet Engine Temperature Control Amplifiers • Electronic Amplifiers • Pressure

Switches for Rockets, Jet Engine and Airframe Applications • Pressure Gauges, Thermocouples • Hydraulic Valves • Jet Engine Afterburner Control Systems.

missile sub-systems ENGINEER

For the Systems Engineer bent on utilizing past experience to "go places," GE's new Aircraft Products Department offers a fine opportunity to guide and integrate all sub-contracting of the missile for bomber defense missile system ... regulating and coordinating schedules, costs, specifications. He will also provide technical coordination between all project sub-systems.

7 to 9 years' experience in missile field including structures, guidance, power plant, and accessory sub-systems.
B.S., E.E., M.E. or A.E. (minimum).

This 3-year old GE Department has expanded at an unusual rate. There is a fine career potential here. New York "Vacationland" location means satisfied living, too!

Write in confidence to:

Mr. C. E. Irwin
Engineering Admin.
Aircraft Products Dept.

GENERAL ELECTRIC

600 Main Street, Johnson City, N. Y.

DU PONT ANNOUNCES

LINO-WRIT 2

The NEW oscillographic paper for critical recording at intermediate frequencies

Here's important news! Du Pont research has developed a new oscillographic paper designed for critical recording at intermediate frequencies. It's Lino-Writ 2 and it gives you clear, high contrast records every time because it is a fast, fog-free, non-staining paper with exceptional latitude. It's made in two types: extra-thin Type *W* and standard-weight Type *B*. Both types take ink or pencil marks readily.

NEW SPEED

New Du Pont Lino-Writ 2 has plenty of extra speed to handle critical recording of intermediate frequencies at high paper travel rates. Thanks to this extra speed, you can use lower lamp voltages with Lino-Writ 2 and minimize lamp failures during a critical test.

WON'T CRACK OR TEAR

You can forget about cracks or tears caused by folding and handling when you use Lino-Writ 2. That's especially true with Type *W*—the strongest, toughest, extra-thin photorecording paper ever produced for commercial oscillographic use. In test after test, Type *W* outlasted every other paper on the market...regardless of whether the paper was handled and folded wet or dry, processed or unprocessed. And you can handle it without a worry

right after stabilization processing.

Type *W* withstands abnormal handling and abuse because it's the only photorecording paper that's made from 100% rag stock.

SPLICE-FREE ROLLS

To decrease the chances of paper failure at the splice during an expensive test, Lino-Writ 2 is supplied in splice-free rolls up to 450' in length at no extra charge.

FITS ALL OSCILLOGRAPHS

New Lino-Writ 2 is available in popular widths and specification numbers to meet the demands of practically all types of oscillographs, including *Century*, *Consolidated*, *General Electric*, *Hathaway*, *Heiland*, *Midwestern* and *Miller*.

SEND FOR FREE BOOKLET

We'll welcome the opportunity to show you how this important new photorecording paper can save you time and money and improve your records of expensive tests. Simply fill out the coupon and we'll immediately send you a free booklet that gives a detailed description of Lino-Writ 2, as well as other Lino-Writ photorecording papers and chemicals. It's worth doing *right now!*

DU PONT
OSCILLOGRAPHIC PRODUCTS



BETTER THINGS FOR BETTER LIVING . . . THROUGH CHEMISTRY

320

E. I. du Pont de Nemours & Co. (Inc.)
Photo Products Department
2420-17 Nemours Building, Wilmington 98, Delaware
Please send me information about new Lino-Writ 2, other photorecording papers, and Du Pont Lino-Writ processing chemicals.

Name _____
Firm _____
Street _____
City _____ State _____

324

JET PROPULSION

S

use be-
made

splice
lied in
charge.

hs and
ctically
onsol-
western

his im-
ou time
re tests
ly send
tion of
cording
!

other
ssing

924

ULSION